Synthetic Routes to ^{18}F-Labelled Gemcitabine and related 2'-Fluoronucleosides

A thesis submitted in accordance with the conditions governing candidates for the degree of

Philosophiae Doctor

by

Jan-Philip Meyer

December 2014

Cardiff School of Pharmacy and Pharmaceutical Science

Cardiff University

Acknowledgements

I want to take the opportunity to thank all my supervisors for their great support. In particular, I want to thank Dr. Andrew Westwell for his guidance in not only research related matters but all sort of challenges that arose along the journey towards the submission of my PhD thesis. Furthermore, I want to express my gratitude to Prof. Chris McGuigan for his fruitful ideas during my group meeting presentations that significantly improved my understanding of how related fields are connected and how important it is to put all assumptions and results to the test. Finally, I thank Dr. Katrin Probst mainly for her assistance in radiochemistry but also for giving me the opportunity to experience various aspects of clinical tracer production. I also would like to thank all members from Andrew's and Chris' lab and the PETIC staff for really nice talks, suggestions and coffee breaks. Additionally, I thank Cancer Research Wales and the British Association for Cancer Research for their financial support and the opportunity to attend interesting scientific conferences. Finally, I would like to express my sincerest appreciation to my family, my fiance (Liz) and my friends in and around Cardiff for their support, motivation and patience.

Abstract

Gemcitabine (2',2'-difluoro-2'-deoxycytidine, dFdC) is an established chemotherapeutic agent used in the treatment of various carcinomas such as lung, breast, bladder and especially pancreatic cancer. However, its general application and bioavailability is compromised due to both poor cell uptake and rapid metabolism by gut and liver cytidine deaminase (CDA). A ^{18}F-gemcitabine positron emission tomography (PET) probe could enable biodistribution studies and the imaging of gemcitabine pharmacodynamics *in vivo*. However, the potential and clinical relevance of a ^{18}F-gemcitabine PET probe would have to be evaluated using appropriate PET tumour models.

In order to approach the synthetic target molecule ^{18}F-dFdC, proof-of-principle studies on more straightforward synthetic targets including ^{18}F-FAU and ^{18}F-FAC (see figure below) were carried out first. An appropriate precursor was synthesised for 2'-stereoselective late-stage radiofluorination based on previously developed conditions. First, the 2'-[^{18}F]fluorinated arabino nucleoside ^{18}F-FAU, which was considered as a rapidly accessible 2'-fluorinated uracil-based dFdC analogue was successfully synthesised in our radiochemical laboratory. Subsequently, this procedure was used as a template method to obtain the cytidine analogue ^{18}F-FAC via a novel synthetic route in moderate radiochemical yield (4.3-5.5%, decay-corrected), high specific activity ($\geq$1700 mCi/μmol) and purity ($\geq$98%) after a synthesis time of 168 min.

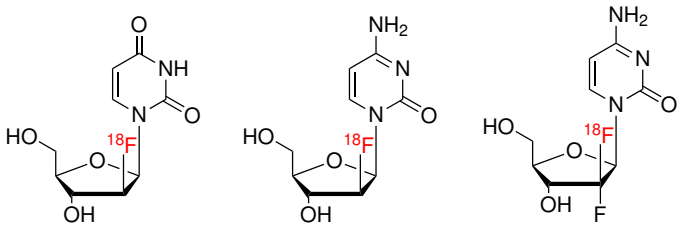

Prior to radiofluorination, experimental and computational methods were used to design a novel precursor that combines stability and reactivity. The selected precursor gave promising RCYs (5-10%) of the ^{18}F-labelled protected intermediate. The impact of temperature and reaction time on radiochemical yield and the stereospecificity of the radiofluorination was investigated in order to determine optimal conditions. The developed radiofluorination method could simplify the production of ^{18}F-FAC for clinical purposes via a fast transfer to automated radiosynthesisers in good manufacturing practice (GMP) labs.

Considering the final target ^{18}F-dFdC, the 2'-carbonyl fluorination precursor used for first radiofluorination studies towards the protected ^{18}F-gemcitabine intermediate was based on previously published results. Radioanalytical data provided evidence that deoxo[^{18}F]difluorination occurred when DAST in combination with [^{18}F]fluoride was used. Low radiochemical yields (0.2-0.3%, decay-corrected) of the 2'-[^{18}F]difluorinated gemcitabine intermediate were achieved. However, extensive studies including the use of simplified radiosynthesisers and modern synthesis techniques such as microwave-assisted synthesis as well as deprotection conditions to give the final target ^{18}F-dFdC have to be carried out in order to assess the potential of this radiochemical approach.

Publications arising from this work

Peer-reviewed journal articles

Jan-Philip Meyer, Katrin Probst, Andrew D. Westwell, Radiochemical synthesis of 2'- and 3'-^{18}F-labelled nucleosides for applications in Positron Emission Tomography Imaging, *J. Label Compd. Radiopharm.*, **2014**, *57* (5), 333-337.

Jan-Philip Meyer, Iuni M.L. Trist, Katrin Probst, Christoper McGuigan, Andrew D. Westwell, A Novel radiochemical approach to 1-(2'-Deoxy-2'-^{18}F-fluoro-β-D-arabino-furanosyl)-cytosine (^{18}F-FAC), *J. Label Compd. Radiopharm* **2014**, *57* (11), 637-644.

Accepted

Jan-Philip Meyer, Andrew D. Westwell, Synthesis of Fluorinated Pharmaceuticals (Chapter 1); Fluorinated Pharmaceuticals: Advances in Medicinal Chemistry (e-book), *Future Science Group*

Published abstracts

Jan-Philip Meyer, Katrin Probst, Christoper McGuigan, Andrew D. Westwell, Synthetic Routes to ^{18}F-labelled Gemcitabine and related 2'-fluoronucleosides, 15th Tetrahedron Symposium (*Tetrahedron*), London, UK, 23-27th June 2014.

Jan-Philip Meyer, Christopher McGuigan, Steven Paisey, Andrew D. Westwell, ^{18}F-Gemcitabine and related 2'-fluoro nucleosides, AACR-NCI-EORTC Molecular Targets and Cancer Therapeutics (*Mol. Cancer Ther.*, **2013**, *12*, B32), Boston, USA, 21-24th October 2013.

Contents

List of abbreviations

Å	Angstrom (1 Å = 10^{-10}m = 0.1 nm)
Bq	Bequerel (1 Bq = 1 decay/sec)
Boc	*tert*-butyl-oxycarbonyl
CDA	cytidine deaminase
CT	Computed Tomography
CD99	Cluster of differentiation 99 (antigen, glycoprotein)
CD8	transmembrane glycoprotein (cell recognition)
COSY	correlation spectroscopy
Ci	Curie (1 Ci = 3.7 × 10^{10} decays/sec = 37 GBq)
dFdC	2,2'-difluoro-2'-deoxycytidine (Gemcitabine)
dCK	deoxycytidine kinase
DNA	deoxyribonucleic acid
DCM	dichloromethane
DAST	diethylaminosulfur trifluoride
DMF	dimethyl formamide
DMSO	dimethyl sulfoxide
DIAD	diisopropyl azodicarboxylate
DMAP	dimethyl aminopyridine
DMP	Dess-Martin periodinane

EoB	End of Bombardment
eV	electronvolt [J]
ESI	eletrospray ionisation
FIAU	2'-fluoro-deoxy-arabino-5-iodouridine
FDG	2-fluoro-deoxy-glucose
FAU	2'-fluoro-deoxy-arabinouridine
FAC	2'-fluoro-deoxy-arabinocytidine
FMAU	2'-fluoro-deoxy-arabino-5-methyluridine
FLT	3'-fluoro-deoxy-L-thymidine
FGI	functional group interconversion
GMP	good manufacturing practice
HSQC	heteronuclear quantum coherence
HSV-TK-1	herpes simplex virus thymidine kinase 1
h	hour
hENT	human concentrative nucleoside transporter
HER2	human epidermal growth factor receptor 2
HPLC	High-pressure liquid chromatograhy
HMPA	hexamethylphosphoramide

K_{222}	Kryptofix 222 (cryptant)
LC	liquid chromatography
MsCl	mesyl chloride
MS	mass spectrometry
MRI	Magnetic Resonance Imaging
M	molar [mol/L]
mL	millilitre
MeCN	acetonitrile
NMR	nuclear magnetic resonance
nca	non-carrier-added
NsCl	nosyl chloride
pTsOH	*para*-toluenesulfonic acid
PETIC	Wales Research and Diagnostic PET Imaging Centre
ppm	parts per million
PK	Pharmacokinetics
PD	Pharmacodynamics
PET	Positron Emission Tomography
pK_a	Acid dissociation constant
QC	quality control

RNA	ribonucleic acid
RR	ribonucleotide reductase
RCY	Radiochemical yield
r.t.	room temperature
R_f	retardation factor
R_t	retention time
SLC	solute carrier family (nucleoside transporter)
Sv	Sievert (1 Sv = 1 joule/kilogram)
SM	starting material
S_N	nucleophilic substitution
TMS	tetramethyl silyl
TsCl	tosyl chloride
THP	tetrahydropyran
TIPDS	tetraisopropyl disilyl
Et_3N	triethyl amine
TK1	thymidine kinase 1
TS	Thymidylate Synthase
TLC	Thin-layer chromatography
THF	tetrahydrofuran
$t_{1/2}$	half-life
TBAF	tetrabutyl ammonium fluoride
UV	ultraviolet

List of Figures

List of Tables

1 Introduction

1.1 Fluorinated nucleoside analogues

1.1.1 Overview

Although fluorine is relatively abundant on earth it is very rare in naturally occurring biologically active compounds. However, regarding medicinal applications the introduction of fluorine into potential drug molecules is common and useful due to both its bioisosterism to a proton substituent and its bioisopolarity to the hydroxy group and the resulting pharmacological properties of the corresponding fluorine containing compounds, such as lipophilicity and metabolic stability[1–3]. The fact that 15-20%[4] of all drugs released worldwide during the last five decades contained one or more fluorine atoms indicates the important role of fluorine in modern medicinal chemistry and general medical applications[5].

Naturally occurring purine nucleosides, such as guanosine, adenosine and inosine, and pyrimidine nucleosides, such as uridine, cytidine and thymidine are not only subunits of deoxyribonucleic acid (DNA) and ribonucleic acid (RNA) of living organisms, but are also important signalling molecules. Extracellular purines, for instance, mediate biological responses, such as neuromodulation and coronary vasodilatation through surface receptors[6–8]. Synthetically modified nucleoside analogues can act as antimetabolites in important biochemical processes and hence represent an important class of antiviral[9] and anticancer[10] therapeutics. These artificial modifications are either performed on the base and/or the sugar

moiety using a wide range of synthetic techniques. 2'- and 3'-fluorinated nucleoside analogues play an important role as both anticancer and antiviral agents[9,10]. The chemical structures of some important fluorinated purine and pyrimidine nucleoside analogues are shown below (Figure **1**). Gemcitabine (**1**), for instance, is used as a first-line treatment of pancreatic adenocarcinoma and non-small cell lung cancer[11] and marketed as Gemzar^{TM} by *Eli Lilly*. Clevudine (**4**) represents another pyrimidine nucleoside analogue which is used as an antiviral agent for the treatment of hepatitis B in south-east asia[12]. Clofarabine (**2**) is a representative of the purine nucleoside analogue family and FDA approved as Evoltra^{TM} for the treatment of acute lymphoblastic leukaemia in children[13]. The ^{18}F-labelled analogues of fluoro-deoxy-L-thymidine (FLT)[14,15] (**3**), fluoro-deoxy-arabinocytidine (FAC)[16] (**5**) and fluoro-deoxy-arabino-5-methyluridine (FMAU)[17] (**6**), for instance, represent a class of interesting biomarkers for positron emission tomography (PET) imaging with pre-clinical and clinical applications. The use of ^{18}F-labelled nucleoside-based PET probes is further discussed in section **1.2.5**.

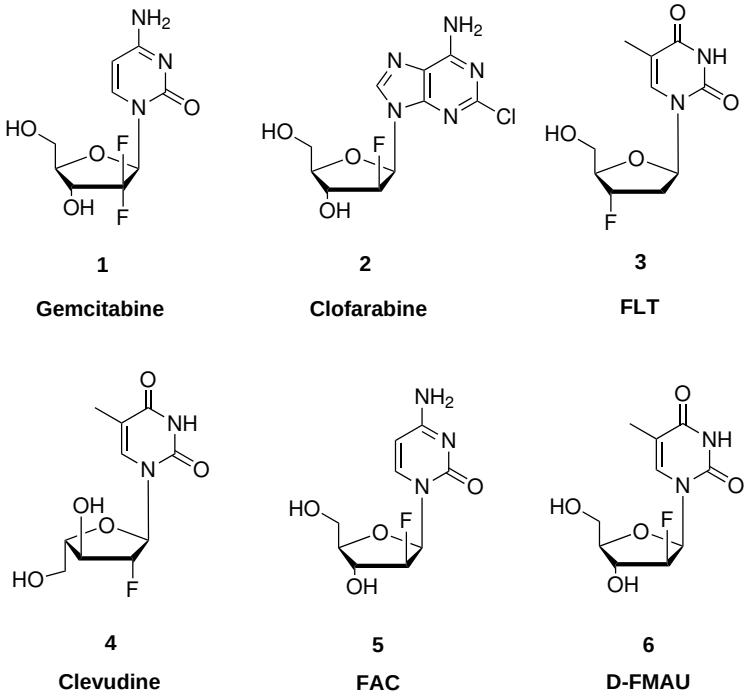

Figure 1: Examples of important fluorinated nucleoside analogues (**1-6**).

Bioisosteric replacement of either a hydrogen atom or a hydroxy group at the 2'- or 3'-position of the ribose moiety through a fluorine atom leads to several interesting properties which are responsible for the pharmacological importance of these fluoro-deoxy-nucleosides[2,3]. Although hydrogen and fluoro substituents are comparable in terms of size and steric effects which is, for instance, important in terms of receptor binding, the overall molecular topology remains almost unaffected[18]. Since the bond lengths of carbon-hydrogen (1.08-1.10 Å) and carbon-fluorine (1.26-1.41 Å) bonds are comparable[19] the steric bulk of the molecule does not change significantly. However, both the pK_a-value and the dipole moment of the molecule may change and affect pharmacokinetic (PK) properties such as logP-values as the fluorine substituent mimics closely a hydroxy group in terms of isopolar behaviour[11]. Furthermore, the incorporation of a fluorine substituent often leads to an increased biological stability of the new compound against oxidative enzymatic modifications due to the high dissociation energy[20] of the carbon-fluorine bond which is in many cases a deliberate feature in drug design.

1.1.2 Mechanism of action

The anticancer and antiviral activity of 2'-fluorinated nucleoside analogues observed in different cell lines initially requires cell uptake by certain nucleoside transporters which are embedded in the cell membrane[21].

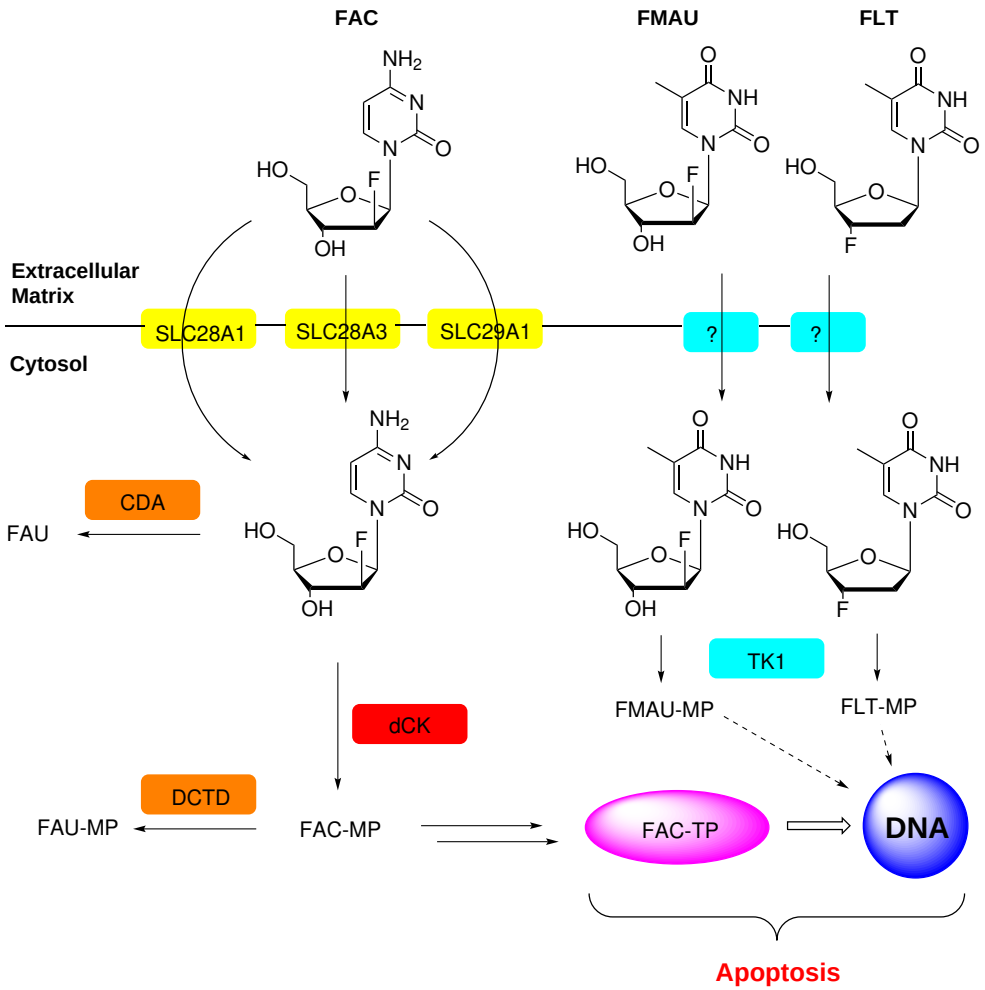

Figure 2: Metabolism and intracellular mode of action of FAC, D-FMAU and FLT.

Most of the nucleoside transporters known so far belong to the solute carrier (SLC) family and are divided into Na^+-dependent human concentrative nucleoside transporters[22] (hCNT/SCL group 28) and Na^+-independent human equilibrative nucleoside transporters[23] (hENT/SCL group 29). Certain transporters within these two groups are specific for particular nucleosides, such as SLC28A2, which is a purine-specific Na^+-cotransporter or SLC28A1, which is a Na^+-dependent pyrimidine-specific transporter, for instance. The 2'-fluorinated nucleoside analogues shown above (Figure **2**) are prodrugs and thus have to undergo certain metabolic transformations, mostly phosphorylations, in order to generate their cytotoxicity[24]. Depending on the phosphorylation stage cytotoxicity occurs due to inhibition of different target enzymes. Intracellular, 1-

(2'deoxy-2'-fluoroarabinofuranosyl)cytosine (**5**, FAC), for instance, is first monophosphorylated to FAC-MP which can either be deactivated by deoxycytidylate deaminase (dCTD) or transformed into the diphosphate FAC-DP which is a potential inhibitor of ribonucleotide reductase (RR)[25]. The triphosphate form FAC-TP represents the actual cytotoxic metabolite that is incorporated into DNA causing chain termination and subsequent apoptosis (Figure **2**)[25].

The described intracellular mechanism of action of FAC is not coercively transferable to any other 2'- or 3'-fluorinated nucleoside analogue nucleoside but should rather be regarded as a model system for a general description of possible intracellular transformations. Depending on the nucleoside analogue and the cell type examined, the mode of action may be different. However, it gives an overview about some important aspects that have to be considered concerning nucleoside analogues as potential drug candidates. Targeting an intracellular pathway to treat a particular disease often raises pharmacological questions such as cell uptake and metabolic deactivation of drug molecules, especially in the case of nucleoside analogues. Gemcitabine will be used as an important example to highlight these pharmacological issues.

1.1.3 Gemcitabine

Initially developed as an antiviral agent[26] 2',2'-difluoro-2'-deoxycytidine (**1**, gemcitabine, dFdC) showed significant activity against leukaemia cell lines *in vitro* in pre-clinical testing[27]. Today, it is used in chemotherapy for the treatment of various carcinomas such as lung, breast, bladder and especially pancreatic cancer[28], both alone or in combination with other chemotherapeutics such as carboplatin[29] or paclitaxel[30].

Gemcitabine shows high cytotoxicity against various cancer cell lines it is thus approved for the first line treatment of advanced and metastatic pancreatic cancer[31]. However, general application and bioavailability are compromised due

to both poor cell uptake and rapid metabolism by gut and liver cytidine deaminase (CDA) resulting in the toxic side product 2',2'-difluoro-2'-deoxyuridine (dFdU)[32]. Hence, gemcitabine is applied intravenously on a frequent schedule in order to extend the systemic exposure time as much as possible. The human terminal plasma half-life of dFdC is about 17 min[33].

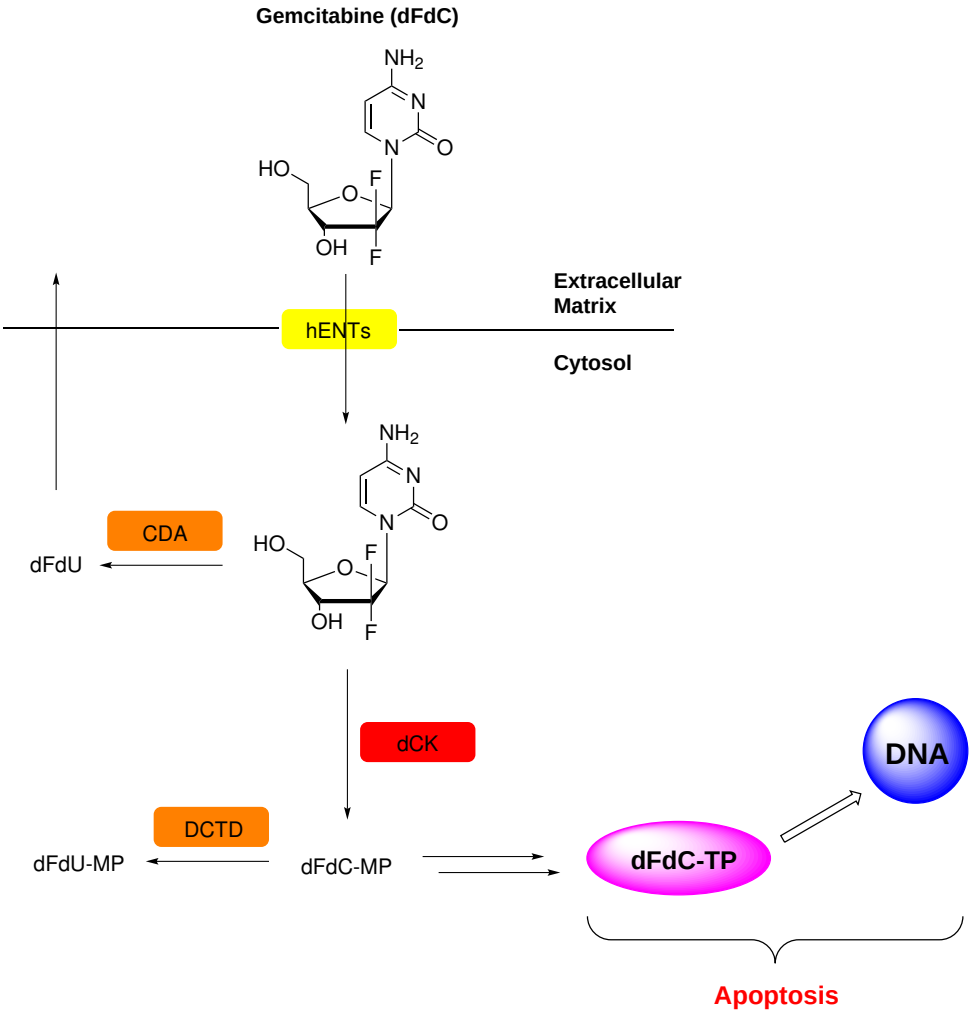

Figure 3: Metabolism and intracellular mode of action of Gemcitabine **1**.

Cellular uptake of dFdC occurs via subtypes of both transporter families hCNT and hENT. Even though dFdC is a substrate of hCNT1-3 and hENT1-2 with varying affinities, hENT1 seems to play a major role for dFdC cell uptake as hENT1-deficient cells show resistance to dFdC treatment[34]. Consequently,

cell uptake is one of the main factors that limit bioavailability of dFdC and nucleoside transporter gene expression constitutes one of the key mechanisms of dFdC sensitivity[35].

Once affiliated by the target cell through active transport either monophosphorylation catalysed by deoxy-cytidine kinase (dCK) or deamination catalysed by deoxy-cytidine deaminase (dCDA)[36] occurs to give pre-activated dFdCMP or deactived dFdU, respectively[37]. In fact, dCK-mediated phosphorylation is the rate-limiting step in the bioactivation sequence of dFdC. Potential prodrugs able to circumvent this step would enhance bioactivation of dFdC while using reduced administration doses which could significantly reduced side-effects such as nausea, vomiting and gastric ulceration[38]. Mutational dCK-deficiency is another mechanism of intrinsic dFdC resistance[39] besides hNT deficiency described above. The mono-phosphate form dFdCMP can either be deactivated to dFdUMP or metabolized to the first active metabolite dFdCDP which is an inhibitor of ribonucleotide reductase (RR) and thus depletes the ribonucleotide pool required for DNA synthesis[40]. Further phosphorylation results in the triphosphate form dFdCTP, the second active and most important metabolite of dFdC which is incorporated into DNA/RNA and hence leads to apoptosis[41].

Since the active nucleotide analogue dFdCTP is a substrate of DNA-polymerase I as its natural counterpart deoxycytidine triphosphate (dCTP), dFdCTP inhibits DNA-polymerase I competitively. Once incorporated into DNA dFdCTP leads to DNA chain termination[42]. Furthermore, incorporation of dFdC into DNA appears to be resistant to the usual mechanisms of DNA repair. However, details concerning this fact still remain unclear[43].

Recently published data indicate that gemcitabine-ProTides are able to bypass these resistance mechanisms[39]. In fact, dFdC-ProTide NUC-1031 (Scheme **1.1**) is currently in Phase I clinical trial for various cancers[39] and consists of a chiral phosphoramidate moiety which represents a pre-activated form of the mono-

phosphate form dFdCMP. The biolabile residues are cleaved in an intracellular step-by-step bioactivation pathway to finally give dFdCMP. This 5'-modification strategy not only bypasses the key rate-limiting monophosphorylation step but also allows transporter-independent uptake of NUC-1031 and improved resistance to CDA-mediated deamination *in-vivo*.

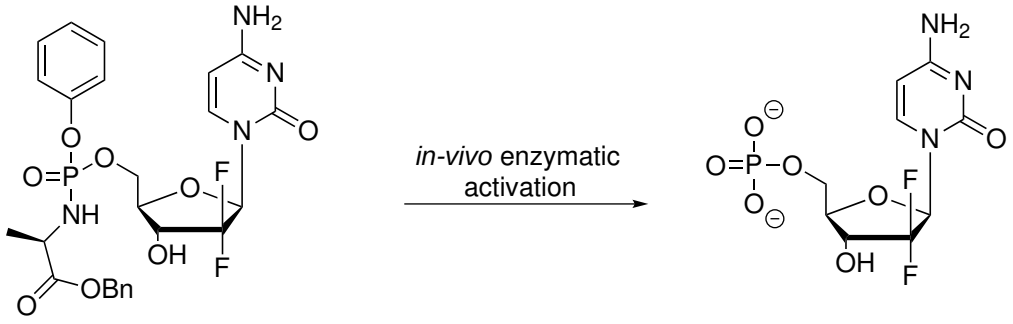

NUC-1031 **dFdCMP**

Scheme 1.1: Intracellular *in-vivo* activation of the novel gemcitabine-ProTide NUC-1031 towards dFdCMP involves different enzymes such as esterases and phosphoramidase-type enzymes.

1.2 Positron emission tomography imaging

Positron emission tomography (PET) imaging is a cross-sectional (tomographic) functional imaging modality that is used to diagnose many types of cancer[44] as well as a variety of other diseases such as gastrointestinal, endocrine and neurological disorders[45]. Even though magnetic resonance imaging (MRI) serves clinically a high spatial resolution in the submillimetre range[46,47], PET is the method of choice for *in vivo* imaging applications, especially in oncology[5]. For instance, according to the molecular imaging and contrast agent database (MICAD), 41% of all molecular imaging probes listed were PET-based[48,49]. Picomolar tracer concentrations[50] and high sensitivity makes PET the imaging modality of choice within pre-clinical, clinical and drug development studies[51].

One of the prime reasons for the importance of PET is the availability of organic positron-emitting radionuclides[52] such as ^{11}C, ^{13}N,^{15}O and ^{18}F that are radionuclides of elements that are occurring in natural and synthetic biologically active compounds. Hence, PET radiotracers can be developed that are chemically and biologically identical or similar to existing natural or synthetic biomolecules and may be able to provide quantifiable information about their pharmacokinetic (PK) and pharmacodynamic (PD) properties *in vivo*[53].

1.2.1 Physical principles of PET imaging

Radioactive decay

The radioactive labelled molecules used in PET imaging contain 'proton-rich' radionuclides that decay under spontaneous emission of a positron (β^+-particle) and a neutrino[54]. The resulting nuclear transmutation of a proton to a neutron within the nucleus does not change the mass number A (sum of all nucleons) of the radioactive atom but reduces the atomic number Z (sum of all protons) by one unit. Consequently, an atom of a chemical element X is transformed into an atom of a chemical element Y that is less by one unit (Z-1)[55] (Equation **1.1**). The nuclear transmutation is exemplified by the β^+-decay of the ^{18}F radionuclide (Equation **1.2**):

$$^{\mathrm{A}}_{\mathrm{Z}}X \rightarrow {}^{\mathrm{A}}_{\mathrm{Z-1}}Y + \mathrm{e}^+ + \mathrm{v_e} \tag{1.1}$$

$$^{18}_{9}\mathrm{F} \rightarrow {}^{18}_{8}\mathrm{O} + \mathrm{e}^+ + \mathrm{v_e} \tag{1.2}$$

Radioactive decay is a statistical process and thus individual nuclear decays are purely random. The radioactive decay can be quantified by the radioactive decay law where the number of disintegrations per unit time (dN/dt) is proportional to the total number N of radioactive nuclei in the probe[56]:

$$\frac{dN}{dt} = -\lambda N \tag{1.3}$$

The decay constant λ is radionuclide-specific[57]. The solution of this first-order differential equation can be written as:

$$N(t) = \mathrm{N}_0 \exp\left(-\lambda t\right) \tag{1.4}$$

The half-life of a radionuclide is defined as the time $\mathrm{t}_{1/2}$ taken for half the radioactive atoms to decay:

$$\frac{N(t = \mathrm{t}_{1/2})}{\mathrm{N}_0} = 0.5 = \exp\left(-\lambda \mathrm{t}_{1/2}\right) \tag{1.5}$$

which leads to the following expression:

$$t_{1/2} = \frac{ln(2)}{\lambda} \tag{1.6}$$

γ-Ray detection and image reconstruction

After emission, the positron travels a certain distance in the tissue while losing energy until it annihilates with an electron into two nearly antiparallel γ-photons that can be detected by external γ-detectors. The loss of energy from the positron is due to Coulomb interactions with electrons of atoms of the surrounding tissue[56]. The distance travelled by a positron until annihilation depends on its initial energy which in turn depends on the radionuclide and imposes a limit of the physical resolution of this modality. The use of different radionuclides[5] (Table **1**) in PET consequently leads to different spatial resolutions[53].

Table 1: Selected radionuclides used in PET imaging

radionuclide	Half-life	β (positron) emission
^{124}I	4.17 days	β^+, 1535 keV (11.8%), 2138 keV (11%)
^{64}Cu	12.7 h	β^+, 653 keV (17.9%), β^-, 578.7 keV (39%)
^{18}F	109.8 min	β^+, 633 keV (96.7%)
^{11}C	20.39 min	β^+, 960 keV (99.8%)
^{13}N	10 min	β^+, 1199 keV (99.8%)
^{18}O	2 min	β^+, 1732 keV (99.9%)

According to the laws of conservation of energy, the electric charge, the linear and angular momentum a positron-electron annihilation event results in two nearly antiparallel (180±0.25°)[56] γ-photons with an energy of 511 keV[58] (Figure **4**). Positron emission tomography imaging uses exactly these two diametrically emitted photons for the reconstruction of the spatial radioactivity distribution within the object. The deviation of the angle between the annihilation photons from the exact 180° angle contributes to the inherent degradation of spatial resolution in all PET detector systems[56].

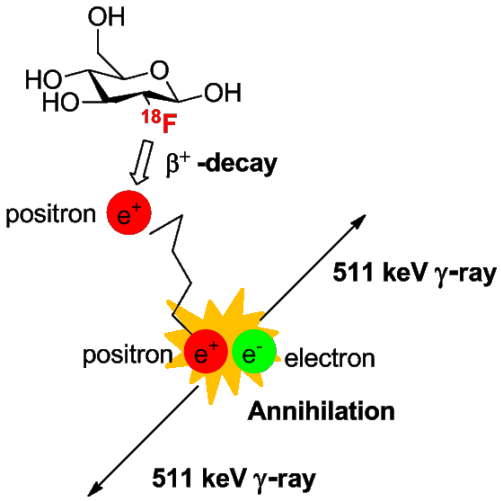

Figure 4: Physical principle of PET showing the annihilation process of an emitted positron with an electron using the PET probe ^{18}F-FDG as an example. The generated nearly antiparallel 511 keV γ-rays are subsequently used to reconstruct the spatial radioactivity distribution within the object.

The 511 keV annihilation γ-photons that reach the external detector system are registered using scintillation crystals. Incoming high energy photons are absorbed and their energy subsequently re-emitted as low energy photons in the range of visible light or near UV[56]. PET scanners may use different material for scintillation crystals such as the inorganic crystals BGO[59] (Bismuth germanate, ($Bi_4Ge_3O_{12}$)), LSO[59,60] (Lutetium orthosilicate, ($Lu_4Si_3O_{12}$)), lanthanum chloride ($LaCl_3$)[61] or lanthanum bromide ($LaBr_3$)[61], among others. Different material results in varying physical characteristics of the scintillation crystals such as energy resolution and light output[62] and hence may influence the sensitivity of the PET scanner[63].

Considering a single PET detector, the scintillation crystals are located at the front of the detector and are coupled with a visible light sensor such as a photomultiplier tube (PMT) or an avalanche photodiode (APD, suitable for PET/MRI systems due to the sensitivity of PMTs to strong magnetic fields)[64] which is located behind the crystal matrix. For instance, a crystal matrix of 64 (8×8) single scintillation crystals may be coupled with 4 PMTs (each PMT is located directly behind 16 single crystals)[55] (Figure **5**, left). Low energy photons that are re-emitted by the scintillation crystal are detected by the PMTs and transformed into an electrical signal. In order to prevent crosstalk between single crystals they are separated by mirror-coated cuts so that the re-emitted low energy photons can only reach the PMTs behind the crystal matrix.

A light-distributor is located between the scintillation crystals and the PMTs to ensure that the low energy photons emitted by one of the 64 single crystals can reach all 4 PMTs (Figure **5**). The single crystal that initially detected the incoming γ-photon can consequently be identified by comparing the different light intensities measured within the PMTs[65,66]. The identification of the single crystal is important in order to locate the annihilation event as precisely as possible to ensure high spatial resolution of the PET scanner[66]. Figure **5** shows a schem-

atic figure (left) and a single PET detector (right)* currently utilised in PET scanners.

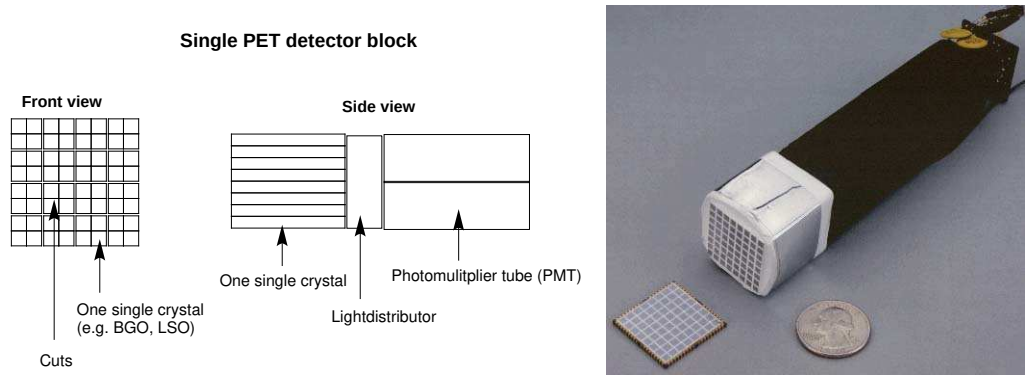

Figure 5: Left: Schematic figure of a scintillation detector. Each detector may contain 64 (8×8) single crystals coupled with 4 PMTs. An incoming γ-photon is registered by one of the 64 crystals which can afterwards be identified by comparing the different light intensities that were measured within the PMTs. However, the detector size limits the spatial resolution. The smaller the detector the better the resolution. Right: A scintillation detector used in modern PET scanners. Usually, several thousand single crystals are utilised in a PET scanner detector system.

The detector system of a PET scanner consists of many single detectors (the number of rings and single detectors may depend on the scanner type) that are arranged perpendicular to the scanner axis in parallel detector rings (Figure **6**, right)†. Each detector generates an electric signal when it registers an incident photon[56]. If the electric signals of two opposite detectors are detected within a coincidence time window (≈6-12 ns)[67] they are considered to be coincident[68]. The coincidence event is assigned to a line of response (LOR) that connects both detectors involved in the detection (Figure **6**, left). Thus, in combination with the measured time difference of the detected photons, positional information of the annihilation event is gained (electronic collimation) without using a physical collimator[55].

*http://cfi.lbl.gov/instrumentation/instrumentation.html
†http://cerncourier.com/cws/article/cern/29248

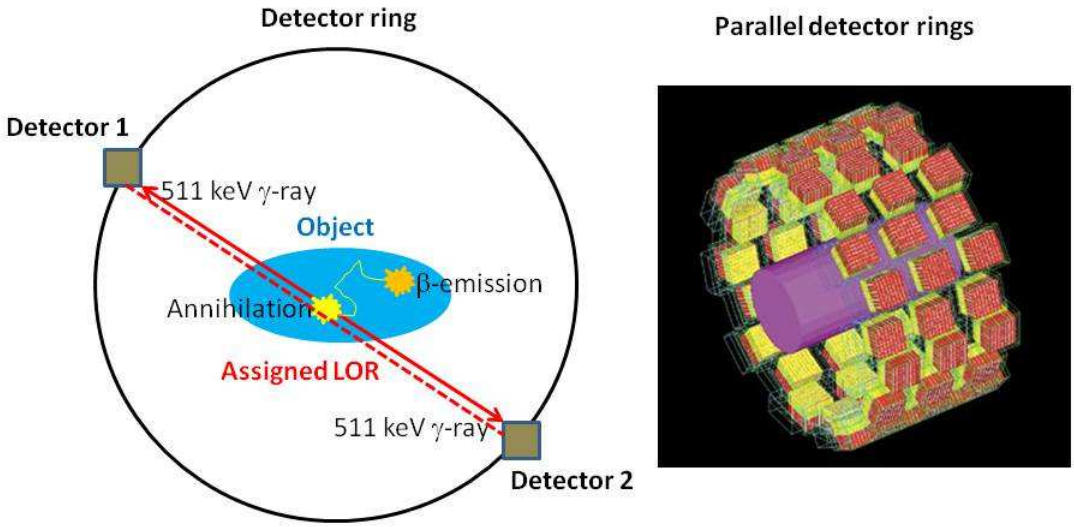

Figure 6: Left: The emitted positron travels a distance within the tissue until it annihilates with an electron and forms two antiparallel 511 keV γ-rays which can be detected by two opposite detectors of the detector ring. A coincidence event is assigned to a line of response (LOR, dashed red line) that enables the localisation of the annihilation event. Right: Schematic figure of parallel detector rings that are arranged perpendicular to the scanner/object axis.

In addition to 'true' coincidences where both annihilation photons reach the detector without being scattered or absorbed random and scattered coincidences are measured during a PET scan[69] (Figure **7**). Furthermore, attenuation, which is the loss of true coincidences due to scatter and absorption of annihilation photons within tissue, must be taken into account for the correction of the acquired raw data in order to obtain a correct quantitation of the radioactivity distribution. Hence, correction algorithms are applied to the acquired raw data in order to keep the degradation of the PET images at a minimum[55,69].

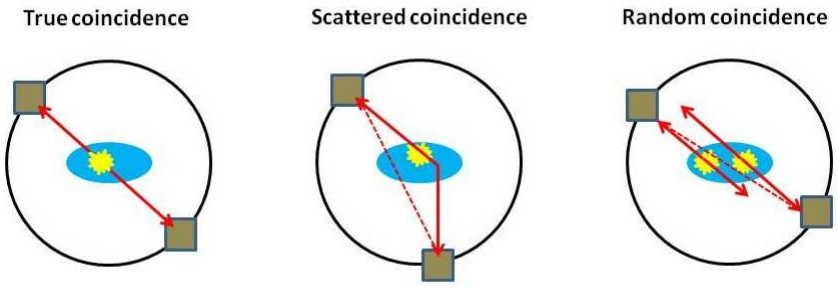

Figure 7: True (left), scattered (middle) and random (right) coincidences are registered in the PET detector ring. Scattered and random coincidences, however, may be assigned to the wrong LOR (dashed red lines). The amount of scattered and random coincidences depends on the volume and attenuation characteristics of the object that is being imaged and has to be corrected from raw data.

For 3D image reconstruction, data acquisition can either be performed in 2D- or 3D-mode depending on the type of acquired data. In 2D-mode, coincidence detection is allowed only within one detector ring (direct) or between detectors of closely neighbouring detector rings (indirect)[70]. However, if coincidences are detected by any detector of any detector ring (cross coincidences), an increased number of coincidence events is detected which in turn leads to an increased sensitivity and a higher signal-to-noise ratio[71,72]. At the same time the amount of detected scatter and random coincidences also increases so that more sophisticated 3D reconstruction algorithms have to be applied. Most scanners have the capability of data acquisition in both 2D- and 3D-mode by retracting septa. Septa are thin rings made of lead or tungsten that can be placed between detector rings to reduce cross coincidences[69]. Furthermore, the combination of PET as a functional imaging technique with computed tomography (CT) as a structural imaging modality not only allows acquisition of both functional and structural data in one study but also improves the quantification of PET data by more accurate correction of attenuation[73]. For that purpose, a CT transmission scan is carried out using an external X-ray source (≈30-120 keV photons) and an attenuation map is generated based on the measured attenuation of the transmission

X-rays[74,75]. The attenuation coefficients obtained from the CT scan are then scaled to reflect the attenuation of the high-energy γ-photons (511 keV) and are applied to the emission data from the PET scans for more accurate attenuation correction[74].

After the raw data have been corrected from scattered and random coincidences, attenuation, as well as detector dead-time, the number of counts assigned to a LOR that connects a pair of opposite detectors is proportional to a line integral of radioactivity along that LOR. Parallel sets of line integrals create projections that are used for image reconstruction[69]. The reconstruction of an image from projections can either be analytical or iterative. Filtered-back projection, for instance, represents an analytical procedure to reconstruct images in 2D-mode and has been widely applied[63,76]. Even though iterative algorithms such as OSEM (Ordered subsets - Expectation maximization)[63,77] require longer computation times, the generated images reflect the radioactivity distribution more accurately. Thus, 3D-mode acquisition and iterative algorithms for image reconstruction are the method of choice in PET imaging supported by advances in information and detector technology[63,69].

The principle of radiotracers

The principle of radiotracers defines a radiotracer as a radiolabelled biologically active molecule that can be used to trace its natural analogue *in vivo* and hence provide information about biological processes in living organisms[78–81]. Regarding PET, a radiolabelled tracer usually consists of a pharmacophore or targeting moiety and a positron-emitting radionuclide[52]. The tracer principle is furthermore based on the fact that the chemical and biological properties of a certain molecule remain unchanged when a stable atom is replaced by a radionuclide of the same element[51,52]. For instance, replacing a ^{19}F-substituent of a certain drug molecule by the positron-emitting radioisotope ^{18}F will not change the behaviour

of this molecule in biological systems[82]. In addition to the isotopic exchange that transforms a natural biologically active molecule into a radiotracer with identical biological properties (isotope tracer), a radiotracer may be chemically different from its natural analogue (analogue tracer)[52]. For instance, ^{11}C-glucose is chemically identical to natural glucose whereas the ^{18}F-labelled glucose analogue 2-[^{18}F]fluoro-2-deoxy-glucose (^{18}F-FDG) is chemically different to natural glucose and hence behaves differently in biological environments. More precisely, ^{18}F-FDG is transported into cells facilitated by glucose transporters (GLUT) and subsequently phosphorylated in the 6-position by hexokinase to form ^{18}F-FDG-6-phosphate. ^{18}F-FDG-6-phosphate, however, is not further metabolised along the glycolytic pathway and thus accumulates inside cells in proportion to their glucose uptake[83]. That is the principle of ^{18}F-FDG PET[84].

Regarding non-invasive functional imaging techniques such as PET, the advantage of replacing a stable and non-radioactive isotope of a certain element by a positron-emitting radionuclide is that the detection of the latter is possible with high sensitivity compared to the stable isotope as the resulting highly energetic annihilation γ-photons may be detected outside the object using sensitive γ-detectors as described above. As a result, the physiological concentrations of radiotracers can be low enough to be considered as 'non-pharmacological', indicating that the tracer has no pharmacodynamic effects[85,86]. Hence, it is possible to gain information about PK parameters such as biodistribution, metabolic rates, retention in target tissue and clearance without disturbing the system or having a toxic effect in organisms[79,86,87]. In fact, PET is an emerging modality in the drug development process and can be used to obtain information about human PK in the early stage of human clinical trials in order to reduce costs and identify poor performing compounds early in the development process[82]. A PET tracer may be used to image a certain biological target or pathway. For that purpose, the tracer must meet specific requirements such as high target specificity, low non-specific binding and a distribution profile that depends on the concentration

of the target[52,88]. Furthermore, the PK of the tracer should match the physical half-life of the utilised radionuclide in order to image the biological process in the appropriate time frame and with an adequate signal-to-noise ratio[52,89]. For instance, the physical half-life of ^{89}Zr (78.41 h) matches the biological half-life of monoclonal anti-bodies ($T_{1/2}$ of days)[90] and hence is used to label monoclonal antibodies for PET studies[91]. Additionally, PET may depend on certain tracer-target interactions such as enzymatic conversion, e.g. phosphorylation in the case of ^{18}F-FDG or ^{18}F-FLT, binding to a specific transporter or receptor, or adsorption in case of [^{18}F]-NaF as a bone-seeking radiotracer[92].

Altogether, more than 500 PET probes are currently available[54] that address various biological targets. However, not every PET probe produces the desired results in terms of target specificity, for instance, and the radiochemical syntheses are often complex and not suitable for automated GMP production and hence human clinical applications[48]. In fact, tracer availability from a synthetic point of view is currently one of the main limitations in PET[48], despite inherent physical limitations such as spatial resolution[93]. The development of novel PET tracers using radionuclides such as ^{18}F, ^{11}C, ^{64}Cu and ^{89}Zr, as well as the improvement of the radiochemical accessibility of existing tracers is of great interest in current PET research[48,53,94].

This research project lies within the field of PET-radiochemistry with focus on the development of novel synthetic routes towards 2'-^{18}F-labelled nucleosides.

1.2.2 Common PET radionuclides

PET imaging can be performed using different positron-emitting radionuclides such as ^{11}C, ^{18}F and ^{15}O. Despite their physical characteristics such as half-life and positron energy, different radionuclides have mostly varying biological applications as they are linked to a certain class of biomolecules. For instance, ^{89}Zr and ^{64}Cu are commonly used for antibody labelling whereas ^{15}O-water or ^{13}N-

ammonia are suitable imaging probes for perfusion studies[95]. Antibody-labelling using either ^{89}Zr or ^{64}Cu-complexes is mostly performed using cycloaddition or 'click'-chemistry[96] to attach the ligand system to the antibody (Scheme **1.2**).[97]

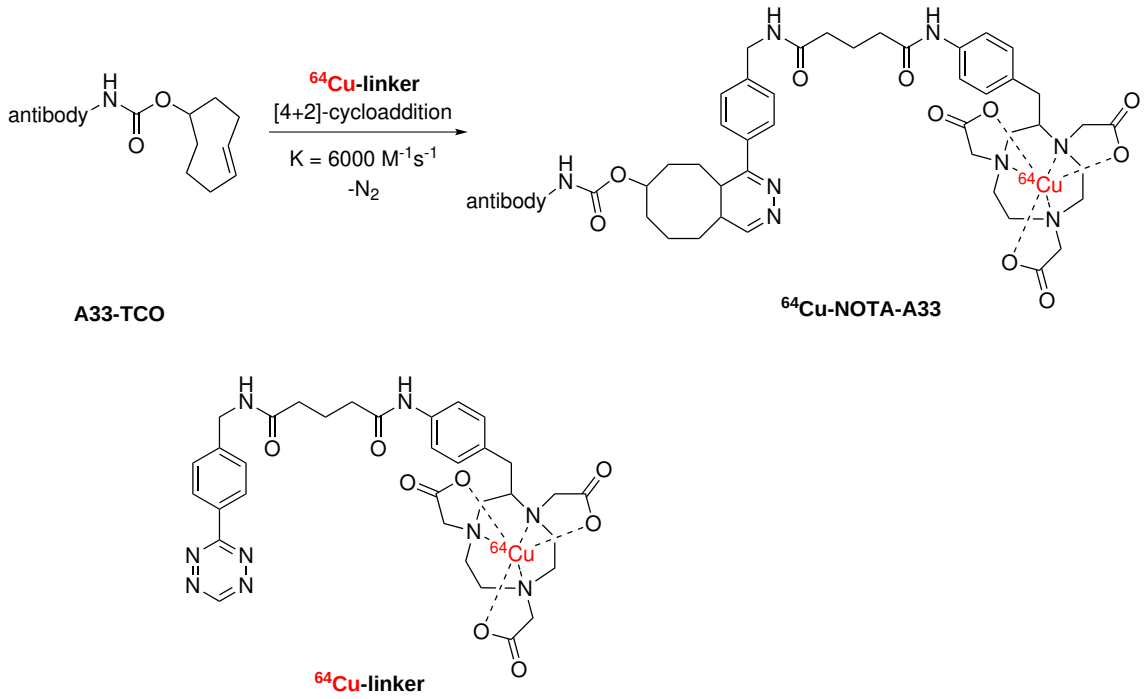

Scheme 1.2: Antibody-labelling with ^{64}Cu using a *trans*-cyclooctene moiety which is attached to the antibody and a tetrazine linked to the ^{64}Cu-complex. The inverse electron-demand Diels-Alder reaction generates nitrogen as a byproduct.

A recent report by Kung *et al.*[98] indicated that ^{64}Cu-labelled anti-CD99 antibody was capable of imaging glycoprotein CD99 expression in mouse xenographs (675 CD99^{+} xenographs). CD99 is a diagnostic marker in routine histologic staining for Ewing sarcoma cells. This study did not only demonstrate that ^{64}Cu-labelled antibody imaging is able to replace invasive histological methods but also that small lesions, otherwise only detectable by MRI but not with ^{18}F-FDG-PET, can be imaged. Similar experiments using ^{89}Zr instead will be repeated[98] as its longer half-life (78.4 h compared to 12.7 h for ^{64}Cu) allows imaging studies at a later time point after injection resulting in a higher signal-to-background ratio

due to clearance of non-bonded antibodies.

As immunotherapy is becoming an alternative and effective way in the treatment of various cancers and other diseases,[99]genetically engineered and ^{64}Cu-labelled minibodies (Mbs, reformatted antibody fragments) were used to image $CD8^+$ T cells in mouse models[100]. The detection and quantification of $CD8^+$ expression in $CD8^+$ lymphomas is critical in the evaluation of treatment response in cancer immunotherapy.

Until a decade ago, ^{124}I has found almost no recognition in PET mostly due to its complex decay pattern where only ≈23% of disintegrations lead to positron emissions[101,102]. However, its well-understood behavior *in vivo* as well as its long half-life of about 4.2 days allows imaging studies of slow and complex PK at low background noise[103]. Indeed, a study by Robinson *et al.* showed that ^{124}I-PET dosimetry using a genetically engineered ^{124}I-labelled antibody fragment was capable of imaging HER2 receptor tyrosine kinase expression in xenograft models, which is potentially useful for planning the treatment of HER2-positive cancer[104]. Another study performed by Jentzen *et al.* used ^{124}I-PET dosimetry in order to estimate therapeutic doses of ^{131}I-radiotherapeutics for patients with differentiated thyroid cancer[105].

Besides ^{18}F, ^{11}C is the most commonly used radionuclide in the early diagnosis of cancer and for monitoring treatment response[106] as its labelling chemistry became more advanced and clinically applicable[53] to a large variety of tracers with broad application[107]. ^{11}C-acetate (Figure **8**), for instance, was found to be superior to ^{18}F-FDG in imaging prostate cancer, especially at an early stage of the disease where ^{18}F-FDG-PET is quite unreliable mainly due to low glucose uptake of most prostate cancers[108]. Reets *et al.* used ^{11}C-methionine ([C-11]-MET, Figure **8**) PET, a marker for tumour uptake of amino acids and protein synthesis, in order to study its potential superior sensitivity to ^{18}F-FDG PET for determination of 3D-target volumes in head and neck cancers prior to

radiotherapy[109]. However, their study demonstrated that ^{18}F-FDG PET is actually superior over [C-11]-MET PET in terms of showing correct target volumes mainly due to low tissue discrimination of [C-11]-MET PET. This result is an example of the actual strength of ^{18}F-FDG PET and its clinical significance and is amongst other reasons explaining why ^{18}F-FDG PET is still the work horse in clinical cancer imaging[110].

^{11}C-acetate ^{11}C-methionine

Figure 8: Structures of the ^{11}C-labelled PET probes ^{11}C-acetate and [C-11]-MET.

Despite the range of different radionuclides potentially available for applications in PET imaging ^{18}F has an outstanding role due to certain properties.

1.2.3 Advantages of the ^{18}F radionuclide

According to the physical data shown above (Table **1**) the ^{18}F radionuclide combines a sufficient half-life for radiosynthesis with an optimal positron energy[111]. A half-life of around 110 minutes enables both an adequate time frame for tracer synthesis (radiofluorination as key synthetic step followed by deprotection and/or other chemical modifications) as well as a minimisation of the radiation dose to the patient[48,112]. Additionally, ^{18}F decays almost exclusively through positron emission (^{18}F decay mode to ^{18}O: β^+-emission (97%) and electron capture (EC, 3%))[113] that have a relatively low energy compared to positrons of other utilised PET radionuclides (see table **1**). Subsequently, the annihilation event into two antiparallel 511 keV γ-rays occurs on average closer to the point of emission which leads to a higher spatial resolution (≈1-2 mm for pre-clinical and 4-5 mm

for clinical PET)[48,52]. Another advantage of using ^{18}F in PET imaging is linked to the common use of fluorine as a bioisosteric substituent in drug molecules as an isotopic exchange does not effect either PK or PD of the bioactive fluorinated molecules[114].

1.2.4 ^{18}F-FDG PET

^{18}F-FDG (**7**) was first synthesised in 1978[115] and the first scans were performed by Shields *et al.*[116] in 1979 at the University of Pennsylvania. Currently, the glucose analogue ^{18}F-FDG (Figure **9**) is the most widely used PET tracer in oncology[117] ($\geq$90% of all scans), mainly for diagnosing and staging various types of cancers[118]. Cells of malignant tumours mainly use glycolysis and subsequent lactic acid fermentation ('Warburg Effect')[119] for the rapid production of energy equivalents needed due to upregulated cell proliferation and cell division.

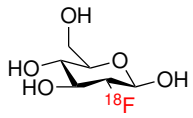

7

Figure 9: Structure of the widely used glucose analogue ^{18}F-FDG (**7**).

The chemically modified 2-position of the pyranose ring does not significantly impact the affinity of ^{18}F-FDG for both the glucose transporter and cytosolic hexokinase[114]. The latter is responsible for intracellular 6-*O*-phosphorylation which traps the tracer inside the cell since charged molecules are not capable of passing the cell membrane. Phosphofructose isomerase, however, does not tolerate the substitution at the 2-position which is why ^{18}F-FDG-6-phosphate remains unmetabolised in the cytosol[114]. Both, increased glucose uptake and phosphorylation are important parameters that distinguish malignant tumour cells from most normal body tissue apart from inflammatory lesions of necrotic

cells, T-cells, bone marrow and the brain, for instance[120]. Hence, ^{18}F-FDG PET lacks specificity due to cells that carry out body functions that require high glucose metabolism. For instance, small lesions located in the bone marrow are not detectable with ^{18}F-FDG-PET due to high background signal and hence require more specific approaches[100]. The development of novel tumour and tissue specific radiotracers is indeed of great interest to current research[48,88] as current clinical practice still depends on a combination of different invasive and non-invasive imaging techniques to fully understand tumour characteristics.

1.2.5 ^{18}F-labelled nucleoside analogues used in PET imaging

As this research project focuses on novel radiosynthetic routes towards ^{18}F-labelled nucleosides, the following section will briefly introduce selected nucleoside-based PET probes by highlighting their application and main limitations.

Overview

As nucleoside analogues such as gemcitabine, clofarabine, and cytarabine are widely used in the treatment of cancer[21,121] (about one in six small molecule anticancer agents are nucleoside-based antimetabolites)[122], ^{18}F-labelled nucleoside PET probes are considered capable of providing a deeper understanding of drug behaviour *in vivo* and important imaging tools towards personalised treatment approaches with nucleoside-based chemotherapy[123]. The multiplicity of interactions that nucleosides undergo in biological environments and the resulting lack of selectivity of nucleoside analogues in cancer treatment[122] makes nucleoside based PET imaging highly desirable for both clinicians and patients with the prospect of individualised nucleoside based chemotherapy[124]. Figure **10** shows structures of some of the most commonly used ^{18}F-labelled nucleosides.

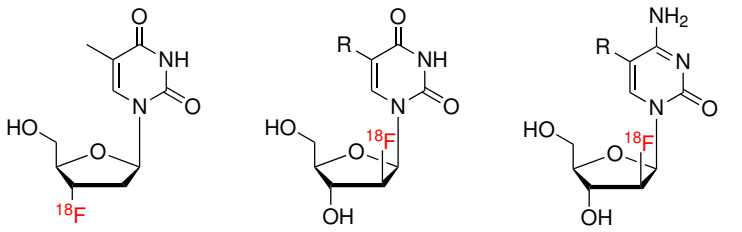

^{18}F-FLT (**8**)

R=H, ^{18}F-FAU (**9**)
R=Me,^{18}F-FMAU (**10**)
R=Et, ^{18}F-FEAU (**11**)
R=F,^{18}F-FFAU (**12**)
R=Br, ^{18}F-FBAU (**13**)
R=I,^{18}F-FIAU (**14**)

R=H,^{18}F-FAC (**15**)
R=I,^{18}F-FIAC (**16**)

Figure 10: Selected ^{18}F-labelled nucleosides (**8-16**) currently used in clinical diagnostics and ^{18}F-PET research.

Although several 2'- and 3'-^{18}F-labelled nucleosides are of great importance as PET probes in clinical diagnostics and PET research[10,125] ^{18}F-FLT is currently the only 2'- or 3'-^{18}F-labelled nucleoside based PET tracer that is routinely used in clinical practice.

The first nucleoside-based PET tracer ^{11}C-thymidine[126] was developed in the early 70s. However, ^{11}C-thymidine was substituted by the much more convenient PET tracer ^{18}F-FLT (**8**) due to both the longer half-life of the ^{18}F radionuclide and an improved biostability *in vivo*[127]. ^{18}F-FLT is synthesised using automated module systems and produced under good manufacturing practice (GMP) guidelines[128,129] for clinical use.

^{18}F-FLT

As a successor of 2-^{11}C-thymidine[126] ^{18}F-FLT shows a higher biostability[127] *in vivo* as it is not a substrate for thymidine phosphorylase. ^{18}F-FLT is accessible via an effective radiochemical synthesis in good RCY (19.8%, decay-corrected) and purity suitable for human production under GMP guidelines[128,129]. Furthermore, the longer half-life of the ^{18}F radionuclide (110 min) simplifies synthesis, quality control and the imaging process significantly (see section **1.4.1**). Hence,

^{18}F-FLT is currently commonly used for the early detection of various cancers[130] and the evaluation of treatment response[131]. After cell uptake by passive diffusion or facilitated transport ^{18}F-FLT is 5'-phosphorylated by TK-1, the key enzyme in the salvage pathway of DNA synthesis, which traps the nucleoside monophosphate inside the cell[132]. This enzyme is significantly upregulated in malignant tissue compared to quiescent cells[133] as the majority of the malignant cell population is in the S-phase of the cell cycle. Thus, ^{18}F-FLT is used as a proliferation marker in clinical oncology. The nucleoside triphosphate ^{18}F-FLT-TP, however, is not incorporated into DNA due to the absence of the 3'-OH group but rather acts as a chain terminator[130], which is why ^{18}F-FLT is not a marker for DNA synthesis[134]. This is a limitation as tumour cells which utilise the *de novo* thymidine salvage pathway via TS catalysed dUMP methylation[135] give a false negative response. However, ^{18}F-FLT PET provides in many cases more distinct information compared to ^{18}F-FDG PET, especially in high-grade tumours where it appears to be more predictive of treatment response and survival[127,136].

^{18}F-FAU

The treatment of colorectal, breast as well as head and neck cancer with thymidylate synthase (TS) inhibitors such as 5-fluorouracil (5-FU)[137] or floxuridine[138] is mainly compromised due to over-expressed TS[139]. As a substrate of TS ^{18}F-FAU seems suitable for imaging TS expression and hence treatment prediction for TS inhibitors such as 5-FU or FAU, respectively. Furthermore, a study[140] using ^{18}F-FAU as a biomarker for the incorporation of the metabolite ^{18}F-FMAU into DNA indicated that FAU could indeed serve as a prodrug in patients with high TS expression. In contrast, however, Sun *et al.*[141] found that ^{18}F-FAU has limited use as a proliferation marker due to its low affinity to thymidine kinase 1 (TK-1) which is even more significant at low tracer concentrations.

^{18}F-FMAU

Unlike ^{18}F-FLT, ^{18}F-FMAU is significantly incorporated into DNA[130] and thus a superior PET probe for proliferation as DNA synthesis is a much more accurate parameter for cellular proliferation than simply TK-1-mediated phosphorylation[142]. *In-vitro* studies[143,144] demonstrated that FMAU retention is proportional to its DNA-incorporation and cytotoxicity. PET studies in dogs[144] showed that ^{18}F-FMAU uptake in highly proliferating tissue such as bone marrow and testicles is significantly higher than in normal tissue indicating that ^{18}F-FMAU might be a strong candidate for imaging DNA synthesis *in vivo*. Indeed, human studies with brain and prostate cancer patients using ^{18}F-FMAU[145] were carried out showing that ^{18}F-FMAU is a reliable marker of DNA-synthesis/cell proliferation with a significantly shorter imaging period (5-11 min, instead of 50-60 min in the case of ^{18}F-FDG).

^{18}F-FAC

Studies reported by Lee *et al.*[124] and Nathanson *et al.*[146] suggest that the developed PET probe ^{18}F-FAC is a promising candidate to determine treatment response to nucleoside analogues based chemotherapy. In fact, ^{18}F-FAC has been used in a non-invasive tumour response study[25] with gemcitabine as the chemotherapeutic agent[147]. Since ^{18}F-labelled gemcitabine is not available as a PET probe, ^{18}F-FAC was expected to reveal some of the unknown metabolic parameters such as cell uptake and deamination and whether or not the outcome of a gemcitabine-based chemotherapy could be predicted. FAC as well as gemcitabine are specific substrates for both deoxycytidine kinase (dCK) and deoxycytidine deaminase (dCDA) which are rate-limiting enzymes in the nucleoside salvage pathway. Hence, ^{18}F-FAC PET may provide a powerful and non-invasive clinical tool to examine potential resistance mechanisms of tumours against these drugs caused by overexpression of deactivating enzymes such as dCDA[147]. Further-

more, lymphoid organs and related immune activation mechanisms have been studied using ^{18}F-FAC PET[16].

1.3 Synthesis of non-radioactive fluorinated nucleosides

With regard to this research project, the following section will focus on the non-radioactive synthesis of 2'- and 3'-fluorinated nucleosides.

1.3.1 Early-step fluorination

The fluorine substituent can be incorporated either early or late during a multi-step synthesis. One approach is to introduce the fluorine substituent before the appropriate base moiety is attached. This is realised by either using fluorine containing starting materials or an early-step fluorination. The *Eli Lilly* synthesis[28,148] of gemcitabine is based on Hertel's general method[149] to synthesise 2'-deoxy-2',2'-difluoro-D-ribofuranosyl nucleosides (Scheme **1.3**). This multi-step synthesis[28] is one among several other approaches to give gemcitabine[28] and starts with the difluorinated precursor ethyl-bromodifluoroacetate **18** and thus exemplifies the use of fluorine containing starting materials.

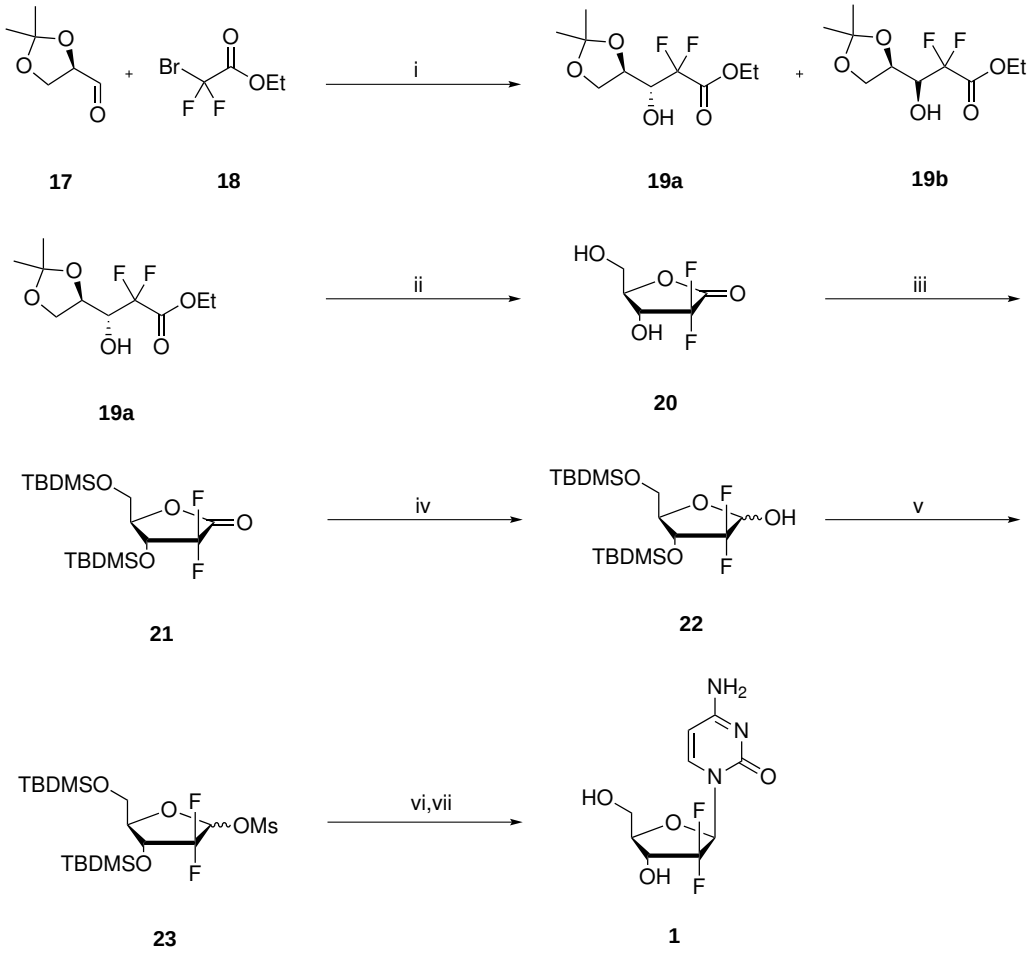

Reagents and conditions: **i)** Zn, THF/Et_2O, reflux, 1 h, 65% (a); **ii)** Dowex 50W-X12, r.t., 4 d, 95% **iii)** TBDMSOTf, 2,6-lutidine, DCM, 12 h, 92%; **iv)** DIBAL-H, toluene, -78°C, 2 h, 79%; **v)** MsCl, Et_3N, DCM, RT, 3 h, 90%; **vi)** bis(trimethylsilyl)-N-acetylcytosine, TMSOTf, DCE, reflux, 15 h; **vii)** AG 50W -X8, MeOH, r.t., 12 h, 10% (β–anomer, after both steps).

Scheme 1.3: Hertel's method for the synthesis of gemcitabine **1**.

The main disadvantage of this approach is the lack of diastereoselectivity when the base moiety is attached and thus includes many separation steps using HPLC. The improved modern synthesis of **1** at least avoids one isomeric separation step due to the preparation of the *gem*-difluorolactone using the electrophilic fluorination reagent N-fluorobenzenesulfonimide (NFSI) and the corresponding monofluorolactone **25**. The latter is an important intermediate in the stereoselective synthesis of clofarabine[148] **2** and thus represents an example for early-step fluorination (Scheme **1.4**).

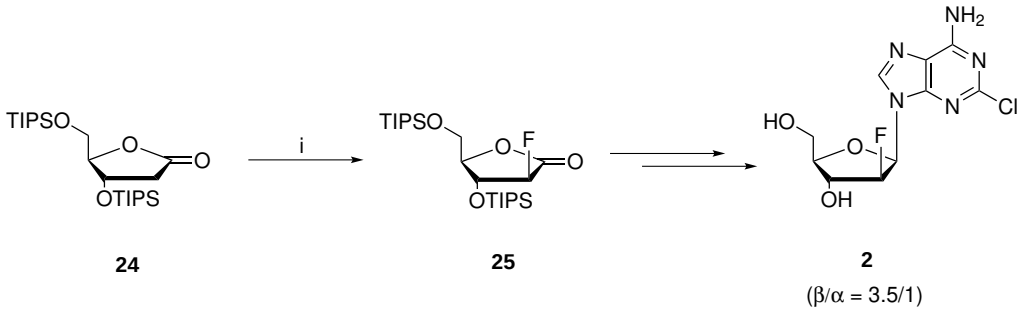

Scheme 1.4: NSFI-mediated fluorination step within the stereoselective synthesis of clofarabine **2**.

Due to synthetic challenges in ^{18}F-radiochemistry primarily caused by the half-life of the ^{18}F radionuclide, late-stage fluorination as an alternative strategy for the introduction of a fluorine substituent will be presented in the following section.

1.3.2 Late-stage fluorination

Organic deoxofluorination agents

Due to a high demand for powerful fluorination methods in pharmaceutical and life sciences, deoxofluorination agents were developed that provide the accessibility of a variety of fluorinated organic compounds including nucleoside analogues.

Initially, it was found that the highly toxic and corrosive inorganic gas SF_4 enabled deoxofluorinations of hydroxy-, carbonyl-, and carboxylic acid compounds into the monofluoro, difluoromethylene, and trifluoromethyl derivatives, respectively[150]. Regarding laboratory safety restrictions and common principles in organic chemistry such as functional group interconversion (FGI), new organic fluorination agents should be able to combine safe handling with efficient and controllable reaction conditions. This led to the development of organic fluorination agents with enhanced stabilities such as DeoxoFluor (**26**, bis(2-methoxyethyl)-aminosulfur trifluoride)[151], DAST (**27**, diethylaminosulfur trifluoride)[152], Xtal-

Fluor E (**28**, (diethylammino)difluorosulfonium tetrafluoroborate) and XtalFluor M (**29**, difluoro(morpholino)sulfonium tetrafluoroborate)[151,153] (Figure **11**).

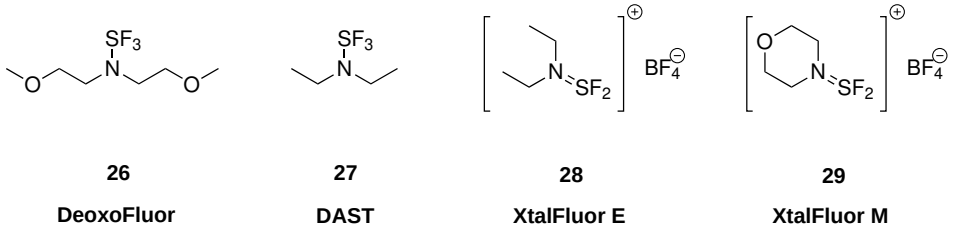

Figure 11: Organic fluorination agents.

These SF_4-based fluorination agents lead to deoxofluorinations according to the following general mechanism[20] (Scheme **1.5**).

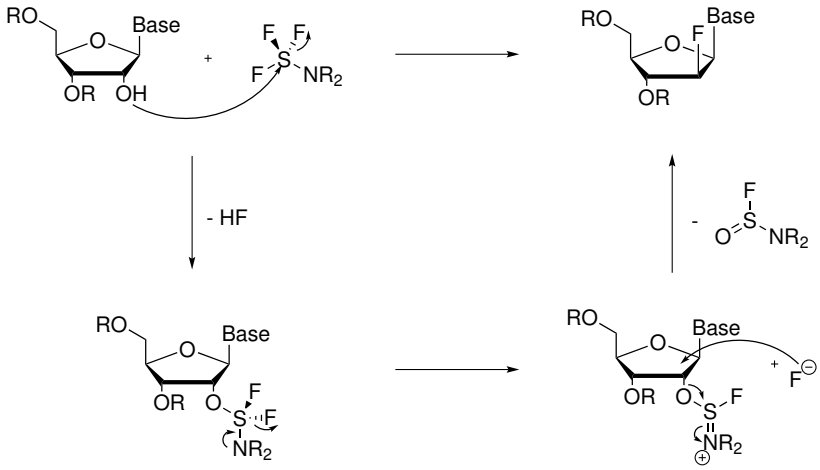

Scheme 1.5: General mechanism of deoxofluorination using SF_4-based fluorination agents.

As mentioned above DAST enables important functional group interconversions that have already been applied to the synthesis of nucleoside analogues[154,155] such as 2'-fluoro-2'-deoxyuridine (**31** ,2'-FU) (Scheme **1.6**).

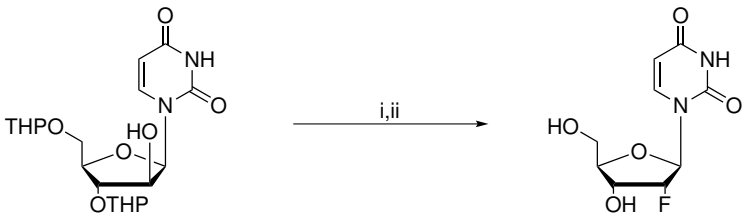

30 **31**

Reagents and conditions: **i)** DAST, pyridine, DCM, 40°C, 12 h, 60%; **ii)** HCl, MeOH.

Scheme 1.6: DAST-promoted deoxofluorination towards 2'-FU (**31**).

Even though widely used in deoxofluorination reactions with a broad spectrum of different substrates[156] DAST was found to be thermally unstable and highly explosive. Furthermore, DAST generates corrosive HF and often olefinic elimination side products. The organic salts XtalFluor^{TM} E (**28**) and M (**29**) allow safer handling as well as high chemo - and stereoselectivities under specific reaction conditions, whereas the reaction mechanism remains the same[153]. Even deoxodifluorinations of aldehydes and ketones towards difluoromethylene compounds are accessible in good yields with XtalFluor reagents[153] (Scheme **1.7**).

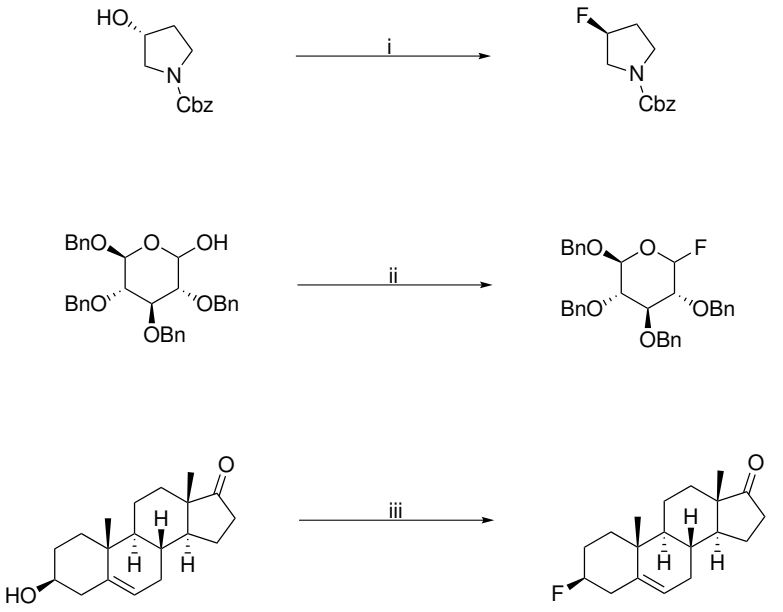

Reagents and conditions: **i)** XtalFluor-M, Et_3N/HF, Et_3N, DCM, -78°C - r.t., 3h, 80%; **ii)** XtalFluor-M, Et_3N/HF, DCM, r.t., 1.5h, 90%; **iii)** XtalFluor-E, Et_3N/HF, DCM, r.t., 16h, 77%.

Scheme 1.7: XtalFluor E (**28**) and M (**29**) enable deoxofluorination reactions with high chemoselectivities in good yields.

A more heat-stable alternative for various deoxofluorinations was reported by using Fluolead[157] (**32**). Several hydroxy- and carbonyl compound could be converted to the corresponding fluoro-, and difluoromethylene derivatives, respectively (Scheme **1.8**).

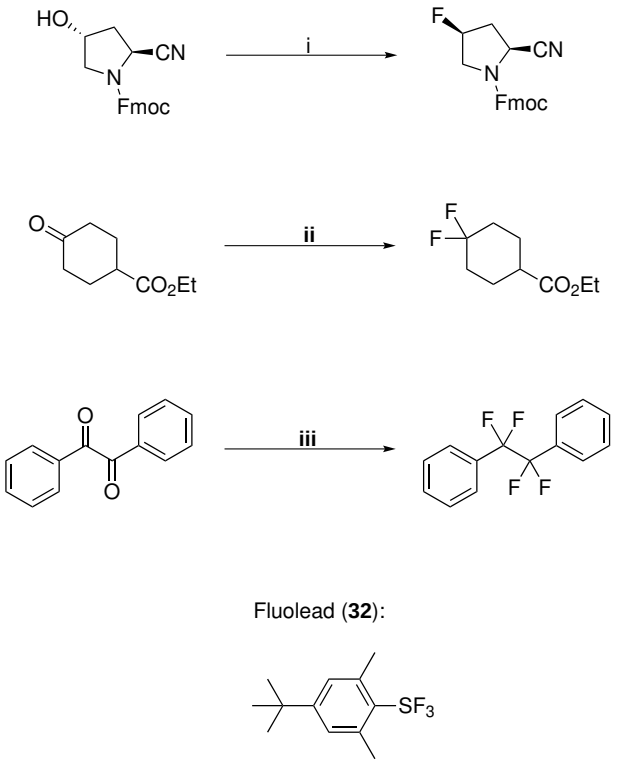

Reagents and conditions: **i) 32** (1.5 eq.), DCM, 0°C 1 h, then r.t., 24 h, 85 %; **ii) 32** (1.5 eq.), py/HF (0.4 eq.), DCM, 0°C - r.t., 3 h, 81 %; **iii) 32** (3 eq.), py/HF (1.7 eq.), toluene, 60°C, 12 h, 88 %.

Scheme 1.8: Fluolead-mediated deoxofluorinations.

Deoxodifluorination of the 2'- and 3'-position of nucleoside analogues

Deoxodifluorination of 5'-O-trityl-3'-ketothymidine **33** to give 5'-O-trityl-3'-deoxy-3',3'-dilfluorothymidine **34** has been reported[158] as a slow transformation with low yields of the *gem*-difluorinated product using DAST (Scheme **1.9**).

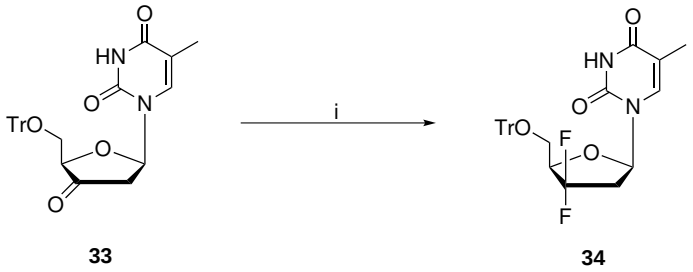

33 **34**

Reagents and conditions: **i)** DAST (3.0 eq.), DCM, r.t., 10 h, 12%

Scheme 1.9: DAST-mediated 3'-deoxodifluorination of 3'-keto precursor **33**.

Regarding the translation towards a deoxodifluorination of an appropriate 2'-keto precursor Kjell *et al.*[159] reported that a reasonable conversion rate could be observed when pyridine/HF was used in addition to DAST. Conversion of the triacetylated precursor **35** using DAST and pyridinium/HF in dry DCM at r.t. gave the *gem*-difluoro derivative in 80% yield after 24 h. Subsequent basic hydrolysis furnished gemcitabine (Scheme **1.10**, top). The study states the indispensable need for pyridine/HF (py/HF) as the first reagent. Hence, a possible reaction mechanism may start with a fluoride anion (from py/HF) to generate an oxyanion at the 2'-position that subsequently attacks DAST to form a leaving group that can in turn be substituted by a second fluoride anion (Scheme **1.10**, bottom).

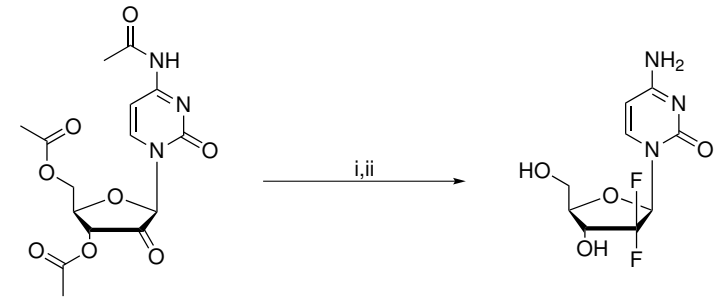

35 **1**

Reagents and conditions: **i)** DAST/pyridine/HF, DCM, 2 d, -78°C - r.t.; **ii)** NaOMe/MeOH, relfux, 1 h.

Mechanism:

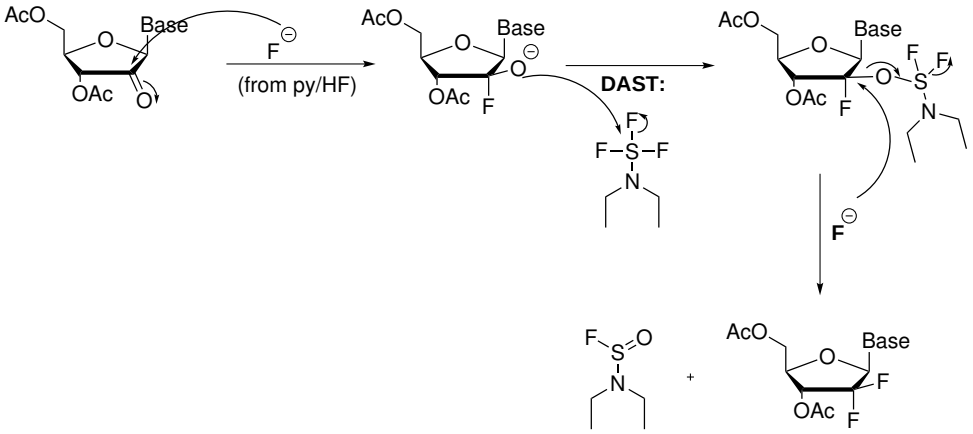

Scheme 1.10: Top: DAST promoted deoxodifluorination of **35** presents a convenient method for the synthesis of *gem*-difluorinated compounds with commercial interest such as gemcitabine (**1**). Bottom: The mechanism explains why an additional fluoride source is needed. Fluoride (from pyridine/HF) attacks the 2'-carbonyl carbon first and forms an oxyanion which in turn reacts with DAST to form a leaving group that can be replaced by another fluoride anion.

The current literature does not provide a broad range of approaches concerning late-stage deoxodifluorinations and thus limits assessments regarding potential applications in radiochemistry. Even though ^{18}F-DAST has been successfully synthesised[153,160] the application in radiosynthesis remains difficult[161–163].

Reactive fluoride salts

Cyclic 2,2'-anhydro precursors are convenient precursors for nucleophilic late-stage fluorination reactions[164,165]. Fluoride salts such as KF, CsF or tetrabutylammonium fluoride (TBAF) can be used as a source for nucleophilic fluoride.

However, the fluoride anion is a strong hydrogen bond acceptor and strong Lewis base as well as a weak nucleophile so that extensive drying processes and anhydrous reaction conditions are indispensable in order to enhance the nucleophilicity of the fluoride anion and obtain reasonable conversion rates[166].

The first late-stage fluorination towards a 2'-fluorinated nucleoside was successfully reported in 1963[167] by using anhydrous HF (Scheme **1.11**). Direct fluorinations of 2,2'-anhydro-1(β-D-arabinofuranosyl)nucleosides **36-38** were carried out in a stainless steel bomb.

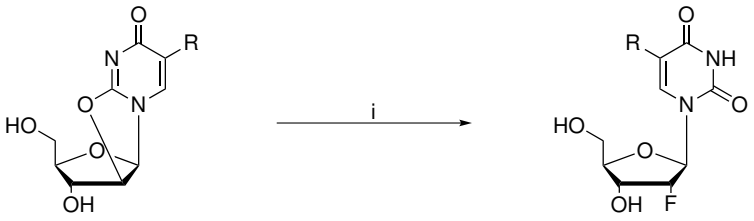

36 R = H
37 R = F
38 R = Me

31 R = H
39 R = F
40 R = Me

Reagents and conditions: **i)** anh. HF, dioxane, 115-118°C, 18 h, 19-45%

Scheme 1.11: First fluoride-mediated ring-opening reaction of 2,2'-anhydro compounds **36-38** using anhydrous HF.

Mengel *et al.*[168] reported in 1978 the successful synthesis of 2'-deoxy-2'-fluorocytidine (FC) **42** via 2,2'-anhydro precursor **41** under much milder conditions using an anhydrous DMF/KF/crown-ether mixture for the nucleophilic ring-opening reaction (scheme **1.12**).

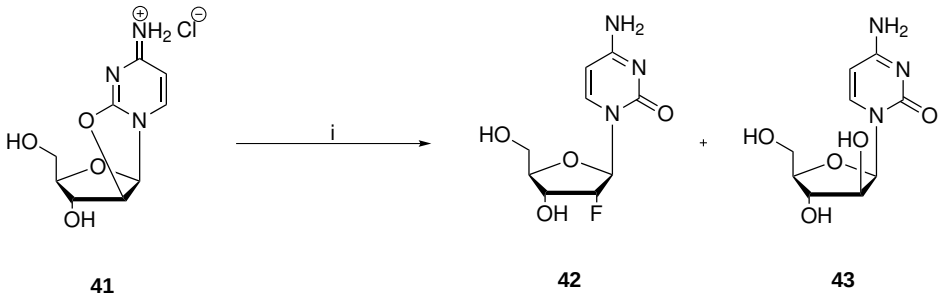

41 **42** **43**

Reagents and conditions: **i)** KF, [18]crown-6, DMF, 120°C, 4 h, 40%.

Scheme 1.12: Fluoride-mediated ring-opening reaction of 2,2'-anhydrocytidine hydrochloride **42** under milder anhydrous conditions.

Even under strictly anhydrous conditions after azeotropic drying with benzene the corresponding hydrolisation product **43** was still obtained illustrating the importance of anhydrous reaction conditions for nucleophilic fluorination reactions.

Crown-ethers and cryptants such as [18]crown-6 or kryptofix-222 (K_{222}) are widely used not only in organic synthesis but also in radiosynthesis due to their cation chelation properties and the generation of a 'naked' fluoride anion[169]. The nucleophilicity of the fluoride anion can be additionally enhanced in polar aprotic solvents. Altogether, anhydrous conditions, polar aprotic solvents and chelating additives such as K_{222} are used in order to provide a nucleophilic fluoride anion.

Even though widely used in radiosynthesis, the incorporation of non-radioactive fluoride into nucleosides using nucleophilic late-stage fluorination has only been rarely reported. The synthesis of fluorinated nucleosides is rather carried out using either early-stage fluorination or late-stage deoxofluorination procedures based on DAST (**27**).

However, Alauddin and co-workers[170] reported the synthesis of FMXU **45** by late-stage fluorination of triflate precursor **44** using a 1 M TBAF solution in dry MeCN (Scheme **1.13**). They further reported similar conditions using [^{18}F]TBAF for the subsequent radiosynthesis of ^{18}F-FMXU.

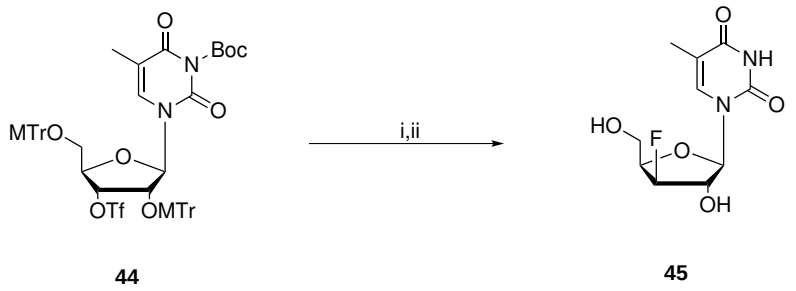

44 **45**

Reagents and conditions: **i)** 1 M TBAF/THF, MeCN, 72-74°C, 20 min, 46%; **ii)** 1 M HCl/MeOH, reflux, 10 min, 70%.

Scheme 1.13: Late-stage fluorination using an anhydrous TBAF/THF solution to give FMXU **45**.

1.4 Radiosynthesis using [^{18}F]fluoride

This section will give an overview of relevant radiosynthetic approaches for the synthesis of 2'- and 3'-^{18}F-labelled nucleosides using [^{18}F]fluoride after a brief introduction to ^{18}F-radiochemistry with ^{18}F-FDG as the most widely used PET tracer. Furthermore, the production of [^{18}F]fluoride, radiochemical analysis, automated radiosynthesisers as well as radiation safety will be briefly introduced at the end of this section.

The radiochemical synthesis of tracers for applications in PET imaging began with the radiochemical synthesis of ^{18}F-FDG[169] and subsequent cerebral glucose imaging in humans in 1978 by Phelps *et al.*[115,116].

Despite the biological principle of ^{18}F-FDG PET as outlined above (Section **1.2.4**), the broad application of ^{18}F-FDG PET in clinical oncology today is mainly due to its highly advanced radiochemical synthesis with radiochemical yields (RCYs, activity of the final tracer divided by the starting activity) between 50-80% (decay-corrected) and specific activities $\geq$350 GBq/μmol using a broad range of automated synthesis modules under good manufacturing practice (GMP) guidelines for human clinical applications[111,171–173] (Scheme **1.14**).

46 ^{18}F-FDG (**7**)

Reagents and condtions: **i)** [^{18}F]fluoride/K_{222}/K_2CO_3, MeCN, 85°C, 3 min, **ii)** NaOH.

Scheme 1.14: Radiochemical synthesis of ^{18}F-FDG using mannose triflate **46** as precursor. Nucleophilic substitution of the triflate leaving group with [^{18}F]fluoride gives the [^{18}F]fluorinated protected intermediate which is converted to ^{18}F-FDG via basic hydrolysis. Cartridge purification and sterilisation give ^{18}F-FDG for clinical applications.

The complex and interdisciplinary nature of PET might be one of the main reasons why the development of novel and more specific PET probes is resource-intensive and time-consuming[94]. Another challenge of a more synthetic nature is certainly the time limitation in synthesis, purification and quality control of PET probes due to the radiochemical decay of the utilised radionuclides. However, progress in information technology and process automation allowed the development of innovative automated radiosynthesisers that enabled automated routine production of several new tracers[174].

Multi-step syntheses towards non-radioactive fluorinated target compounds utilise either fluorine containing starting materials or early-stage fluorinations[148] due to the high C-F binding energy and the resulting chemical stability. However, considering radioactive decay and safety restrictions, radiofluorinations have to be carried out at a later stage of the synthesis of ^{18}F-labelled tracers. Pharmaceutical standard radiolabelled tracers should be synthesised and purified within three half-lives of the utilised radionuclide[53]. These restrictions led to the development of new synthetic methods and the increased implementation of automated synthesisers and modern synthetic techniques such as microwave assisted and flow synthesis[112].

1.4.1 Radiosynthesis of 2'- and 3'-^{18}F-labelled nucleosides

Early-stage radiosynthesis implies that radiofluorination is carried out at the sugar moiety before the appropriate nucleobase is attached at the 1-position of the ribose moiety. Late-stage radiofluorination on the other hand uses an intact and activated (protected) nucleoside for radiosynthesis[85].

Early-stage radiofluorination

Several 5-substituted uridine - and cytidine-based 2'-^{18}F-arabino nucleosides have been synthesised via early-step radiofluorination within the last 15 years. The general approach starts with a [^{18}F]fluoride-mediated nucleophilic substitution of a leaving group at the 2-position of a protected ribose moiety followed by a base coupling reaction that furnishes the desired nucleoside.

In 2003, Mangner *et al.*[175] reported the radiochemical synthesis of the arabino nucleosides ^{18}F-FAU, ^{18}F-FMAU, ^{18}F-FBAU, and ^{18}F-FIAU based on the route presented below with a synthesis time of ≈180 min (Scheme **1.15**).

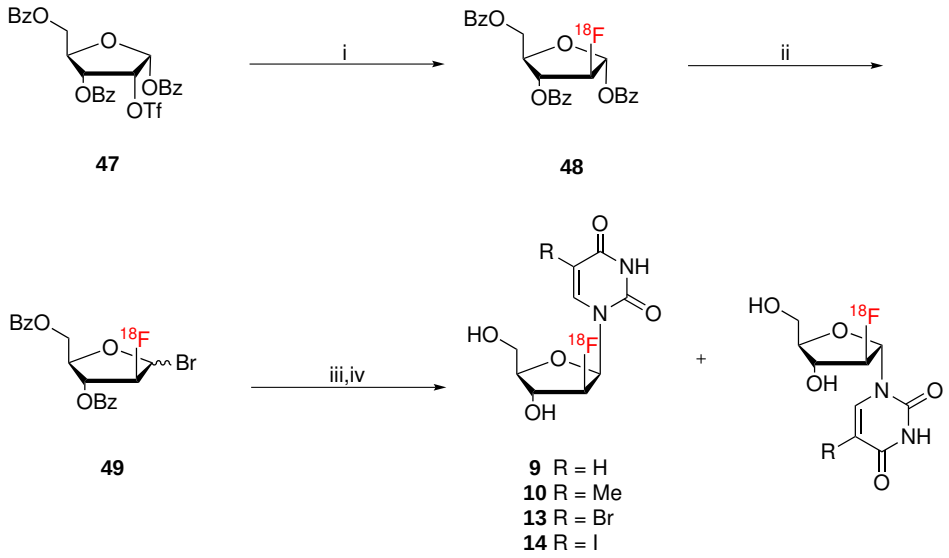

Reagents and conditions: **i)** [^{18}F]fluoride/K_{222}, DMF, 150°C, 5 min, 70-80%; **ii)** HBr/AcOH, DCM, 125°C, 15 min, 80-90%; **iii)** 2,4-bis-O-(trimethylsilyl)uracil (**9**), 2,4-bis-O-(trimethylsilyl)thmidine (**10**), 2,4-bis-O-(trimethylsilyl)-5-bromouracil (**13**), 2,4-bis-O-(trimethylsilyl)-5-Iodouracil; (**14**), $CHCl_3$, 150°C, 30 min, 70-80%; **iv)** NaOMe/MeOH, MeCN, 20°C for 10 min, 80-90%.

Scheme 1.15: Radiosynthesis of uridine-based arabino nucleosides. Reported RCYs (decay-corrected) of the desired β-isomer: 34.7±11.2% (^{18}F-FAU), 42.1±2.1% (^{18}F-FMAU), 40.0±3.1% (^{18}F-FBAU), and 34.6±7.3% (^{18}F-FIAU).

The protected triflate precursor **47** reacted first with [^{18}F]fluoride/kryptofix to perform the nucleophilic substitution reaction at high temperatures. The 2-^{18}F-labelled compound **48** contains the ^{18}F-substituent in the right stereochemical orientation. Bromination and subsequent condensation with the appropriate 2,4-bis-*O*-(trimethylsilyl)pyrimidines produced mixtures of β- and α-isomers (β/α=6.6-8.6) of the nucleosides depending on reaction solvent and temperature as reported by Howell *et al*[176]. Deprotection was followed by semi-preparative HPLC purification which enabled the separation of the isomers. The labelling reactions were carried out using a remote-controlled reactor.

Even though the nucleoside-based radiotracers were obtained in good RCY and high purities, this synthetic approach could not be used for human tracer production according to GMP regulations[177] mostly due to its complexity. In 2011, Cai *et al.*[178] synthesised the uridine-based nucleosides ^{18}F-FAU, ^{18}F-FEAU,

^{18}F-FFAU, ^{18}F-FBAU and ^{18}F-FIAU in reasonable RCYs (4.1-10%) with high radiochemical purity (≥99%) and specific activities (380±35 Ci/mmol) using a novel one-pot strategy that may simplify their use in clinical routine production. The main advantages of this approach were the removal of the bromination step and the shorter synthesis time (≈150 min) (Scheme **1.16**). However, the RCYs and the selectivity for the desired β-isomers were lower.

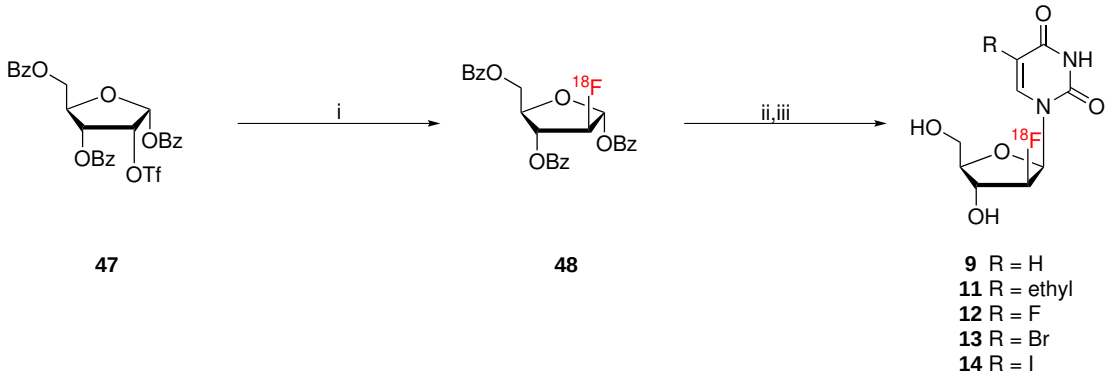

Reagents and conditions: **i)** [^{18}F]fluoride/K_{222} or [^{18}F]TBAF, MeCN, 85°C, 20 min; **ii)** 2,4-bis-O-(trimethylsilyl) uracil (**9**), 2,4-bis-O-(trimethylsilyl)-5-ethyluracil (**11**), 2,4-bis-O-(trimethylsilyl)-5-fluorouracil (**12**), 2,4-bis-O-(trimethylsilyl)-5-bromouracil (**13**), 2,4-bis-O-(trimethylsilyl)-5-Iodouracil (**14**), HMDS, TMSOTf, MeCN, 85 °C, 1 h, **iii)** KOMe, MeOH.

Scheme 1.16: Advanced one-pot radiosynthesis of pyrimidine nucleosides gave almost a 1:1 mixture of the α- and β-isomers. The RCYs (decay-corrected, n = 4) of the desired β-isomers were reported as 5.4±1.0% (^{18}F-FAU), 4.1±0.8% (^{18}F-FEAU), 5.5±0.9% (^{18}F-FFAU), 8.0±2.5% (^{18}F-FBAU) and 9.9±0.4% (^{18}F-FIAU).

Furthermore, Zhang *et al.* reported an improved radiosynthesis of the nucleoside derivatives ^{18}F-FIAU, ^{18}F-FMAU and ^{18}F-FEAU in terms of RCY by using a microwave assisted synthesis. Their findings led to the conclusion that the TMSOTf-catalysed coupling reaction of the sugar moiety and the protected base can be accelerated by microwave assisted heating.

Despite significant improvements of the conditions of these labelling reactions and the automated production of these uridine-based arabino nucleosides, their use in routine clinical applications remains challenging.

Radu *et al.*[16] reported the radiosynthesis of the cytidine-based nucleoside ^{18}F-FAC (**15**) in good RCY (20-30%, decay-corrected) and high radiochemical purities (≥99%). The synthesis scheme (Scheme **1.17**) was similar to the route towards 2'-^{18}F-labelled uridine-based nucleosides presented above. Hence, radiofluorination was carried out first followed by bromination of the 1-position of the sugar moiety and subsequent base coupling using the O- and N-TMS-protected pyrimidine base. Amaraesekera *et al.*[179] developed a radiochemical approach to give ^{18}F-FAC using a newly developed radiosynthesis module with high-pressure capabilities that furnished the tracer ^{18}F-FAC in high RCYs (39±5%, decay-corrected, n = 13), high radiochemical purities (≥99%) and specific activities (≥37 GBq/μmol) with a synthesis time of 240 min.

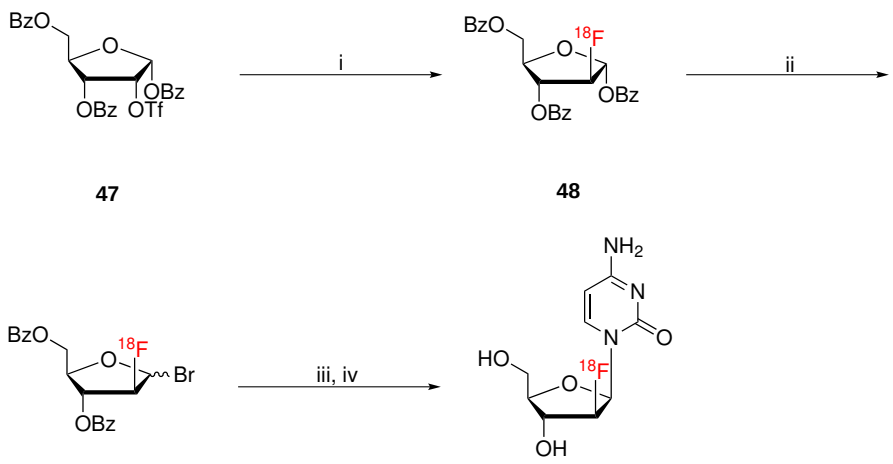

Reagents and conditions: **i)** [^{18}F]fluoride, K_{222}, DMF, 165°C, 15 min; **ii)** 30% HBr/AcOH, dichlorethane, 80°C, 10 min; **iii)** bis(trimethylsilyl)cytosine, dichlorethane, 160°C, 30 min; **iv)** NaOMe/MeOH, 100°C, 5 min

Scheme 1.17: Current radiochemical approach to give ^{18}F-FAC.

The same synthetic route was tested by Lazari *et al.*[180] to synthesise the ^{18}F-labelled nucleoside analogues ^{18}F-FAC and ^{18}F-FMAU using a specifically

developed radiosynthesiser. In case of ^{18}F-FAC, a decay-corrected RCY of 31±5% (n = 6) with specific activities between 37-44 GBq/μmol were reported. The synthesis time was 160 min. This method is currently used to produce ^{18}F-FAC for clinical trials to image the deoxycytidine kinase (dCK)-status of cancer patients carried out by Michael Phelps and co-workers*. Even though this method is fully automated further studies have to show whether this method will be applicable for clinical routine production.

Late-stage radiofluorination

A reproducible and efficient late-stage radiofluorination towards 2'- and 3'-labelled nucleoside analogues may enable a faster transfer to routine production of these PET probes[177]. In 2000, Machulla *et al.*[165] reported the synthesis of ^{18}F-FLT (**8**) via both the unprotected anhydro thymidine precursor **50** and the 5'-O-DMT-protected precursor **51** (Scheme **1.18**). Different radiochemical yields were reported for precursor **50** (5.3±1.2%) and precursor **51** (14.3±3.3%) with a synthesis time of 90 min in case of precursor **51**.

*http://sofiebio.com/products/probes/

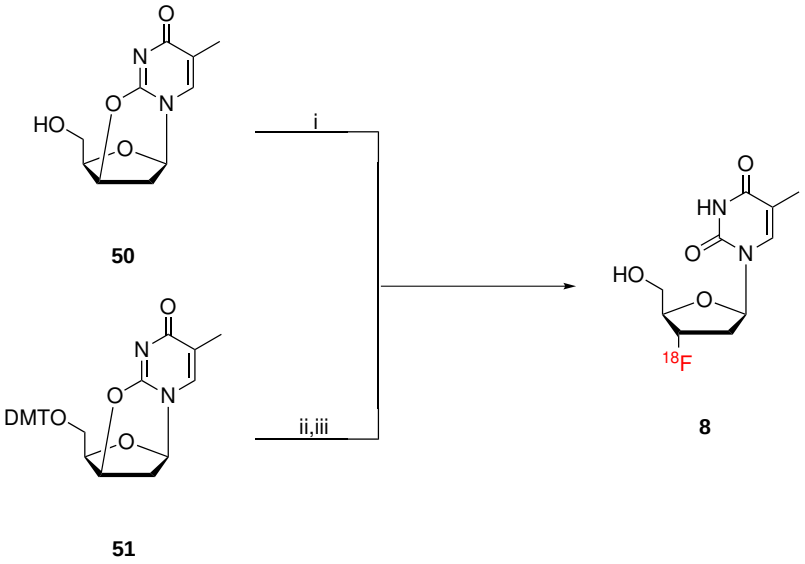

Reagents and conditions: **i)** [^{18}F]fluoride/K_{222}, DMSO, 130 °C, 30 min; **ii)** [^{18}F]fluoride/K_{222}, DMSO, 160 °C, 10 min; **iii)** 1 M HCl, 50 °C, 10 min.

Scheme 1.18: Radiochemical synthesis of ^{18}F-FLT **8** via the 2,3'-anhydro precursors **50** and **51**.

In order to increase reactivity at the 3'-position, several 3'-activated precursors with different leaving groups were synthesised by Martin *et al.*[128] in order to reduce both the reaction temperature and the reaction time. The synthesis of ^{18}F-FLT using a N^3-Boc-5'-dimethoxytrityl-protected 3'-*p*-nitrobenzenesulfonate (nosylate) precursor **52** (Scheme **1.19**) gave ^{18}F-FLT in 19.8% RCY (decay-corrected) with a synthesis time of 85 min.

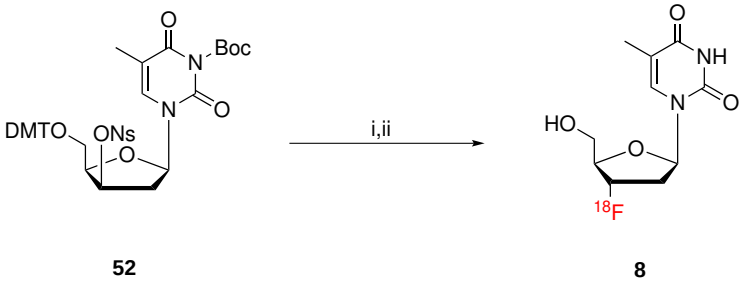

Reagents and conditions: **i)** [^{18}F]fluoride/K_{222}, MeCN, 105 °C, 4 min; **ii)** HCl, 100°C, 4 min, then NaOH.

Scheme 1.19: Advanced radiochemical synthesis of ^{18}F-FLT (**8**) using the 3'-nosylated precursor **52**.

The protected nosylate precursor **52** reacts with dried [^{18}F]fluoride/K_{222} in anhydrous acetonitrile. The deprotection step is carried out using a 1 M HCl-solution at 105 °C for 4 minutes and subsequent HPLC purification yields ^{18}F-FLT in high radiochemical purity. Possible side products such as the 2',3'-olefinic elimination product can easily be separated from the ^{18}F-labelled product[128,181].

In 2004, S.J. Oh *et al.*[129] presented a high-yielding radiochemical synthesis of ^{18}F-FLT using precursor **52** and a fully automated synthesis module. Decay-corrected RCYs of up to 50.5±5.2% were reported with specific activities of 3.3-7.7 Ci/mmol after a synthesis time of 60±5 min. Even high starting activities (≈37 GBq) gave RCYs of 48% after HPLC purification. Additionally, full automation made the synthesis suitable for clinical routine production[129].

A study by Javed *et al.* using microreactors[15] demonstrated the potential of continuous-flow systems by obtaining 63% decay-corrected RCY for ^{18}F-FLT using the above described synthetic route[182]. Furthermore, purification using custom-made solid-phase extraction cartridges furnished ^{18}F-FLT in high purities consistent with standards required by the U.S. Pharmacopeia[182].

At the present time, the proliferation marker ^{18}F-FLT remains the only 2'- or 3'-^{18}F-labelled nucleoside that is used routinely in human clinical applications[85]. The radiochemical synthesis of ^{18}F-FLT that is currently used for clinical applications is based on the approach presented in scheme **1.19**.

2'-^{18}F-labelled arabino nucleoside analogues are of great interest in both preclinical research and clinical oncology mainly due to their variable applicability as outlined above (Section **1.2.5**). For instance, 2'-^{18}F-labelled arabino nucleosides have been used as reporter gene probes for targets such as HSV-TK-1 and are strong candidates for imaging other important biological targets such as dCK[124] within the nucleoside salvage pathway[183,184]. However, introducing the ^{18}F-substituent in the 2'-arabino-position of an intact nucleoside was considered as difficult, if not impossible[177]. The main reason for the difficulty is the high

potential of 2'-activated labelling precursors to form the anhydro side product due to the nucleophilicity of the C-2 carbonyl group of the pyrimidine moiety after base-mediated N^3-H deprotonation (Scheme **1.20**).

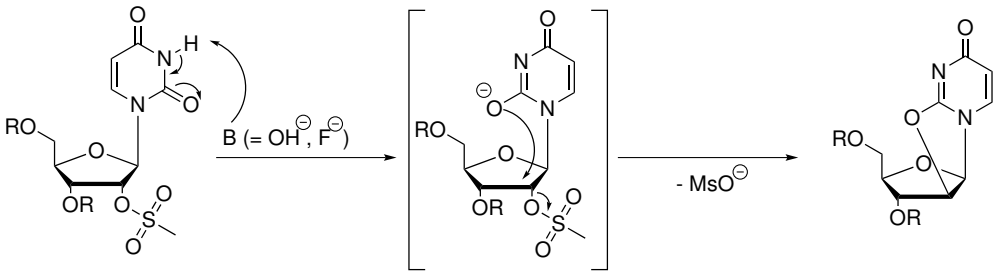

Scheme 1.20: Base-mediated formation of the anhydro side product under elimination of the leaving group (exemplified by commonly used sulfonic ester derivatives) through nucleophilic attack of the C-2 carbonyl oxygen at the 2'-position.

However, N^3-protection with electron withdrawing groups such as *tert*-butyloxycarbonyl (Boc) could successfully prevent 2'-activated precursor molecules from forming 2,2'-cyclic compounds as it was shown by Alauddin *et al.*[177,185] with the development a new radiosynthesis of ^{18}F-FMAU (**10**, Scheme **1.21**) using precursor **53**. Even though this is a low yielding labelling reaction (2.0% RCY, decay-corrected), high specific activities ($\geq$1.8 Ci/mmol) and radiochemical purities ($\geq$99%) with a synthesis time of 95-100 min were reported. Further investigations carried out by Alauddin *et al.*[177] regarding the effect of different 2'-leaving and 3',5-protection groups, however, could not improve the RCY of ^{18}F-FMAU.

In contrast, the radiosynthesis of the ribo analogue 2'-[^{18}F]fluoro-deoxy-uridine using a 2'-nosylated precursor gave the ^{18}F-labelled product in 26.5$\pm$1.4% RCY and high radiochemical purities after a synthesis time of 70$\pm$10.5 min[186] exemplifying the difference in the syntheses of 2'-^{18}F-labelled ribo and arabino nucleosides.

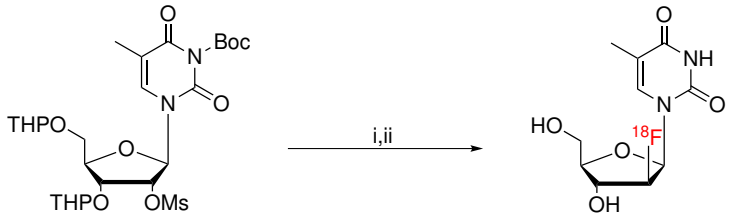

53 **10**

Reagents and conditions: **i)** [^{18}F]fluoride/K_{222}, MeCN, 80°C, 20 min; **ii)** 1 M HCl/MeOH, 80°C,10 min.

Scheme 1.21: Late-stage radiofluorination gave ^{18}F-FMAU (**10**).

1.4.2 Production of [^{18}F]fluoride

In a cyclotron (cyclic particle accelerator) or linear particle accelerator ^{18}O-enriched water is bombarded with highly energetic protons (ca. 18 MeV) to yield non-carrier-added [^{18}F]fluoride present as [^{18}F]-HF[187] and dissolved in ^{18}O-enriched target water via the ^{18}O(p,n)^{18}F nuclear reaction[188]. Specific activities of the produced [^{18}F]fluoride may be ≥370 GBq/μmol[52]. Even though radioactivity levels can reach harmful thresholds (e.g. low milli-Sievert per hour (mSv/h) levels) during a single cyclotron run, the concentration of [^{18}F]fluoride for the synthesis of PET tracers in routine production is still very low compared to precursor concentrations[88]. The following equation **1.7** shows that the concentration of [^{18}F]fluoride hardly exceeds low micromolar levels. For instance, an initially delivered activity A of 80 GBq from the cyclotron dissolved in 1 mL of ^{18}O-enriched water would lead to the following concentration of [^{18}F]fluoride:

$$c([^{18}F]) = \frac{A}{N_A}\frac{t_{(1/2)}}{ln(2)\cdot V} = 1.261\mu mol/L \tag{1.7}$$

This equation can be derived from equation **1.8** and the relation c = n/V.

1.4.3 Specific activity

Since all radioactive atoms eventually decay the area under the time-activity curve equals the total number N of radioactive atoms in the sample:

$$N = A\frac{t_{1/2}}{ln(2)} \tag{1.8}$$

Dividing N by Avogadro's number N_A ($N_A = 6.022\times10^{23}$ mol^{-1}) gives the molar amount of ^{18}F-labelled tracer in the sample. Together with the molar weight of the radiotracer the specific activity (SA) of the sample can be calculated. The SA is defined as the radioactivity per unit of material and is mostly given as the radioactivity per gram or moles of tracer[188]. However, this approach assumes that all molecules of the sample are labelled with ^{18}F and hence gives the theoretical maximum SA. The actual specific activity of a synthesised tracer may be lower as traces of ^{19}F (carrier) might have been present during radiofluorination even after a non-carrier-added (nca) production of [^{18}F]fluoride. Possible sources of carrier are Teflon tubing[189] and ion-exchange cartridges[190], among others.

The actual SA of a radiotracer can be calculated by determining the ratio of ^{18}F-labelled tracer to the total amount of tracer (sum of radioactive and non-radioactive tracer)[187]. The total amount of tracer can be determined by HPLC using a UV detector for UV-active compounds or refractive index-/conductivity detectors for compounds with low molar absorptivities such as FDG[191,192]. Assuming that the tracer is UV-active and sufficiently concentrated, the intensity of the detected UV-signal that corresponds to the radiotracer during an HPLC run would enable the calculation of the total amount of tracer by using a calibration curve previously determined with different concentrations of non-radioactive standard[187].

1.4.4 Automated synthesis modules

The production of radiopharmaceuticals is in many ways different to regular pharmaceutical chemistry. Reaction time, purification and analysis of the final ^{18}F-labelled tracer have to be performed in a time frame according to the half-life of the utilised radionuclide (rule of thumb is 3 times the half-life of the radionuclide). Hence, the use of automated synthesis modules in radiochemistry laboratories is advantageous. In particular, tracer production for pre-clinical and clinical applications requires fast and reproducible synthesis and purification procedures[193]. Computer-controlled reaction modules are placed in lead-shielded fume hoods or hot cells for labelling reactions with high activities in order to minimise the radiation exposure to staff. Graphic visualisation of the radiochemical synthesis on a computer screen allows monitoring of the reaction sequences during radiotracer production.

Several suppliers (General Electric, Eckert & Ziegler, IBA etc.) offer different automated synthesis modules, either specifically developed for a particular tracer or flexible to conduct radiochemical syntheses for different tracers utilising different radionuclides. The IBA Synthera® module system, for instance (Figure **12**)*, may be used for ^{18}F-FDG production.

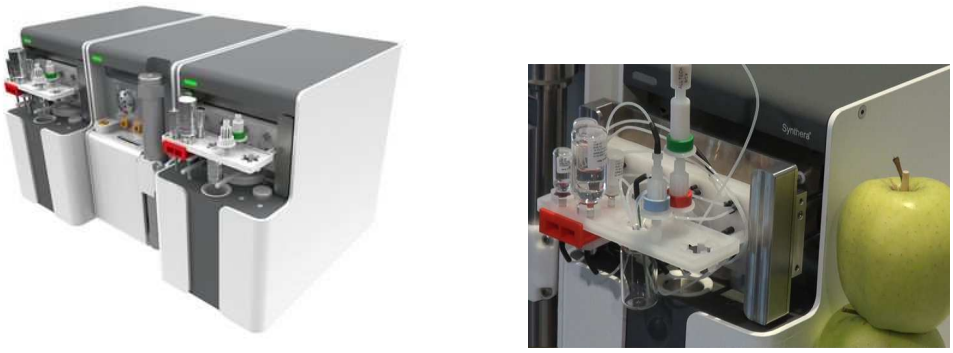

Figure 12: Synthera synthesis module (left) with the integrated fluidic processor (IFP) (right) that carries out the labelling reaction.

*taken from: http://www.iba-radiopharmasolutions.com/products/chemistry

The development of automated synthesis modules has significantly contributed to the wide use and commercialisation of the radiotracer ^{18}F-FDG. Other clinically relevant radiotracers such as ^{18}F-FLT[194] and ^{18}F-FMISO[195] may be synthesised in a ^{18}F-FDG-like manner via nucleophilic radiofluorination and subsequent hydrolysis/deprotection and can hence be produced using ^{18}F-FDG-based synthesis modules with appropriate modifications in programming and hardware[196].

However, more complex radiochemical syntheses with more reaction and/or purification steps require more advanced module systems in order to ensure the automated procedure gives the particular tracer with the desired RCY and radiochemical purity and in a fast and reproducible manner[111]. Examples for such radiosynthesisers are the TracerLab FX® (GE Medical Systems, USA) (Figure **13**, left)†, the FastLab® (GE Medical Systems, USA) for cassette-based productions as well as the All-in-One® (Trasis S.A., Belgium) (Figure **13**, right)‡ and the Eckert & Ziegler module systems (Eckert & Ziegler Eurotope GmbH, Germany).

Figure 13: GE TracerLab FX N Pro module system (left) and the Trasis All-in-One system (right).

†taken from: http://www3.gehealthcare.com/en/products/categories/pet-radiopharmacy/
‡taken from: http://www.trasis.com/

1.4.5 Analysis and quality control of radiotracers

The analysis and quality control (QC) of radiopharmaceuticals is not only important for pre-clinical and clinical applications but also for the development of PET probes and novel radiochemical syntheses. In order to ensure that a newly developed synthetic route yields the desired radiolabelled product with the appropriate RCY, (radio)chemical purity, specific activity and sterility, different analytical techniques have to be performed. Table **2** gives an overview over the most relevant test parameters and analytical methods. In case of PET radiopharmaceuticals for clinical use, all synthetic methods and analytical tests have to be validated according to the GMP guidelines of the appropriate country[57].

Table 2: Analysis and QC for PET radiopharmaceuticals

QC test	Criteria/subject of test	Test method
Sterility	Batch needs to be sterile	Bacteria growth (incubation over 2 weeks
Pyrogenicity	Batch needs to be apyrogenic	Limulus amebocyte lysate (LAL) test
Appearance	Colour/clarity	Visual inspection
Isotonicity	Batch needs to be isotonic	Osmometry (crysocopy)
pH	7.4 (ideal), slightly higher or lower	pH-Meter
Radionuclidic purity	Radionuclides must be pure prior to use	γ-spectroscopy
Chemical purity	Impurities/solvent traces must be reduced or harmless	HPLC/GC
Radiochemical purity	Individual limits (set by national Pharmacopeia)	Radio-HPLC, radio-TLC

Radio-TLC and Radio-HPLC are routinely performed techniques in the development of novel PET tracers that enable the characterisation of labelling reactions.

Radio-HPLC, for instance, allows the simultaneous detection of both the UV, refractive index- or conductivity as well as the radioactivity profile of a radioactive sample[197]. Flow-cell radioactivity analysis is the method of choice as it provides

real-time analysis of the HPLC run. An alternative method is the analysis of fractions by microplate scintillation counting. The detection of radioactivity in a radio-HPLC detector may be conducted using NaI(Tl) or BGO scintillation crystals that register the annihilation γ-photons and re-emit low energy photons that can be converted into an electrical signal by coupled photomultiplier tubes[197]. The detection unit is usually shielded from background radiation and visible light sources[198]. Certain radioactivity detectors in radio-HPLC systems use the 12 ns coincidence time window in order to discriminate annihilation γ-rays from background radiation and hence increase sensitivity. Additionally, the tubing for the mobile phase inside the detector unit can be coiled to form a helix in order to reduce the effective velocity of the mobile phase and thus increase the length of the active detector which may also lead to an increased sensitivity[198].

The radionuclidic purity of a synthesised PET tracer can be determined by recording γ-spectra and only allowing the 511 keV peak as well as the 1022 keV sum peak that are characteristic for PET tracer[171]. However, since most PET radionuclides yield the same γ-spectra the physical half-life of the utilised radionuclide can be calculated for radionuclidic purity confirmation by measuring the activity of the sample at different time points using the following equation[199]:

$$t_{1/2} = -ln2(\mathrm{t_2} - \mathrm{t_1})/ln\frac{\mathrm{A_2}}{\mathrm{A_1}} \tag{1.9}$$

1.4.6 Radiation safety and monitoring

Prior to any work involving radioactivity all personnel must complete a mandatory radiation safety and monitoring training course. During work with radioactivity personal film badges (finger, torso, head) must be worn in addition to standard lab protective cloth in order to monitor and assess radiation doses. The annual effective dose limit in accordance to the Ionising Radiations Regulations 1999 (IRR) for the whole body of a radiation worker of age 18 or above is 20

mSv[200]. The annual dose limit for hands, forearms, feet and ankles is 500 mSv and the dose limit for the lens of the eye is 150 mSv[200].

In general, radiation protection and monitoring in accordance to IRR aims for a dose as low as reasonably achievable/practical (ALARA/ALARP)[57], and ensures that exposure to ionising radiation of staff members does not exceed the dose limits. This can be accomplished by spending a minimal amount of time near the radiation source while keeping the greatest distance possible. Increasing the distance between the radiation source and the staff member reduces the exposure rate according to the inverse square law[201]. Furthermore, shielding devices are used in order to minimise the radiation dose to staff members and patients. In order to work in PET radiochemistry labs and hot cells, lead walls with a width of $\geq$4 cm are required to effectively shield the 511 keV photons[201]. Altogether, a good work practice is essential including the compliance with all radiation safety regulations as well as the use of safety and radiation monitoring devices such as electronic personal dosimeters (EPD) and personal film batch dosimeters.

2 Research aims and objectives

The overall aim of this research project is the radiochemical synthesis of ^{18}F-gemcitabine. Although several synthetic routes towards gemcitabine have already been accomplished the radiochemical synthesis of ^{18}F-labelled gemcitabine has never been achieved. Therefore, ^{18}F-gemcitabine poses serious challenges and an entirely new synthetic approach due to the requirement for radiofluorination at a late stage of the synthesis. It was envisaged that a ^{18}F-gemcitabine PET probe may enable the visualisation of the PK and PD of this important anticancer drug *in vivo*. However, biological evaluations using appropriate cancer models would have to be carried out in order to validate the clinical potential of this tracer.

The development of novel radiosynthetic routes to 2'-^{18}F-labelled gemcitabine analogues such as ^{18}F-FAU and ^{18}F-FAC is the primary objective of this research project in order to establish routes that might enable a translation to the late-stage synthesis of the *gem*-2'-difluoro system.

The figure below (Figure **14**) shows the time line of this project together with the ^{18}F-labelled target compounds.

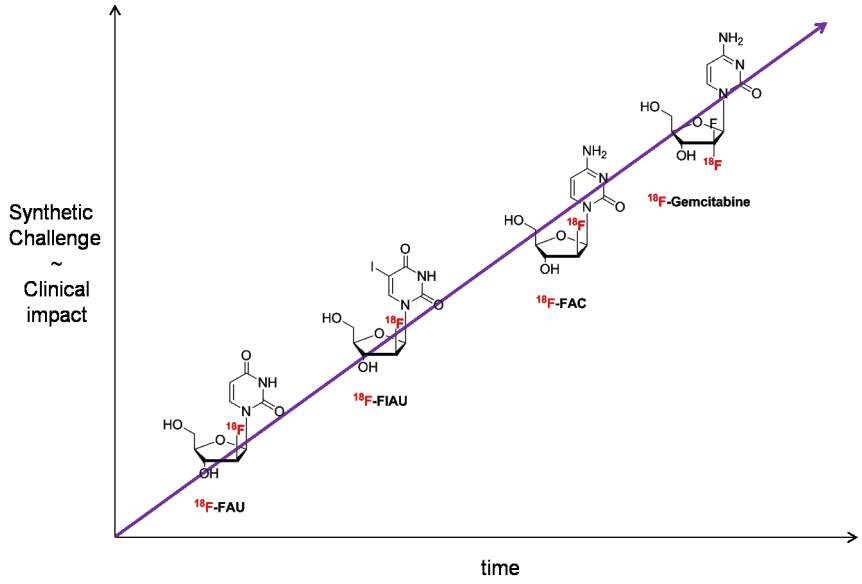

Figure 14: ^{18}F-labelled target molecules of this research project.

Once methods for non-radioactive late-stage synthesis of 2'-fluoro-nucleosides are established, radiosynthesis of the correspondent mono-[^{18}F]fluorinated analogues ^{18}F-FAU, ^{18}F-FIAU and ^{18}F-FAC (Figure **15**) will be carried out at PETIC (Wales Positron Emission Tomography Imaging Centre). The development of a novel and efficient late-stage radiochemical synthesis of ^{18}F-FAC is of particular interest as the current radiochemical approach to this newly developed and clinically relevant tracer is complex and hence difficult to translate to routine tracer production.

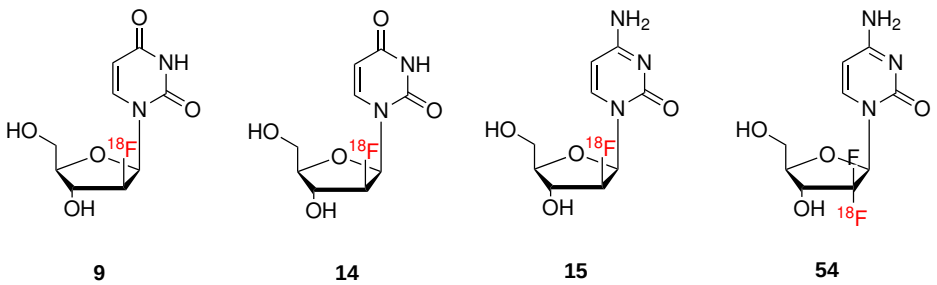

Figure 15: Structures of the mono-[^{18}F]fluorinated target molecules ^{18}F-FAU (**9**), ^{18}F-FIAU (**14**) and ^{18}F-FAC (**15**) as well as the final target compound ^{18}F-gemcitabine (**54**).

Finally, it will be investigated whether results obtained during late-stage radiosynthesis of 2'-monofluorinated nucleosides can be applied to a synthesis of the 2',2'-difluoro system of gemcitabine. For this purpose, the synthesis of an appropriate 2'-activated gemcitabine precursor will be pursued prior to commencing non-radioactive fluorination and radiofluorination studies towards ^{18}F-gemcitabine as the final target of this research project.

3 Results and discussion

3.1 Non-radioactive late-stage fluorinations

3.1.1 Fluorination of protected 2,2'-anhydro uridines

Apart from the target molecules ^{18}F-FAU and ^{18}F-FAC that contain the fluorine substituent in the 2'-arabino-position, the 2'-fluorinated nucleosides 2'-fluoro-2'-deoxyuridine (**31**, 2'-FU) and 2'-fluoro-2'-deoxy-methyluridine (**40**, 2'-FMU) (Figure **16**) were considered as the first targets within this project. It was envisaged that these 2'-fluorinated nucleoside analogues could be accessible via fluorination of appropriate 2,2'-anhydro precursors. Furthermore, fluoride-mediated ring-opening reactions towards 2'-fluorinated nucleosides was of interest due to possible applications in radiochemistry[164].

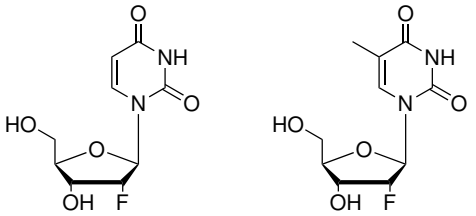

31 **40**

Figure 16: Structures of 2'-FU (**31**) and 2'-FMU (**40**).

Mitsunobu reaction of uridine (**55**) and 5-methyluridine (**56**) using diisopro-

pyl azodicarboxylate (DIAD) and triphenylphosphine[202] furnished 2,2'-anhydro-β-D-arabinofuranosyluracil (**57**) and 2,2'-anhydro-β-D-arabinofuranosylthymine (**58**), respectively, in moderate yields (Scheme **3.1**). The absence of the amine proton signal of the pyrimidine moieties at around 9.5 ppm in the ^{1}H NMR spectra confirmed that the anhydro compounds were formed.

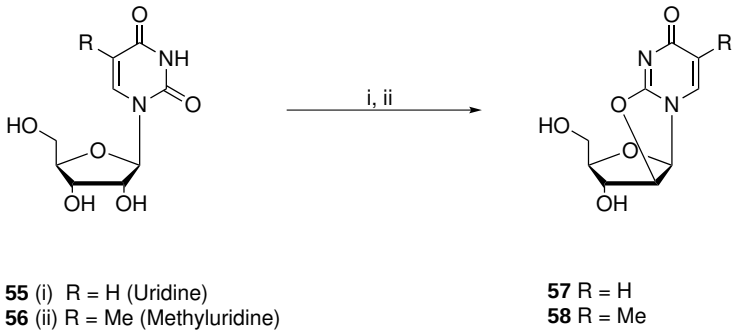

55 (i) R = H (Uridine)
56 (ii) R = Me (Methyluridine)

57 R = H
58 R = Me

Reagents and conditions: **i)** DIAD, PPh_3, MeCN, -20°C - 0°C, 5 h, 56%; **ii)** DIAD, PPh_3 MeCN, -20°C - 0°C, 3 h, 51%

Scheme 3.1: Intramolecular cyclisation towards the anhydro derivatives (**57**) and (**58**).

Purification of the anhydro compounds **57** and **58** was carried out using silica gel column chromatography and gradient elution with EtOAc/MeOH. Reaction control by TLC indicated both full conversion of the starting compound and no side product formation such as the 2,3'-anhydro compound. Subsequently, the remaining hydroxy groups at the 3'- and 5'-positions were protected using different protecting groups (Scheme **3.2**) in order to study their impact on fluorination reactions as well as to minimise side reactions during fluorination. The most common protecting group used in radiochemistry for late-stage fluorinations at the 2'-position is the 2-tetrahydropyranyl (THP)-group[185,186], mostly due to its ease of removal through acidic hydrolysis. THP-protection of anhydro compounds **57** and **58** was carried out using an excess of 3,4-dihydro-2*H*-pyran and equimolar amounts of *p*-toluenesulfonic acid in dry THF. Column chromatography furnished

the protected compounds **59** and **60** in 77-84% yield. The reaction gave a clean profile without side product formation according to TLC.

Although the THP protecting group can be attached and removed efficiently, NMR analysis, however, remains difficult due to the formation of one additional stereocenter per THP group. In this case, a mixture of four diastereomers was obtained. Nevertheless, column chromatography purification of the crude product using a low flow rate enabled separation of two pairs of diastereomers which could be adequately analysed by NMR. Furthermore, product formation was confirmed by mass spectrometry (ESI-MS).

In order to study whether silica based protecting groups allow simultaneous fluorination and deprotection or rather cause side effects during fluorination, anhydro compounds **57** and **58** were treated with 1,3-dichloro-1,1,3,3-tetraisopropyldisiloxane[203,204] in a pyridine/DMF mixture at r.t. for 13-15 h. The corresponding TIPDS-protected compounds **61** and **62** were obtained in good yields (71-84%) after purification by column chromatography. Although these reactions were carried out under anhydrous conditions it is worth noting that around 10-12% of the hydrolysed disiloxane compound was recovered in both cases which limited the yield of these reactions.

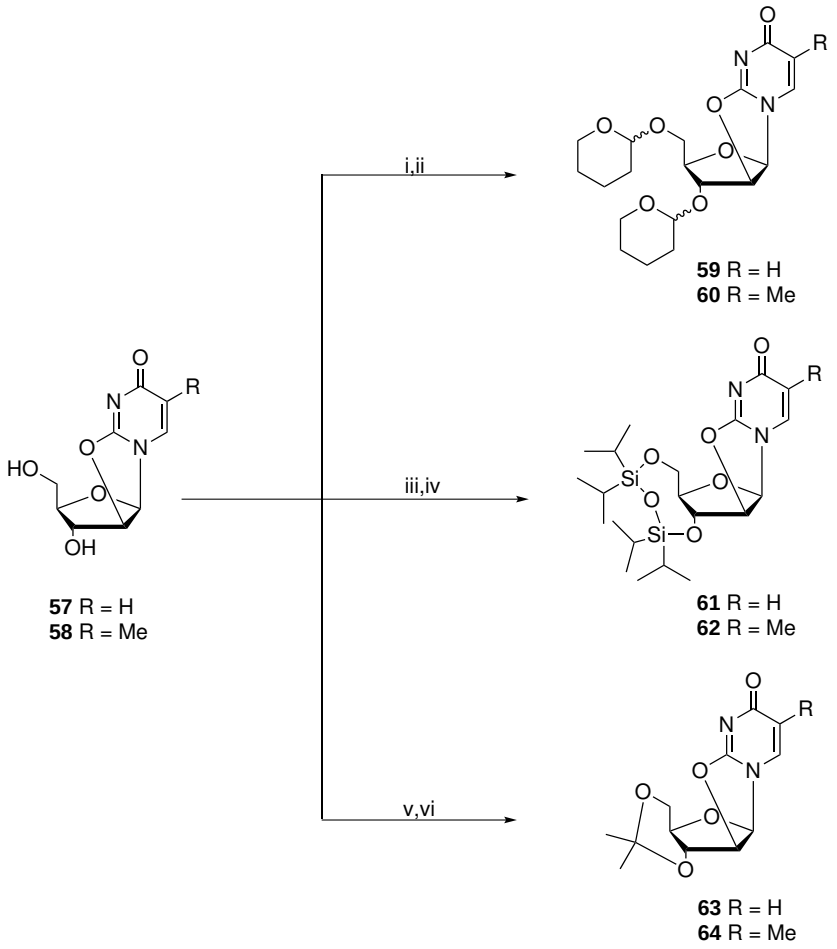

Reagents and conditions: **i)** DHP, pTsOH, THF, 0°C - r.t., 3 h, 84%; **ii)** DHP, pTsOH, THF, 0°C - r.t., 3 h, 77%; **iii)** $TIPDSCl_2$, pyridine, DMF, r.t., 16 h, 71%; **iv)** $TIPDSCl_2$, pyridine, DMF, r.t., 12 h, 84%; **v)** acetone, conc. HCl, 0°C - r.t., 16 h, 85%; **vi)** acetone, conc. HCl, 0°C - r.t., 15 h, 88%.

Scheme 3.2: Simultaneous protection of the remaining 3' and 5' hydroxy groups towards first fluorination precursors **59-64**.

The corresponding acetonides **63** and **64** were found to be stable and could be synthesised in high yields (85-88%) by treating the 2,2'-anhydro precursors **57** and **58** with catalytic amounts of hydrochloric acid in acetone as solvent[205]. The amount of hydrochloric acid is obviously crucial in this reaction in terms of product formation. It was found that addition of a catalytic amount (≈20 μL) of 37% HCl furnished a clean reaction profile and high yields.

Table **3** gives an overview of the first fluorination reactions (Scheme **3.3**)

carried out with the protected precursors **59-64** as starting materials. Solvent, reaction time and temperature as well as the fluoride salts were varied. All reactions were carried out using anhydrous solvents under argon atmosphere. Each reaction was performed on a 100 mg scale with 3 equivalents of the fluoride salt and a solvent volume of 4 mL. A reaction time of 12 h was considered as the maximum time.

59 (i) R = H, PG = THP
60 (ii) R = Me, PG = THP
61 (iii) R = H, PG = TIPDS
62 (iv) R = Me, PG = TIPDS
63 (v) R = H, PG = acetonide
64 (vi) R = Me, PG = acetonide

Scheme 3.3: General scheme for the fluorination of compounds **59-64**.

Table 3: Fluoride-mediated ring-opening reactions of anhydro compounds **59-64** tested under different conditions.

starting material	fluoride source	solvent (T [°C])	time [h]	yield [%]	comment
59,60	CsF	MeCN (85)	6-12	n/a	SM recovered
59,60	CsF	DMF (145)	3-12	n/a	SM recovered
59,60	KF/K_{222}	DMSO (180)	2-8	n/a	SM recovered
61,62	KF/K_{222}	MeCN (85)	6-10	n/a	deprotection
61,62	CsF	DMF (145)	3-12	n/a	deprotection
61,62	KF/K_{222}	DMSO (180)	2-6	n/a	deprotection
63,64	KF/K_{222}	MeCN (85)	4	n/a	SM recovered
63,64	CsF	DMF (145)	3-6	n/a	SM recovered
63,64	KF/K_{222}	DMSO (180)	1-2	n/a	SM recovered

The desired 2'-fluorinated compounds could not be obtained under the above

described conditions. The THP (**59,60**) and acetonide (**63,64**) protected precursors were recovered from the reaction mixture by column chromatography after reaction times stated in table **3**. The obtained NMR data for these compounds and the starting materials were consistent. The TIPDS-protected compounds **61** and **62** were deprotected under these conditions. The corresponding anhydro compounds **57** and **58** were recovered and confirmed by NMR spectroscopy. A ^{19}F-signal with an estimated chemical shift of around -190 ppm, however, could not be observed in any case confirming that nucleophilic ring-opening by fluoride did not occur, at least not on a scale which was detectable by UV.

All solvents used in this reactions were dried in order to ensure anhydrous reaction conditions. The fluorination agents, however, were used without performing azeotropic drying procedures prior to reactions which is a standard procedure in radiochemical synthesis since [^{18}F]fluoride is delivered in low quantities and as an aqueous solution in ^{18}O-enriched target water[128,170,177]. Properly dried fluoride/kryptofix in combination with dry solvents could change the outcome of these reactions significantly. Another reason for the observed results might be the high stability of the anhydro compounds. Lewis-acid activation via the pyrimidine moiety may increase the likelihood of the fluoride-mediated ring-opening event.

3.1.2 Nucleophilic fluorination of 2'-activated nucleoside precursors

Since direct fluorination of the 2,2'-anhydro nucleoside precursors **59-64** could not be achieved under the above stated conditions, the preparation and testing of several nucleoside precursors containing a leaving group at the 2'-position seemed to be the next reasonable step towards the 2'-fluorinated nucleosides 2'-FMU (**40**) and FAU (**65**) as the first fluorinated arabino nucleoside (Figure **17**).

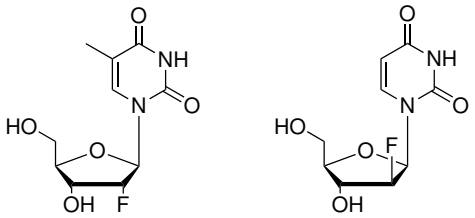

Figure 17: Structures of the target molecules 2'-FMU (**40**) and FAU (**65**).

For this purpose, hydroxide mediated ring-opening reaction of compounds **60** and **64** was performed using a 10 M sodium hydroxide solution in methanol at reflux temperature for 4 h and 5 h, respectively (Scheme **3.4**).

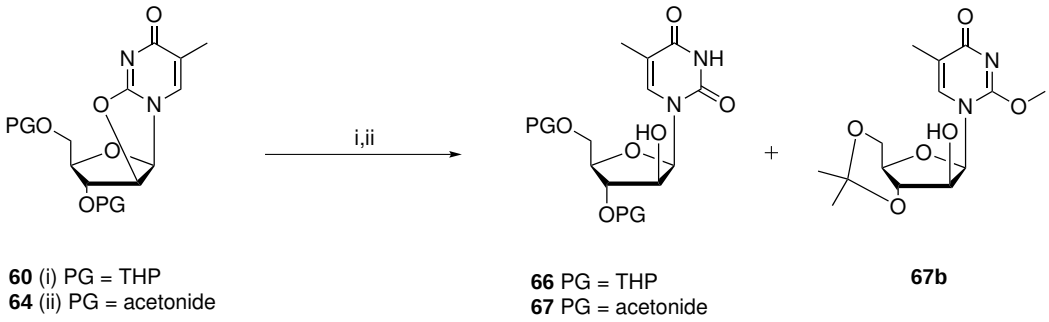

Reagents and conditions: **i)** 10 M NaOH, MeOH, reflux, 4 h, 47%; **ii)** 10 M NaOH, MeOH, reflux, 5 h, 59%

Scheme 3.4: Hydrolysis of compounds **60** and **64** gave the corresponding protected 2'-hydroxy arabino nucleosides **66** and **67**.

The same reaction was reported for THP protected 2,2'-anhydro uridine (**59**) and 2,2'-anhydro 5-methyluridine (**60**) using 1 M NaOH solution[206]. In the case of **60** and **64**, however, significant product formation only occurred using harsh conditions with a 10 M NaOH solution in MeOH at reflux temperature. Additionally, these harsh conditions led to side product formation. In the case of THP protected compound **60**, the TLC showed full conversion of the starting material

and two new spots corresponding to the desired product (**66**, 47%) and a side product (35%) with R_f-values (5% MeOH/DCM) of 0.2 and 0.4, respectively. The product was analysed and confirmed by both NMR spectroscopy as well as mass spectrometry. Since a comparable reaction profile was observed for the reaction of the acetonide protected compound **64** the side product was further studied due to clean one- and two dimensional NMR spectra in the case of compound **64**. The ^{1}H NMR spectrum gave signals corresponding to 21 instead of 18 protons indicating an additional methyl group at 3.57 ppm. Finally, (^{1}H,^{1}H)-COSY and HSQC spectra in combination with MS analysis led to the conclusion that the methoxy-group acted as a competitive nucleophile which was generated under these harsh conditions from solvent molecules. Methoxy-mediated ring-opening furnished finally the observed 2-methoxy side product **67b** with lower polarities in comparison to the desired products (see Experimental Part).

The 2'-hydroxy arabino analogues (**66**) and (**67**) were converted to the corresponding 2'-(*p*-nitrobenzenesulfonyl) (-nosyl) compounds **68** and **69** using *p*-nitrobenzenesulfonyl chloride (NsCl) and dry pyridine in anhydrous DCM at r.t. in good yields (68-84%, Scheme **3.5**). The nosylate precursor **51** furnished good RCY (14-18 %, decay-corrected) in case of ^{18}F-FLT[128,162] as presented in section **1.4.1**.

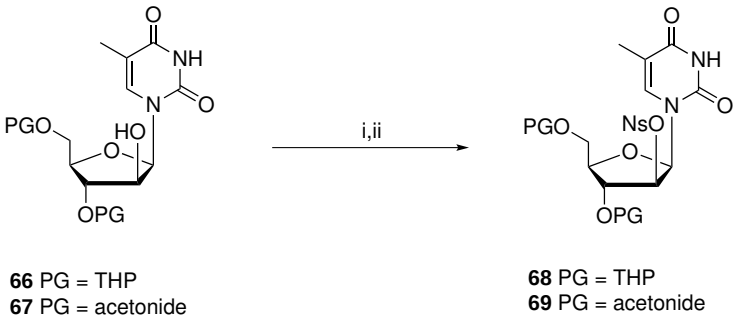

66 PG = THP
67 PG = acetonide

68 PG = THP
69 PG = acetonide

Reagents and conditions: **i)** NsCl, pyrdine, DCM, r.t., 15 h, 68%; **ii)** NsCl, pyrdine, DCM, r.t., 8 h, 84%.

Scheme 3.5: Nosylation of compounds **66** and **67** furnished the nosylate precursor **68** and **69**.

The nosylate precursors **68** and **69** were treated with KF/K_{222} in either dry MeCN or DMF at appropriate reflux temperatures for different reaction times (2-12 h) as shown below (Scheme **3.6**, table **4**).

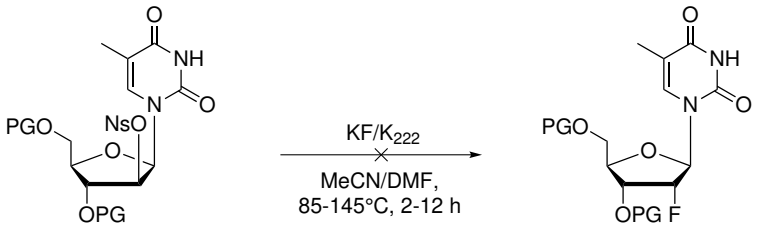

68 PG = THP
69 PG = acetonide

Scheme 3.6: Fluoride-mediated nucleophilic substitution using nosylate precursor **68** and **69** did not occur. Instead, the appropriate anhydro intermediates were obtained.

Table 4: Results of the fluoride-mediated nucleophilic substitution of the nosylate precursors **68** and **69**.

starting material	fluoride source	solvent (T [°C])	time [h]	yield [%]	comment
68	KF/K_{222}	MeCN (85)	3-12	n/a	anhydro cmpd **60**
68	KF/K_{222}	DMF (145)	3-12	n/a	anhydro cmpd **60**
69	KF/K_{222}	MeCN (85)	4-12	n/a	anhydro cmpd **64**
69	KF/K_{222}	DMF (145)	4-12	n/a	anhydro cmpd **64**

In place of the 2'-fluorinated compounds the corresponding anhydro intermediates **60** and **64** were obtained and confirmed by NMR and MS. That led to the conclusion that the reaction stopped at the stage of the anhydro intermediate. However, since the leaving group is in an unfavoured "up" (arabino)-position regarding a nucleophilic attack of the carbonyl oxygen of the pyrimidine moiety, the anhydro formation reaction most likely follows a S_{N_1}-mechanism as illustrated below (Scheme **3.7**). A S_{N_1}-mechanism was additionally supported by the use of polar aprotic solvents, high reaction temperatures and a good leaving group. Furthermore, the fluoride anion competes with the 2-carbonyl oxygen to attack the activated 2'-position. Hence, reducing the nucleophilicity of the 2-carbonyl oxygen could increase the likelihood of a fluoride attack. In fact, Turkman *et al.*[185] reported that Boc-protection of the N^3 of the base moiety successfully prevented the formation of the anhydro derivative during radiosynthesis.

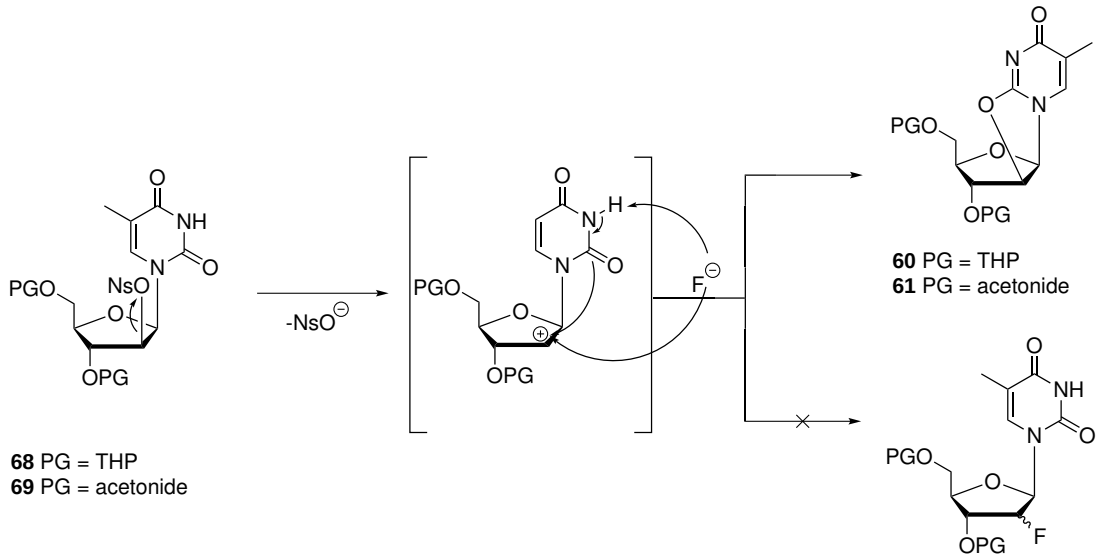

68 PG = THP
69 PG = acetonide

60 PG = THP
61 PG = acetonide

Scheme 3.7: Possible mechanism that explains the results obtained during the fluorination of the nosylate precursors **68** and **69**. The fluoride anion can also act as a base and hence trigger anhydro formation through NH-deprotonation.

The next logical step was Boc-protection of the nosylate precursors **68** and **69** following reported procedures[162]. For this purpose, compounds **68** and **69** were treated with Boc_2O and 4-DMAP in dry THF at r.t. for 14 h (Scheme **3.8**).

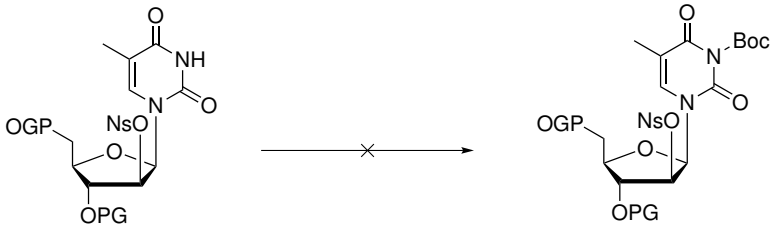

68 PG = THP
69 PG = acetonide

Reaction conditions: **i)** Boc_2O, DMAP, THF, r.t., 14 h.

Scheme 3.8: Anhydro formation triggered under basic conditions.

In both cases, however, anhydro compounds **60** and **64** were obtained and thus Boc-protection did not occur. Based on that results, it was assumed that

a base-mediated cyclisation towards the corresponding anhydro compounds took place, which seems reasonable due to the proposed mechanism of the anhydro formation (Scheme **3.7**). Thus, N^3-Boc-protection had to be carried out before leaving group introduction at the 2'-position in order to prevent the formation of anhydro compounds.

Therefore, TMS-protection of the 2'-OH group was accomplished first before the N^3-position was Boc-protected. TMS-protected compound **70** was obtained in 73% yield. Additionally, it is worth noting that addition of Et_3N (1%) prevents the TMS-group from being hydrolysed on the silica gel column during purification. Boc-protection was carried out directly followed by selective deprotection of the TMS-group through addition of *p*TsOH (2 eq.) to the reaction mixture. Column purification furnished compound **71** in an good overall yield (53%). Nosylation of the free 2'-OH group of the Boc-protected compound **71** was carried out using nosyl chloride and pyridine in anhydrous DCM. Fluorination precursor **72** was obtained after purification in an acceptable yield (53%) (Scheme **3.9**).

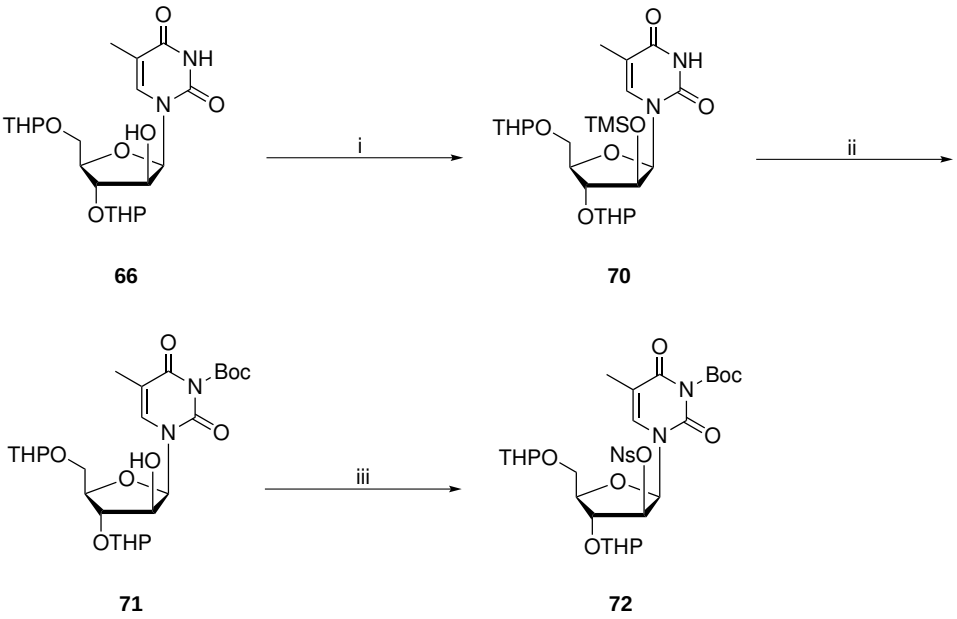

66 70 71 72

Reagents and conditions: **i)** TMSCl, Et_3N, DCM, 0°C - r.t., 2.5 h, 73%; **ii)** Boc_2O, DMAP, THF, r.t., 14 h, then pTsOH, 0°C - r.t., 40 min, 53%; **iii)** NsCl, pyrdine, DCM, r.t., 3 h , 53%.

Scheme 3.9: Synthetic scheme to give the fluorination precursor **72**.

Prior to nucleophilic fluorination of the nosylate precursor **72**, XtalFluor-mediated deoxofluorination of Boc-protected hydroxy compound **71** was performed in order to obtain the reference compound for the purpose of comparison. The treatment of compound **71** with a freshly prepared mixture of XtalFluor M and Et_3N/HF in anhydrous DCM at -78 °C led to the desired product 2'-FMU. After full conversion of the starting material an aqueous HCl/MeOH solution was added furnishing the fully deprotected fluorinated compound 2'-FMU (**40**) in 25% yield (Scheme **3.10**). Target compound **40** was fully characterised and confirmed by analytical comparison with commercially available 2'-FMU. This is the first time that deoxofluorination was performed using the new DAST-derivative XtalFluor M (**29**).

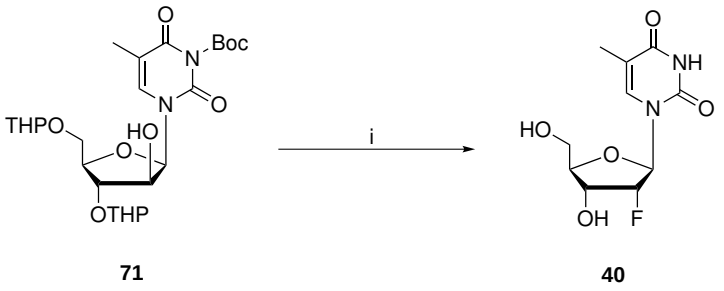

71 **40**

Reagents and conditions: **i)** XtalFluor M, Et_3N/HF, DCM, -78°C - r.t., 3 h, then HCl/MeOH, r.t., 1 h, 25%.

Scheme 3.10: XtalFluor M enabled fluorination of hydroxy precursor **71**. Subsequent deprotection furnished 2'-FMU (**40**).

However, when treated with KF/K_{222} or TMAF in dry MeCN at reflux temperature (Scheme **3.11**, table **5**) nosylate precursor **72** did not lead to the desired 2'-fluoro compound. Reaction control using LC-MS did not show any evidence for the formation of the fluorinated derivative.

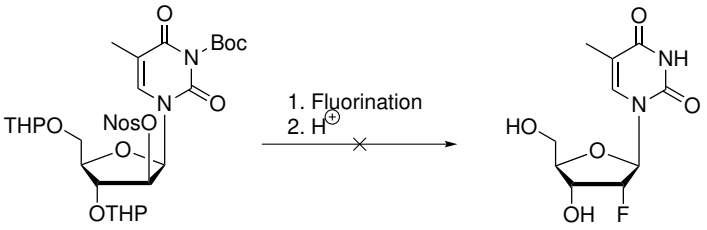

72 **40**

Scheme 3.11: Fluoride-mediated nucleophilic substitution towards **40** did not occur.

Table 5: Fluorination results using precursor **72**.

starting material	fluoride source	solvent (T [°C])	time [h]	yield (**40**) [%]	comment
72	KF/K_{222}	MeCN (85)	3-6	n/a	decomposition
72	KF/K_{222}	DMF (145)	2-4	n/a	decomposition
72	TMAF	MeCN (85)	8-12	n/a	SM recovered
72	TMAF	DMF (145)	2-4	n/a	decomposition

Although tetramethylammonium fluoride (TMAF)[20] was considered as a milder and more soluble fluorination agent it did not lead to the formation of the desired compound 2'-FMU. Hence, it was assumed that the nosyl group may be replaced by another less reactive leaving group in order to accomplish a better stability-to-reactivity ratio of the corresponding fluorination precursor.

For this purpose the arabino analogue of 2'-FU, 2'-fluoro-2'-deoxy-arabino-uridine (FAU) **65**, was synthesised using a mesylate precursor based on a procedure reported by Turkman *et al.*[185] for the radiosynthesis of the 5-methylated analogue ^{18}F-FMAU. The corresponding mesylate precursor **79** was synthesised via the route shown in scheme **3.12**. TIPDS-protection of commercially available uridine (**55**) was carried out using dichloro-1,1,3,3-tetraisopropyldisiloxane in dry pyridine/DMF. 3',5'-TIPDS-protected uridine (**73**) was furnished in 88% yield after column purification. TMS-protection of the remaining 2'-hydroxy group gave compound **74** in 79% yield. N^3-Boc-protection and subsequent selective deprotection of the TMS-group furnished hydroxy compound **75** in 63% overall yield. Mesylation of the free 2'-OH group using mesyl chloride and Et_3N in dry DCM gave **76** in 82% yield. Tosylation product **77** was obtained in 44% yields, however, it did not prove to be stable when stored at r.t. for longer then 24 h. Hence, the synthesis of a tosylate precursor was discontinued.

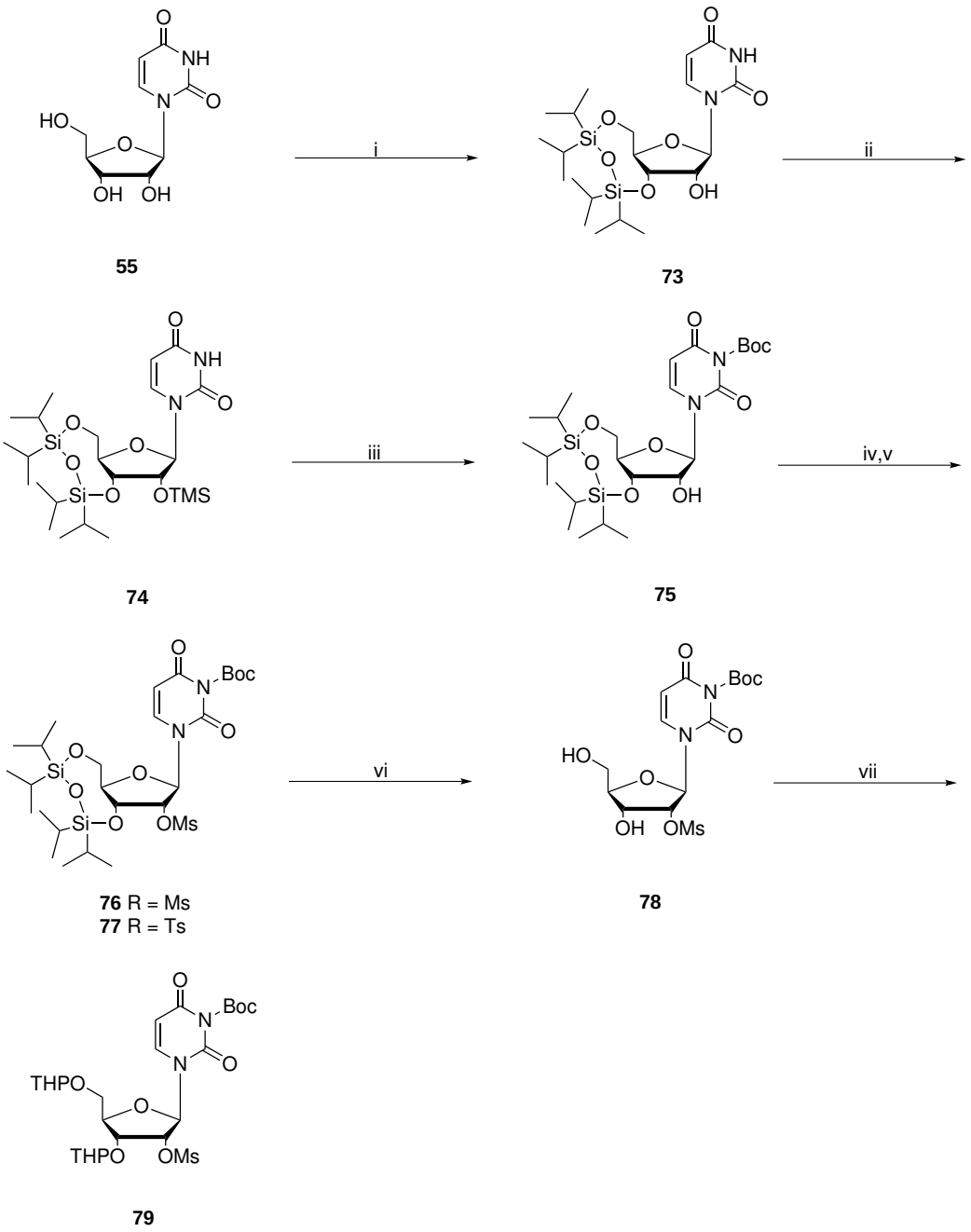

Reagents and conditions: **i)** $TIPDSCl_2$, pyridine, DMF, 0°C - r.t., 14 h, 88%; **ii)** TMSCl, Et_3N, DCM, 0°C - r.t., 2 h, 79%; **iii)** Boc_2O, DMAP, THF, r.t., 16 h then pTsOH, 1 h, 63%; **iv)** MsCl, Et_3N, DCM, 0°C - r.t., 3 h, 82%; **v)** TsCl, Et_3N, DCM, r.t., 24 h, 44%; **vi)** TBAF, THF,r.t., 40 min, 90%; **vii)** DHP, pTsOH, THF, 0°C - r.t., 4 h, 65%.

Scheme 3.12: Synthetic scheme towards the mesylated fluorination precursor **79**.

Tetrabutylammonium fluoride (TBAF) mediated deprotection of the bidentate protection group furnished compound **78** in 90% yield. THP-protection of the 3'- and 5'-hydroxy groups was carried out using an excess of 3,4-dihydro-2*H*-

pyran and an equimolar amount of *p*TsOH to obtain mesylate precursor **79** in 65% yield and high purities. Mesylate precursor **79** was tested using several fluoride salts and different reaction conditions as summarised below (Scheme **3.13**, table **6**).

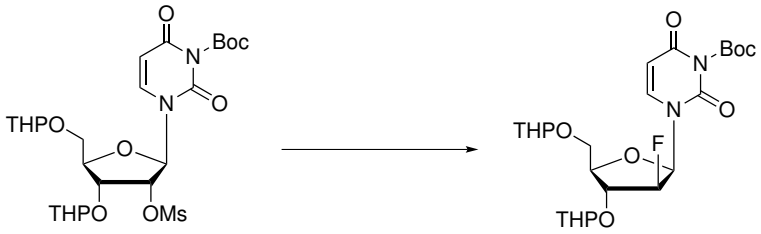

79 **80**

Scheme 3.13: Fluoride-mediated nucleophilic substitution towards the protected 2'-fluoro-arabinonucleoside **80**.

Table 6: Fluorination results using mesylate precursor **79**.

starting material	fluoride source	solvent (T [°C])	time [h]	yield (**80**) [%]	comment
79	KF/K_{222}	MeCN (85)	8-12	n/a	SM recovered
79	KF/K_{222}	DMF (145)	3-5	n/a	decomposition
79	TMAF	MeCN (80)	8-12	n/a	SM recovered
79	TMAF	DMF (145)	4-8	n/a	SM recovered
79	TBAF/THF	MeCN (80)	2.5	51	-

Fluorinated intermediate **80** was obtained in MeCN at 80 °C for 2.5 h using TBAF/THF (3.0 eq.) and confirmed by NMR and ESI-MS. Since TBAF is only available as the trihydrate and very difficult to dry[207,208], the anhydrous solution of TBAF in THF was considered as a reasonable option since it was already successfully used in the synthesis of FMXU[170] (**46**, scheme **1.13**). Acid mediated hydrolysis of protected intermediate **80** using 1 M HCl/MeOH solution furnished the target compound FAU **65** in acceptable yield (62%) (Scheme **3.14**) after column purification.

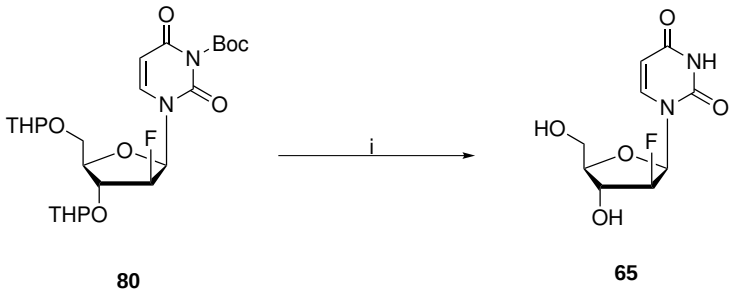

80 65

Reagents and conditions: **i)** 1 M HCl/MeOH, reflux, 1 h, 62%.

Scheme 3.14: Acidic deprotection of **80** furnished the final compound FAU (**65**).

Full NMR characterisation in combination with MS and melting point (mp) determination confirmed the desired product. The correct conformation of the fluoro-substituent was derived from the coupling constants of the ribose protons according to the Karplus relation. The corresponding ^{1}H and ^{19}F NMR spectra of the mesylate precursor **79**, the fluorinated intermediate **80** and FAU **65** are shown in the appendix. The absence of the characteristic mesyl group singlets at around 3.25 ppm illustrate the successful substitution by the fluoride nucleophile.

3.2 Radiochemical synthesis of ^{18}F-FAU and ^{18}F-FIAU

In this section the results regarding a novel late-stage radiofluorination approach towards the 2'-^{18}F-labelled uridine analogues ^{18}F-FAU (**9**) and ^{18}F-FIAU (**14**) are presented.

The current radiochemical approach to give the uridine-based nucleosides ^{18}F-FAU (**9**) and ^{18}F-FIAU (**14**) is based on the early radiofluorination method reported by Cai *et al.*[178] (Scheme **3.15**):

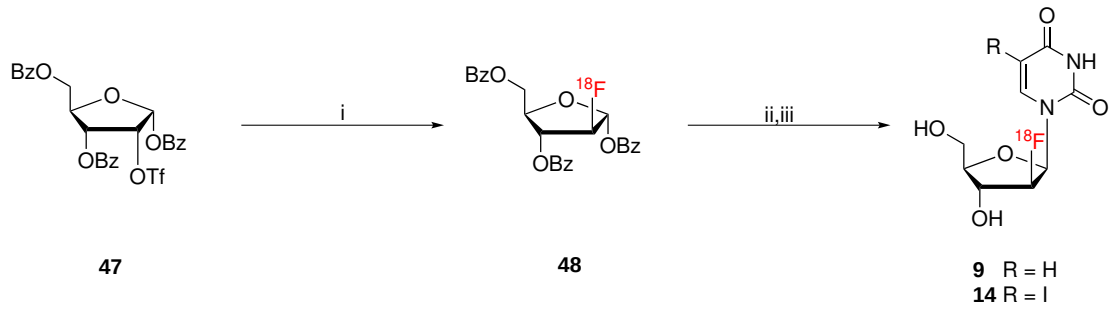

47 **48** **9** R = H **14** R = I

Reagents and conditions: **i)** [^{18}F]fluoride/K_{222} or [^{18}F]TBAF, MeCN, 85°C, 20 min; **ii)** 2,4-bis-O-(trimethylsilyl)uracil (**9**), 2,4-bis-O-(trimethylsilyl)-5-Iodouracil (**14**), HMDS, TMSOTf, MeCN, 85 °C, 1 h; **iii)** KOMe, MeOH.

Scheme 3.15: Current radiosynthesis of the uridine-based nucleoside analogues ^{18}F-FAU (**9**) and ^{18}F-FIAU (**14**).

Decay-corrected RCYs of 5.4±1.0% (^{18}F-FAU) and 9.9±0.4% (^{18}F-FIAU) with specific activities of 380±35 Ci/mmol and high radiochemical purities (≥99%) were reported. The synthesis time was 150 min. The radiochemical syntheses of these tracers were carried out on automated synthesis modules. Routine production of these tracers, however, remains challenging.

3.2.1 ^{18}F-FAU

Since the late-stage fluorination of FAU-precursor **79** could be successfully demonstrated, the subsequent radiochemical synthesis of its labelled analogue ^{18}F-FAU was carried out. First, the radiochemical synthesis of the ^{18}F-labelled intermediate **81** was conducted in order to investigate whether [^{18}F]fluoride could be incorporated by nucleophilic substitution (Scheme **3.16**).

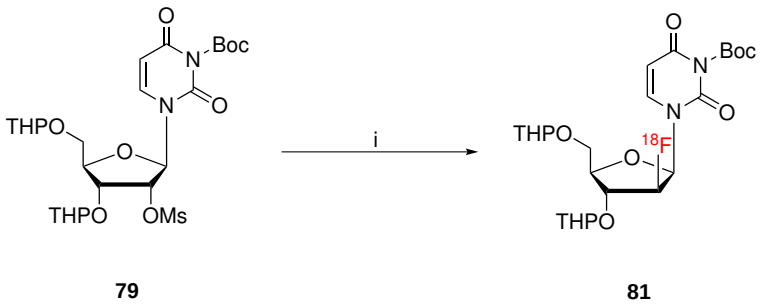

79 **81**

Reaction conditions: **i)** [^{18}F]fluoride/K_{222}, MeCN/DMF/DMSO, 90-140 °C.

Scheme 3.16: [^{18}F]fluoride-mediated nucleophilic substitution towards the protected 2'-^{18}F-labelled FAU-intermediate **81**.

Radiofluorinations were carried out using 3 GBq activity (≈5 nmoles of [^{18}F]fluoride) which was delivered from the cyclotron as an aqueous solution. Hence, a drying procedure was carried out (ca. 20 min) after [^{18}F]fluoride was released from the ion-exchange (QMA) cartridge. Various polar aprotic solvents such as MeCN, DMF and DMSO and different reaction temperatures (90-140 °C), with reaction times no longer than 30 min were tested regarding radioactive decay. Table **7** gives an overview of the results from conducted radiofluorinations using different reaction conditions.

Table 7: Analytical radiochemical yields of **81** using different reaction conditions.

run	solvent	T [°C]	t [min]	RCY [%] (n = 3)
1	MeCN	90	20	0.7±0.5
2	MeCN	90	30	0.9±0.3
3	DMF	100	20	2.3±0.7
4	DMF	120	20	8.7±1.1
5	DMF	120	30	5.2±0.9
6	DMF	140	20	3.9±1.0
7	DMSO	120	20	2.3±0.6
8	DMSO	140	20	1.4±0.6

The analytical RCY of compound **81** was determined using radio-TLC. The table shows that maximum yields were found with DMF, 120 °C and 20 min reaction time.

The peak width of the radio-TLC experiment using the crude reaction mixture (Figure **18**) is most likely due to incomplete evaporation of high boiling reaction solvents such as DMF and DMSO prior to the TLC experiment.

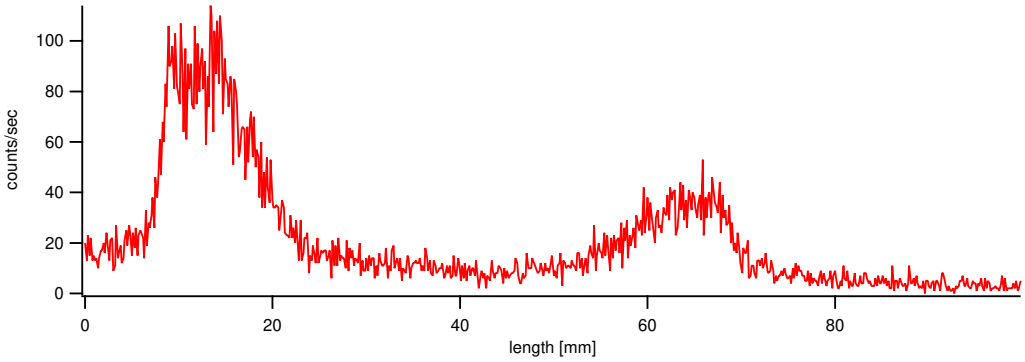

Figure 18: Radio-TLC of the crude reaction mixture showing the radioactivity signal of the fluorinated intermediate (R_f=0.65; 5% MeOH/DCM) and the unreacted [^{18}F]fluoride near the baseline.

Labelling reactions were carried out using [^{18}F]fluoride/K_{222}/K_2CO_3 instead of [^{18}F]TBAF since the drying procedure was easier to perform (less prone to decomposition[207,209]) in the module system and the conditions were adjusted for [^{18}F]fluoride/K_{222}/K_2CO_3. Consequently, precursor **79** (10 mg) was dissolved in dry DMF under a flow of nitrogen. The solution was then added to [^{18}F]fluoride/K_{222} in a V-vial under a nitrogen atmosphere. The resulting mixture was stirred at the appropriate temperature (90-140 °C) for the given time (20-30 min). Table **7** shows that the highest RCY (8.7%) for **81** was obtained at 120 °C for 20 min in dry DMF. The crude reaction mixture was purified using AL (Normal-phase alumina) and C18 (Reversed-phase C-18) cartridges to trap unreacted [^{18}F]fluoride and organic residues, respectively. The radioactive intermediate **81** was released with EtOAc (2 mL) into a V-vial containing water (2 mL). The mixture was extracted to further remove unreacted [^{18}F]fluoride from the organic layer. Subsequently, radio-TLC (Figure **19**) and radio-HPLC (Figure **20**) samples spiked with non-radioactive reference compound **80** for co-elution were analysed.

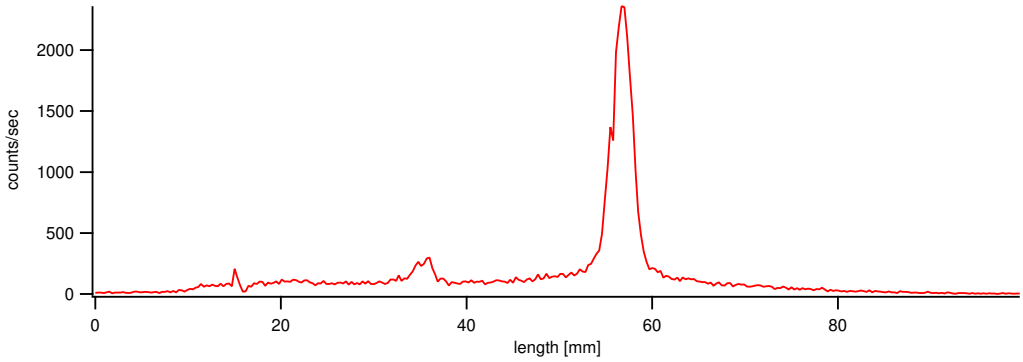

Figure 19: Radio-TLC of the purified reaction mixture using pre-conditioned Al and C18 cartridges for purification. The radioactive intermediate could be identified at around 57 mm by co-elution with the non-radioactive reference standard.

Radio-HPLC with isocratic co-elution (20% H_2O/MeCN) of both the non-radioactive and the radioactive compound at approx. 6.3 min further confirmed that the ^{18}F-labelled intermediate **81** was obtained (Figure **18**). Additionally, **81** was confirmed by LC-MS where the Na^+-adduct with a mass to charge ratio of 535.79 ($[M + Na]^+$)) was found indicating the intermediate ion with a mass of 513.54 ($[M^+]$).

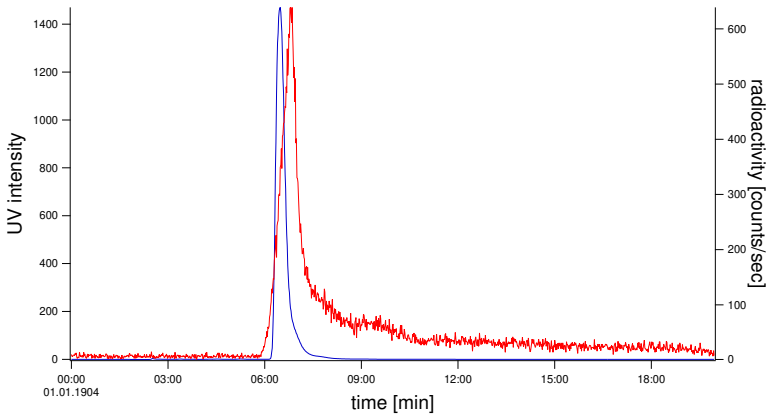

Figure 20: Superimposed radioactivity and UV traces of the purified ^{18}F-labelled intermediate (Al and C18 cartridge followed by extraction) using analytical radio-HPLC and non-radioactive reference standard, respectively (isocratic 20% H_2O/MeCN; 1.0 mL/min flow rate).

The next step involved acid-catalysed deprotection to give the nucleoside tracer ^{18}F-FAU (Scheme **3.16**).

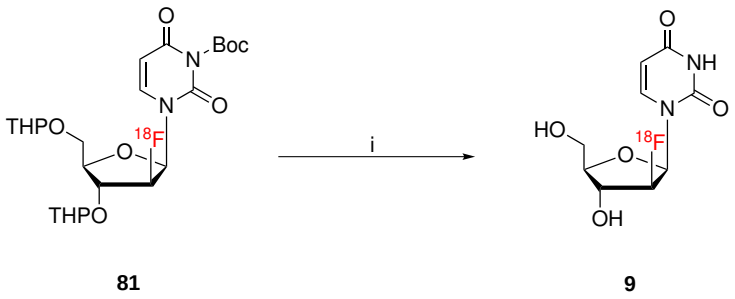

81 **9**

Reaction conditions: **i)** 1 M HCl/MeOH, 70°C, 8 min.

Scheme 3.17: Acid-catalysed deprotection gave ^{18}F-FAU **9**.

The radiofluorination step was carried out using optimal conditions (run 4, Table **7**). The eluted EtOAc-solution from the cartridge containing **81** was flushed back into the reactor. The solvent was then removed under a stream of nitrogen at 80 °C before 1 M HCl/MeOH-solution (0.4 mL) was added to the reaction vial. The reactor was heated up to 70 °C for 8 min. A test reaction carried out using an appropriate amount of the non-radioactive reference compound **80** indicated that deprotection is complete after 5 min under these conditions. The mixture was subsequently neutralised with 1 M NaOH solution (0.5 mL). The reaction mixture was then loaded onto a semi-preparative HPLC column via a 10 mL injection-loop. The product fraction was collected after 13.5 min of isocratic elution (10% MeCN/H_2O, 3 mL/min flow rate) in a vial containing isotonic NaCl-solution. The product solution was then flushed through a sterility filter into the final product vial.

Analytical radio-HPLC (10% MeCN/H_2O, 1 mL/min flow rate) of the final product confirmed ^{18}F-FAU was furnished by co-elution with the non-radioactive

reference compound FAU (Figure **19**). ^{18}F-FAU was obtained with a RCY of 2.8-3.9% (decay-corrected, n = 3) in high radiochemical purities (≥95%) and specific activities ≥42 GBq/μmol with a synthesis time of 178 min.

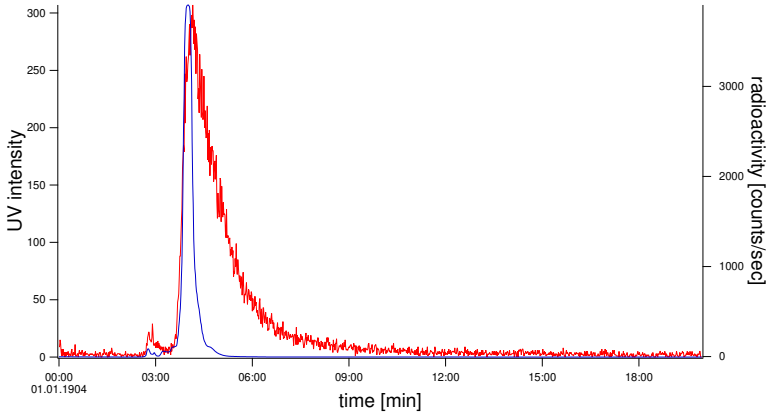

Figure 21: Superimposed radioactivity and UV traces of analytical radio-HPLC of purified ^{18}F-FAU and non-radioactive reference standard FAU (**65**), respectively (isocratic elution with 10% MeCN/H_2O; 1.0 mL/min flow rate).

This was the first time that ^{18}F-FAU was synthesised via a late-stage fluorination procedure. This approach was based on previously published data for the radiosynthesis of the uridine analogue ^{18}F-FMAU by Alauddin *et al.*[177,185]. However, due to the proof-of-principle character of this reaction further optimisations towards an improved radiosynthesis of ^{18}F-FAU were not carried out.

3.2.2 ^{18}F-FIAU

In collaboration with Dr. Steven Paisey from PETIC at the Cardiff University Hospital, we aimed to synthesise the FAU-analogue ^{18}F-FIAU (**14**) via a novel synthetic route based on the results obtained from the previously described ^{18}F-FAU study. Ultimately, ^{18}F-FIAU was supposed to be tested as a PET reporter probe for herpes simplex virus thymidine kinase 1 (HSV-TK-1) in a newly developed cancer model at the Cardiff School of Medicine. As FIAU and thus ^{18}F-FIAU are substrates for HSV-TK-1 but not substrates of the mammalian

thymidine kinase 1 (TK-1)[210], genetically engineered stem cells that express the HSV-TK-1 gene could selectively trap ^{18}F-FIAU in the cell through phosphorylation[211]. It was envisaged that *in vivo* imaging of stem cell localisation and, if enzyme expression is conditional, cell differentiation could be monitored by PET with potential applications in stem cell therapy[212].

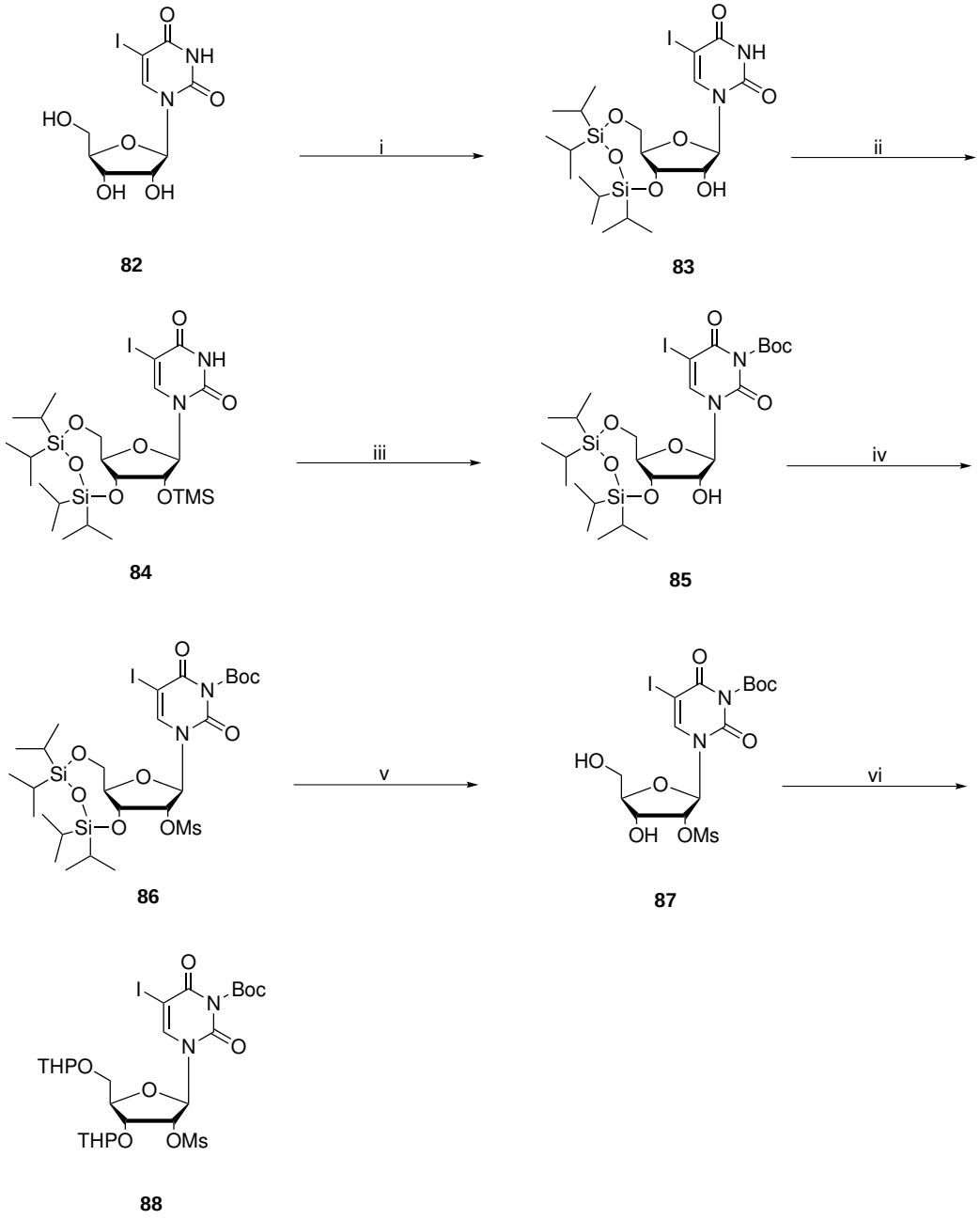

Reagents and conditions: **i)** $TIPDSCl_2$, pyridine, 0°C - r.t., 24 h, 77%; **ii)** TMSCl, Et_3N, DCM, 0°C - r.t., 2 h, 91%; **iii)** Boc_2O, DMAP, THF, r.t., 16 h then pTsOH, r.t., 1 h, 58%; **iv)** MsCl, Et_3N, DCM, 0°C - r.t., 3 h, 87%; **v)** TBAF, THF, r.t., 40 min, 72%; **vi)** DHP, pTsOH, THF, 0°C - r.t., 4 h, 55%.

Scheme 3.18: Synthetic scheme towards the mesylated fluorination precursor **88**.

The precursor synthesis was performed according to the FAU-precursor synthesis. Starting with commercially available 5-iodouridine (**82**) the first step involved the 3',5'-TIPDS-protection in dry pyridine at ambient temperature furnishing compound **83**[213] in 77% yield followed by TMS-protection of the remaining hydroxy group at the 2'-position. It is noteworthy that the yield of the TMS-protection could be significantly improved (≥30%) by slow and dropwise addition of the TMSCl at low temperatures (≤-5 °C). Subsequent N^3-Boc-protection and *p*TsOH-mediated TMS-deprotection gave compound **85** as a white foamy solid in 58% yield. Mesylation was carried out in dry DCM using MsCl and Et_3N. The reaction profile was clean and full conversion of the starting material could be observed after 3 h. TBAF-mediated deprotection of the bidentate protecting group occurred within 45 min at ambient temperature. The resulting crude oil was used without further purification for reaction scales ≥500 mg for the subsequent THP-protection step. The dried crude mixture was dissolved in dry DCM under inert atmosphere followed by the addition of an excess of 3,4-dihydro-2*H*-puran and an equimolar amount of *p*TsOH. Full conversion of the starting material was observed after 4 h. The THP-protected product **88** was detected by TLC as two close spots under UV-light (254 nm), each spot corresponding to one pair of diastereomers. The two pairs of diastereomers could be separated and purified by column chromatography using an EtOAc/hexane gradient. Analytical HPLC gave a purity of ≥97% with a yield of 55% for precursor **88**.

The radiochemical synthesis was performed based on the ^{18}F-FAU-synthesis. However, the non-radioactive reference standard **89** for the radiolabelled ^{18}F-FIAU-intermediate was not available as non-radioactive fluorinations proved to be challenging (Scheme **3.19**, top). Different reaction conditions were tested using either KF/K_{222} or TBAF as fluorination agent and MeCN or DMF as solvents at reflux temperatures (90-160 °C) for 1-2 h. However, analytical evidence for the fluorinated intermediate **89** could not be provided. Consequently, radiofluorinations with subsequent deprotection were carried out (Scheme **3.19**, bottom)

as the non-radioactive reference standard FIAU was commercially available and thus enabled analysis of the reaction mixture with radio-HPLV and radio-TLC via co-elution.

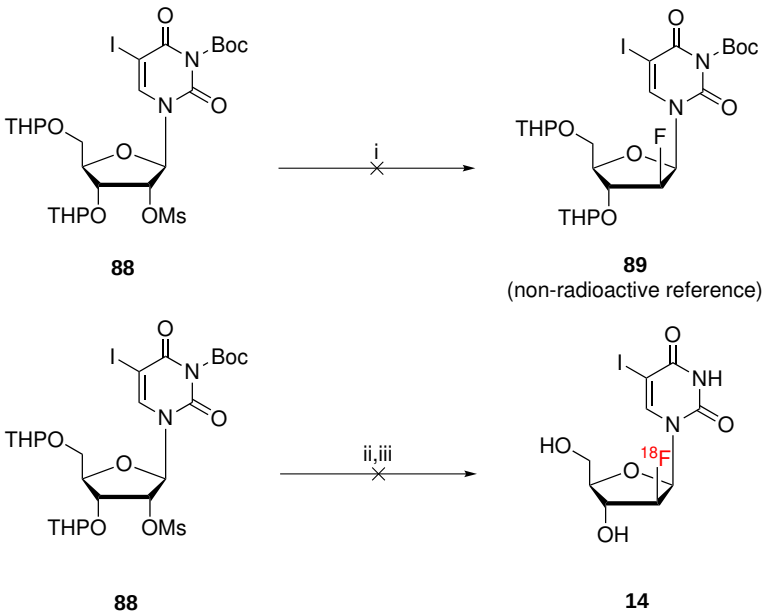

Reaction conditions: **i)** KF/K_{222} or TBAF, MeCN/DMF, 90-140°C, 1-2 h; **ii)** [^{18}F]fluoride/K_{222}, DMF/DMSO, 100 - 140°C, 20 min, **iii**) 1 M HCl/MeOH, 70°C, 8 min.

Scheme 3.19: Non-radioactive fluorination did not yield the intermediate **89**. Furthermore, the radiochemical approach as outlined above to give ^{18}F-FIAU **14** was not successful.

Radiofluorination and subsequent deprotection were carried out in the same reaction vial. Reaction solvent and temperature were varied. The reaction time as well as the conditions for the deprotection step (1 M HCl, 80 °C, 10 min) were not changed (Table **8**).

Table 8: Tested radiofluorination conditions to give ^{18}F-FIAU

run	solvent	T [°C]	t [min]	RCY [%] (n = 2)
1	DMF	100	20	n/a
2	DMF	120	20	n/a
3	DMF	130	20	n/a
4	DMF	140	20	n/a
5	DMSO	130	20	n/a
6	DMSO	140	20	n/a

The target compound ^{18}F-FIAU (**14**) could not be obtained using different reaction conditions.

Radio-TLC as well as radio-HPLC experiments were carried out using co-elution with the non-radioactive reference compound FIAU. However, ^{18}F-FIAU could not be obtained under the reaction conditions shown in table **8**. The only observed radioactivity peak was due to unreacted [^{18}F]fluoride.

Further investigations regarding the late-stage synthesis of ^{18}F-FIAU were discontinued, mainly due to reasons of time but also because the stem cells could not be provided. The translation of the findings from the ^{18}F-FAU synthesis to ^{18}F-FIAU proved to be more challenging then expected even though the target molecules are similar in their chemical structure. That is an indicator for the general complexity of radiochemistry.

3.3 Radiochemical synthesis of ^{18}F-FAC

As outlined in section (**1.4.1**), ^{18}F-FAC is currently synthesised via the following route[180] (Scheme **3.20**):

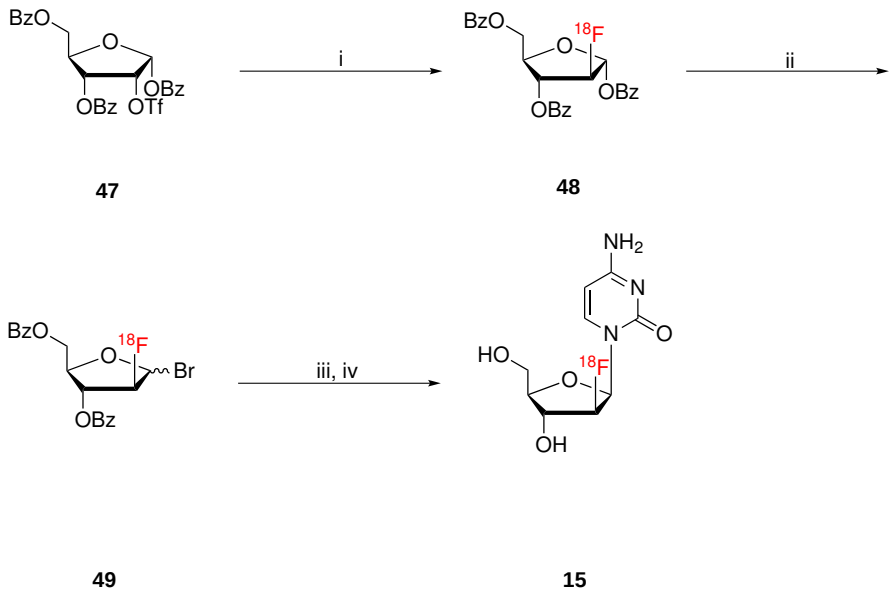

Reagents and conditions: **i)** [^{18}F]fluoride, K_{222}, DMF, 165°C, 15 min; **ii)** 30% HBr/AcOH, dichlorethane, 80°C, 10 min; **iii)** bis(trimethylsilyl)cytosine, dichlorethane, 160°C, 30 min; **iv)** NaOMe/MeOH, 100°C, 5 min

Scheme 3.20: Current radiochemical approach to give ^{18}F-FAC.

A novel automated radiosynthesis module (ELIXYS) was developed in order to synthesise ^{18}F-FAC following the route in scheme **3.20** and suitable for clinical application[180]. Decay-corrected RCY of 31±5 (n = 6) with specific activities between 37-44 GBq/μmol and a synthesis time of 160 min were reported. Clinical routine production of this radiotracer, however, has not been reported so far.

A late-stage and FDG-like radiosynthesis may simplify the application of ^{18}F-FAC in clinical routine production and hence could have a significant impact on the availability of 2'-[^{18}F]fluorinated arabino cytidine derivatives such as ^{18}F-FAC and ^{18}F-FIAC in clinical use. The following section describes a novel late-stage radiofluorination approach to give ^{18}F-FAC.

3.3.1 Precursor development

The greatest challenge from a synthetic point of view is the rational design and synthesis of an appropriate fluorination precursor which combines an activated, electrophilic position at the 2'-position of the sugar moiety with stability against decomposition when handled at high temperatures (≥100 °C) and under basic conditions.

The development of a novel late-stage radiochemical approach towards ^{18}F-FAC (**15**) was based on the idea that a rational design of a potential precursor may be advantageous prior to ^{18}F-labelling reactions. In order to develop a novel precursor for the radiofluorination of the 2'-arabino position of cytidine derivatives the idea of radiofluorination of an intact nucleoside moiety was applied. The main challenge of this new approach was the rational design of a precursor that combined reactivity and stability in a way that radiofluorination at high temperatures could be carried out with acceptable conversion rates while the heat- and base-mediated anhydro-formation was kept at a minimum.

Despite experimental data, a quantitative method for the characterisation of the thermal stability of precursors was desirable. Next to base-mediated N^3/N^4-H deprotonation, the electric charge density of the 2-carbonyl oxygen of the pyrimidine moiety was considered as a measurement for the potential to undergo an intramolecular nucleophilic attack at the 2'-position to form undesired anhydro side products. Hence, the electric charge density of a family containing N^4-substituted cytidine derivatives was calculated. Base-mediated N-H deprotonation, however, was not considered for the calculations. Molecular dynamic calculations were performed to yield energetically minimised conformations from which sixteen were selected in order to cover the conformational space. The net electric charge of all atoms of these compounds were calculated using the GAMESS[214] software with support from Dr. Andrea Brancale and Iuni Trist. The net electric charge of the 2-carbonyl oxygen was subsequently averaged for

each compound. In addition to the cytidine derivatives **90-94**, selected uridine derivatives were included to give a reference value as well as to show the impact of the 4-amino group on the electric charge density of the 2-carbonyl oxygen (Table **9**). The N-substituents were chosen with regard to their synthetic accessibility and deprotection mechanisms that are suitable for radiochemical syntheses and GMP environments in terms of efficient removal and the use of hazardous chemicals, respectively (Figure **23**).

Furthermore, the N^3−nitro-2'-(methanesulfonyl)uridine **96** was considered as a standard value since the N^3−nitro-2'-(trifluoromethanesulfonyl)uridine derivative **97** (Figure **22**) was previously reported as successfully synthesised and thermally stable[215]. Thus, N-nitro-substitution decreases the electron density on the 2-carbonyl oxygen and prevents base-mediated N-H deprotonation to an extent which allows the conversion of the 2'-hydroxy group into a triflate group (a very good leaving group) without formation of the cyclic 2,2'-anhydro compound.

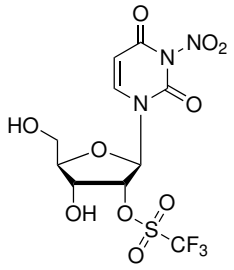

97

Figure 22: Compound **97** was found to be stable even though the triflate group represents a good leaving group. Hence, the N^3-nitro substituent withdraws enough electron density and prevents base-mediated N-H deprotonation so that the 2-carbonyl oxygen is not attacking the 2'-position.

However, according to the existing literature[215] no radiofluorination method could be applied to a N^3−nitro uridine-based precursor. Hence, N-nitro protection was not considered as a potential protecting group strategy.

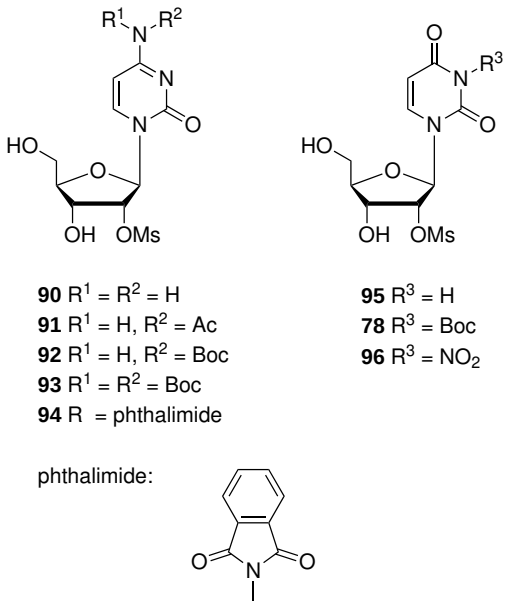

Figure 23: Selected cytidine- (**90-94**) and uridine-based (**95,78,96**) nucleosides for electric charge density calculations.

Table 9: Net electric charge densities Ω calculated for the 2-carbonyl oxygen.

Compound	R^1	R^2	R^3	Ω
90	H	H		-0.911±0.09
91	H	Ac		-0.901±0.05
92	H	Boc		-0.860±0.01
93	Boc	Boc		-0.825±0.06
94	phthalimide	phthalimide		-0.814±0.08
95			H	-0.838±0.02
78			Boc	-0.770±0.03
96			NO_2	-0.589±0.10

The results shown in table **9** indicated that the net electric charge at the 2-carbonyl oxygen was reduced when H-substitution at the N^4 (N^3 for uridine derivatives) with an electron-withdrawing group was performed. Furthermore, it showed that the stronger the electron-withdrawing effect of the substituent(s) the lower the calculated electron density at the 2-carbonyl oxygen. For instance, double N^4-Boc-protection (**93**) decreased the electron density more then single N^4-Boc-protection (**92**) and N^4-acetylation (**91**), respectively. In order to translate

the difference of the calculated electric net charge into a measurable dimension, compounds **91** and **93** were tested for their ability to decompose and to form the appropriate cyclic anhydro compounds. Intramolecular cyclisation of compound **91** is shown in scheme **3.21**.

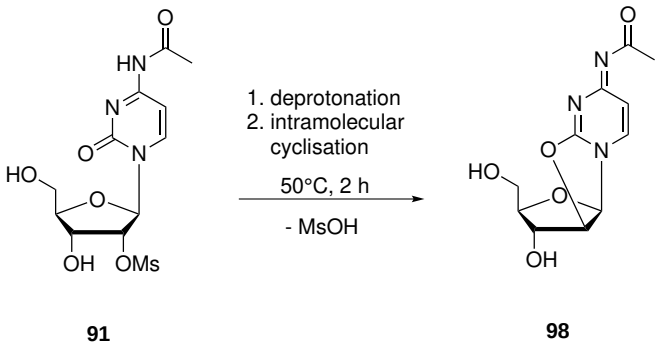

91 **98**

Scheme 3.21: Intramolecular cyclisation of compound **91** gave the cyclisation product **98**

Therefore, a NMR sample of compound **91** was heated up to 50 °C. ^{1}H NMR spectra were recorded hourly. Figure **24** shows that almost full conversion to anhydro compound **98** occurred within 2 h.

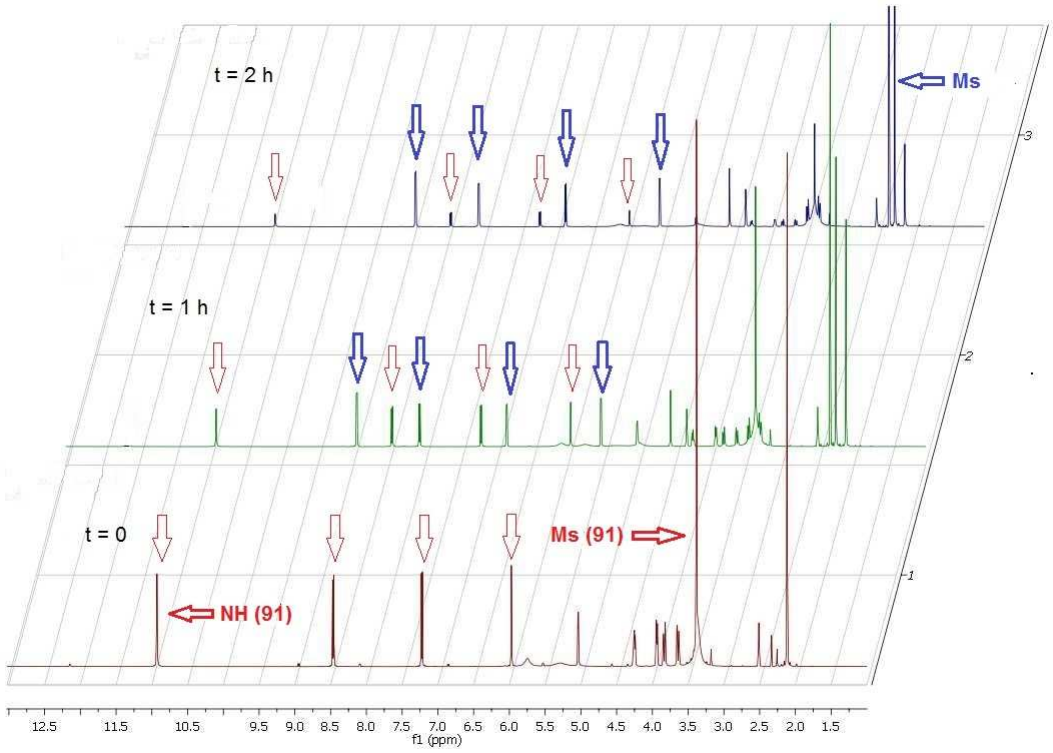

Figure 24: Decomposition of compound **91**. The signals in red correspond to compound **91**, the signals in blue to the anhydro compound **98**.

Chemical shifts of the amino proton (11.5 to 12.25 ppm) and the ribose protons showed the conversion into the cyclic nucleoside compound. Furthermore, the vanishing signal of the mesyl group at 3.5 ppm also indicated the decomposition since the free mesylate should show a different chemical shift which indeed was observed at around 2.3 ppm next to the methyl-signal of the acetamide.

^{13}C-NMR chemical shifts also indicated anhydro formation. Additionally, ESI-MS was performed in order to show the change in the molecular mass. In fact, the increasing intensity of the *m/z*-signal 268 ($[M + H]^+$) further confirmed the formation of compound **98**. The same results were obtained for the benzoylated derivative **106**. Subsequent THP-protection of the 3'- and 5'- hydroxy groups of **91** increased its thermal stability, presumably due to steric hindrance of the intramolecular nucleophilic attack. However, temperatures $\geq$80 °C also led to decomposition, which was reliably monitored by TLC.

The double N^4-Boc-protected compound **93**, however, indicated a significantly increased stability as shown in figure **25**. Recorded proton NMR spectra did not show the formation of the cyclic compound **99** after 2 h at 80 °C (Figure 25). the observed stability of compound **93** looked promising with regard to radiofluorination reactions. Additionally, carbon NMR spectra and recorded MS data supported the stability of compound **93**.

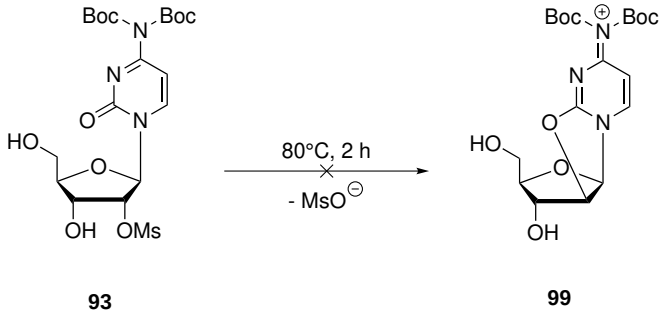

93 **99**

Scheme 3.22: Compound **93** did not form the cyclisation product **99** after 2 h at 80 °C.

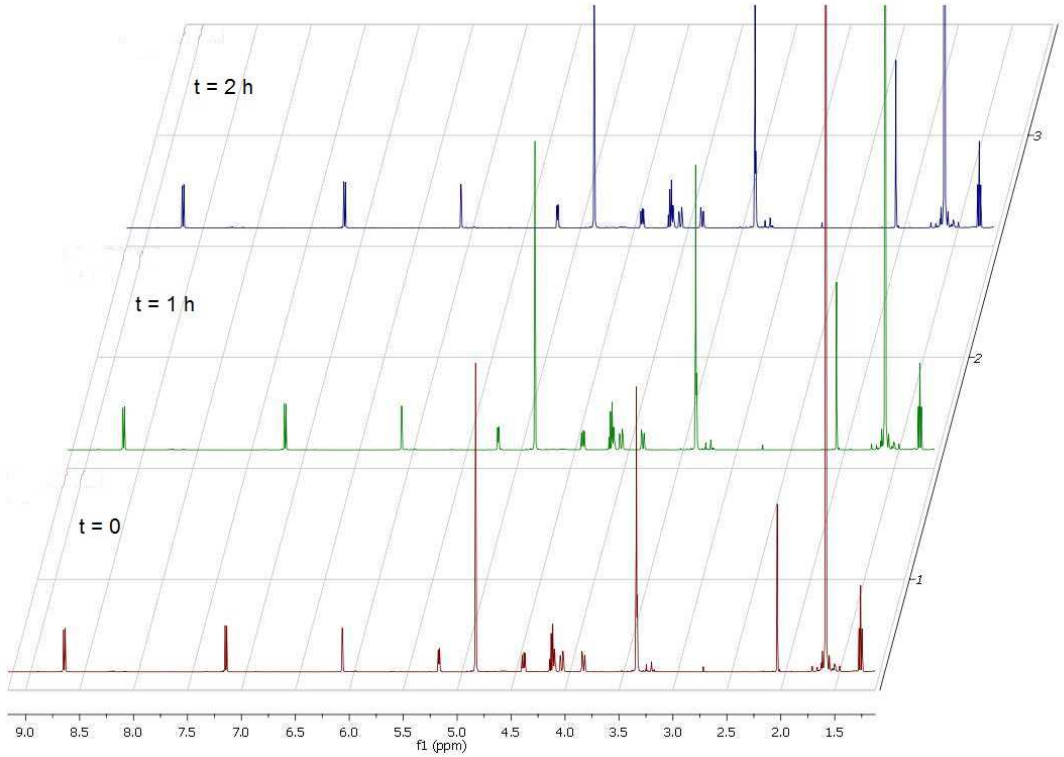

Figure 25: Even after 2 h at 80 °C compound **93** was not converted into the cyclic species **99**. The increased stability led to the synthesis of fluorination precursor **119**. Additionally, acid-labile N^4-Boc-protection was the protection strategy of choice regarding a possible THP-protection of the hydroxy groups.

Hence, both the calculated and experimental data led to the conclusion that N^4/N^3-electron withdrawing groups have a measurable and quantifiable effect on the electron density at the 2-carbonyl oxygen. Depending on the strength of its electron withdrawing nature a N^4/N^3-protecting group may influence the stability of a 2'-activated nucleoside analogue regarding 2,2'-intramolecular cyclisation.

However, these results did not explain to what extend the electron withdrawing effect of the Boc-protecting groups contributed to the observed stability of compound **93**, or whether it was a result of the disubstitution of both amino protons preventing base-mediated cyclisation. Hence, it was assumed that the disubstituted N^4-diacetyl- and N^4-dibenzoyl compounds might have similar stabilities. Their synthesis, however, proved not to be successful and thus appropriate stability experiments could not be carried out. The inaccessibility of these

compounds was a surprising result as double N^4-Boc-protection was performed in good yields.

Finally, compound **93** was selected for further studies. In accordance to previous experiments, the combination of N-Boc-protection with 3'/5'-O-THP-protection was the protection strategy of choice. This led to the development of precursor **119** (Scheme **3.28**).

3.3.2 Precursor synthesis

TIPDS-protection of the 3'- and 5'-OH groups of N^4-acetylcytidine (**100**) and N^4-benzoylcytidine (**101**) furnished compounds **102** and **103** in good yields (67-77%). Coevaporation with dry pyridine prior to the reaction was found to be crucial for yields $\geq$60%. Subsequent mesylation was carried out using mesyl chloride and Et_3N in anhydrous DCM under inert atmosphere and furnished compounds **104** and **105** in yields between 82-88%. TBAF-mediated deprotection of the TIPDS-group furnished compounds **91** and **106** which were used for stability experiments (Scheme **3.23**).

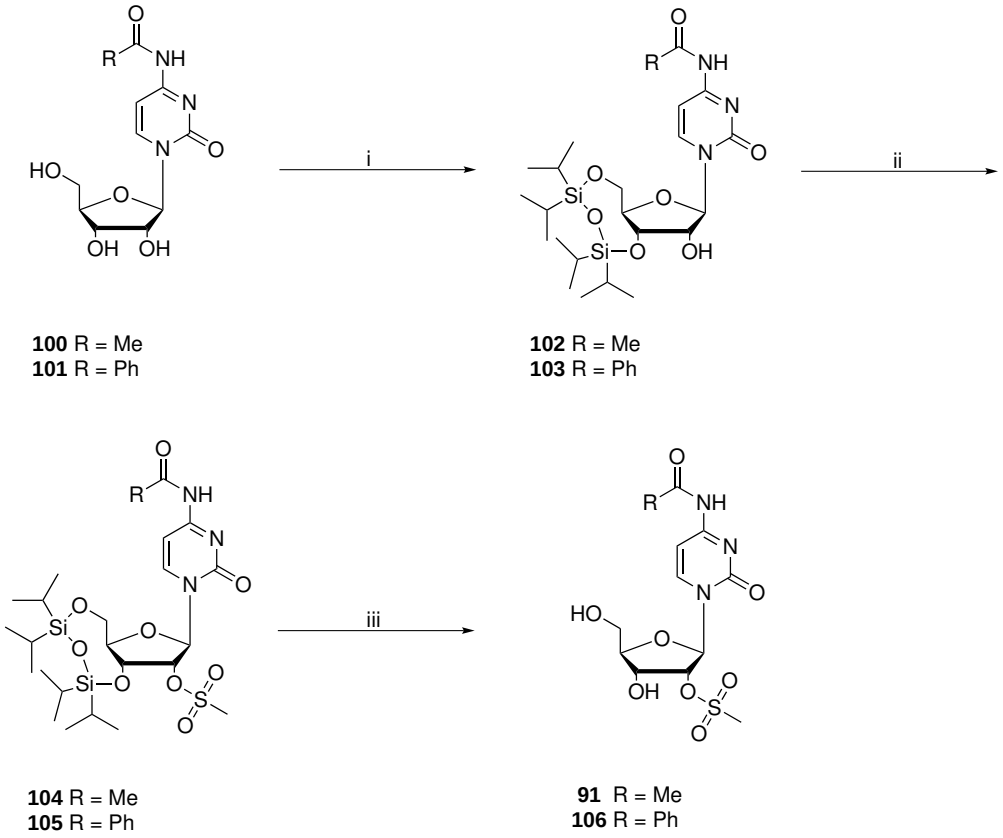

Reaction conditions: **i)** $TIPDSCl_2$, pyridine, 0°C - r.t., 18 h, 67-77%; **ii)** MsCl, Et_3N, DCM, 0°C - r.t., 2 h, 82-88%; **iii)** TBAF, THF, r.t., 30 min, 57-63%.

Scheme 3.23: Synthetic scheme towards the mesylated compounds **91** and **106**.

As a proof-of-principle study, the influence of a better leaving group at the 2'-position of the N^4-acetyl cytidine derivative **91** was investigated by synthesising the 2'-tosylated compound **107**. Compound **107**, however, was found to be even less thermally stable than the 2'-mesylated counterpart (Scheme **3.24**).

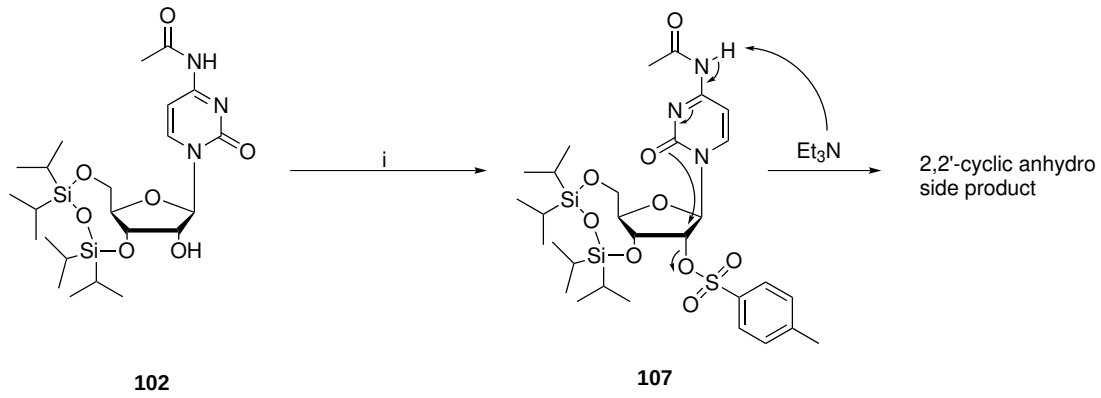

Reagents and conditions: **i)** TsCl, Et_3N, DCM, r.t., 6 h

Scheme 3.24: The 2'-tosylated derivative decomposed even faster than compound **91** supporting previous assumptions about leaving group abilities and their influence on 2,2'-intramolecular cyclisations.

Double N^4-acetylation/benzoylation was investigated using compounds **108** and **109** as starting materials according to published results[216]. However, the disubstituted products could not be observed. Reaction time and temperature were varied as well as higher amounts of the acetylating agent were tested (Scheme **3.25**).

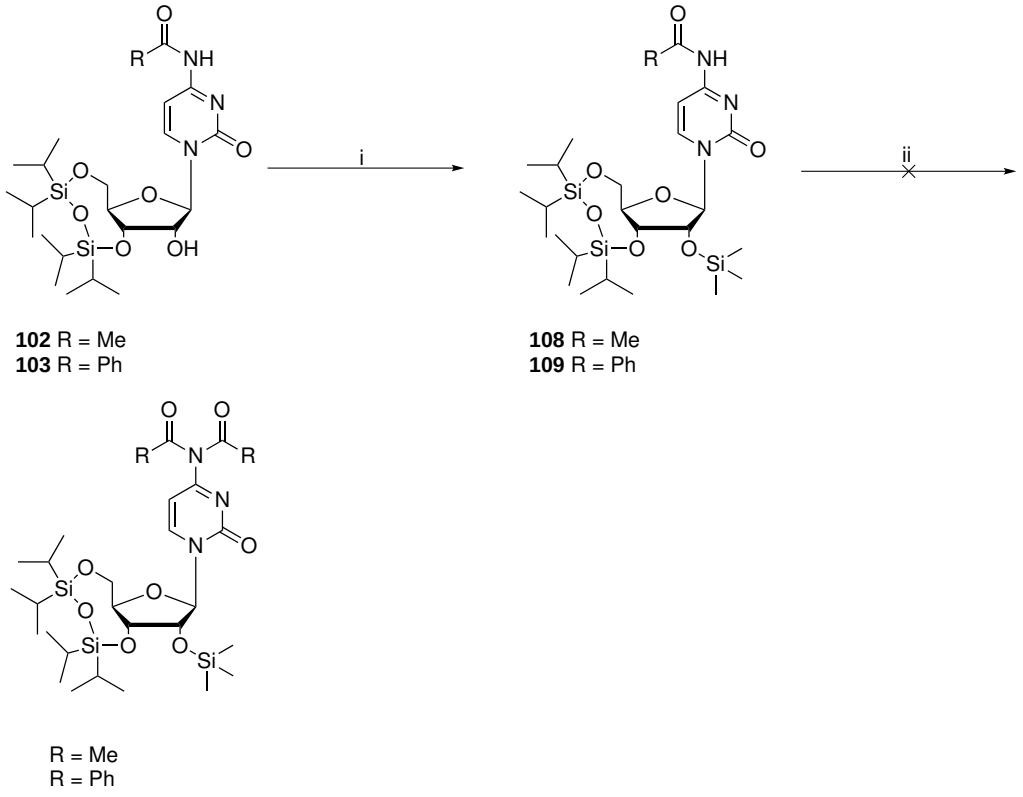

Reaction conditions: **i)** TMSCl, Et_3N, DCM, 0°C - r.t., 3 h, 73-82%; **ii)** either AcCl, Ac_2O or BzCl in DCM/THF/dioxane, 0°C/r.t./reflux, 2-12 h.

Scheme 3.25: N^4-acetylation/benzoylation of **108** and **109** could not be achieved using different reaction conditions.

Starting from commercially available cytidine (**110**) compounds **113** and **114** could be successfully synthesised. Phthalimide **113** was obtained by converting the 4-amino-group of compound **112** into the cyclic diamide using phthaloyl chloride and DMAP in dry pyridine[217]. The desired product gave a strong UV signal (254 nm) with R_f=0.8 (DCM/MeOH=94/6). Coevaporation with dry pyridine prior to the reaction and dropwise addition of a phthaloyl chloride solution in DCM furnished **113** in 69% yield. Additionally, compound **114** was successfully synthesised using similar conditions as for compounds **75** and **85** except a higher excess of di-tert-butyl dicarbonate. The starting material was completely converted after 5 h and no other spot on the TLC according to the mono-protected

intermediate could be found. NMR and ESI-MS confirmed that compound **114** was successfully obtained in 77% yield (Scheme **3.26**).

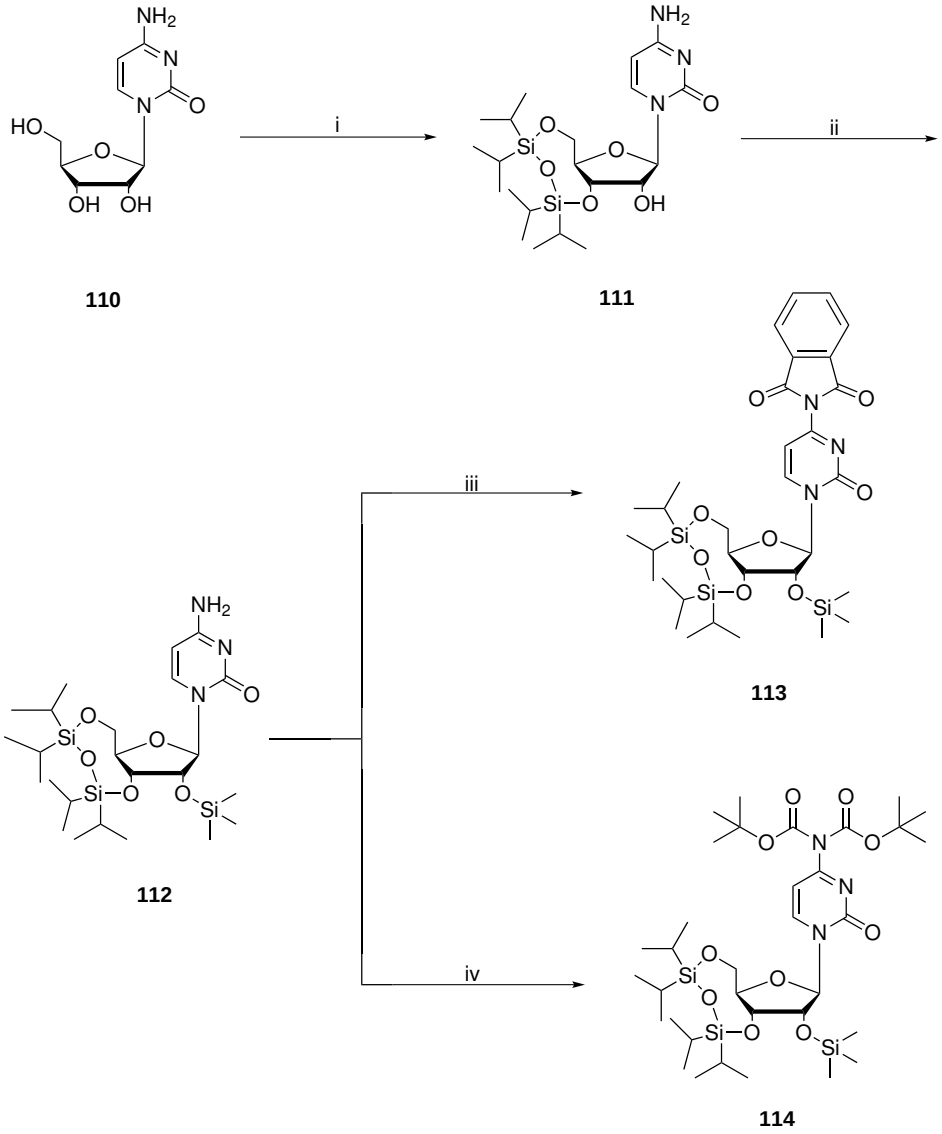

Reaction conditions: **i)** $TIPDSCl_2$, pyridine, 0°C - r.t., 18 h, 81%; **ii)** TMSCl, Et_3N, DCM, 0°C - r.t., 2 h, 83%; **iii)** phthaloyl chloride, DMAP, pyridine, 0°C - r.t., 4 h, 69%; **iv)** Boc_2O, DMAP, DCM, r.t., 5 h, 77%.

Scheme 3.26: Formation of the 4-amino-protected compounds **113** and **114**. TIPDS and subsequent TMS protection starting from commercially available cytidine furnished **112** which was then converted to the 4-amino-protected derivatives **113** and **114**.

Di-tert-butyl dicarbonate had to be used in 5 equivalents or higher in order to fully convert the starting material into the di-Boc protected compound **114**. Otherwise both the single (**114b**) and double **114** Boc-protected compounds

were isolated. The straightforward synthesis of **114** is surprising considering the unsuccessful attempts to synthesise the double acetylated- and benzoylated derivatives. Compounds **113** and **114** were then treated with *p*TsOH in dry DCM at 0 °C in order to selectively deprotect the 2'-position. In case of **114**, the addition of *p*TsOH was performed slowly over a time period of 15 min in order to avoid cleavage of the Boc-groups. Subsequent mesylation of **115** and **116** furnished **117** and **118** in good yields (65-71%) (Scheme **3.27**).

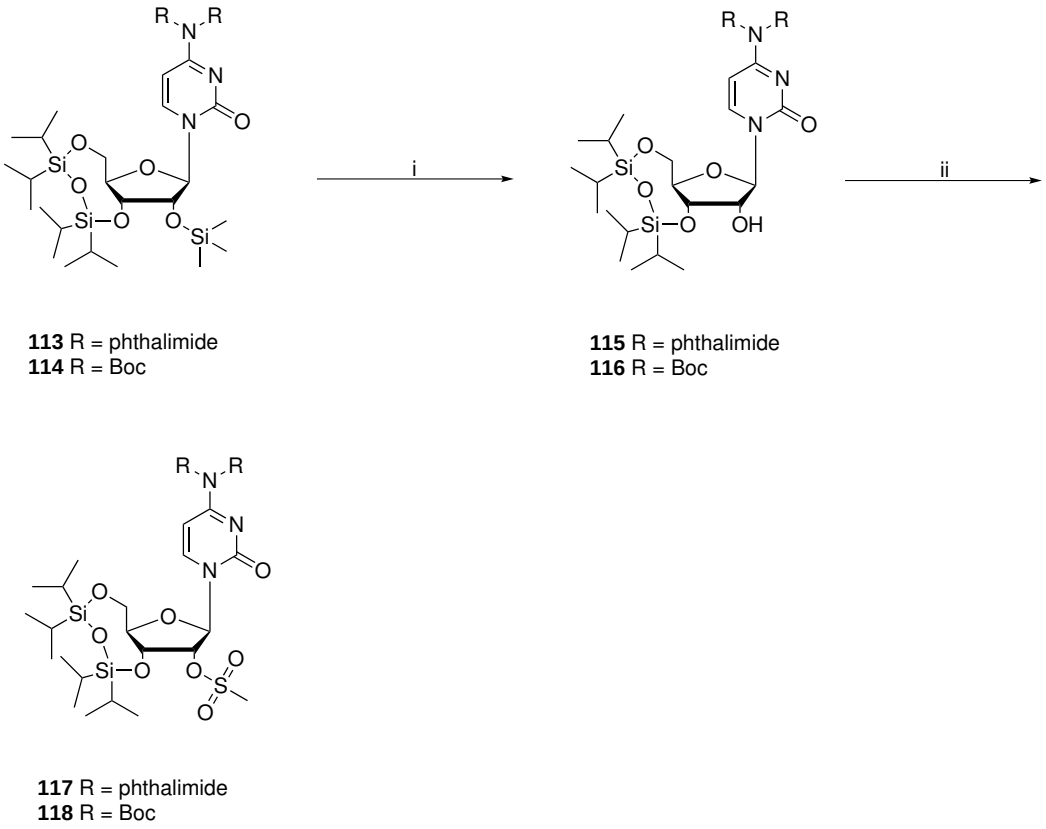

113 R = phthalimide
114 R = Boc

115 R = phthalimide
116 R = Boc

117 R = phthalimide
118 R = Boc

Reaction conditions: **i)** pTsOH, DCM, 0°C, 30 min, 62-66%; **ii)** MsCl, Et_3N, DCM, 0°C - r.t., 2 h, 65-71%

Scheme 3.27: Selective 2'-deprotection and subsequent mesylation furnished compounds **117** and **118**.

The Boc-protected precursor was considered as more suitable for automated synthesis modules as N^4-deprotection should be more straight forward compared

to the phthalimide which usually involves chemicals such as $NaBH_4$ or methyl amine and long reaction times[218,219]. Furthermore, treating compound **117** with fluoride-containing agents for deprotection did not lead to the desired compound **94**.

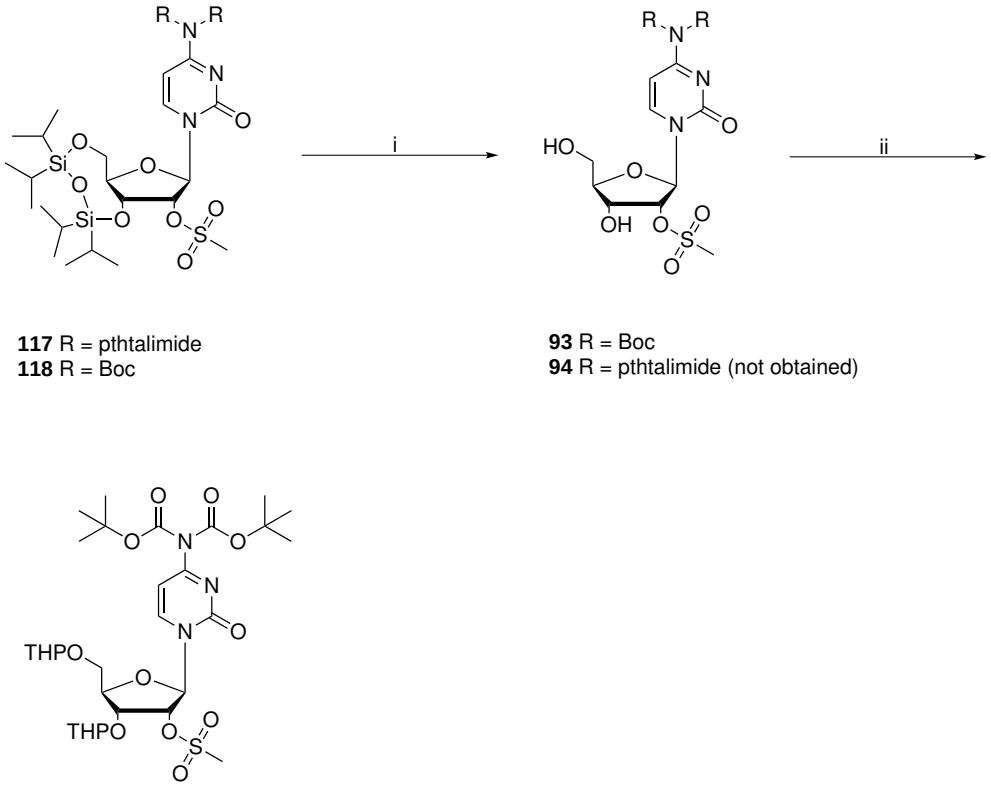

Scheme 3.28: Selective TIPDS-deprotection gave the intermediate **93** which was used for stability studies. Subsequent THP-protection furnished FAC-precursor **119** as a mixture of four diastereomers in moderate yields and high purities.

Based on these results, the corresponding fluorination precursor **119** was synthesised. Precursor **119** was obtained in good yield (47%), as an off-white powder and as a mixture of four diastereomers with coincidental ratios. The purity was determined using analytical HPLC and calculated for ≥98% (Scheme **3.28**).

The non-radioactive reference compound **120** was obtained by treating precursor **119** with an anhydrous 1 M TBAF/THF solution in DMF at 110 °C for 2 h according to the method previously described for the FAU-intermediate **80** (Scheme **3.29**). The accessibility of this compound was crucial as it allowed identification of the ^{18}F-labelled intermediate after radiofluorination via co-injection.

Despite ESI-MS, ^{19}F NMR was used to confirm the product by showing four distinguishable fluorine signals each corresponding to one of the four diastereomers that are present due to the THP-protecting groups (see Appendix). Intermediate **120** was obtained in moderate yields (29%) and high purities (≥98%) which was considered as the most important factor for HPLC purposes.

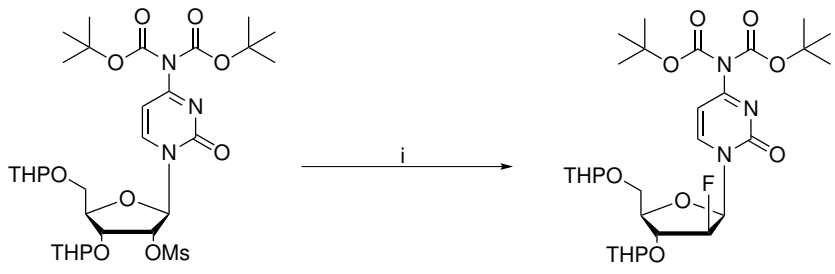

FAC-precursor (119) **FAC-intermediate (120)**

Reagents and conditions: **i)** 1 M TBAF/THF, DMF, 110°C, 100 min, 29%

Scheme 3.29: TBAF-mediated fluorination furnished the FAC-intermediate **120** as a mixture of four diastereomers in moderate yields.

3.3.3 Radiochemistry

Subsequent radiofluorinations to give the ^{18}F-FAC-intermediate **121** were carried out using dried [^{18}F]fluoride/K_{222}/$KHCO_3$ in different solvents and at various temperatures (Scheme **3.30**). [^{18}F]fluoride was released from the QMA cartridge using a K_{222}/$KHCO_3$-solution. Table **10** shows the analytical RCYs calculated using radio-TLC.

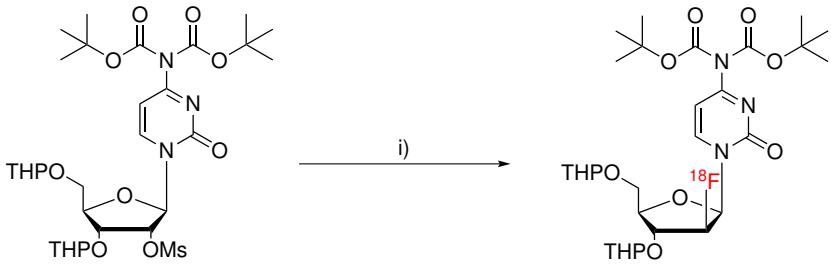

FAC-precursor **(119)** ^{18}F-FAC-intermediate **(121)**

Reaction conditions: **i)** [^{18}F]fluoride/K_{222}, 90-130°C, solvent, 20-30 min.

Scheme 3.30: Radiofluorination of precursor **119** furnished the radioactive intermediate **121**.

The highest RCY (9.4%) of **121** was obtained using DMF at 110 °C for 20 minutes (Table **10**, Figure **26**). MeCN or *t*BuOH as solvent did not show any conversion. However, higher temperatures and longer reaction times led to decreased RCY, presumably due to increased formation of the anhydro intermediate. Furthermore, less basic reaction conditions by using $KHCO_3$ instead of K_2CO_3 led to an improved RCY.

Table 10: Analytical radiochemical yields of **121** using different reaction conditions.

run	solvent	T [°C]	t [min]	RCY [%] (n = 3)
1	tBuOH	95	20	n/a
2	MeCN	90	20	n/a
3	DMF	90	20	1.3±0.3
4	DMF	95	20	2.6±0.2
5	DMF	100	20	4.9±0.6
6	DMF	105	20	7.7±0.8
7	DMF	110	20	9.4±0.8
8	DMF	110	30	7.9±0.6
9	DMF	115	20	6.9±0.5
10	DMF	120	20	4.1±0.4
11	DMF	125	20	2.3±0.2
12	DMF	130	20	1.8±0.2

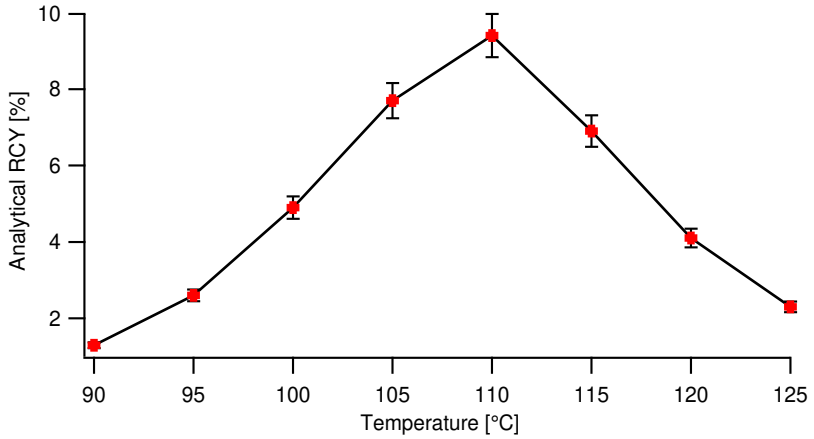

Figure 26: Analytical RCY of precursor **119** plotted against the reaction temperature. The reactions were carried out in DMF with 20 min reaction time. Despite the balance between precursor stability and reactivity, the reaction temperature displays another crucial parameter for radiofluorination.

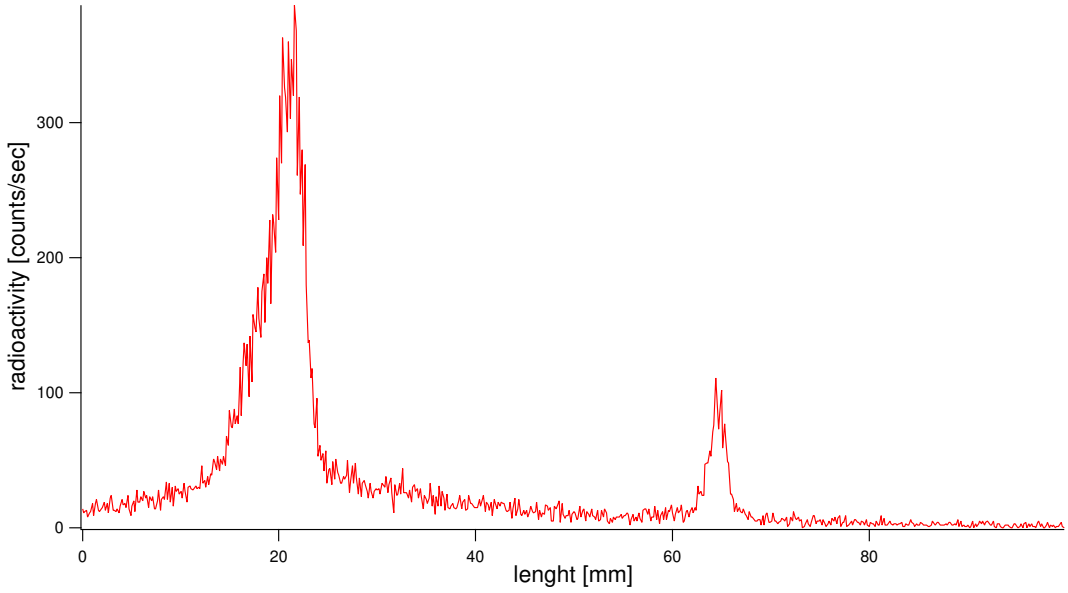

Figure 27: Radio-TLC chromatogram of the crude reaction mixture after radiofluorination.

After trapping unreacted [^{18}F]fluoride on an Al cartridge and organic residues on a C18 cartridge, the ^{18}F-labelled intermediate **121** was released using EtOAc (3 mL). Product confirmation was carried out by radio-TLC and radio-HPLC with co-injection of the non-radioactive reference standard **120** (Figure **28,29**).

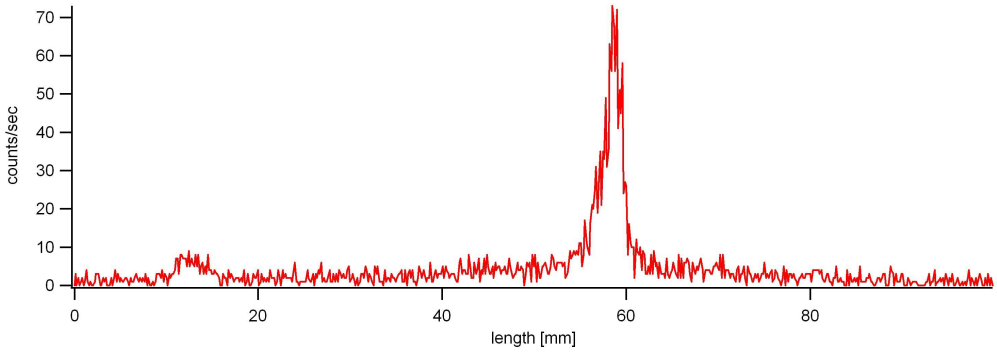

Figure 28: Radio-TLC chromatogram of the EtOAc-phase after purification of the [^{18}F]fluorinated intermediate **121** using Al and C18 cartridges.

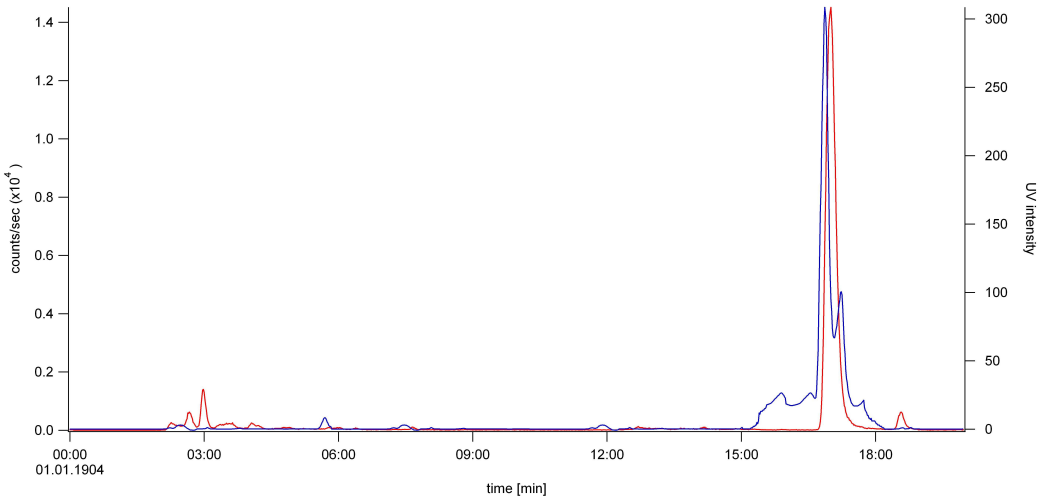

Figure 29: Radio-HPLC chromatogram of the purified (Al/C18 cartridge) [^{18}F]fluorinated intermediate **121** (red trace) with co-injected reference compound **120** (blue (UV) reference peak)

After elution of the labelled intermediate from the Al cartridge with EtOAc into a clean V-vial, the solvent was removed at 90 °C under a stream of nitrogen in a separate heating module. 2 M HCl solution was added to the dried residue and then stirred at 95 °C for 20 min (Scheme **3.31**, top). Neutralisation with 2 M NaOH solution was followed by semi-preparative HPLC purification. ^{18}F-FAC was eluted after 22.5 minutes at a flow rate of 3.5 mL/min using 3% MeCN/H_2O as the mobile phase. After collection of the product the HPLC solvent was removed under reduced pressure and a stream of nitrogen. The radioactive product was taken up in saline and subsequently flushed through a sterility filter to obtain a sterile and clean aqueous solution of ^{18}F-FAC.

An aliquot of the purified sterile sample was analysed by HPLC (Figure **30**) via co-elution of both possible 2'-^{19}F-isomers FC and FAC (Scheme **3.31**, bottom) as reference. The obtained ^{18}F-labelled product was confirmed as the desired target compound ^{18}F-FAC. Radiochemical reactions were carried out using starting activities between 2.5-55 GBq. Final product activities of 134-1045 MBq were obtained resulting in RCY of 4.3-5.5% (n = 6, decay-corrected from end of bom-

bardment (EoB)) with high radiochemical purities (≥98%) and specific activities ≥1700 mCi/μmol. The total synthesis time was 168 min after the end of bombardment (EoB).

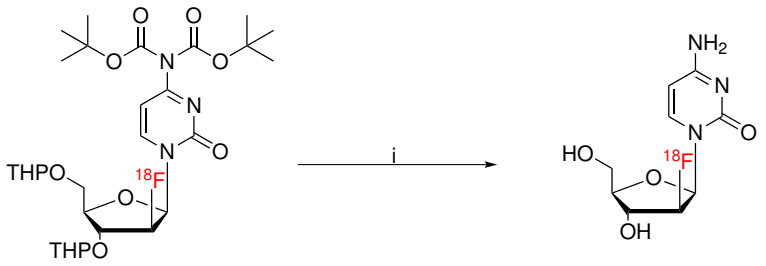

121 **^{18}F-FAC (15)**

Reaction conditions: **i)** 2 M HCl, 95°C, 20 min.

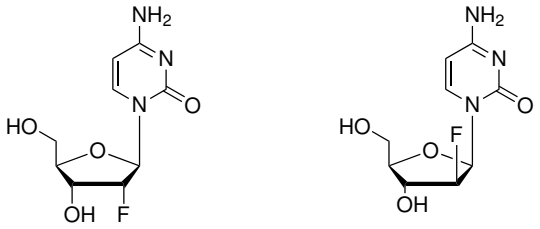

FC (42) **FAC (5)**

Scheme 3.31: top: deprotection scheme towards the ^{18}F-labelled nucleoside ^{18}F-FAC; bottom: structure of the two possible 2'-fluoro stereoisomers 2'-fluorocytidine (FC, **42**) and 2'-fluoroarabinocytidine (FAC, **5**).

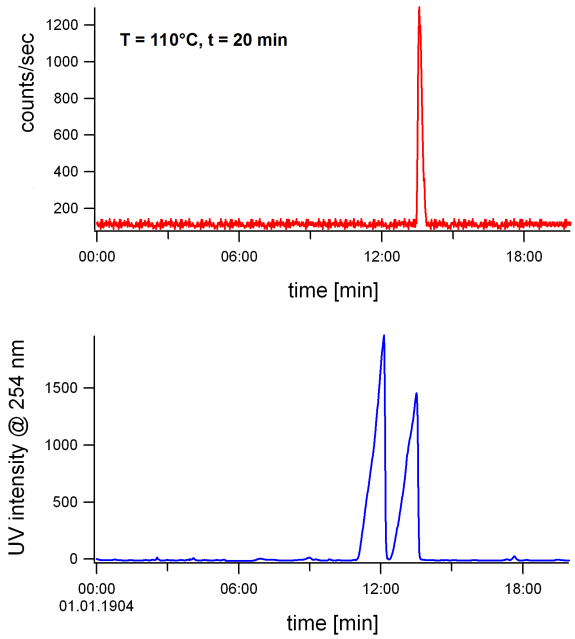

Figure 30: The purified and sterilised product solution was analysed by radio-HPLC and co-elution of both stereoisomers and reference standards FC (R_t=11.7 min) and FAC (R_t=13.1 min) showing that the correct stereoisomer was obtained.

A carrier-added synthesis was performed and the resulting product solution stored for 48 h for decay. Subsequently, the sample was characterised by LC-MS showing a single signal with the *m/z*-values of 245.4 (5%) $[(M + H)^+]$ and 267.7 (95%) $[(M + Na)^+]$, respectively. Furthermore, the influence of reaction time and temperature on the stereospecific outcome of this radiofluorination reaction was studied. The diagrams below show radioactivity traces recorded after different reaction temperatures and reaction times (Figure **31**).

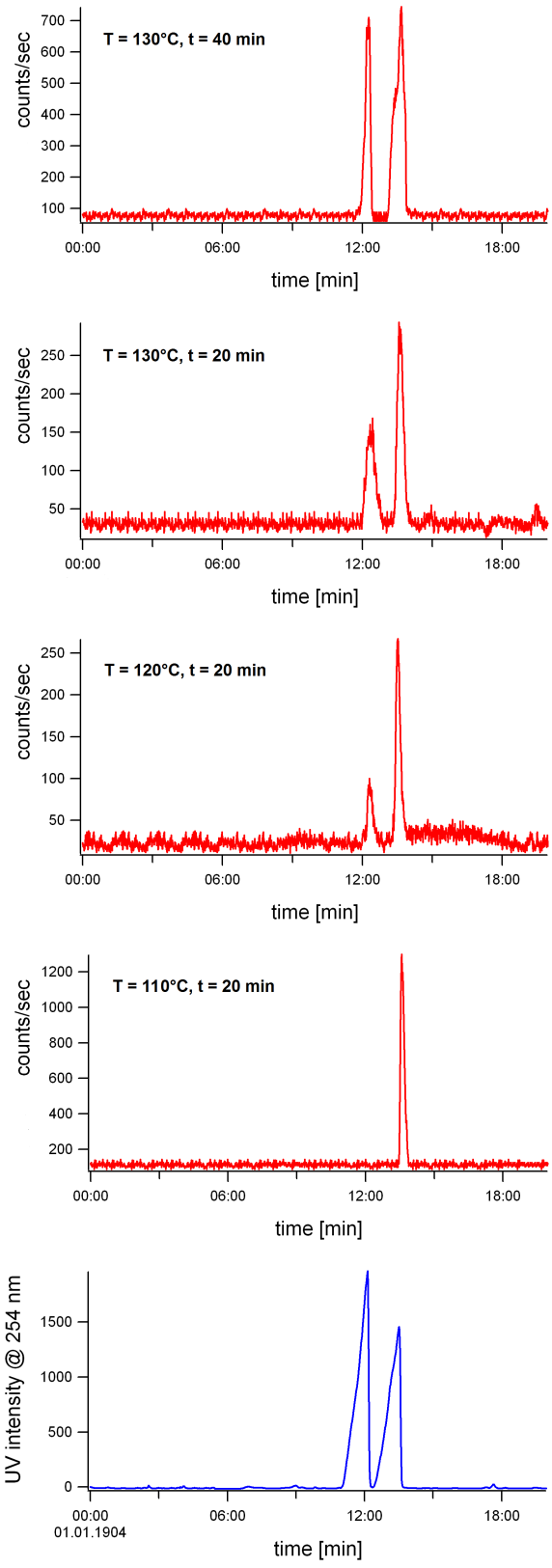

Figure 31: Increased reaction temperature and longer reaction times led to anhydro formation and subsequently to the formation of 2'-^{18}F-FC shown by the increasing intensity of the radioactivity signal at ≈11.8 min. That may explain the decrease in the observed RCY for the desired arabino compound (Table **10**). Both radioactive isomers ^{18}F-FAC to ^{18}F-FC were collected in one fraction during semi-preparative HPLC purification.

The chromatograms above (Figure **31**) show the temperature and reaction time dependence of the stereochemical outcome of the radiofluorination reaction and hence support previous assumptions regarding the 2,2'-intramolecular cyclisation (Scheme **3.32**). Increased reaction temperature and longer reaction times led to the formation of the 2,2'-cyclic anhydro side product which in turn gave the 2'-[^{18}F]fluoro-ribo isomer. Hence, the ratio of ^{18}F-FAC to ^{18}F-FC decreases when reaction temperature and time increase which is indicated by the consecutively increasing radioactivity signal at ≈12 min, which, as co-injection shows, corresponds to the 2'-[^{18}F]fluoro-ribo-isomer.

Due to the instability of Boc-protecting groups during radiofluorinations, most likely due to *in situ* generation of hydrogen fluoride from remaining trace water, the cleavage of a Boc group may lead to the formation of a N^4-mono-Boc protected intermediate (**122**) which in turn may undergo base-mediated intramolecular cyclisation as shown in Scheme **3.32**. Subsequent nucleophilic attack of [^{18}F]fluoride at the 2'-position would lead to the formation of the 2'-[^{18}F]fluoro-ribo isomer ^{18}F-FC.

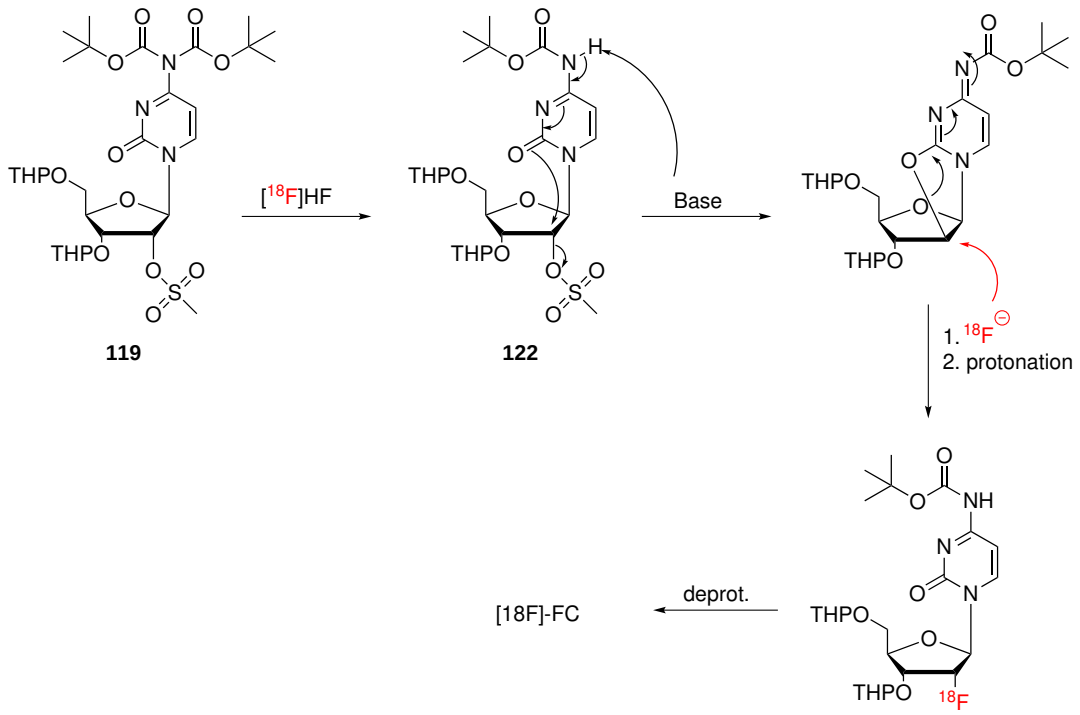

Scheme 3.32: Single (or double) deprotection of the Boc groups would enable base-mediated intramolecular cyclisation of N^4-single Boc-protected compound **122**. ^{18}F-mediated nucleophilic attack of the 2'-position would lead to the observed 2'-[^{18}F]fluoro-ribo isomer ^{18}F-FC.

This newly developed radiochemical approach to give ^{18}F-FAC applied the principle of a late-stage radiofluorination for the first time to a cytidine-based nucleoside. Even though the RCY of this method is low compared to the reported RCY of the latest method (31±5%)[180], less steps after radiofluorination and an ^{18}F-FDG-like synthetic route (radiofluorination followed by deprotection) using an intact nucleoside moiety may simplify the use of this tracer in routine production. However, the results presented in this section concerning ^{18}F-FAC should be regarded as first trials. Further investigations using different radiochemistry set-ups (e.g. different radiosynthesisers, microwave-assisted synthesis, continuous-flow systems) have to be carried out in order to validate the clinical potential of this method.

3.4 Radiochemical approach towards ^{18}F-gemcitabine

2'-carbonyl nucleosides were the only reported 2'-activated nucleoside analogues that enabled a late-stage formation of the *gem*-difluoro system. Consequently, the proposed synthetic approach (Scheme **3.33**) towards ^{18}F-gemcitabine (**54**) was based on previously published data[159] concerning a 2'-deoxodifluorination as presented in section **1.3.2**. Considering the mechanism (Scheme **3.34**, top) of the 2'-deoxodifluorination of a 2'-keto nucleoside, it was assumed that [^{18}F]fluoride could replace pyridine/HF as an additional fluoride source in a labelling reaction (Scheme **3.34**, bottom). [^{18}F]fluoride would hence be incorporated first by forming an oxyanion at the 2'-position which then could react with DAST. Subsequent nucleophilic substitution of the generated leaving group by fluoride may lead to the 2'-difluorinated and ^{18}F-labelled gemcitabine intermediate **123** (Schemes **3.33** and **3.34**).

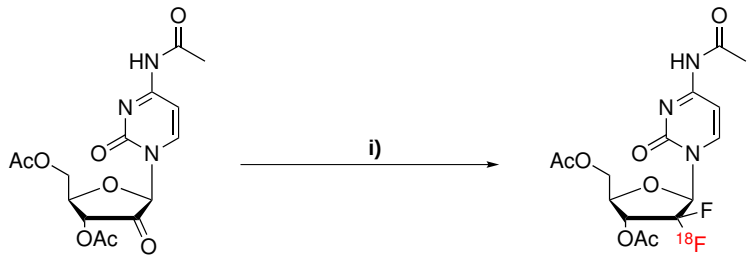

35 **123**

Reaction conditions: **i)** [^{18}F]fluoride/K_{222}, DAST/XtalFluor/Fluolead, MeCN/DMF, 30-120 °C, 60-90 min.

Scheme 3.33: Proposed synthetic scheme towards a ^{18}F-labelled *gem*-difluoro system as present in the ^{18}F-gemcitabine intermediate **123**. In comparison to the reported non-radioactive deoxodifluorination carried out at r.t. for 24 h in anhydrous DCM with 80% conversion, the time of the labelling reaction is restricted due to the half-life of ^{18}F. Thus, higher reaction temperatures in higher boiling polar aprotic solvents were used in order to compensate shorter reaction times.

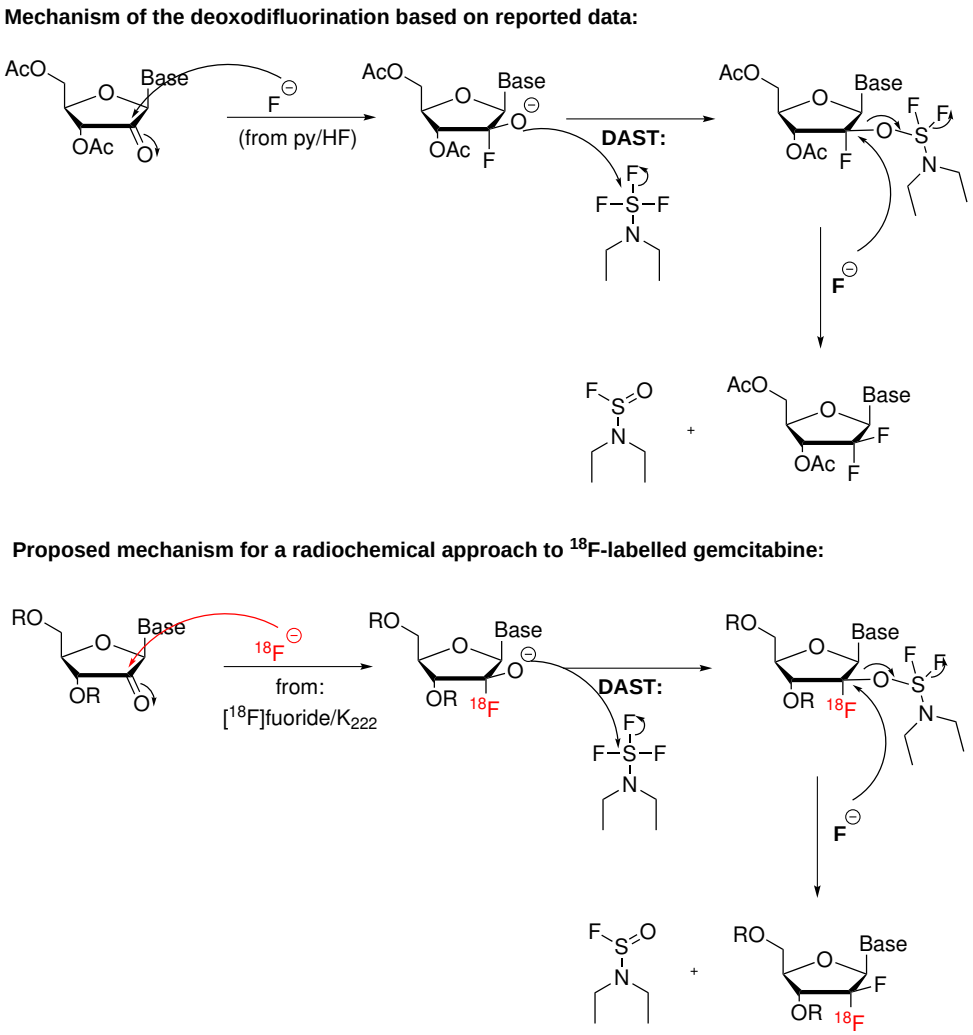

Scheme 3.34: Top: Mechanism of the reported non-radioactive deoxodifluorination towards gemcitabine. Bottom: Hypothetical mechanism of a labelling reaction to give intermediate **123** using [^{18}F]fluoride as an additional fluoride source.

Based on the results from the previous chapter involving the radiosynthesis of ^{18}F-FAC, the first thoughts regarding an appropriate precursor with an activated 2'-position for deoxodifluorination resulted in structure **124** (Figure **32**).

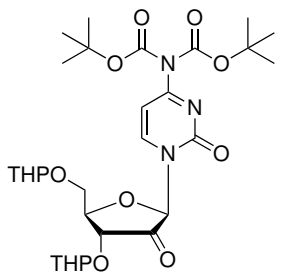

124

Figure 32: Proposed structure of a novel gemcitabine precursor based on previous results.

Consequently, 2'-oxidation of compound **116** using DMP-oxidation conditions was successfully carried out furnishing 2'-keto compound **125** in 57% yield (Scheme **3.35**).

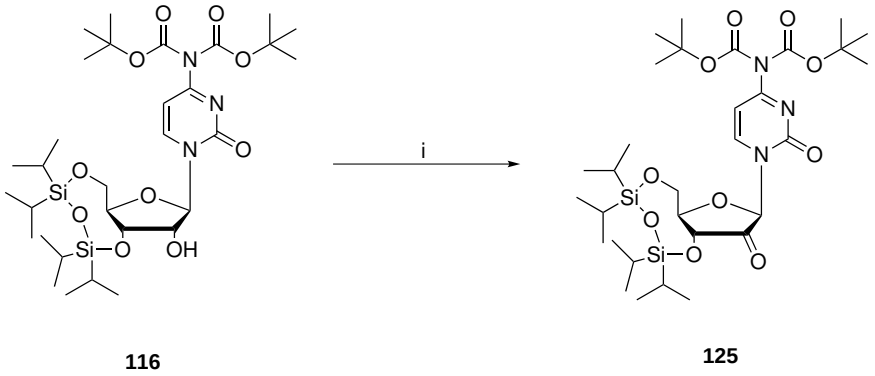

116 **125**

Reaction conditions: **i)** DMP, DCM, r.t., 24 h, 61%

Scheme 3.35: 2'-oxidation of **116** was successful using DMP.

However, all attempts to cleave the 3',5'-protecting group failed. Compound **125** formed side products such as the fully deprotected nucleoside when treated with TBAF or related fluoride containing reagents. The second reason why this approach was finally abandoned was the fact that acid-labile protecting groups such as Boc and THP might be cleaved during the reaction with HF-generating agents such as DAST and Fluolead.

Precursor **35** was adopted from previously published data[159] as outlined in section **1.3.2** and synthesised by using the TIPDS-protected cytidine derivative **102**. Subsequent 2'-oxidation to give the 2'-carbonyl compound **126** was carried out using both Dess-Martin Periodinan (DMP) reagent and classic Swern oxidation conditions (Scheme **3.36**). Both methods furnished the desired 2'-carbonyl compound **126** in moderate yields (49-55%). Swern oxidation was preferred due to less costly material and shorter reaction times.

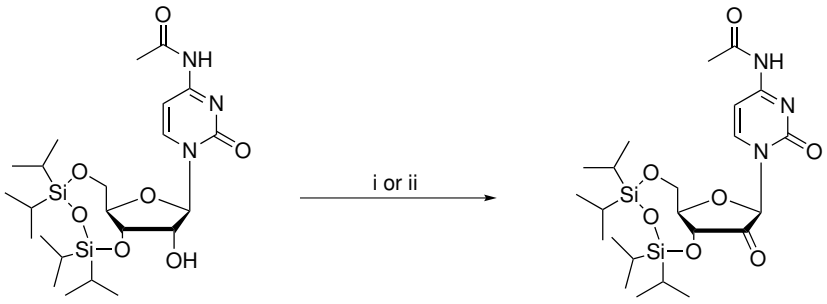

102 **126**

Reagents and conditions: **i)** DMP, DCM, r.t., 24 h, 55%; **ii)** oxalyl chloride, DMSO, Et_3N, DCM, -78°C - r.t., 1 h, 49%.

Scheme 3.36: Synthetic scheme towards the 2'-carbonyl compound **126**. Both DMP and Swern oxidation furnished **126** in 49-55% yield.

According to published data[159], TIPDS deprotection and subsequent acetylation of the 3'- and 5'-hydroxy groups were carried out using anhydrous Et_3N/HF in DCM for deprotection followed by acetylation using acetyl chloride in dry DCM at r.t. After basic work-up of the reaction mixture, two consecutive column purifications were required in order to obtain precursor **35** in high purities ($\geq$98%) and moderate overall yield (32%) (Scheme **3.37**).

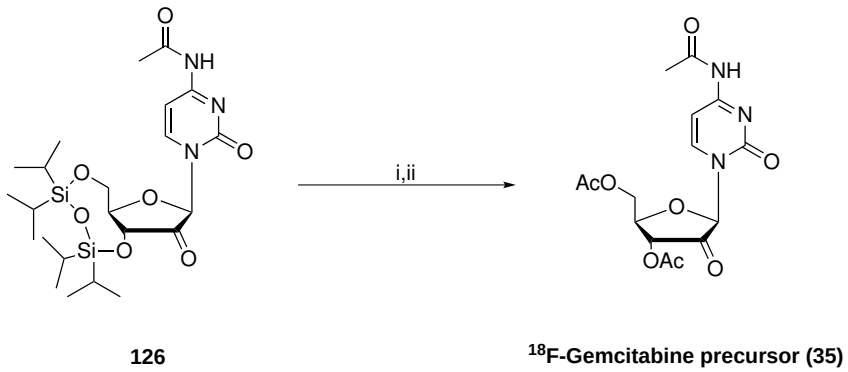

126 **^{18}F-Gemcitabine precursor (35)**

Reagents and conditons: **i)** Et_3N/HF, DCM, r.t., 45 min; **ii)** AcCl, Et_3N, DCM, 0°C - r.t., 24 h, 32% overall yield.

Scheme 3.37: Et_3N/3HF-mediated deprotection and subsequent acetylation furnished gemcitabine precursor **35**.

The alternative route towards precursor **35** via cyclic anhydro compound **127** was investigated by my 4th year MPharm project student Josephine Sze. It was found that this route is faster but furnishes lower overall yields (Scheme **3.38**). **127** is hydrolised under basic conditions and the 2'-hydroxy product was filtered off and purified. Oxidation of compound **128** furnished precursor **35** in 43% yield and high purities (≥98%).

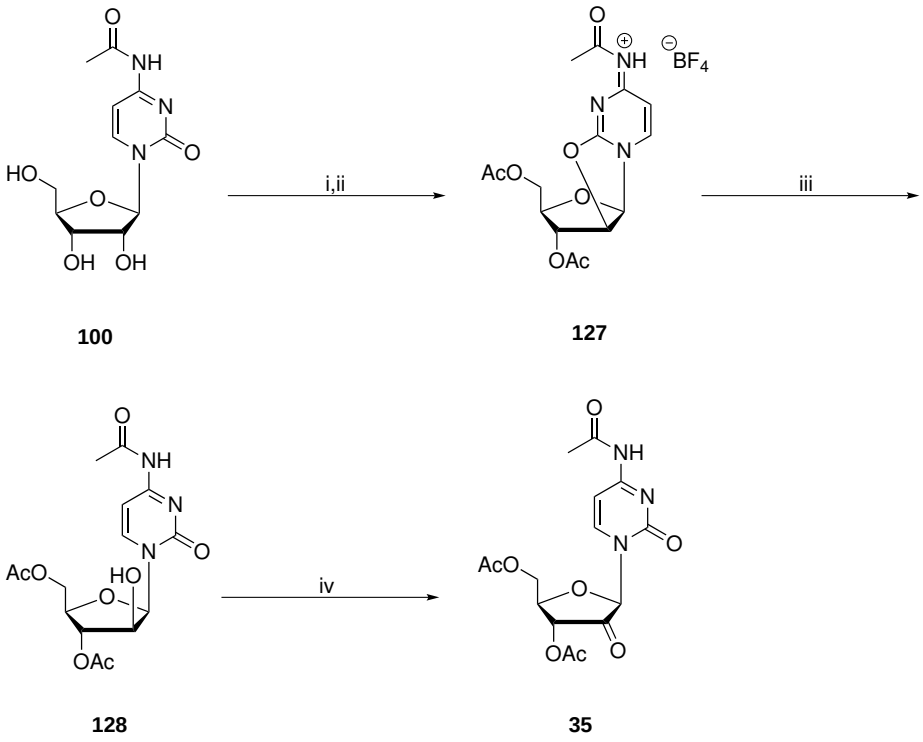

Reagents and conditons: **i)** BF_3/OEt_2, MeCN, reflux, 1 h; **ii)** AcCl, reflux, 2 h, 39% (overall)
iii) sat. $NaHCO_3$, r.t., 24 h, 54%; **iv)** DMP, MeCN, 0°C - r.t., 24 h, 43%.

Scheme 3.38: Alternative synthetic route to give gemcitabine precursor **35**.

After successful synthesis of precursor **35**, the 2'-difluorinated reference compound **129** for the analysis of labelling reactions with radio-TLC and radio-HPLC was synthesised via acetylation of all available hydroxy and amino groups of commercially available gemcitabine. Compound **129** was obtained in high yield (93%) (Scheme **3.39**).

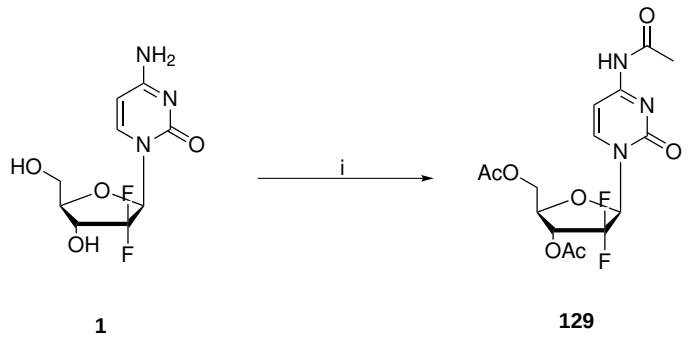

1 **129**

Reagents and conditions: **i)** AcCl, Et_3N, DCM, r.t., 24 h, 93%

Scheme 3.39: Synthesis of the *gem*-2'-difluoro reference standard **129** starting with commercially available gemcitabine.

Prior to labelling reactions, non-radioactive test reactions were carried out in order to investigate whether the 2'-difluorinated intermediate **129** could be synthesised using an organic fluorination agent such as DAST and an additional fluoride source such as pyridinium hydrogen fluoride at higher temperatures and shorter reaction times with regard to subsequent radiofluorinations (Scheme **3.40**).

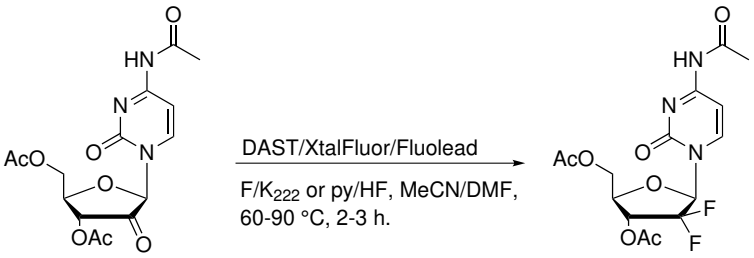

35 **129**

Scheme 3.40: Non-radioactive fluorination of precursor **35** to give the *gem*-2'-difluoro reference standard **129**.

Precursor **35** was treated with different organic fluorination agents (OFA) in combination with either KF/K_{222} or pyridinium hydrogen fluoride (py/HF) as summarised in table **11**. In general, precursor **35** (20 mg) was dissolved in the

reaction solvent (1 mL) under inert atmosphere before either KF/K_{222} or py/HF (1 eq.) was added to the mixture. A solution of the organic fluorination agent (10 eq.) in the reaction solvent (0.2 mL) was then added dropwise to the reaction mixture before heating.

Table 11: Results of the non-radioactive 2'-deoxodifluorinations using precursor **35**.

run	OFA	add. fluoride source	solvent (T [°C])	t [h]	yield (**129**) [%] (n = 1)
1	DAST	KF/K_{222}	MeCN (60)	3	n/a
2	DAST	py/HF	MeCN (90)	2	n/a
3	DAST	KF/K_{222}	DMF (60)	3	n/a
4	DAST	py/HF	DMF (90)	2	n/a
5	XtalFluor M	KF/K_{222}	MeCN (60)	3	n/a
6	XtalFluor M	py/HF	MeCN (90)	2	n/a
7	XtalFluor M	KF/K_{222}	DMF (60)	3	n/a
8	XtalFluor M	py/HF	DMF (90)	2	n/a
9	Fluolead	KF/K_{222}	MeCN (60)	3	n/a
10	Fluolead	py/HF	MeCN (90)	2	n/a
11	Fluolead	KF/K_{222}	DMF (85)	3	n/a
12	Fluolead	py/HF	DMF (145)	2	n/a

Deoxodifluorinations in presence of an organic fluorination agent (OFA = DAST, XtalFluor M, Fluolead; 10 eq. relative to precursor) and either py/HF or KF/K_{222} (1 eq.) using precursor **35** (20 mg, 51.4 μmol) in 1.2 mL solvent. However, the *gem*-difluoro intermediate **129** could not be observed.

Evidence for compound **129** could not be provided under the reaction conditions shown in table **11**. The crude reaction mixtures were analysed by TLC, ESI-MS and HPLC. Even though the starting material was fully converted after the given reaction time side products could not be identified.

Although non-radioactive test reactions did not yield the 2'-difluorinated intermediate **129**, a series of radiofluorination reactions was carried out (Scheme **3.41**). The radiochemistry set-up in the hot cells as well as the Eckert & Ziegler module system enabled more reproducible reaction conditions. Furthermore, the detection of radioactivity by using radio-TLC and radio-HPLC systems offered a higher sensitivity in comparison to UV detectors. Consequently, lower concentra-

tions of ^{18}F-labelled compounds can be detected. Table **12** shows the conditions of the labelling reactions carried out using the Eckert & Ziegler module system.

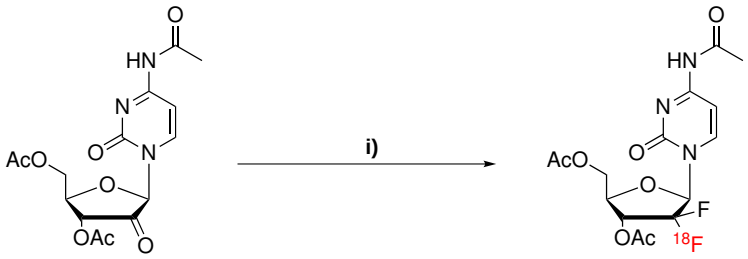

35 **123**

Reaction conditions: **i)** [^{18}F]fluoride/K_{222}, DAST/XtalFluor/Fluolead, MeCN/DMF, 30-120 °C, 60-90 min.

Scheme 3.41: Labelling reaction to give the radioactive gemcitabine intermediate **123**.

Table 12: [^{18}F]fluorination reactions using precursor **35**.

Run	OFA (eq.)	[^{18}F]fluoride [GBq]	T [°C]	t [min]	solvent	RCY [%] (n = 1)
1	Fluolead (5.0)	5	70	60	MeCN	n/a
2	Fluolead (5.0)	5	90	60	MeCN	n/a
3	Fluolead (10.0)	8	60, 100	30, 30	DMF	n/a
4	Fluolead (10.0)	8	60, 120	30, 50	DMF	n/a
5	Fluolead (10.0)	10	50, 85	30, 50	MeCN	n/a
6	XtalFluor (10.0)	8	40, 80	30, 50	MeCN	n/a
7	XtalFluor (10.0)	8	50, 90	30, 60	MeCN	n/a
8	DAST (5.0)	8	30, 50	30, 30	MeCN	n/a
9	DAST (10.0)	8	30, 50	30, 50	MeCN	n/a
10	DAST (5.0)	8	50, 85	30, 30	MeCN	0.2±0.1*
11	DAST (10.0)	8	50, 85	30, 60	MeCN	0.3±0.05*
control	DAST (10.0)	8	50, 85	30, 60	MeCN	n/a

*n = 3; Deoxodifluorination reactions in presence of an organic fluorination agent (OFA = DAST, XtalFluor M, Fluolead; eq. relative to precursor) and 5-10 GBq of [^{18}F]fluoride. Each run was carried out using a total solvent volume of 400 μL and precursor **35** (10 mg, 2.7 μmol). The control run was performed without precursor **35** present. The influence of temperature and reaction time on the formation of the ^{18}F-labelled gemcitabine intermediate **123** was investigated using radio-HPLC by co-elution with the non-radioactive reference standard **129**. Radio-HPLC provided evidence that experiments 10 and 11 furnished intermediate **123** in very low RCY (0.2-0.3%, decay-corrected).

After azeotropic drying of [^{18}F]fluoride/K_{222}, precursor **35** (10 mg) dissolved in reaction solvent (0.2 mL) was added. Subsequently, the organic fluorination agent dissolved in reaction solvent (0.2 mL) was added to the reaction mixture. The reaction was stirred (60-90 min) at temperatures between 30-120 °C before the reaction mixture was analysed using radio-HPLC.

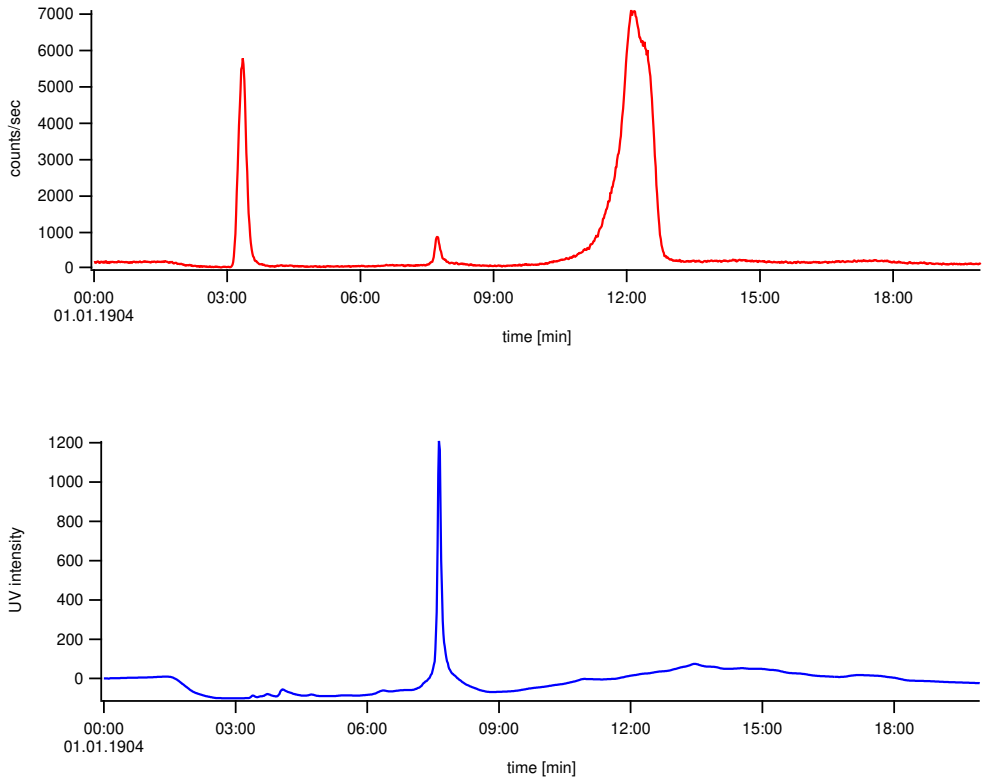

Figure 33: Radioactivity-trace (top) and UV-trace (bottom) of the HPLC chromatogram of run 11. The ^{18}F-labelled *gem*-difluoro intermediate **123** was co-eluted (isocratic, 50% MeCN/H_2O) with the non-radioactive reference compound at R_t=7.9 minutes.

Analytical radio-HPLC (60% MeCN in H_2O) of the crude reaction mixture with co-elution of the non-radioactive standard **129** gave the chromatograms shown above (Figure **33**) for run 11. Figure **33** showed that the UV signal of the reference standard (bottom) matched a radioactivity signal of the reaction mixture (top) providing evidence that the [^{18}F]fluorinated intermediate **123** had

been formed. HPLC experiments without co-elution of **129** did not show a corresponding UV signal which excluded the possibility of the formation of considerable amounts of non-radioactive intermediate **129** during the reaction. The radioactivity signal at ≈3.2 min was due to unreacted [^{18}F]fluoride. The radioactivity signal at ≈12 min was observed in all runs including the control reaction without precursor **35** present. Thus, it was assumed that the radioactivity peak at ≈12 min could correspond to a ^{18}F-labelled DAST species. The [^{18}F]fluorinated intermediate **123** could be purified using Al and C18 cartridges.

One explanation for the low RCY (0.2-0.3%) may be the complex mechanism of the deoxodifluorination that was proposed in scheme **3.34**. The non-radioactive difluorination reaction reported by Kjell *et al.*[159] (Scheme **1.10**) indicated 80% conversion after 24 h at r.t. Hence, it was assumed that higher temperatures during radiofluorination were needed in order to compensate a shorter reaction time due to radiochemical decay. However, DAST is not stable at high temperatures[151] which led to the assumption that DAST was decomposing during the labelling reaction resulting in a low yield of the desired product **123**. Furthermore, treating carbonyl compounds with DAST can lead to side product formation due to elimination reactions[220,221]. Longer reaction times were tested (up to 3 h at 80 °C) but no significant improvement of the RCY could be observed.

Even though the calculated RCY of the ^{18}F-labelled gemcitabine intermediate **123** is very low a deoxodifluorination with incorporation of [^{18}F]fluoride at the 2'-position of an intact nucleoside could be demonstrated for the first time. The detection of the radioactive intermediate **123** provided supporting evidence for the mechanism that was proposed in scheme **3.34**. However, in order to evaluate the relevance of this approach for future biological applications of the final tracer ^{18}F-gemcitabine (**54**) test reactions to improve the RCY as well as the deprotection step to give the final compound **54** have to be investigated.

4 Conclusion

The objective of this research project was the development of novel and efficient radiosynthetic routes to ^{18}F-labelled gemcitabine and related 2'-^{18}F-labelled nucleosides for applications in positron emission tomography (PET) imaging. Currently, the synthetic accessibility of ^{18}F-labelled uridine- and cytidine-based nucleosides is limited[177,178]. The clinical potential and broad applicability of these tracers, ranging from reporter gene imaging[212] to the assessment of nucleoside salvage pathway activity[147], justify the need of new and efficient radiosynthetic procedures. In order to address this demand, the presented research project focused on nucleophilic late-stage radiofluorinations with the intention to develop novel and fast radiochemical approaches towards 2'-^{18}F-labelled nucleosides. Proof-of-concept studies based on uridine-derived 2'-^{18}F-labelled nucleosides were followed by the development of novel late-stage radiofluorination approaches towards the cytidine-based nucleosides ^{18}F-FAC and finally ^{18}F-gemcitabine. The latter is a new PET probe which has not yet been synthesised and thus posed serious challenges and an entirely new synthetic approach.

Non-radioactive late-stage fluorination reactions as proof-of-principle studies were initially performed, which led to a solid understanding of the reactivity and stability of different precursors for 2'-fluorinated nucleosides. The major finding was that an optimal balance between precursor reactivity and stability is key in order to successfully conduct nucleophilic late-stage fluorinations. This was demonstrated by the non-radioactive late-stage synthesis of FAU (**65**) which in turn enabled late-stage radiofluorinations carried out at the Wales Research and

Diagnostic Positron Emission Tomography Centre (PETIC) at Cardiff University Hospital. Radiofluorination reactions towards ^{18}F-FAU (**9**) were performed using the Eckert & Ziegler module system with highest RCYs in DMF at 120 °C. ^{18}F-FAU was purified and identified via both radio-TLC and radio-HPLC using co-injected non-radioactive reference compound as internal standard. RCYs were calculated to 2.8-3.9% (decay-corrected, n = 3) with high radiochemical purities (≥95%) and specific activities ≥42 GBq/μmol after a synthesis time of 178 min. This was the first time that ^{18}F-FAU was synthesised via late-stage radiofluorination. However, due to the proof-of-principle character of this study further investigations towards an improved radiochemical synthesis were discontinued. Instead, the findings of the ^{18}F-FAU synthesis were used as a template for a novel radiosynthetic approach to the structurally related uridine analogue ^{18}F-FIAU with regard to potential applications in reporter gene imaging. Despite the structural similarity of both compounds, which justified comparable reaction conditions and set-ups, non-radioactive fluorinations as well as radiofluorinations using the 2'-mesylated precursor **88** were not successful under the tested conditions.

Previous results and experiences with radiofluorinations could subsequently be used to develop a novel late-stage radiochemical approach to give ^{18}F-FAC (**15**), a PET probe previously developed by Radu *et al.* and currently in clinical trials. This methodology involved computational and experimental analysis of the precursor stability followed by an extensive investigation of the RCY of the labelling reactions and proof of the correct stereochemical outcome of this reaction. The final product ^{18}F-FAC was obtained with RCYs between 4.3-5.5% (n = 6, decay-corrected), high radiochemical purities (≥98%) and specific activities ≥1700 mCi/μmol. The total synthesis time was 168 min after the end of bombardment (EoB)[222]. Future studies regarding an improved radiosynthesis of ^{18}F-FAC should include test reactions using simplified and cassette-based radiosynthesisers such as the IBA SynthERA or the GE FastLab/TracerLab module

systems. This would be a crucial step forward in terms of the translation of this radiochemical approach to a GMP facility. The reaction could then be further tested regarding reproducibility and RCY. Furthermore, [^{18}F]TBAF should be used in continuing investigations as an alternative fluorination agent to evaluate improvements in RCY. The newly developed route offers an advantage over the latest reported synthetic method as it utilises a 'FDG-like' radiochemical approach with radiofluorination and subsequent deprotection. The reaction started with an intact (protected) nucleoside avoiding base coupling reactions and subsequent separations of the α- and β-stereoisomers after radiofluorination. Hence, this approach may simplify the production of ^{18}F-FAC in GMP hot cells. However, the RCY is still low compared to reported RCYs for ^{18}F-FAC (31±5%)[180] and thus further testing is needed to demonstrate the actual clinical potential of this synthetic approach.

Considering the final target of this research project it was envisaged that a ^{18}F-gemcitabine PET probe may enable the evaluation of pharmacokinetic and pharmacodynamic parameters of this widely applied anticancer drug *in vivo*, which may have significant impact on future treatment planning using nucleoside-based chemotherapy. However, the clinical relevance of ^{18}F-gemcitabine as a PET probe would have to be evaluated using appropriate *in vivo* cancer models.

3',5'-O-diacetyl-N^4-acetyl-2'-ketocytidine (**35**) was used as a precursor for first radiochemical approaches towards the target molecule ^{18}F-gemcitabine (**54**). Compound **35** was based on previously published data[159] demonstrating that deoxodifluorination of **35** can be achieved when treated with DAST and pyridinium hydrogen fluoride. Based on that finding, it was assumed that [^{18}F]fluoride/K$_{222}$ could substitute pyridinium hydrogen fluoride as the additional fluoride source in a radiosynthetic approach. Consequently, radiofluorination reactions using precursor **35** were carried out under different conditions testing several organic fluorination agents (DAST, XtalFluor M, Fluolead), varying reaction times (1-

2 h) and temperatures (40-90 °C). Radio-HPLC experiments provided evidence that the ^{18}F-labelled gemcitabine intermediate **123** was obtained in very low RCY (0.2-0.3%, decay-corrected) after a synthesis time of 212 minutes. That finding provided supporting evidence for the proposed mechanism of this radioactive deoxodifluorination. However, the reaction mechanism included that the incorporation of [^{18}F]fluoride and [^{19}F]fluoride occurred in distinct steps during the reaction implying that each ^{18}F-gemcitabine molecule would be single labelled. Considering the presence of organic fluorination agents such as DAST, it seemed reasonable to assume that [^{18}F]fluoride competed with [^{19}F]fluoride in both incorporation steps potentially leading to non-radioactive, single and double ^{18}F-labelled compounds. Hence, future tests including the determination of the specific activity as well as the improvement of the RCY are indispensable in order to make this approach significant for future applications. Furthermore, the subsequent deprotection step to give the final compound has to be carried out to produce a sufficient amount of ^{18}F-gemcitabine needed for biological evaluations. Altogether, extensive investigations have yet to be conducted in order to identify the potential of this synthetic approach. Further radiosynthetic improvements should include the use of simplified synthesisers (e.g. GE TracerLab) and cassette-based synthesis modules in order to reduce potential sources of error. In addition, the application of this radiochemical approach using microwave-assisted radiosynthesis and mircoreactor technology[223,224] could lead to higher RCYs and cleaner reaction profiles due to milder and more controllable reaction conditions.

Altogether, it could be demonstrated that rationally designed radiochemical approaches are capable of providing new synthetic routes towards challenging PET probes such as ^{18}F-labelled nucleoside analogues that were the focus of this research project. In particular, the newly developed radiosynthesis of ^{18}F-FAC may prove useful in future routine applications providing that an improved synthetic procedure is transferable to GMP facilities. Despite considerable advances in the synthesis of ^{18}F-labelled nucleosides within the last decade, further invest-

igations have to be carried out in order to make ^{18}F-labelled nucleosides such as ^{18}F-FMAU, ^{18}F-FIAU and ^{18}F-FAC applicable for clinical routine production. This may include novel and simplified radiosynthetic approaches with as few steps after radiofluorination as possible and the improvement of RCY and reproducibility of established synthetic routes. Late-stage radiofluorinations as reported here and elsewhere[177,185,222] may be able to meet these requirements if appropriate precursors and reaction conditions can be developed. Additional studies should focus on the development of innovative radiosynthesisers (e.g. ELIXYS[180]) that are capable of providing nucleoside-based PET tracers of clinical standard in terms of yield, purity and reproducibility. This progression would help to address the growing demand for novel and more specific PET probes in pre-clinical and clinical research as well as clinical routine application.

5 Experimental Part

5.1 General information

5.1.1 Analytics

Proton (^{1}H) NMR spectra were measured on a BrukerAvance Ultra Shield (500 MHz) spectrometer at ambient temperature. Data were recorded as follows: chemical shift in ppm from internal reference tetramethylsilane on the δ scale, multiplicity (s = singlet; d = doublet; t = triplet; m = multiplet), coupling constant (Hz), integration, and assignment. Carbon (^{13}C) NMR spectra were measured on a BrukerAvance Ultra Shield (125 MHz) spectrometer at ambient temperature. Chemical shifts were recorded in ppm from the solvent resonance employed as the internal standard (deuterochloroform at 77.00 ppm). Fluorine (^{19}F) NMR spectra were recorded on a BrukerAvance Ultra Shield (474 MHz) spectrometer at ambient temperature.

For thin-layer chromatography (TLC) analysis throughout this work, Merck precoated TLC plates (silica gel 60 GF_{254}) were used. Mass spectrometry analysis (LC-ESI-MS) was performed on either an AGILENT 6430 T-Quadrupol spectrometer (PETIC) or on a Bruker micro-TOF. High-resolution mass spectrometry (ESI-HRMS) were carried out by the National Mass Spectrometry Facility (Swansea, Wales, UK). Melting points were determined using an uncalibrated Griffin 220V melting point apparatus.

5.1.2 Solvents and chemicals

In experiments that required dry solvents, ether and THF were freshly distilled from Na/benzophenone. Acetic anhydride, DMF and acetone were dried over P_2O_5. Toluene and dichloromethane were freshly distilled from CaH_2. All anhydrous solvents were stored over 4Å molecular sieves. All other chemicals had synthetic-grade and were used as commercially available. All reagents and solvents were used as supplied from Sigma-Aldrich without further purification. All nucleoside-based starting materials were purchased from Carbosynth Ldt UK. Column chromatography was performed using Fluka silica gel (35-70 mm) as stationary phase.

5.2 Experimental data

5.2.1 Nucleoside nomenclature

The positions of the carbon and hydrogen atoms of all nucleoside analogues throughout this thesis were labelled as follows:

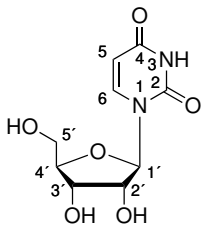

Assignments of the proton and carbon chemical shifts observed in the NMR spectra are related to the atom numbering shown above. All other substituents were assigned using appropriate abbreviations. Furthermore, all known compounds (according to the SciFinder data base) are provided with references. All

novel compounds are fully characterised. Thermally unstable compounds were as fully analysed as possible.

5.2.2 Procedures and spectral data

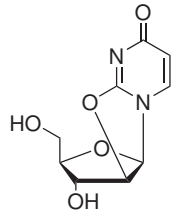

57 ,$C_9H_{10}N_2O_5$, MW: 226.19

2,2'-anhydro-uridine (57).[225] Uridine (**55**, 0.52 g, 2,1 mmol) was suspended in anhydrous MeCN (20 mL). Triphenylphosphine (1.39 g, 5.3 mmol) was added and the suspension was stirred at -20 °C for 20 min. Diisopropyl azadicarboxylate (1.32 mL, 6.7 mmol) was added dropwise to the solution. The mixture was stirred at 0 °C for 5 h. The solution was poured into cold EtOAc (50 mL) (-20 °C) and stirred for additional 20 min. The white precipitate was filtered and washed with cold EtOAc (30 mL). Purification of the crude product by column chromatography on SiO_2 (eluent: EtOAc/MeOH, 100/0 to 90/10) gave 0.25g (56%) of the anhydro-compound as a white powder; mp 233-236 °C (lit.[225] 234-237 °C); R_f=0.55 (6% MeOH/DCM); ^{1}H NMR (500 MHz, DMSO-d_6) δ 8.02 (d, J = 7.8 Hz, 1 H, H-6), 5.93 (d, J = 7.5 Hz, 1 H, H-5), 5.58 (s, 1 H, H-1'), 4.52 (s, 1 H, H-2'), 4.48 (dd, J = 12.8, 1.6 Hz, 1 H, H-5') 4.42 (m, 1 H, H-3'), 4.32 (m, 1 H, H-4'), 4.10 (dd, J = 11.8, 1.1 Hz, 1 H, H-5'); ^{13}C NMR (125 MHz, d_6-DMSO) δ 168.1 (C-4), 158.3 (C-2), 136.1 (C-6), 116.2 (C-5), 102.2 (C-1'), 87.5 (C-4'), 77.6 (C-2'), 73.1 (C-3'), 68.2 (C-5'); MS (ESI) *m/z* 261.2 $[M + Cl]^-$.

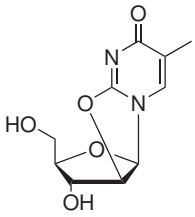

58, $C_{10}H_{12}N_2O_5$, MW: 240.21

2,2'-anhydro-5-methyluridine (58).[226] 5-methyluridine (**56**, 200mg, 0.76 mmol) and PPh_3 (510 mg, 1.94 mmol) were suspended in dry MeCN (4.5 mL) at -20 °C. The resulting suspension was stirred at this temperature for 20 min before diisopropyl azadicarboxylate (0.5 mL, 2.33 mmol) was added dropwise. The yellowish mixture was stirred at 0 °C for 3 h. After completion of the reaction the mixture was concentrated under reduced pressure. Cold EtOAc (15 mL) was added to the solid residue and the resulting white precipitate was filtered and washed with cold EtOAc (10 mL). The crude product was purified by column chromatography on SiO_2 (eluent: EtOAc/MeOH, 100/0 to 90/10 v/v) to furnish 110 mg (51%) of compound as a white solid; mp 224 °C (lit.[167] 227-228 °C); R_f=0.55 (6% MeOH/DCM); ^{1}H NMR (500 MHz, DMSO-d_6) δ 7.94 (s, 1 H, H-6), 5.52 (m, 2 H, H-1', H-2'), 5.25 (s, 1 H, OH-3'), 4.49 (dd, J = 12.8, 1.6 Hz, 1 H, H-5'), 4.47 (s, 1 H, OH-5'), 4.38 (m, 1 H, H-3'), 4.33 (m, 1 H, H-4'), 4.07 (dd, J = 12.7, 0.8 Hz, 1 H, H-5'), 1.81 (s, 3 H, methyl); ^{13}C NMR (125 MHz, d_6-DMSO) δ 171.0 (C-4), 156.6 (C-2), 139.2 (C-6), 117.4 (C-5), 100.0 (C-1'), 87.1 (C-4'), 76.9 (C-2'), 74.4 (C-3'), 71.1 (C-5'), 12.7 (CH_3); MS (ESI) *m/z* 275.4 $[M + Cl]^-$.

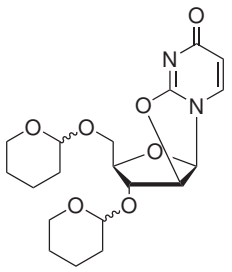

59, $C_{19}H_{26}N_2O_7$, MW: 394.42

3',5'-O-bis-tetrahydropyranyl-2,2'-anhydro-uridine (59).[227] Anhydro compound **57** (200 mg, 0.84 mmol) was suspended in dry THF (6 mL) before *p*TsOH (200 mg, 1.1 mmol) and 3,4-dihydro-2*H*-pyran (0.8 mL, 8.3 mmol) were added to the suspension at 0 °C. The resulting mixture was stirred at r.t. for 3 h. After completion of the reaction the mixture was neutralised with triethylamine (0.3 mL) and stirred for additional 10 min. The solution was diluted with brine (20 mL) and extracted with EtOAc (3 × 30 mL). The combined organic layer was washed with brine (2 × 15 mL), dried over Na_2SO_4 and concentrated. The residue was purified by column chromatography on SiO_2 (eluent: EtOAc/hexane, 50/50 to 70/30 v/v) to obtain 57 mg (84%) of the title compound as a white foam (four diastereomers); R_f=0.6 (4% MeOH/DCM); ^{1}H NMR[186] (500 MHz, $CDCl_3$) δ 7.11-7.05 (4s, 4 H, H-6), 6.05-5.88 (m, 4 H, H-5), 5.21-5.11 (m, 4 H, H-1'), 4.49-4.43 (m, 4 H), 3.95-3.82 (m, 16 H), 3.79-3.60 (m, 12 H), 3.52-3.37 (m, 12 H), 1.91-1.50 (m, 48 H); MS (ESI) *m/z* 429.3 $[M + Cl]^-$.

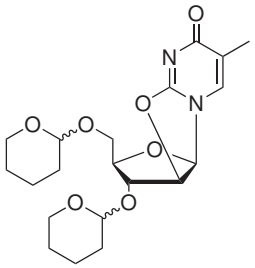

60, $C_{20}H_{28}N_2O_7$, MW: 408.45

3',5'-O-bis-tetrahydropyranyl-2,2'-anhydro-5-methyluridine (60).[227] The title compound was obtained from compound **58** as described for compound **64** in 77% yield after purification by column chromatography on SiO_2 (eluent: EtOAc/hexane, 40/60 to 60/40 v/v) as a white foam (four diastereomers); R_f=0.55 (4% MeOH/DCM); ^{1}H NMR (500 MHz, $CDCl_3$) δ 6.55-6.47 (4s, 4 H, H-6), 5.37-5.31 (m, 4 H, H-1,), 4.58-4.55 (m, 4 H), 3.99-3.7 (m, 16 H), 3.66-3.59 (m, 12 H), 3.52-3.37 (m, 12 H), 2.19-2.11 (m, 12 H, CH_3), 1.91-1.50 (m, 48 H); MS (ESI) *m/z* 443.2 $[M + Cl]^-$.

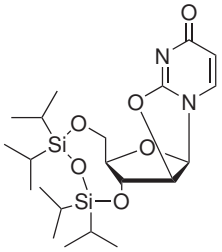

61, $C_{21}H_{36}N_2O_6Si_2$, MW: 468.69

3',5'-O-(1,1,3,3-tetraisopropyldisiloxane-1,3-diyl)-2,2'-anhydrouridine (61).[215] [228] Anhydro compound **57** (42 mg, 0,18 mmol) was coevaporated with dry pyridine (2 × 3 mL) before dry DMF (4 mL) was added under an argon atmosphere. Pyridine (0.2 mL) and dichloro-1,1,3,3-tetraisopropyldisiloxane (0.12 mL, 0.37 mmol) were added dropwise to the solution at ambient temperature. The resulting mixture was stirred at r.t. for 16 h. After full conversion

of the starting material the mixture was poured onto ice in a separation funnel followed by an extraction with diethyl ether (3 × 10 mL). The combined organic layer was washed with brine (2 × 10 mL), dried over Na_2SO_4 and concentrated. Purification of the crude product by column chromatography on SiO_2 (eluent: EtOAc/hexane, 50/50 v/v) gave 64 mg (71%) of the protected compound as colorless needles; mp 183 °C (lit.[228] 179-180 °C), R_f=0.65 (4% MeOH/DCM); ^{1}H NMR (500 MHz, $CDCl_3$) δ 7.36 (d, J = 7.9 Hz, 1 H, H-6), 5.82 (d, J = 8.0 Hz, 1 H, H-5), 4.53 (m, 1 H, H-1'), 4.38 (m, 2 H-2', H-3'), 4.34 (dt, J = 6.5, 3.5 Hz, 1 H, H-4'), 3.90 (dd, J = 11.7, 3.3 Hz, 1 H, H-5'), 3.77 (dd, J = 12.1, 3.5 Hz, 1 H, H-5'), 0.98 - 1.16 (m, 28 H, ^{i}Pr); ^{13}C NMR (125 MHz, $CDCl_3$) δ 165.5 (C-4), 148.9 (C-2), 137.2 (C-6), 112.8 (C-5), 92.2 (C-1'), 82.4 (C-4'), 76.2 (C-3'), 73.1 (C-5'), 71.5 (H-2'), 18.4 (CH_3), 18.1 (CH_3), 17.7 (CH_3), 17.6 (CH_3), 17.2 (CH_3), 17.0 (CH_3), 16.9 (CH_3), 13.7 (CH_3), 13.1 (CH), 13.0 (CH), 12.9 (CH), 12.8 (CH); MS (ESI) *m/z* 491.2 $[M + Na]^+$

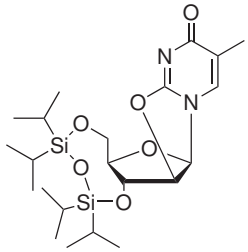

62, $C_{22}H_{38}N_2O_6Si_2$, MW: 482.72

3',5'-O-(1,1,3,3-tetraisopropyldisiloxane-1,3-diyl)-2,2'-anhydro-5-methyluridine (62).[228] Compound **58** (35 mg, 0.14 mmol) was coevaporated with dry pyridine (2 × 3 mL) before dry DMF (1.5 mL) was added under an argon atmosphere. Pyridine (0.3 mL) and dichloro-1,1,3,3-tetraisopropyldisyloxane (0.05 mL, 0.155 mmol) were added dropwise to the solution at r.t. The resulting mixture was stirred at for 12 h. After full conversion of the starting material the mixture was poured onto ice (15 g) in a separating funnel and extrac-

ted with EtOAc (3 × 10 mL). The combined organic layer was washed with brine (2 × 10 mL), dried over Na_2SO_4 and concentrated to furnish a yellow oil. Purification of the crude product by column chromatography on SiO_2 (eluent: EtOAc/hexane, 40/60 to 60/40 v/v) gave 57 mg (84%) of the title compound as a white powder; mp 175-176 °C (lit.[228] 179-180 °C); R_f=0.6 (3% MeOH/DCM); ^{1}H NMR (500 MHz, $CDCl_3$) δ 7.48 (s, 1 H, H-6), 5.85 (d, J = 3.4 Hz, 1 H, H-1'), 4.49 (m, 1 H, H-2'), 4.38 (m, 1 H, H-3'), 4.30 (dt, J = 6.3, 3.3 Hz, 1 H, H-4'), 3.98 (dd, J = 12.3, 3.2 Hz, 1 H, H-5'), 3.82 (dd, J = 12.3, 3.4 Hz, 1 H, H-5'), 1.95 (s, 3 H, methyl), 1.02 - 1.13 (m, 28 H, ^{i}Pr); ^{13}C NMR (125 MHz, $CDCl_3$) δ 163.8 (C-4), 149.8 (C-2), 135.9 (C-6), 110.7 (C-5), 91.2 (C-1'), 82.2 (C-4'), 76.0 (C-3'), 72.2 (C-5'), 44.3 (C-2'), 17.5 (CH_3), 17.4 (CH_3), 17.3 (CH_3), 17.2 (CH_3), 17.1 (CH_3), 17.0 (CH_3), 16.9 (CH_3), 13.3 (CH_3), 13.08 (CH), 13.0 (CH), 12.8 (CH), 12.6 (CH_3), 12.5 (CH); MS (ESI) *m/z* 517.2 $[M + Cl]^-$.

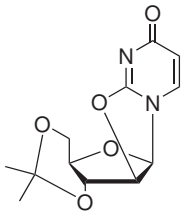

63, $C_{12}H_{14}N_2O_5$, MW: 266.25

3',5'-O-propylidene-2,2'-anhydro-uridine (63). Anhydro compound **57** (96 mg, 0,42 mmol) was suspended in absolute acetone (4 mL) before a catalytic amount of concentrated hydrochloric acid (25 μL) was added dropwise to the solution at 0 °C. The resulting mixture was stirred at r.t. for 16 h. After full conversion of the starting material the mixture was neutralised with saturated $NaHCO_3$. The mixture was diluted with water (15 mL) and extracted with EtOAc (3 × 15 mL). The combined organic layer was washed with brine (2 × 15 mL), dried over Na_2SO_4 and concentrated. Purification of the crude product by column

chromatography on SiO_2 (eluent: EtOAc/hexane, 70:30 to 90/10 v/v) gave 94 mg (85%) of the title compound as a white solid; mp 185-188 °C; R_f=0.5 (5% MeOH/DCM); ^{1}H NMR (500 MHz, $CDCl_3$) δ 7.36 (d, J = 8.1 Hz, 1 H, H-6), 5.78 (d, J = 7.2 Hz, 1 H, H-5), 5.70 (d, J = 2.2 Hz, 1 H, H-1'), 5.02 (dd, J = 6.5, 2.3 Hz, 1 H, H-2'), 4.92 (dd, J = 6.5, 3.7 Hz, 1 H, H-3'), 4.38 (td, J = 5.5, 3.8 Hz, 1 H, H-4'), 3.84 (dd, J = 11.5, 5.7 Hz, 1 H, H-5'), 3.74 (dd, J = 11.5, 5.3 Hz, 1 H, H-5'), 1.59 (s, 3 H, methyl), 1.38 (s, 3 H, methyl). ^{13}C NMR (125 MHz, $CDCl_3$) δ 163.7 (C-4), 150.1 (C-2), 142.5 (C-6), 114.7 (C-5), 102.7 (C-1'), 94.9 (C-4'), 86.7 (C-2'), 84.5 (C-3'), 82.1 (C-5'), 44.1 ($C_{quat.}$, acetal), 27.2 (CH_3), 25.3 (CH_3); MS (ESI) *m/z* 301.2 $[M + Cl]^-$.

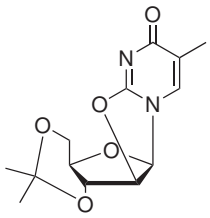

64, $C_{13}H_{16}N_2O_5$, MW: 280.28

3',5'-O-propylidene-2,2'-anhydro-5-methyluridine (64). Anhydro compound **58** (50 mg, 0.22 mmol) was suspended in absolute acetone (4 mL) at r.t. before a catalytic amount of 37% HCl solution (25 μL) was added dropwise at 0 °C. After 15 h stirring at r.t. and complete conversion of the starting material the colorless solution was neutralised with saturated $NaHCO_3$. The mixture was diluted with water (20 mL) and extracted with EtOAc (3 × 10 mL). The combined organic layer was washed with brine (2 × 15 mL), dried over Na_2SO_4 and concentrated. The crude residue was purified by column chromatography on SiO_2 (eluent: EtOAc/hexane, 90/10 to 80/20 v/v) to give 56 mg (88%) of the title compound as a white solid; mp 202-204 °C; R_f=0.55 (5% MeOH/DCM); ^{1}H NMR (500 MHz, $CDCl_3$) δ 7.16 (s, 1 H, H-6), 5.67 (s, 1 H, H-1'), 5.04 (dd, J =

6.5, 2.0 Hz, 1 H, H-2'), 4.92 (dd, J = 6.4, 3.7 Hz, 1 H, H-3'), 4.35 (td, J = 5.5, 3.9 Hz, 1 H, H-4'), 3.84 (dd, J = 11.4, 5.8 Hz, 1 H, H-5'), 3.74 (dd, J = 11.4, 5.5 Hz, 1 H, H-5'), 1.98 (s, 3 H, methyl), 1.65 (s, 3 H, methyl), 1.21 (s, 3 H, methyl). ^{13}C NMR (125 MHz, $CDCl_3$) δ 164.1 (C-4), 150.5 (C-2), 138.4 (C-6), 114.7 (C-5), 111.2 (C-1'), 95.0 (C-4'), 86.8 (C-2'), 84.4 (C-3'), 82.3 (C-5'), 44.1 ($C_{quat.}$, acetal), 26.9 (CH_3), 25.3 (CH_3), 12.3 (CH_3); MS (ESI) *m/z* 315.4 [M + Cl]$^-$; HRMS (ESI) calcd for $C_{13}H_{16}N_2O_5Cl$ (= [M + Cl]$^-$) *m/z* 315.1911, found 315.1902.

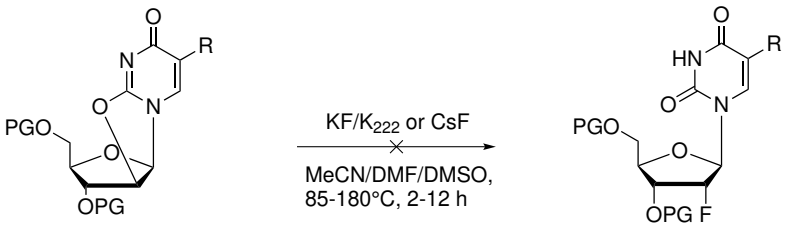

59 (i) R = H, PG = THP
60 (ii) R = Me, PG = THP
61 (iii) R = H, PG = TIPDS
62 (iv) R = Me, PG = TIPDS
63 (v) R = H, PG = acetonide
64 (vi) R = Me, PG = acetonide

General procedure for the fluorination of precursors 59-64: The fluorination precursor (100 mg) was dissolved in reaction solvent (MeCN/DMF/DMSO, 4 mL) under inert atmosphere before either KF/K_{222} or CsF (3 eq.) was added to the solution. The mixture was stirred at the appropriate temperature (85-180 °C) for the given time (2-12 h). Reaction control using TLC was performed hourly. However, the desired fluorinated compounds could not be observed using the stated conditions. The reaction mixtures were purified using column chromatography to recover the starting material or the deprotected compounds **57** and **58** using appropriate gradients as stated in the above procedures.

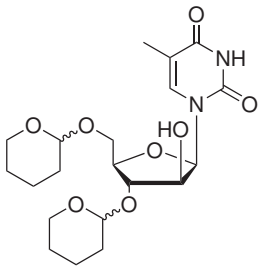

66, $C_{20}H_{30}N_2O_8$, MW: 426.46

3',5'-O-(bis-tetrahydropyranyl)-2'-arabino-5-methyluridine (66).[155] Compound **60** (270 mg, 0.66 mmol) was dissolved in MeOH (4.0 mL) at r.t. before 10 M NaOH (0.1 mL) was added dropwise. The reaction mixture was stirred at reflux temperature for 4h. After full conversion of the starting material the mixture was neutralised with glacial acetic acid. The reaction mixture was diluted with water (10 mL) and extracted with EtOAc (3 × 20 mL). The combined organic layer was washed with brine, dried over Na_2SO_4 and concentrated. The resulting crude residue was purified by silica gel chromatography (eluent: EtOAc/hexane, 80/20 to 100/0 v/v) to give 89.5 mg (47%) of the desired product as a white powder (four diastereomers); R_f=0.65 (4% MeOH/DCM); ^{1}H NMR[229] (500 MHz, $CDCl_3$) δ 9.50-9.39 (4s, 4 H, N-H), 7.79-7.61 (4s, 4 H, H-6), 6.13-5.91 (4s, 4 H, H-1') 5.02-4.87 (m, 4 H), 4.75-4.69 (m, 4 H), 4.34-4.20 (m, 12 H), 3.87-3.69 (m, 12 H), 3.59-3.39 (m, 24 H), 1.95-1.90 (4s, 12 H), 1.82-1.49 (m, 40 H); MS (ESI) *m/z* 449.2 $[M + Na]^+$.

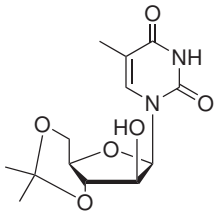

67, $C_{13}H_{18}N_2O_6$, MW: 298.29

3',5'-O-propylidene-2'-arabino-5-methyluridine (67). Protected anhydro compound **64** (170 mg, 0.61 mmol) was dissolved in MeOH (4.0 mL) at r. t. before 10 M NaOH (0.1 mL) was added dropwise. The reaction mixture was stirred at reflux temperature for 5h before it was neutralised with glacial acid. The reaction mixture was diluted with water (10 mL) and extracted with EtOAc (3 × 10 mL). The combined organic layer was washed with brine, dried over Na_2SO_4 and concentrated. The resulting crude residue was purified by silica gel chromatography (eluent: EtOAc/hexane, 80/20 to 100/0 v/v) to give 117 mg (59%) of the desired product as a white powder; mp 187-189 °C; R_f=0.5 (5% MeOH/DCM); ^{1}H NMR (500 MHz, $CDCl_3$) δ 9.17 (s, 1 H, N-H), 7.16 (d, J = 1.1 Hz, 1 H, H-6), 5.53 (d, J = 3.1 Hz, 1 H, H-1'), 5.11 (dd, J = 6.5, 3.1 Hz, 1 H, H-2'), 5.00 (dd, J = 6.5, 3.6 Hz, 1 H, H-3'), 4.29 (dt, J = 6.4, 3.4 Hz, 1 H, H-4'), 3.93 (dd, J = 12.1, 2.7 Hz, 1 H, H-5'), 3.82 (dd, J = 12.1, 3.7 Hz, 1 H, H-5'), 2.56 (s, 1 H, O-H), 1.93 (s, 3 H, CH_3), 1.60 (s, 3 H, CH_3), 1.38 (s, 3 H, CH_3); ^{13}C NMR (125 MHz, $CDCl_3$) δ 163.8 (C-4), 150.7 (C-2), 138.9 (C-6), 114.3 (C-5), 111.3 (C-1'), 95.8 (C-4'), 86.9 (C-2'), 83.2 (C-3'), 80.4 (C-5'), 62.7 ($C_{quat.}$, acetal), 27.0 (CH_3), 25.3 (CH_3), 12.2 (CH_3); MS (ESI) *m/z* 299.3 $[M + H]^+$; HRMS (ESI) calcd for $C_{13}H_{18}N_2O_6Cl$ (= $[M + Cl]^-$) *m/z* 335.1911, found 335.1917.

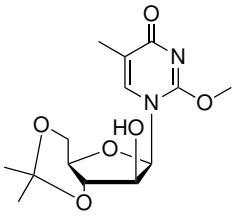

67b, $C_{14}H_{20}N_2O_6$, MW: 313.32

3',5'-O-propylidene-2'-arabino-2-O-methyl-5-methyluridine (67b). As a side product from the reaction to compound **67**, nucleoside **67b** was obtained in 22% yield as a colourless oil; R_f=0.7 (5% MeOH/DCM); ^{1}H NMR (500 MHz, $CDCl_3$) δ 7.72 (d, J = 2.0 Hz, 1 H, H-6), 5.61 (d, J = 2.7 Hz, 1 H, H-1'), 5.21 (dd, J = 6.2, 2.9 Hz, 1 H, H-2'), 5.10 (dd, J = 6.7, 3.5 Hz, 1 H, H-3'), 4.43 (m, 1 H, H-4'), 3.96 (dd, J = 11.8, 2.8 Hz, 1 H, H-5'), 3.88 (s, 3 H, CH_3), 3.73 (dd, J = 12.0, 2.9 Hz, 1 H, H-5'), 2.74 (s, 1 H, O-H), 1.95 (s, 3 H, CH_3), 1.69 (s, 3 H, CH_3), 1.41 (s, 3 H, CH_3); ^{13}C NMR (125 MHz, $CDCl_3$) δ 162.5 (C-4), 154.6 (C-2), 139.1 (C-6), 118.9 (C-5), 112.1 (C-1'), 98.2 (C-4'), 88.8 (C-2'), 85.4 (C-3'), 81.1 (C-5'), 67.8 ($C_{quat.}$, acetal), 58.7 (CH_3); 28.1 (CH_3), 25.8 (CH_3), 13.1 (CH_3); MS (ESI) *m/z* 314.2 $[M + H]^+$.

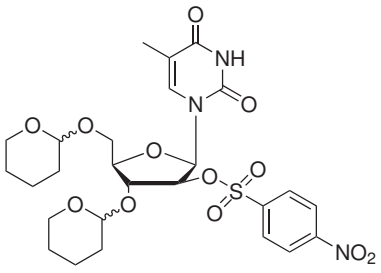

68, $C_{26}H_{33}N_3O_{12}S$, MW: 611.62

3',5'-O-(bis-tetrahydropyranyl)-2'-arabino-(*p*-nitrobenzenesulfonyl)-5-methyluridine (68). Pyridine (3 mL) and nosyl chloride (100 mg, 0.45 mmol) were added to a solution of compound **66** (135 mg, 0.32 mmol) in dry DCM (3

mL). The yellowish solution was stirred at r.t. for 15 h. After completion of the reaction the solution was diluted with water (15 mL) and extracted with DCM (3 × 10 mL). The combined organic layer was washed with brine, dried over Na_2SO_4 and concentrated. The crude residue was purified by silica gel chromatography (eluent: EtOAc/hexane, 20/80 to 50/50 v/v) to give 112 mg (68%) of the desired product as a yellow solid (four diastereomers); R_f=0.65 (4% MeOH/DCM); ^{1}H NMR (500 MHz, $CDCl_3$) δ 9.09-8.86 (4s, 4 H, N-H), 8.42-8-35 (m, 8 H), 8.15-7.98 (m, 8 H), 7.27-7.22 (m, 4 H), 7.19-7.02 (m, 8 H), 6.06-5.80 (m, 8 H), 4.88-4.27 (m, 32 H), 3.92-3.72 (m, 12 H), 3.59-3.42 (m, 12 H), 1.95 (4s, 12 H), 1.84-1.63 (m, 24 H); MS (ESI) *m/z* 612.2 $[M + H]^+$.

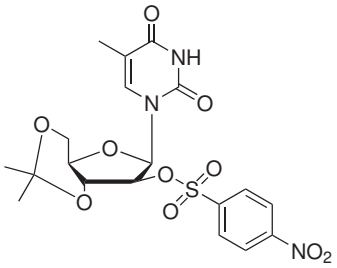

69, $C_{19}H_{21}N_3O_{10}S$, MW: 483.45

3',5'-O-propylidene-2'-arabino-(*p*-nitrobenzenesulfonyl)-5-methyl-uridine (69). Pyridine (1.0 mL) and nosyl chloride (32 mg, 0.14 mmol) were added to a solution of hydroxy compound **67** (40 mg, 0.14 mmol) in dry DCM (2.0 mL) under vigorous stirring at r.t. The resulting solution was stirred at room temperature for 8 h. After full conversion of the starting material the solution was diluted with water (10 mL) and extrated with DCM (3 × 10 mL). The combined organic layer was washed with 5% H_2SO_4 (15 mL), saturated sodium bicarbonate solution (15 mL) and brine, dried over Na_2SO_4 and concentrated. Purification of the resulting crude solid by column chromatography on SiO_2 (eluent: EtOAc/hexane, 40/60 to 80/20 v/v) furnished 57 mg (84%) of the title

compound as a white solid; mp 223-225 °C; R_f=0.6 (5% MeOH/DCM); ^{1}H NMR (500 MHz, $CDCl_3$) δ 9.94 (1 H, s, N-H), 8.37 (d, J = 8.7 Hz, 2 H, $H_{arom.}$), 8.11 (d, J = 8.7 Hz, 2 H, $H_{arom.}$), 7.05 (s, 1 H, H-6), 5.50 (d, J = 0.8 Hz, 1 H, H-1'), 5.06 (dd, J = 6.4, 1.2 Hz, 1 H, H-2'), 4.83 (dd, J = 6.3, 3.9 Hz, 1 H, H-3'), 4.46 - 4.40 (m, 2 H, H-4', H-5'), 4.37 - 4.33 (m, 1 H, H-5'), 1.94 (s, 3 H, CH_3), 1.54 (s, 3 H, CH_3), 1.33 (s, 3 H, CH_3); ^{13}C NMR (125 MHz, $CDCl_3$) δ 163.1 (C-4), 149.8 (C-2), 149.1 (C-6), 140.6 ($C_{arom.}$), 138.1 (2 C, $CH_{arom.}$), 128.5 (2 C, $CH_{arom.}$), 128.0 ($C_{arom.}$), 113.5 (C-5), 95.4 (C-1'), 84.7 (C-2'), 83.3 (C-4'), 80.0 (C-3'), 69.9 (C-5'), 25.9 ($C_{quat.}$, acetal), 24.2 (CH_3), 20.0 (CH_3), 11.1 (CH_3); MS (ESI) *m/z* 484.3 $[M + H]^+$.

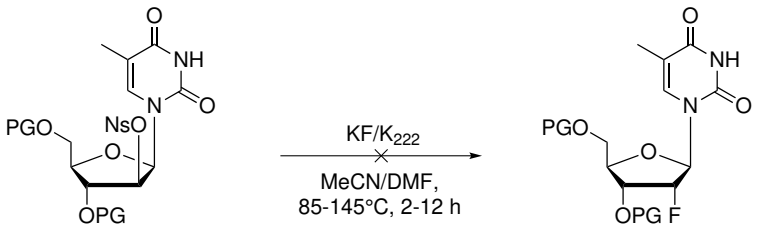

68 PG = THP
69 PG = acetonide

General procedure for the fluorination of precursors 68 and 69: The fluorination precursor (100 mg) was dissolved in anhydrous solvent (MeCN/DMF, 4 mL) under inert atmosphere before KF/K_{222} (3 eq.) was added to the solution. The mixture was stirred at the appropriate temperature (85-145 °C) for the given time (3-12 h). Reaction control using TLC was performed hourly. However, the desired fluorinated compounds could not be observed using the described conditions. The reaction mixtures were purified using column chromatography to recover the deprotected compounds **60** and **64** using appropriate gradients as stated in the above procedures.

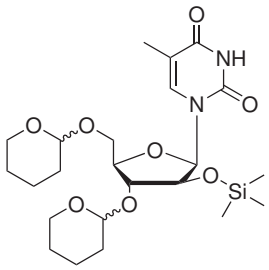

70, $C_{23}H_{38}N_2O_8Si$, MW : 498.64

3',5'-O-(bis-tetrahydropyranyl)-2'-arabino-(trimethylsilyl)-5-methyluridine (70). Triethylamine (0.3 mL, 2.5 mmol) and trimethylsilyl chloride (0.2 mL, 1.5 mmol) were added dropwise to a solution of compound **66** (200 mg, 0.47 mmol) in dry DCM at 0 °C. The solution was stirred at r.t. for 2.5 h. After full conversion of the starting material the solution was diluted with water (25 mL) and extracted with DCM (3 × 20 mL). The combined organic layer was washed with brine, dried over Na_2SO_4 and concentrated in vacuo. The crude residue was purified by by column chromatography on SiO_2 (eluent: Et_3N/EtOAc/hexane, 1/59/40 to 1/69/30) to obtain 172 mg (73%) of the title compound as a colourless oil (four diastereomers); R_f=0.7 (4% MeOH/DCM); HPLC: ≥94% (R_t=8.2 min, isocr. 30% MeCN/H_2O); ^{1}H NMR (500 MHz, $CDCl_3$) δ 9.80-9.68 (4s, 4 H, N-H), 7.63-7.53 (4s, 4 H, H-6), 6.17-5.99 (4s, 4 H, H-1'), 4.93-4.69 (m, 8 H), 4.33-4.18 (m, 12 H), 3.92-3.65 (m, 16 H), 3.53-3.42 (m, 8 H), 1.87-1.84 (4s, 12 H), 1.79-1.38 (m, 48 H), 0.17-0.09 (m, 36 H); MS (ESI) *m/z* 533.2 $[M + Cl]^-$.

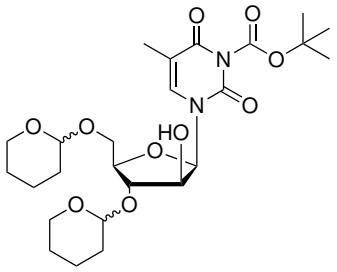

71 $C_{25}H_{38}N_2O_{10}$, MW : 526.58

N^3-Boc-3',5'-O-(bis-tetrahydropyranyl)-2'-arabino-5-methyluridine (71). DMAP (42 mg, 0.34 mmol) and di-tert-butyl dicarbonate (150 mg, 0.68 mmol) were added to a solution of compound **70** (170 mg, 0.34 mmol) at r.t. and the resulting mixture was strirred for 14 h. After complete conversion of the starting material *p*-toluenesulfonic acid (130 mg, 0.68 mmol) was added slowly and the solution was stirred for additional 40 min. The remaining solution was then concentrated under reduced pressure. The crude residue was purified by by column chromatography on SiO_2 (eluent: EtOAc/hexane, 50/50 v/v) to furnish 95 mg (53%) of the title compound as a white foam (four diastereomers); R_f=0.5 (3% MeOH/DCM); HPLC: ≥96% (R_t=10.9 min, isocr. 35% MeCN/H_2O); ^{1}H NMR (500 MHz, $CDCl_3$) δ 7.71-7.29 (4s, 1 H, H-6), 5.92-5.70 (4s, 1 H, H-1'), 4.85-4.80 (m, 1 H), 4.69-4.64 (m, 1 H), 4.52-4.43 (m, 1 H), 4.38-4.18 (m, 2 H), 3.98-3.71 (m, 5 H), 3.52-3.40 (m, 2 H), 1.89 (s, 3 H), 1.85-1.67 (m, 5 H), 1.58-1.54 (m, 9 H), 1.53-1.44 (m, 7 H); MS (ESI) *m/z* 550.1 $[M + Na]^+$.

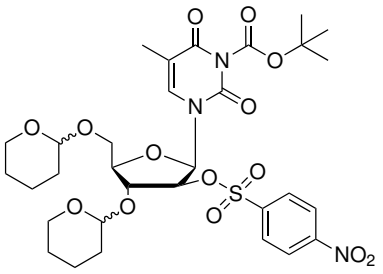

72, $C_{31}H_{41}N_3O_{14}S$, MW : 711.73

N^3-Boc-3',5'-O-(bis-tetrahydropyranyl)-2'-arabino-(*p*-nitrobenzene -sulfonyl)-5-methyluridine (72). Pyridine (5 mL) and nosyl chloride (190 mg, 0.86 mmol) were added to the solution of compound **71** (300 mg, 0.57 mmol) in dry DCM (5 mL) at r.t. The resulting mixture was stirred for 3 h. After completion of the reaction the solution was diluted with water (30 mL) and extracted with DCM (3 × 15 mL). The combined organic layer was washed with brine, dried over Na_2SO_4 and concentrated. The crude residue was purified by silica gel chromatography (eluent: EtOAc/hexane, 20/80 to 40/60 v/v) to furnish 205 mg (53%) of the title compound as a yellow oil (four diastereomers), R_f=0.6 (2% MeOH/DCM); ^{1}H NMR (500 MHz, $CDCl_3$) δ 8.40-8.36 (m, 2 H), 8.13-8.08 (m, 2 H), 7.36-7.13 (m, 3 H), 5.82-5.50 (m, 1 H), 4.93-4.09 (m, 7 H), 3.92-3.70 (m, 2 H), 3.54-3.41 (m, 2 H), 1.95-1.92 (m, 3 H), 1.87-1.58 (m, 5 H), 1.58-1.54 (m, 9 H), 1.51-1.41 (m, 5 H); MS (ESI) *m/z* 718 $[M + Na]^+$.

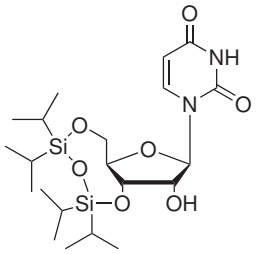

73, $C_{21}H_{38}N_2O_7Si_2$, MW : 500.73

3',5'-O-(1,1,3,3-tetraisopropyldisiloxane-1,3-diyl)-uridine (73).[230] Uridine (**55**, 770 mg, 3.17 mmol) was coevaporated with dry pyridine (2 × 3 mL) before it was dissolved in anhydrous DMF (10 mL) under an argon atmosphere. The solution was cooled to 0 °C before dry pyridine (10 mL) and dichloro-1,1,3,3-tetraisopropyldisiloxane (1.0 g, 3.17 mmol) were added to the solution. The mixture was stirred at r.t. for 14 h. After completion of the reaction the mixture was diluted with water and extracted with DCM (3 × 30 mL). The combined organic layer was washed with brine (30 mL), dried over Na_2SO_4 and

concentrated. The crude residue was purified by column chromatography on SiO_2 (eluent: EtOAc/hexane, 50/50 to 80/20 v/v) to give 1.29 g (82%) of the title compound as a white foam; mp 166-169 °C (lit.[230] 172°C); R_f=0.45 (4% MeOH/DCM); ^{1}H NMR (500 MHz, $CDCl_3$) δ 9.92 (s, 1 H, N-H), 7.79 (d, J = 8.1 Hz, 1 H, H-6), 5.76 (s, 1 H, H-1'), 5.72 (d, J = 8.2 Hz, 1 H, H-5), 4.32 (dd, J = 8.9, 4.7 Hz, 1 H, H-5'), 4.23 (m, 2 H, H-2', H-3'), 4.18 (dt, J = 9.0, 2.1 Hz, 1 H, H-4'), 4.02 (dd, J = 13.3, 2.6 Hz, 1 H, H-5'), 3.84 (d, 1.9 Hz, 1 H, O-H), 1.15-0.95 (m, 28 H, ^{i}Pr); ^{13}C NMR (125 MHz, $CDCl_3$) δ 163.5 (C-4), 150.3 (C-2), 139.9 (C-6), 101.9 (C-5), 90.9 (C-1'), 81.7 (C-4'), 75.2 (C-2'), 68.9 (C-3'), 60.2 (C-5'), 17.5 (CH_3), 17.4 (CH_3), 17.3 (CH_3), 17.2 (CH_3), 17.0 (CH_3), 17.0 (CH_3), 16.9 (CH_3), 16.8 (CH_3), 13.4 (CH), 13.0 (CH), 12.9 (CH), 12.5 (CH); MS (ESI) *m/z* 523.3 $[M + Na]^+$.

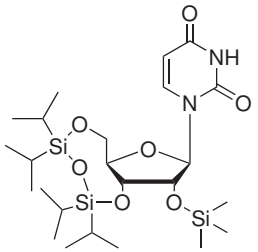

74$C_{24}H_{46}N_2O_7Si_3$, MW : 558.89

3',5'-O-(1,1,3,3-tetraisopropyldisiloxane-1,3-diyl)-2'-(trimethylsilyl)-uridine (74).[230] To a solution of compound **73** (2.65 g, 5.45 mmol) in dry DCM (50 mL) were added triethylamine (3.8 mL, 26.3 mmol) and trimethylsilyl chloride (2.1 mL, 16.1 mmol) dropwise at -10 °C. The solution was allowed to warm up to r.t. and to stir for 2 h. The reaction mixture was then poured onto ice water in a separation funnel and was extracted with DCM (3 × 50 mL). The combined organic layer was washed with brine (50 mL), dried over Na_2SO_4 and concentrated. Purification by column chromatography on SiO_2 (eluent: Et_3N/EtOAc/hexane, 1/19/80 to 1/49/50 v/v) gave 2.35 g (78%) of compound as a white foam; mp

177-178 °C (lit.[230] 184°C); R_f=0.55 (6% MeOH/DCM); ^{1}H NMR (500 MHz, $CDCl_3$) δ 9.80 (s, 1 H, N-H), 7.98 (d, J = 8.1 Hz, 1 H, H-6), 5.69 (d, J = 8.1 Hz, 1 H, H-5), 5.60 (d, J = 1.6 Hz, 1 H; H-1'), 4.27 (d, J = 13.6 Hz, 1 H, H-5'), 4.17 (m, 2H, H-2', H-3'), 4.08 (ddd, J = 9.4, 3.6, 1.5 Hz, 1 H, H-4'), 3.99 (d, J = 13.6 Hz, 1 H, H-5'), 1.16-0.92 (m, 28 H, ^{i}Pr), 0.21 (s, 9 H, TMS); ^{13}C NMR (125 MHz, $CDCl_3$) δ 163.9 (C-4), 149.8 (C-2), 139.5 (C-6), 101.0 (C-5), 91.1 (C-1'), 81.3 (C-4'), 76.2 (C-2'), 67.8 (C-3'), 59.2 (C-5'), 17.3 (CH_3), 17.2 (CH_3), 17.1 (CH_3), 17.0 (CH_3), 16.8 (CH_3), 16.8 (CH_3), 16.7 (CH_3), 16.6 (CH_3), 13.2 (CH), 13.0 (CH), 12.7 (CH), 12.6 (CH), 0.0 (3 C, CH_3, TMS); MS (ESI) *m/z* 581.2 [M + Na]$^+$.

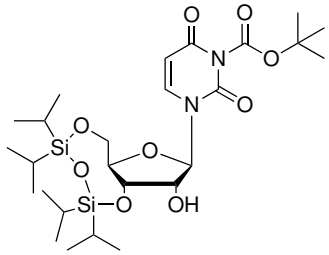

75, $C_{26}H_{46}N_2O_9Si_2$, MW : 586.82

N^3-Boc-3',5'-O-(1,1,3,3-tetraisopropyldisiloxane-1,3-diyl)-uridine (75). Di-tert-butyl dicarbonate (1.85 g, 8.5 mmol) and DMAP (500 mg, 4.15 mmol) were added to a solution of compound **74** (2.32 g, 4.15 mmol) in dry THF (50 mL) at r.t. The resulting mixture was stirred for 16 h. After full conversion of the starting material *p*-toluenesulfonic acid (1.6 g, 8.3 mmol) was added. The mixture was stirred for additional 50 min, cooled to 0 °C, and neutralised with triethylamine (1.1 mL). The reaction mixture was diluted with water (30 mL) and extracted with EtOAc (3 × 50 mL). The combined organic layer was washed with brine (50 mL), dried over Na_2SO_4 and concentrated. Purification by column chromatography on SiO_2 (eluent: EtOAc/hexane, 30/70 to 60/40 v/v) furnished 1.41 g (58%, overall yield) of the desired compound as a white foam; mp 202-

204 °C; R_f=0.5 (40% EtOAc/hexane); ^{1}H NMR (500 MHz, $CDCl_3$) δ 7.68 (d, J = 8.2 Hz, 1 H, H-6), 5.72 (s, 1 H, H-1'), 5.71 (d, J = 8.3 Hz, 1 H, H-5), 4.36 (dd, J = 8.8, 4.9 Hz, 1 H, H-3'), 4.20 (m, 2 H, H-2', H-4'), 4.11 (dd, J = 10.8, 2.3 Hz, 1 H, H-5'), 4.00 (dd, J = 13.3, 2.8 Hz, 1 H, H-5'), 2.94 (s, 1H, OH), 1.61 (s, 9 H, TMS), 1.14-0.90 (m, 28 H, ^{i}Pr); ^{13}C NMR (125 MHz, $CDCl_3$) δ 160.1 (C-4), 148.3 (C-2), 147.6 (C-6), 139.2 (C=O, Boc), 101.5 (C-5), 90.9 (C-1'), 86.8 (C-4'), 81.9 (C-2'), 75.1 (C-3'), 68.9 (C-5'), 60.0 (C_{tert}, Boc), 27.4 (3 C, CH_3, Boc), 17.4 (CH_3), 17.4 (CH_3), 17.2 (CH_3), 17.2 (CH_3), 17.0 (CH_3), 17.0 (CH_3), 16.9 (CH_3), 16.8 (CH_3), 13.4 (CH), 12.9 (CH), 12.9 (CH), 12.5 (CH); MS (ESI) *m/z* 609.9 $[M + Na]^+$; HRMS (ESI) calcd for $C_{26}H_{47}N_2O_9Si_2$ (= $[M + H]^+$) *m/z* 587.2815, found 587.2804.

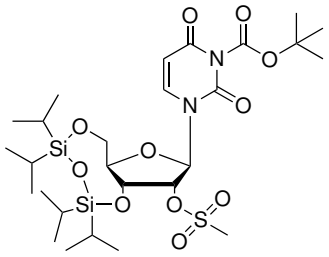

76, $C_{27}H_{48}N_2O_{11}SSi_2$, MW : 664.91

N^3-Boc-3',5'-O-(1,1,3,3-tetraisopropyldisiloxane-1,3-diyl)-2'-O-(methanesulfonyl)-uridine (76). Triethyl amine (1.6 mL, 11.5 mmol) and mesyl chloride (0.55 mL, 5.1 mmol) were added to a solution of compound **75** (1.35 g, 2.3 mmol) in dry DCM (20 mL) at 0 °C. The mixture was stirred at this temperature for additional 10 min before it was allowed to warm up to r.t and was stirred for 1.5 h. After full conversion of the starting material the mixture was diluted with sat. $NaHCO_3$-solution and extracted with DCM (2 × 20 mL). After drying over Na_2SO_4 and concentration in vacuo the resulting crude oil was purified by column chromatography on SiO_2 (eluent: EtOAc/hexane, 15/85 to 40/60 v/v) to obtain 1.13 g (74%) of the title compound as a white foam; mp

187-188 °C; R_f=0.55 (20% EtOAc/hexane); ^{1}H NMR (500 MHz, $CDCl_3$) δ 7.80 (d, J = 8.3 Hz, 1 H, H-6), 5.81 (s, 1 H, H-1'), 5.75 (d, J = 8.3 Hz, 1 H, H-5), 5.04 (d, J = 4.4 Hz, 1 H, H-2'), 4.35 (dd, J = 9.6, 4.5 Hz, 1 H, H-5'), 4.28 (d, J = 13.7 Hz, 1 H, H-3'), 4.12 (dd, J = 9.6, 2.0 Hz, 1 H, H-4'), 4.01 (dd, J = 13.7, 2.5 Hz, 1 H, H-5'), 3.26 (s, 3 H, CH_3, mesyl), 1.63 (s, 9 H, CH_3, Boc), 1.16-0.92 (m, 28 H, ^{i}Pr); ^{13}C NMR (125 MHz, $CDCl_3$) δ 161.5 (C-4), 148.8 (C-2), 146.9 (C-6), 139.5 (C=O, Boc), 102.2 (C-5), 92.1 (C-1'), 85.9 (C-4'), 82.1 (C-2'), 75.3 (C-3'), 68.7 (C-5'), 60.8 (Ctert, Boc), 38.5 (CH_3, mesyl), 26.3 (3 C, CH_3, Boc), 17.6 (CH_3), 17.5 (CH_3), 17.4 (CH_3), 17.1 (CH_3), 17.0 (CH_3), 16.9 (CH_3), 16.9 (CH_3), 16.6 (CH_3), 14.1 (CH), 12.8 (CH), 12.6 (CH), 12.2 (CH); MS (ESI) *m/z* 665.9 $[M + H]^+$; HRMS (ESI) calcd for $C_{27}H_{49}N_2O_{11}SSi_2$ (= $[M + H]^+$) *m/z* 665.8529, found 665.8533.

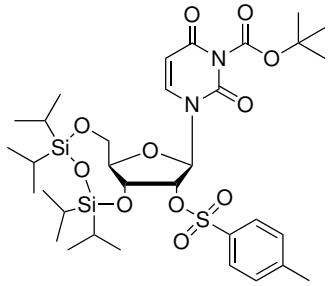

77, $C_{33}H_{52}N_2O_{11}SSi_2$, MW : 741.01

N^3-Boc-3',5'-O-(1,1,3,3-tetraisopropyldisiloxane-1,3-diyl)-2'-O-(p-toluenesulfonyl)-uridine (77). Compound **75** (200 mg, 0.38 mmol) was dissolved in dry DCM (4 mL) before Et_3N (0.53 mL, 1.52 mmol), nosyl chloride (290 mg, 1.52 mmol) and DMAP (94 mg, 0.76 mmol) were added to the solution at r.t. under an argon atmosphere. The solution was stirred for 24 h. After full conversion of the starting material the reaction was quenched by pouring it onto ice. The mixture was extracted with DCM (3 × 15 mL) and the combined organic layer was washed with brine, dried over Na_2SO_4 and concentrated under reduced

pressure in a water bath which was kept below 40 °C. The resulting crude product was purified by column chromatography on SiO_2 (eluent: EtOAc/hexane, 60/40 to 50/50 v/v) to give 81 mg of **77** (44%) as a white foam; R_f=0.4 (EtOAc/hexane, 60/40); ^{1}H NMR (500 MHz, $CDCl_3$) δ 7.88 (d, J = 6.5 Hz, 2 H, H_{arom}), 7.60 (d, J = 8.3 Hz, 2 H, H_{arom}), 7.34 (d, J = 8.1 Hz, 1 H, H-6), 5.70 (d, J = 8.3 Hz, 1 H, H-5), 5.09 (d, J = 4.8 Hz, 1 H, H-1'), 4.46 (dd, J = 9.3, 4.8 Hz, 1 H, H-2'), 4.21 (d, J = 13.5 Hz, 1 H, H-5'), 4.09 - 4.05 (m, 2 H, H-3',5'), 4.00 (dt, J = 13.5, 2.3 Hz, 1 H, H-4'), 2.45 (s, 3 H, CH_3), 1.64 (s, 9 H, Boc, CH_3), 1.14 - 0.89 (m, 28 H, ^{i}Pr); MS (ESI) *m/z* 742.1 $[M + H]^+$.

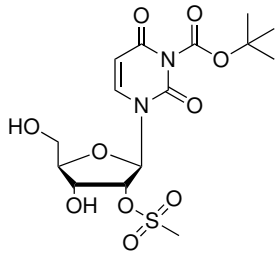

78, $C_{15}H_{22}N_2O_{10}S$, MW : 422.41

N^3-Boc-2'-O-(methanesulfonyl)-uridine (78). TBAF (125 mg, 0.4 mmol) was added to a stirring solution of compound **76** (80 mg, 0.12 mmol) in dry THF (3 mL) at r.t. The mixture was stirred for 30 min. After completion of the reaction the solvent was removed in vacuo. The resulting crude residue was purified by column chromatography on SiO_2 (eluent: EtOAc/hexane, 90/10 to 100/0 v/v) to obtain 38 mg (76%) of the title compound as a white foam; mp 223-225 °C; R_f=0.55 (6% MeOH/DCM); ^{1}H NMR (500 MHz, $CDCl_3$) δ 7.88 (d, J = 8.3 Hz, 1 H, H-6), 5.87 (s, 1 H, H-1'), 5.72 (d, J = 8.2 Hz, 1 H, H-5), 5.07 (dd, J = 4.5, 3.2 Hz, 1 H, H-3'), 4.40 - 4.36 (m, 1H, H-4'), 4.03 (d, J = 6.6 Hz, 1 H, H-2'), 3.91 (d, J = 11.2 Hz, 1 H, H-5'), 3.77 (d, J = 11.2 Hz, 1 H, H-5'), 3.15 (s, 3 H, CH_3, mesyl), 1.51 (s, 9 H, CH_3, Boc); ^{13}C NMR (125 MHz, $CDCl_3$) δ 160.1 (C-4), 147.8 (C-2), 146.9 (C-6), 139.4 (C=O, Boc), 101.5 (C-5), 87.7 (C-1'), 86.6

(C-2'), 83.4 (C-4'), 80.6 (C-3'), 67.2 (C-5'), 59.5 (Ctert, Boc), 37.9 (CH_3, mesyl), 26.7 (3 C, CH_3, Boc); MS (ESI) *m/z* 450.5 $[M + Na]^+$.

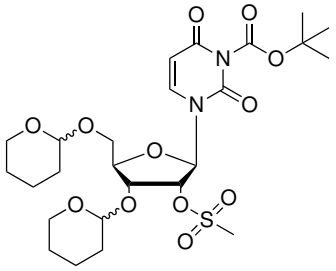

79, $C_{25}H_{38}N_2O_{12}S$, MW : 590.64

N^3-Boc-3',5'-O-(bis-tetrahydropyranyl)-2'-O-(methanesulfonyl)-uridine (79). *p*TsOH (270 mg, 1.4 mmol) and DHP (0.6 mL, 7.0 mmol) were added to a solution of compound **78** (300 mg, 0.71 mmol) in dry THF (8 mL) at 0 °C. The solution was allowed to warm up to r.t. and was stirred for 3 h. The solution was then neutralised with triethylamine (0.25 mL). The neutral mixture was diluted with water (20 mL) and extracted with DCM (3 × 15 mL). The combined organic layer was washed with brine (50 mL), dried over Na_2SO_4 and concentrated. Twofold purification by column chromatography on SiO_2 (eluent: EtOAc/hexane, 10/90 to 30/70 v/v) furnished 234 mg (56%) of the desired compound **79** as a white foam (four diastereomers). A small portion (1.5 mg) was further characterised by analytical HPLC. The precursor was found to be ≥98% pure (R_t=7.5-8.2 min, 80% MeCN/H_2O); R_f=0.6 (15% EtOAc/hexane); ^{1}H NMR (500 MHz, $CDCl_3$) δ 8.14-8.07 (4s, 4 H, H-6), 5.96-5.90 (4s, 4 H, H-1'), 5.71-5.67 (4s, 4 H, H-5), 5.15-5.10 (m, 4 H), 4.79-4.66 (m, 8 H), 4.52-4.44 (m, 4 H), 4.34-4.29 (m, 4 H), 4.25-4.07 (m, 4 H), 3.88-3.62 (m, 12 H), 3.56-3.49 (m, 8 H), 3.22-3.21 (4s, 8 H), 1.84-1.63 (m, 24 H), 1.62-1.56 (4s, 36 H, Boc, CH_3), 1.56-1.40 (m, 28 H, THP); MS (ESI) *m/z* 613.7 $[M + Na]^+$; HRMS (ESI) calcd for $C_{25}H_{39}N_2O_{12}S$ (= $[M + H]^+$) *m/z* 591.3730, found 591.3732.

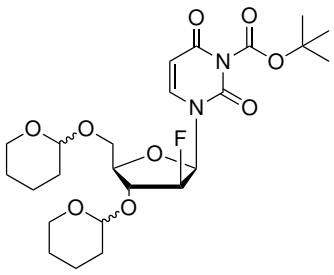

80, $C_{24}H_{35}FN_2O_9$, MW : 514.54

N^3-Boc-3',5'-O-bis-tetrahydropyranyl-2'-fluoro-arabino-uridine (80). Fluorination precursor **79** (100 mg, 0.17 mmol) was dissolved in dry acetonitrile (3 mL) at r.t under an argon atmosphere in an oven dried Schlenk flask. 1 M TBAF solution in dry THF (0.5 mL, 0.5 mmol) was added dropwise to the solution. The resulting mixture was stirred at 80 °C for 2.5 h. After completion of the reaction the solvent was removed under reduced pressure. The crude residue was purified by column chromatography on SiO_2 (eluent: EtOAc/hexane, 15/85 to 20/80 v/v) to furnish the fluorinated compound **80** (42 mg, 51%) as a colourless oil (four diastereomers); A small portion (≈1 mg) was further characterised by analytical HPLC. The fluorinated intermediate was found to be ≥95% pure (R_t=6.3 min, 80% MeCN/H_2O); R_f=0.45 (15% EtOAc/hexane); ^{1}H NMR (500 MHz, $CDCl_3$) δ 7.62-7.53 (4s, 4 H, H-6), 6.20-6.11 (4s, 4 H, H-1'), 5.70-5.67 (m, 4 H, H-5)), 5.25-4.97 (m, 4 H, H-2'), 4.75-4.61 (m, 8 H, H-4', THP), 4.52-4.29 (m, 4 H, H-3'), 4.21-4.14 (m, 4 H, H-5'), 3.98-3.88 (m, 4 H, H-5'), 3.82-3.73 (m, 4 H, THP), 3.66-3.58 (m, 4 H, THP), 3.56-3.49 (m, 8 H, THP), 1.81-1.61 (m, 20 H, THP), 1.57 (s, 36 H, Boc, CH_3), 1.53-1.38 (m, 32 H, THP); ^{19}F NMR (471 MHz, $CDCl_3$) δ -198.46, -198.70, -199.24, -199.44; MS (ESI) *m/z* 537.3 $[M + Na]^+$; HRMS (ESI) calcd for $C_{24}H_{36}FN_2O_9$ (= $[M + H]^+$) *m/z* 515.2911, found 515.2916.

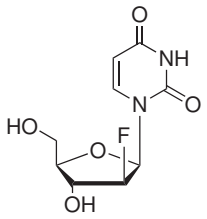

65, $C_9H_{11}FN_2O_5$, MW : 246.19

2'-deoxy-2'-fluoroarabino-uridine (65).[231] Compound **80** (70 mg, 0.14 mmol) was dissolved in MeOH (4 mL) before 1 M HCl solution (1 mL) was added dropwise. The mixture was stirred at 60 °C for 1 h. After full conversion of the starting material saturated $NaHCO_3$ (2 mL) was added to the mixture. After concentration in vacuo the crude product was purified by column chromatography on SiO_2 (eluent: DCM/MeOH, 90/10 v/v) to obtain 21 mg (62%) of **65** as a white powder; mp 164-165 °C (lit.[231] 159-162 °C); R_f=0.3 (10% MeOH/DCM); ^{1}H NMR (500 MHz, $CDCl_3$) δ 11.43 (s, 1 H, N-H), 7.72 (d, J = 8.1 Hz, 1 H, H-6), 6.11 (dd, J = 16.0, 4.3 Hz, 1 H, H-3'), 5.89 (d, J = 4.9 Hz, 1 H, OH-3'), 5.65 (d, J = 8.1 Hz, 1 H, H-5), 5.09 (dd, J = 6.6, 4.3 Hz, 1 H, H-2'), 4.99 (dd, J = 4.1, 3.3 Hz, 1 H, H-1'), 4.22 (ddd, J = 19.8, 7.8, 4.6 Hz, 1 H, H-4'), 3.80 (q, J = 4.7 Hz, 1 H, OH-5'), 3.65 (dd, J = 11.5, 4.8 Hz, 1 H, H-5'), 3.58 (dd, J = 11.8, 5.6 Hz, 1 H, H-5'); ^{13}C NMR (125 MHz, $CDCl_3$) δ 163.0 (C-4), 150.2 (C-2), 141.1 (C-6), 101.0 (C-5), 95.4 (d, ^{1}J(C,F) = 191.8 Hz, C-2'), 83.2 (d, ^{2}J(C,F) = 16.5 Hz, C-1'), 72.7 (d, ^{2}J(C,F) = 23.9 Hz, C-3'), 59.9 (C-5'), 48.4 (C-4'); ^{19}F NMR (474 MHz, $CDCl_3$) δ -198.6; MS (ESI) *m/z* 281 $[M + Cl]^-$.

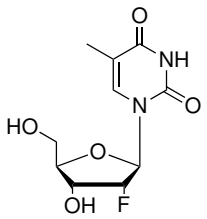

40, $C_{10}H_{13}FN_2O_5$, MW : 260.22

2'-deoxy-2'-fluoro-5-methyl-uridine (40).[232]

via deoxofluorination of compound 71 using XtalFluor M:

A freshly prepared solution of XtalFluor M and $Et_3N{\cdot}3HF$ in dry DCM (2 mL) was added to a solution of compound **71** (200 mg, 0.38 mmol) in dry DCM (3 mL) dropwise at -78 °C. The solution was allowed to heat up slowly to r.t. and stirred for 3 h. A freshly prepared 1 M solution of HCl in MeOH (5 ML) was added to the solution. The mixture was stirred for an additional 30 min. The solution was then neutralised by adding sat. $NaHCO_3$-solution and concentrated in vacuo. The obtained crude product was purified by column chromatography on SiO_2 (eluent: DCM/MeOH, 90/10 v/v) to obtain 23 mg (25%) of the title compound as colourless needles; mp 155-157 °C (lit.[232] 149-150 °C); R_f=0.45 (10% MeOH/DCM); ^{1}H NMR (500 MHz, $CDCl_3$) δ 11.30 (s, 1 H, N-H), 7.77 (d, J = 0.8 Hz, 1 H, H-6), 5.93 (dd, J = 17.6, 2.3 Hz, 1 H, H-3'), 5.52 (d, J = 6.3 Hz, 1 H, OH-3'), 5.14 (t, J = 4.7 Hz, 1 H, OH-5'), 5.02 (ddd, J = 53.2, 4.4, 2.4 Hz, 1 H, H-2'), 4.24 - 4.15 (m, 1 H, H-4'), 3.78 (d, J = 12.2 Hz, 1 H, H-5'), 3.61 (dt, J = 12.3, 3.5 Hz, 1 H, H-5'), 1.77 (s, 3 H, CH_3); ^{13}C NMR (125 MHz, $CDCl_3$) δ 163.6 (C-4), 150.3 (C-2), 136.2 (C-6), 109.0 (C-5), 93.3 (d, J = 186.1 Hz, C-2'), 86.8 (d, J = 34.0 Hz, C-1'), 83.3, 67.6 (d, J = 16.1 Hz, C-3'), 59.6 (C-5'), 11.8 (C-4'); ^{19}F NMR (474 MHz, $CDCl_3$) δ -202.7; MS (ESI) *m/z* 295 $[M + Cl]^-$.

via fluorination of compound 72 using either KF/K_{222} or TMAF:

Fluorination precursor **72** (100 mg, 141 μmol) was placed in an oven-dried

Schlenk flask and dissolved in anhydrous solvent (MeCN/DMF, 4 mL) under inert atmosphere before either KF/K_{222} or TMAF (3 eq.) was added to the solution. The mixture was stirred at the appropriate temperature (85-145 °C) for the given time (2-12 h). Reaction control using TLC was performed hourly. However, the desired fluorinated and protected intermediate could not be observed using the stated conditions. Hence, the deprotection step to give **40** was not carried out. The reaction mixtures were purified using column chromatography to recover the starting material using appropriate gradients as stated in the above procedures.

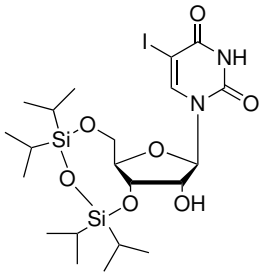

83, $C_{21}H_{37}IN_2O_7Si_2$, MW : 612.60

3',5'-O-1,1,3,3-tetraisopropyl-1,3-disiloxane-5-iodouridine (83).[213] 5-iodouridine **82** (500 mg, 1.35 mmol) was coevaporated twice with dry pyridine (3 mL) and then dissolved in dry pyridine (10 mL) under an argon atmosphere. The solution was cooled to 0 °C before 1,3-dichloro-1,1,3,3-tetraisopropyldisiloxane (0.43 mg, 1.35 mmol) was added dropwise to the cold solution. The reaction mixture was stirred at r.t for 16 h. After full conversion of the starting material pyridine was removed in vacuo by azeotropic co-evaporation with toluene. The crude product was purified by column chromatography on SiO_2 (eluent: DCM/MeOH, 96/4 to 94/6 v/v) to give **83** (569 mg, 0.92 mmol, 69%) as a white foam; R_f=0.55 (8% MeOH/DCM); ^{1}H NMR (500 MHz, $CDCl_3$) δ 10.17 (s, 1H, N-H), 8.03 (s, 1H, H-6), 5.68 (s, 1H, H-1'), 4.28 (dd, J = 8.7, 4.9 Hz, 1H, H-5'), 4.21 - 4.20 (m, 2H, H-3', H-2'), 4.19 - 4.18 (m, 1H, H-4'), 4.04 (s, 1H, OH-2'), 3.98 (dd, J = 13.5,

2.7 Hz, 1H, 5'-H), 1.10 - 0.98 (m, 28H, H-^{i}Pr); ^{13}C NMR (125 MHz, $CDCl_3$) δ 160.4 (C-4), 150.3 (C-2), 144.1 (C-6), 91.5 (C-1'), 82.1 (C-4'), 75.0 (C-2'), 68.7 (C-3'), 68.5 (C-5), 59.9 (C-5'), 17.7 (CH), 17.6 (CH), 17.4 (CH), 17.2 (CH), 17.1 (CH_3), 17.0 (CH_3), 17.0 (CH_3), 16.8 (CH_3), 13.5 (CH_3), 13.0 (CH_3), 12.7 (CH_3), 12.5 (CH_3); MS (ESI) *m/z* 635.2 $[M + Na]^+$.

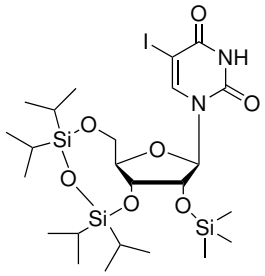

84, $C_{24}H_{45}IN_2O_7Si_3$, MW : 684.78

3',5'-O-1,1,3,3-tetraisopropyl-1,3-disiloxane-2'-O-(trimethylsilyl)-5-iodouridine (84). Compound **83** (300 mg, 0.94 mmol) was dissolved in dry DCM (5 mL) under an argon atmosphere and the solution was cooled to -10 °C. Triethylamine (0.36 mL, 2.5 mmol) and trimethylsilyl chloride (0.2 mg, 1.5 mmol) were added dropwise before the cooling bath was removed and the mixture was then stirred at r.t. for 5 h. After full conversion of the starting material the reaction mixture was poured onto a cold saturated aqueous solution of $NaHCO_3$. The mixture was extracted with DCM (3 × 15 mL). The combined organic layer was washed with brine (20 mL), dried over Na_2SO_4 and concentrated. The crude product was purified via column chromatography on SiO_2 (eluent: DCM/MeOH, 98/2 to 96/4 v/v) to give **84** (275 mg, 0.40 mmol, 82%) as a white foam; mp 76-79 °C; R_f=0.65 (5% MeOH/DCM); ^{1}H NMR (500 MHz, $CDCl_3$) δ 9.94 (s, 1H, H-3), 8.19 (s, 1H, H-6), 5.53 (s, 1H, H-1'), 4.27 (d, J = 13.7 Hz, 1H, H-5'), 4.22 - 4.17 (m, 2H, H-3', H-2'), 4.10 (dd, J = 9.4, 4.0 Hz, 1H, H-4'), 3.98 (dd, J = 13.7, 2.5 Hz, 1H, H-5'), 1.16 - 0.91 (m, 28H, H-^{i}Pr), 0.20 (s, 9H, H-TMS); ^{13}C NMR (125

MHz, $CDCl_3$) δ 160.4 (C-4), 149.8 (C-2), 143.7 (C-6), 91.6 (C-1'), 81.5 (C-4'), 76.1 (C-2'), 67.8 (C-3'), 67.6 (C-5), 59.0 (C-5'), 17.6 (CH), 17.4 (CH), 17.2 (CH), 17.0 (CH), 16.9 (CH_3), 16.8 (CH_3), 16.7 (CH_3), 13.3 (CH_3), 12.7 (CH_3), 12.7 (2 C, CH_3), 12.6 (CH_3), 0.1 (3 C, CH_3-TMS); MS (ESI) *m/z* 708 $[M + Na]^+$; HRMS (ESI) calcd for $C_{24}H_{45}IN_2O_7Si_3$ (= $[M + H]^+$) *m/z* 685.1652, found 685.1650.

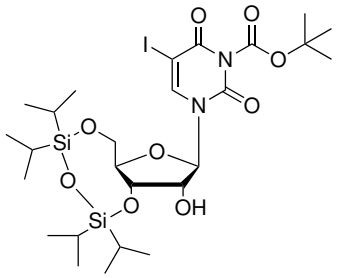

85, $C_{26}H_{45}IN_2O_9Si_2$, MW : 712.72

N^3-Boc-3',5'-O-1,1,3,3-tetraisopropyl-1,3-disiloxane-5-iodouridine (85). Compound **84** (250 mg, 0.36 mmol) was dissolved in dry DCM under an argon atmosphere before 4-(dimethylamino)-pyridine (44 mg, 0.36 mmol) and di-tert-butyl dicarbonate (94 mg, 0.43 mmol) were added to the solution. The reaction mixture was stirred at r.t for 15 h. After full conversion of the starting material *p*-toluenesulfonic acid monohydrate (143 mg, 0.72 mmol) was added and the resulting suspension was stirred at r.t. for additional 2 h. After completion of the reaction the mixture was cooled to 0 °C before triethylamine (0.13 mL, 0.72 mmol) was added dropwise. The solution was then poured onto a saturated $NaHCO_3$-solution and was extracted with DCM (3 × 15 mL). The combined organic layer was dried over Na_2SO_4 and concentrated. The crude product was purified via column chromatography on SiO_2 (eluent: cyclohexane/EtOAc, 90/10 to 85/15 v/v) to give 163 mg (58%) of **85** as a white foam; mp 82-84 °C; R_f=0.7 (5% MeOH/DCM); ^{1}H NMR (500 MHz, $CDCl_3$) δ 7.81 (s, 1H, H-6), 5.63 (s, 1H, H-1'), 4.38 (dd, J = 8.6, 5.2 Hz, 1H, H-3'), 4.19 (dd, J = 13.1, 2.2 Hz, 1H, H-5'),

4.09 (d, J = 5.2 Hz, 1H, H-2'), 4.05 (dt, J = 8.6, 2.6 Hz, 1H, H-4'), 3.99 (dd, J = 13.1, 3.0 Hz, 1H, H-5'), 2.91 (s, 1H, OH-2'), 1.67 (s, 9H, Boc), 1.17 - 0.92 (m, 28H, H-^{i}Pr); ^{13}C NMR (125 MHz, $CDCl_3$) δ 161.3 (C-4), 157.4 (C=O, Boc) 150.8 (C-2), 141.3 (C-6), 91.7 (C-1'), 81.9 (C-4'), 75.23 (C-2'), 69.55 (C-3'), 69.17 (C-5), 63.69 (C-5'), 60.21 ($C_{quat.}$, Boc), 29.43 (3 C, CH_3, Boc), 17.70 (CH_3), 17.55 (CH_3), 17.43 (CH_3), 17.24 (CH_3), 17.05 (CH_3), 16.98 (CH_3), 16.94 (CH_3), 16.85 (CH_3), 13.42 (CH), 12.97 (CH), 12.74 (CH), 12.55 (CH); MS (ESI) *m/z* 726 [M + Na]$^+$; HRMS (ESI) calcd for $C_{26}H_{49}IN_3O_9Si_2$ (= [M + NH_4]$^+$) *m/z* 730.2047, found 730.2048.

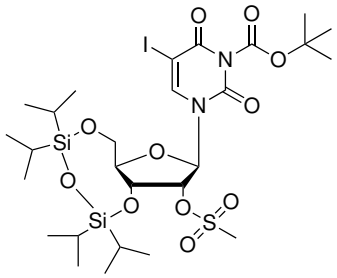

86, $C_{27}H_{47}IN_2O_{11}SSi_2$, MW : 790.81

N^3-Boc-3',5'-O-1,1,3,3-tetraisopropyl-1,3-disiloxane-2'-O-methylsulfonyloxy-5-iodouridine (86). Compound **85** (520 mg, 0.7 mmol) was dissolved in dry DCM under an argon atmosphere and cooled to -10 °C before triethylamine (0.5 mL, 3.5 mmol) and methanesulfonyl chloride (0.2 mL, 2.6 mmol) were added dropwise to the solution. The resulting mixture was stirred at this temperature for 10 minutes beefore it was allowed to warm up to r.t. and stirred for additional 2 h. After full conversion of the starting material the solution was then poured onto cold brine and was extracted with DCM (3 × 20 mL). The combined organic layer was dried over Na_2SO_4 and concentrated. The crude product was purified via column chromatography on SiO_2 (eluent: cyclohexane/EtOAc, 90/10 v/v) to furnish 512 mg (88%) of the title compound **86** as a white foam;

mp 92 °C; R_f=0.45 (2% MeOH/DCM); ^{1}H NMR (500 MHz, $CDCl_3$) δ 8.06 (s, 1H, H-6), 5.75 (s, 1H, H-1'), 5.06 (d, J = 4.6 Hz, 1H, H-2'), 4.36 (dd, J = 9.5, 4.6 Hz, 1H, H-3'), 4.28 (d, J = 13.8 Hz, 1H, H-4'), 4.11 (dd, J = 9.5, 2.0 Hz, 1H, H-5'), 4.00 (dd, J = 13.8, 2.5 Hz, 1H, H-5'), 3.23 (s, 3H, Ms), 1.61 (s, 9H, Boc), 1.14 - 0.90 (m, 28H, H-^{i}Pr); ^{13}C NMR (125 MHz, $CDCl_3$) δ 157.4 (C-4), 147.7 (C-2), 146.5 (C=O, Boc), 142.2 (C-6), 89.5 (C-1'), 87.6 (C-2'), 82.5 (C-4'), 82.2 (C-3'), 67.8 (C-5), 66.6 (C-5'), 58.6 ($C_{quat.}$, Boc), 39.2 (CH_3, Ms), 27.2 (3 C, CH_3), Boc), 17.7 (CH_3), 17.6 (CH_3), 17.4 (CH_3), 17.2 (CH_3), 17.0 (CH_3), 16.9 (CH_3), 16.8 (CH_3), 16.8 (CH_3), 13.6 (CH), 12.9 (CH), 12.7 (CH), 12.6 (CH); MS (ESI) *m/z* 813 $[M + Na]^+$; HRMS (ESI) calcd for $C_{27}H_{51}IN_3O_{11}SSi_2$ (= $[M + NH_4]^+$) *m/z* 808.1822, found 808.1826.

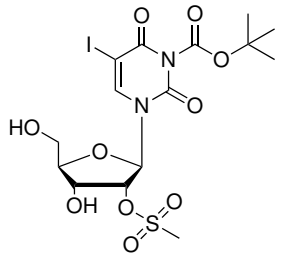

87, $C_{15}H_{21}IN_2O_10S$, MW : 548.30

N^3-Boc-2'-O-methylsulfonyloxy-5-iodouridine (87). TBAF (2.3 g, 7.1 mmol) was added to a stirring solution of compound **86** (1.87 g, 2.36 mmol) in dry THF (35 mL) at r.t. The mixture was stirred for 40 min. After completion of the reaction the solvent was removed in vacuo. The resulting crude residue was purified by column chromatography on SiO_2 (eluent: EtOAc/hexane, 85/15 to 95/5 v/v) to obtain 856 mg (48%) of the title compound (**87**) as a white foam; mp 143 °C; R_f=0.45 (7% MeOH/DCM); ^{1}H NMR (500 MHz, $CDCl_3$) δ 8.57 (s, 1H), 5.93 (d, J = 2.3 Hz, 1H), 5.11 (dd, J = 4.5, 2.5 Hz, 1H), 4.55 - 4.47 (m, 1H), 4.15 - 3.97 (m, 3H), 3.90 (d, J = 11.4 Hz, 1H), 3.22 (s, 3H), 3.18 - 3.12 (m, 1H), 1.56 (s, 10H); ^{13}C NMR (125 MHz, $CDCl_3$) δ 159.4 (C-4), 144.7 (C-2), 145.6

(C-6), 139.2 (C=O, Boc), 102.2 (C-5), 87.7 (C-1'), 86.5 (C-2'), 82.2 (C-4'), 79.1 (C-3'), 65.3 (C-5'), 58.4 ($C_{quat.}$, Boc), 38.5 (CH_3, mesyl), 25.9 (3 C, CH_3, Boc); MS (ESI) *m/z* 571.3 $[M + Na]^+$.

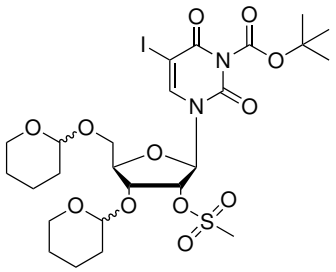

88, $C_{25}H_{37}IN_2O_12S$, MW : 716.54

N^3-Boc-3',5'-O-bis-tetrahydropyranyl-2'-O-methylsulfonyloxy-uridine (88). TBAF (2.3 g, 7.1 mmol) was added to a solution of **87** (1.87 g, 2.36 mmol) in dry THF (35 mL) at r.t. under nitrogen. The resulting yellow solution was stirred at r.t. for 40 min. After completion of the reaction the solvent was removed in vacuo and the resulting dried crude mixture was then used for the next step. *p*TsOH (1.02 g, 5.4 mmol) and DHP (2.5 mL, 27 mmol) were added to a solution of the crude compound **87** in THF (38 mL) at 0 °C. The solution was allowed to warm up to r.t. and stirred for 3 h. After completion of the reaction the solution was neutralised with triethyl amine (1.2 mL). The neutral mixture was diluted with water (20 mL) and extracted with DCM (3 × 30 mL). The combined organic layer was washed with brine (50 mL), dried over Na_2SO_4 and concentrated. Purification of the crude residue by column chromatography on SiO_2 (eluent: EtOAc/hexane, 10/90 to 30/70 v/v) furnished 586 mg (35%, overall yield) of the desired title compound **88** as a white foam (4 diastereomers); a small portion (1.5 mg) was further characterised by analytical HPLC. The precursor was found to be ≥97% pure (R_t=4.1, 6.9-7.2 min, 80% MeCN/H_2O); R_f=0.5 (8% MeOH/DCM); ^{1}H NMR (500 MHz, $CDCl_3$) (1 diastereomer) δ 8.27 (s, 1 H, H-6),

5.98 (d, J = 3.2 Hz, 1 H, H-1'), 5.16 (dd, J = 4.6, 3.3 Hz, 1 H, THP) 4.59 (t, J = 4.3 Hz, 1 H, H-3'), 4.49 (dd, J = 6.2, 4.9 Hz, 1 H, H-2'), 4.36 (d, J = 6.3 Hz, 1 H, H-4'), 4.25 (dd, J = 12.0, 1.5 Hz, 1 H, H-5'), 3.99 (dd, J = 11.5, 1.5 Hz, 1 H, H-5'), 3.96 - 3.91 (m, 1 H, THP), 3.87 - 3.72 (m, 4 H, THP), 3.56 - 3.47 (m, 4 H, THP), 3.19 (s, 3 H, CH_3, mesyl), 1.90 - 1.69 (m, 6 H, THP), 1.56 (s, 11 H, THP, Boc); MS (ESI) *m/z* 739 $[M + Na]^+$; HRMS (ESI) calcd for $C_{25}H_{38}IN_2O_{12}S$ (= $[M + H]^+$) *m/z* 717.4458, found 717.4452.

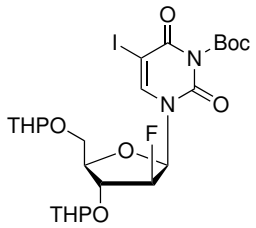

89, $C_{24}H_{34}FIN_2O_9$, MW : 644.44

N^3-Boc-3',5'-O-bis-tetrahydropyranyl-2'-fluoro-arabino-5-iodo-uridine (89). Fluorination precursor **88** (30 mg, 0.047 mmol) was dissolved in dry MeCN or DMF (1-2 mL) at r.t under an argon atmosphere in an oven dried Schlenk flask. Either KF/K_{222} (3-6 eq.) or 1 M TBAF/THF solution (3-10 eq.) was added to the solution. The resulting mixture was stirred at temperatures between 90-160 °C for 1-2 h. The reaction was monitored using TLC and LC-MS. Even though the starting material was converted after the reaction time evidence for the desired fluorinated product **89** could not be provided.

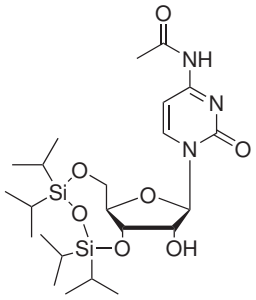

102, $C_{23}H_{41}N_3O_7Si_2$, MW : 527.76

3',5'-O-(1,1,3,3-tetraisopropyldisiloxane-1,3-diyl)-N^4-acetylcytidine (102).[233] N^4-acetylcytidine (**100**, 2.0g, 7.0 mmol) was coevaporated two times with dry pyridine (4 mL) before it was dissolved in dry pyridine (50 mL) at r.t. under nitrogen atmosphere. The whitish suspension was cooled to 0 °C before dichloro-1,1,3,3-tetraisopropyldisyloxane (2 mL, 6.3 mmol) was added dropwise to the suspension. The ice bath was removed and the resulting mixture stirred at r.t. for 16h. After completion of the reaction the solvent was removed in vacuo and the resulting crude mixture diluted with DCM (60 mL). The solution was washed with brine (2 × 30 mL), dried over Na_2SO_4 and concentrated. The remaining pyridine was removed by co-evaporation with toluene. The resulting crude product was subsequently purified via column chromatography on SiO_2 (eluent: hexane/EtOAc, 90/10 to 70/30 v/v) to furnish 2.65 g (82%) of the desired compound as a white foam; mp 157-159 °C; R_f=0.4 (8% MeOH/DCM); ^{1}H NMR (500 MHz, $CDCl_3$) δ 10.19 (s, 1 H, NH), 8.22 (d, J = 7.5 Hz, 1 H, H-6), 7.46 (d, J = 7.5 Hz, 1 H, H-5), 5.82 (s, 1 H, H-1'), 4.29 - 4.25 (m, 2 H, H-4', H-5') 4.22 (m, 1 H, H-2') (dd, J = 13.4, 2.3 Hz, 1 H, H-5'), 3.56 (s, 1 H, OH-2'), 2.30 (s, 3 H, acetyl), 1.13 - 0.97 (m, 28H, H-^{i}Pr); ^{13}C NMR (125 MHz, $CDCl_3$) δ 170.2 (C-4), 162.2 (C=O, acetyl), 154.1 (C-2), 143.2 (C-6), 95.7 (C-1'), 90.7 (C-5), 80.8 (C-4'), 74.4 (C-2'), 67.8 (C-3'), 58.9 (C-5'), 24.2 (CH_3), 16.5 (CH_3), 16.4 (CH_3), 16.3 (CH_3), 16.2 (CH_3), 16.0 (CH_3), 15.9 (CH_3), 15.8 (CH_3), 15.8 (CH_3), 12.4 (CH), 12.0 (CH), 11.9 (CH), 11.5 (CH); MS (ESI) *m/z* 550.2 $[M + Na]^+$.

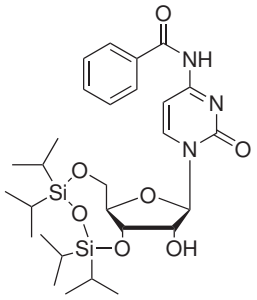

103, $C_{28}H_{43}N_3O_7Si2, MW : 589.83$

3',5'-O-(1,1,3,3-tetraisopropyldisiloxane-1,3-diyl)-N^4-benzoylcytidine (103).[231] N^4-benzoylcytidine (**101**, 1.2 g, 2.5 mmol) was coevaporated with dry pyridine (2 × 4 mL) before it was dissolved in dry pyridine (25 mL) at r.t. under nitrogen atmosphere. The suspension was cooled to 0 °C before dichloro-1,1,3,3-tetraisopropyldisyloxane (1.0 mL, 3.17 mmol) was added dropwise to the suspension. The icebath was removed and the resulting mixture stirred at r.t. for 16 h. After completion of the reaction the solvent was removed in vacuo and the resulting crude mixture diluted with DCM (30 mL). The solution was washed with brine (2 × 30 mL), dried over Na_2SO_4 and concentrated. The remaining pyridine was removed by coevaporation with toluene. The resulting crude product was subsequently purified by column chromatography on SiO_2 (EtOAc/hexane, 90/10 to 70/30 v/v) to furnish 1.29 g (63%) of **103** as a white foam; mp 131-133 °C (lit.[231] 142 °C); R_f=0.55 (7% MeOH/DCM); ^{1}H NMR (500 MHz, $CDCl_3$) δ 9.16 (s, 1 H, NH), 8.27 (d, J = 7.5 Hz, 1 H, C-6), 7.93 (d, J = 7.4 Hz, 1 H, C-5), 7.77 - 7.43 (m, 5 H, benzoyl), 5.86 (s, 1 H, H-1'), 4.32 - 4.23 (m, 5 H), 4.02 (dd, J = 13.4, 2.4 Hz, 1 H, H-5'), 1.16 - 0.94 (m, 28 H, H-^{i}Pr); ^{13}C NMR (125 MHz, $CDCl_3$) δ 162.6 (C=O, benzoyl), 154.8 (C-4), 149.5 (C-2), 144.5 (C-6), 136.3 (C_{arom}), 132.9 (CH_{arom}), 129.2 (2 C, CH_{arom}), 127.4 (CH_{arom}), 123.7 (CH_{arom}), 96.4 (C-1'), 91.6 (C-5), 82.1 (C-4'), 77.4 (C-2'), 74.3 (C-3'), 68.5 (C-5'), 17.5 (CH_3), 17.4 (CH_3), 17.3 (2 C, CH_3), 17.0 (2 C, CH_3), 16.9 (CH_3), 16.8 (CH_3), 13.4 (CH), 13.0 (CH), 12.9 (CH), 12.4 (CH); MS (ESI) *m/z* 612.1 [M + Na]$^+$.

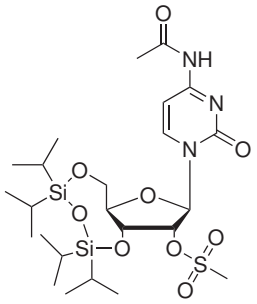

104, $C_{24}H_{43}N_3O_9SSi_2$, MW : 605.85

3',5'-O-(1,1,3,3-tetraisopropyldisiloxane-1,3-diyl)-2'-O-(methanesulfonyl)-N^4-acetylcytidine (104). Et_3N (2.7 mL, 19.0 mmol) and MsCl (0.8 mL, 9.5 mmol) were added dropwise to a solution of **103** (2.0 g, 3.8 mmol) in dry DCM (40 mL) under nitrogen atmosphere at -10 °C. The cooling bath was removed after 10 minutes and the solution was stirred at rt for additional 2 hours. After full conversion of the starting material the solution was poured into brine in a separation funnel and extracted with DCM (2 × 50 mL). The combined organic layer was dried over Na_2SO_4 and concentrated. Purification by column chromatography on SiO_2 (DCM/MeOH 98/2 to 97/3 v/v) gave 1.73 g (75%) the title compound **98a** as a white foam; R_f=0.55 (6% MeOH/DCM); ^{1}H NMR (500 MHz, $CDCl_3$) δ 10.18 (s, 1 H, NH), 8.23 (d, J = 7.6 Hz, 1 H, H-6), 7.50 (d, J = 7.6 Hz, 1 H, H-5), 5.89 (s, 1 H, H-1'), 5.02 (d, J = 4.4 Hz, 1 H, H-2'), 4.33 - 4.26 (m, 2 H, H-3',H-4'), 4.17 (dd, J = 9.7, 1.5 Hz, 1 H, H-5'), 4.03 (dd, J = 13.6, 2.2 Hz, 1 H, H-5'), 3.34 (s, 3 H, Ms), 2.30 (s, 3 H, acetyl), 1.13 - 1.01 (m, 28 H, H-^{i}Pr); ^{13}C NMR (125 MHz, $CDCl_3$) δ 171.1 (C-4), 163.4 (C=O, acetyl), 154.7 (C-2), 143.7 (C-6), 97.0 (C-1'), 89.3 (C-5), 82.6 (C-4'), 82.0 (C-2'), 66.5 (C-3'), 59.1 (C-5'), 39.2 (CH_3, mesyl), 24.9 (CH_3, acetyl), 17.4 (CH_3), 17.4 (CH_3), 17.3 (CH_3), 16.9 (CH_3), 16.8 (CH_3), 16.8 (CH_3), 16.7 (CH_3), 14.2 (CH_3), 13.4 (CH), 13.1 (CH), 13.0 (CH), 12.6 (CH); MS (ESI) *m/z* 628 $[M + Na]^+$.

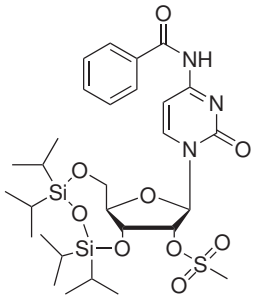

105, $C_{29}H_{45}N_3O_9SSi_2$, MW : 667.92

3',5'-O-(1,1,3,3-tetraisopropyldisiloxane-1,3-diyl)-2'-O-(methanesulfonyl)-N^4-benzoylcytidine (105). Et_3N (0.65 mL, 3.4 mmol) and MsCl (0.35 mL, 2.5 mmol) were added dropwise to a solution of **103** (1.0 g, 1.7 mmol) in dry DCM (16 mL) under nitrogen atmosphere at -10 °C. The cooling bath was removed after 10 minutes and the solution was stirred at r.t. for an additional 2 h. After full conversion of the starting material the solution was poured onto cold brine in a separation funnel and extracted with DCM (2 × 50 mL). The combined organic layer was dried over Na_2SO_4 and concentrated. Purification by column chromatography on SiO_2 (DCM/MeOH 98/2 to 97/3 v/v) gave 690 mg (61%) of the title compound as a white foam; R_f=0.7 (4% MeOH/DCM); ^{1}H NMR (500 MHz, $CDCl_3$) δ 9.45 (s, 1 H, NH), 8.24 (d, J = 7.5 Hz, 1 H, H-6), 7.95 - 7.88 (m, 2 H, benzoyl), 7.57 (m, 2 H, benzoyl, H-5), 7.47 (m, 2 H, benzoyl), 5.85 (s, 1 H, H-1'), 4.98 (d, J = 4.5 Hz, 1 H, H-2'), 4.30 - 4.25 (m, 2 H, H-3', H-4'), 4.14 (dd, J = 9.7, 1.7 Hz, 1 H, H-5'), 4.00 (dd, J = 13.7, 2.4 Hz, 1 H, H-5'), 3.29 (s, 3 H, mesyl), 1.15 - 0.90 (m, 28 H, H-^{i}Pr); ^{13}C NMR (125 MHz, $CDCl_3$) δ 166.9 (C=O, benzoyl), 162.8 (C-4), 154.2 (C-2), 143.5 (C-6), 133.2 (C_{arom}), 128.9 (2 C, CH_{arom}), 127.4 (2 C, CH_{arom}), 96.5 (CH_{arom}), 88.8 (C-5), 82.7 (C-1'), 81.8 (C-4'), 66.6 (C-2'), 58.9 (C-3'), 53.0 (C-5'), 39.2 (CH_3, mesyl), 17.4 (CH_3), 17.4 (CH_3), 17.3 (CH_3), 17.2 (CH_3), 16.9 (CH_3), 16.8 (CH_3), 16.8 (CH_3), 16.7 (CH_3), 13.4 (CH), 12.9 (CH), 12.8 (CH), 12.6 (CH); MS (ESI) *m/z* 690.1 $[M + Na]^+$.

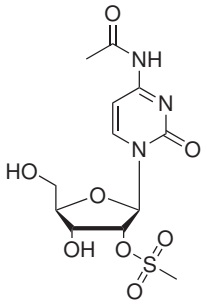

91, $C_{12}H_{17}N_3O_8S$, MW : 363.34

2'-O-(methanesulfonyl)-N^4-acetylcytidine (91). TBAF (2.65 g, 8.4 mmol) was added to a solution of **104** (1.71 g, 2.8 mmol) in dry THF (35 mL) at r.t. under nitrogen. The yellow solution was stirred at r.t. for 40 min. After full conversion of the starting material the solvent was evaporated in vacuo while the water bath was kept below 30 °C. The resulting crude product was purified by column chromatography on SiO_2 (DCM/MeOH 94/6 to 90/10 v/v) to give the title compound **100** (552 mg, 41%) as a white foam. R_f=0.35 (9% MeOH/DCM); ^{1}H NMR (500 MHz, $CDCl_3$) δ 10.93 (s, 1 H, NH), 8.46 (d, J = 7.5 Hz, 1 H, H-6), 7.22 (d, J = 7.5 Hz, 1 H, H-5), 5.97 (d, J = 2.1 Hz, 1 H, H-1'), 5.04 (dd, J = 4.8, 2.1 Hz, 1 H, H-2'), 4.25 (dd, J = 7.5, 4.9 Hz, 1 H, H-3'), 3.94 (dt, J = 7.6, 2.4 Hz, 1 H, H-4'), 3.83 (dd, J = 12.4, 2.2 Hz, 1 H, H-5'), 3.64 (dd, J = 12.5, 2.8 Hz, 1 H, H-5'), 3.38 (s, 3 H, mesyl), 2.12 (s, 3 H, acetyl); ^{13}C NMR (125 MHz, $CDCl_3$) δ 171.0 (C=O, acetyl), 162.7 (C-4), 154.3 (C-2), 145.0 (C-6), 95.5 (C-1'), 88.1 (C-5), 83.8 (C-4'), 82.1 (C-2'), 66.3 (C-3'), 58.9 (C-5'), 38.4 (CH_3, mesyl), 24.5 (CH_3, acetyl); MS (ESI) *m/z* 386 $[M + Na]^+$.

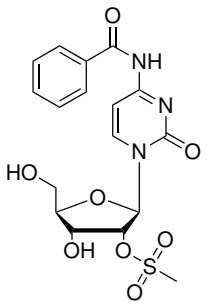

106, $C_{17}H_{19}N_3O_8S$, MW : 425.41

2'-O-(methanesulfonyl)-N^4-benzoylcytidine (106). TBAF (0.75 g, 2.3 mmol) was added to a solution of **105** (0.5 g, 0.75 mmol) in dry THF (15 mL) at r.t. under a nitrogen atmosphere. The yellow solution was stirred at r.t. for 40 min. After full conversion of the starting material the solvent was evaporated in vacuo while the water bath was kept below 30 °C. The resulting crude product was purified by column chromatography on SiO_2 (DCM/MeOH 94/6 to 90/10 v/v) to give the title compound (193 mg, 45%) as a white foam; R_f=0.45 (9% MeOH/DCM); ^{1}H NMR (500 MHz, $CDCl_3$) δ 11.30 (s, 1 H, NH), 8.55 (d, J = 7.0 Hz, 1 H, H-6), 8.03 - 7.99 (m, 2 H, $H_{arom.}$), 7.67 - 7.60 (m, 1 H, $H_{arom.}$), 7.52 (m, 2 H, $H_{arom.}$), 7.39 (d, J = 5.8 Hz, 1 H, H-5), 6.03 (d, J = 2.2 Hz, 1 H, H-1'), 5.79 - 5.77 (m, 1 H, H-5'), 5.34 (s, 1 H, H-2'), 5.09 (dd, J = 4.8, 2.3 Hz, 1 H, H-3'), 4.30 (s, 1 H, OH-3'), 3.97 (dt, J = 7.6, 2.6 Hz, 1 H, H-4'), 3.85 (s, 1 H, OH-5'), 3.67 (dd, J = 12.4, 2.4 Hz, 1 H, H-5'), 3.40 (s, 3 H, CH_3, mesyl); MS (ESI) *m/z* 426.4 $[M + H]^+$.

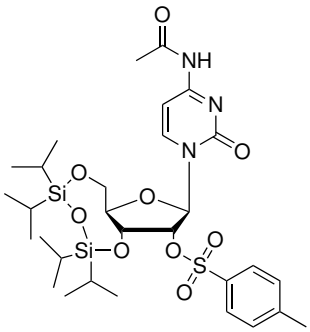

107, $C_{30}H_{47}N_3O_9SSi_2$, MW : 681.94

3',5'O-(1,1,3,3-tetraisopropyldisiloxane-1,3-diyl)-2'-O-(*p*-toluenesulfonyl)-N^4-acetylcytidine (107). Compound **102** (200 mg, 0.38 mmol) was dissolved in dry DCM (4 mL) before Et_3N (0.53 mL, 1.52 mmol), pTsCl (290 mg, 1.52 mmol) and DMAP (94 mg, 0.76 mmol) were added to the solution at r.t. under an argon atmosphere. The solution was stirred for 24 h. After full conversion of the starting material the reaction was quenched by pouring it onto ice. The mixture was extracted with DCM (3 × 15 mL) and the combined organic layer was washed with brine, dried over Na_2SO_4 and concentrated under reduced pressure in a water bath which was kept below 40 °C. The resulting crude product was purified by column chromatography on SiO_2 (eluent: EtOAc/hexane, 60/40 to 50/50 v/v) to give 71 mg of **98b** (44%) as a white foam; R_f=0.4 (EtOAc/hexane, 60/40); ^{1}H NMR (500 MHz, $CDCl_3$) δ 10.42 (s, 1 H, NH), 8.17 (d, J = 7.6 Hz, 1 H, H-6), 7.97 (d, J = 8.3 Hz, 2 H, Harom), 7.48 (d, J = 7.6 Hz, 1 H, H-5), 7.33 (d, J = 8.1 Hz, 2 H, H_{arom}), 5.75 (s, 1 H, H-1'), 5.21 (d, J = 4.4 Hz, 1 H, H-2'), 4.36 (dd, J = 9.5, 4.4 Hz, 1 H, H-4'), 4.27 (d, J = 13.5 Hz, 1 H, H-5'), 4.15 (d, J = 8.6 Hz, 1 H, H-3'), 4.00 (dd, J = 13.6, 2.4 Hz, 1 H, H-5'), 2.43 (s, 3 H, CH_3, tosyl), 2.32 (s, 3 H, CH_3, acetyl), 1.14-0.83 (m, 28 H, H-^{i}Pr); ^{13}C NMR (125 MHz, $CDCl_3$) δ 171.3 (C-4), 163.4 (C=O, acetyl), 154.5 (C-2), 144.5 (C-6), 144.4 ($C_{arom.}$), 134.5 ($C_{arom.}$), 129.6 (2 C, $CH_{arom.}$), 128.0 (2 C, $CH_{arom.}$), 96.9 (C-1'), 89.9 (C-4'), 82.3 (C-2'), 82.1 (C-3'), 66.8 (C-5'), 59.3 (CH_3, tosyl), 24.9 (CH_3, acetyl), 21.6 (CH_3), 17.4 (CH_3), 17.4 (CH_3), 17.3 (CH_3), 17.3 (CH_3), 16.9

(CH_3), 16.8 (3 C, CH_3), 13.3 (CH), 12.9 (CH), 12.8 (CH), 12.6 (CH); MS (ESI) *m/z* 682.5 $[M + H]^+$.

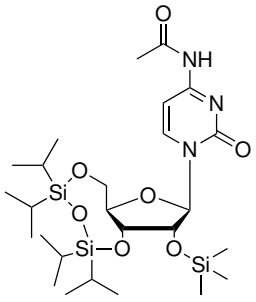

108, $C_{26}H_{49}N_3O_7Si_3$, MW : 599.94

3',5'-O-(1,1,3,3-tetraisopropyldisiloxane-1,3-diyl)-2'-O-(trimethylsilyl)-N^4-acetylcytidine (108). Compound **102** (2.39 g, 4.5 mmol) was dissolved in dry DCM (50 mL) under an argon atmosphere and the solution was cooled to -10 °C. Triethylamine (3.15 mL, 22.6 mmol) and trimethylsilyl chloride (1.15 mL, 9.0 mmol) were added dropwise before the cooling bath was removed and the mixture was then stirred at r.t. for 2.5 h. After full conversion of the starting material the reaction mixture was poured onto a cold saturated aqueous solution of $NaHCO_3$. The mixture was extracted with DCM (3 × 50 mL). The combined organic layer was washed with brine (50 mL), dried over Na_2SO_4 and concentrated. The crude product was purified via column chromatography on SiO_2 (eluent: DCM/MeOH, 98/2 to 96/4 v/v) to give 2.06 g (76%) of **98a** as a white foam; mp 145-147 °C; R_f=0.3 (6% MeOH/DCM); ^{1}H NMR (500 MHz, $CDCl_3$) δ 11.05 (s, 1 H, NH), 8.21 (d, J = 6.9 Hz, 1 H, H-6), 7.33 (d, J = 7.3 Hz, 1 H, H-5), 5.51 (s, 1 H, H-1'), 4.23 - 3.99 (m, 4 H, H-2',3',4',5'), 3.89 (dd, J = 12.6, 1.9 Hz, 1 H, H-5'), 2.20 (s, 3 H, CH_3, acetyl), 1.09 - 0.71 (m, 28 H, H-^{i}Pr), 0.07 (s, 9 H, TMS); ^{13}C NMR (125 MHz, $CDCl_3$) δ 171.3 (C-4), 162.8 (C=O, acetyl), 154.6 (C-2), 143.7 (C-6), 96.1 (C-5), 91.6 (C-1'), 81.3 (C-4'), 75.9 (C-2'), 67.4 (C-3'), 59.3 (C-5'), 24.26 (CH_3, acetyl), 17.3 (CH_3), 17.2 (CH_3), 17.1

(CH_3), 16.9 (CH_3), 16.7 (CH_3), 16.7 (CH_3), 16.6 (CH_3), 16.6 (CH_3), 13.2 (CH), 13.1 (CH), 12.6 (CH), 12.5 (CH), 0.02 (3 C, CH_3, TMS); MS (ESI) *m/z* 601.0 [M + H]$^+$; HRMS (ESI) (M + H)$^+$ calcd for $C_{26}H_{48}N_3O_7SSi_3$ *m/z* 600.2951, found 600.2947.

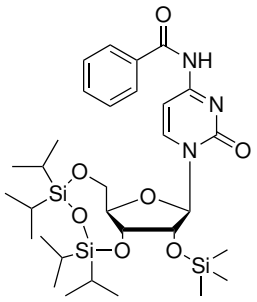

109, $C_{31}H_{51}N_3O_7Si_3$, MW : 662.01

3',5'-O-(1,1,3,3-tetraisopropyldisiloxane-1,3-diyl)-2'-O-(trimethylsilyl)-N^4-acetylcytidine (109). Compound **103** (2.1 g, 3.6 mmol) was dissolved in dry DCM (45 mL) under an argon atmosphere and the solution was cooled to -10 °C. Triethylamine (2.56 mL, 18.1 mmol) and trimethylsilyl chloride (0.92 mL, 7.2 mmol) were added dropwise before the cooling bath was removed and the mixture was then stirred at r.t. for 3.5 h. After full conversion of the starting material the reaction mixture was poured onto a cold saturated aqueous solution of $NaHCO_3$. The mixture was extracted with DCM (3 × 50 mL). The combined organic layer was washed with brine (50 mL), dried over Na_2SO_4 and concentrated. The crude product was purified via column chromatography on SiO_2 (eluent: DCM/MeOH, 99/1 to 97/3 v/v) to give 2.07 g (84%) of **109** as a white foam; mp 161-164 °C; R_f=0.4 (6% MeOH/DCM); ^{1}H NMR (500 MHz, $CDCl_3$) δ 11.10 (s, 1 H, NH), 8.23 (d, J = 7.0 Hz, 1 H, H-6), 8.11 - 8.04 (m, 2 H, $H_{arom.}$), 7.82 - 7.71 (m, 2 H, $H_{arom.}$), 7.48 - 7.41 (m, 1 H, $H_{arom.}$), 7.31 (d, J = 7.3 Hz, 1 H, H-5), 5.41 (s, 1 H, H-1'), 4.19 - 3.93 (m, 4 H, H-2',3',4',5'), 3.91 (dd, J = 12.4, 1.8 Hz, 1 H, H-5'), 1.05 - 0.78 (m, 28 H, H-^{i}Pr), 0.12 (s, 9 H, TMS);

^{13}C NMR (125 MHz, $CDCl_3$) δ 171.3 (C-4), 162.8 (C=O, acetyl), 154.3 (C-2), 143.7 (C-6), 139.0 (C_{arom}), 131.2 (CH_{arom}), 126.1 (2 C, CH_{arom}), 124.1 (CH_{arom}), 122.2 (CH_{arom}), 96.1 (C-5), 91.6 (C-1'), 81.3 (C-4'), 75.9 (C-2'), 67.4 (C-3'), 59.3 (C-5'), 17.3 (CH_3), 17.2 (CH_3), 18.1 (CH_3), 16.9 (CH_3), 16.8 (CH_3), 16.7 (CH_3), 16.6 (CH_3), 16.5 (CH_3), 13.1 (CH), 13.0 (CH), 12.6 (CH), 12.5 (CH), 0.02 (3 C, CH_3, TMS); MS (ESI) *m/z* 663.2 $[M + H]^+$.

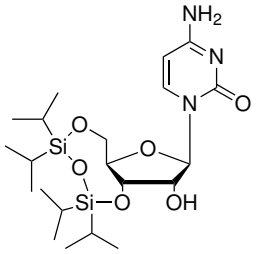

111, $C_{21}H_{39}N_3O_6Si_2$, MW : 485.72

3',5'-O-(1,1,3,3-tetraisopropyldisiloxane-1,3-diyl)-cytidine (111).[234] Cytidine (**110**, 2.3 g, 9.48 mmol) was coevaporated with dry pyridine (2 × 4 mL) before it was suspended in dry pyridine (40 mL) at r.t. under a nitrogen atmosphere. The suspension was cooled to 0 °C before dichloro-1,1,3,3-tetraisopropyldisiloxane (2.0 mL, 6.32 mmol) was added dropwise to the suspension. The icebath was removed and the resulting mixture stirred at r.t. for 5 h. After completion of the reaction the solvent was removed in vacuo. The remaining pyridine was removed by coevaporation with toluene. The resulting crude mixture was subsequently purified by column chromatography on SiO_2 (eluent: DCM/MeOH, 96/4 to 92/8 v/v) to furnish 2.68 g (78%) of the desired compound as a white powder; mp 177 °C; R_f=0.25 (6% MeOH/DCM); ^{1}H NMR (500 MHz, $CDCl_3$) δ 8.26 (s, 1 H, NH), 7.83 (s, 1 H, NH), 7.81 (d, J = 7.6 Hz, 1 H, H-6), 5.87 (d, J = 7.6 Hz, 1 H, H-5), 5.69 (s, 1H, H-1'), 5.55 (s, 1 H, OH-2'), 4.17 (d, J = 13.1 Hz, 1 H, H-5'), 4.11 - 4.00 (m, 3 H, H-2', H-3', H-4'), 3.92 (dd, J = 13.4, 2.1 Hz, 1 H, H-5'), 1.15 - 0.92 (m, 28 H, H-^{i}Pr); ^{13}C NMR (125 MHz, $CDCl_3$) δ 167.2 (C-2),

156.8 (C-4), 141.2 (C-6), 94.4 (C-5), 91.9 (C-1'), 80.2 (C-4'), 77.3 (C-2'), 67.2 (C-3'), 58.4 (C-5'), 17.3 (CH_3), 17.2 (CH_3), 17.0 (CH_3), 16.9 (CH_3), 16.9 (CH_3), 16.4 (CH_3), 16.2 (CH_3), 15.5 (CH_3), 13.2 (CH), 12.7 (CH), 12.6 (CH), 12.5 (CH); MS (ESI) *m/z* 508.2 $[M + Na]^+$.

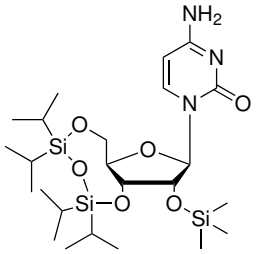

112, $C_{24}H_{47}N_3O_6Si_3$, MW : 557.90

3',5'-O-(1,1,3,3-tetraisopropyldisiloxane-1,3-diyl)-2'-O-(trimethylsilyl)-cytidine (112). Compound **111** (2.39 g, 4.5 mmol) was dissolved in dry DCM (50 mL) under an argon atmosphere and the solution was cooled to -10 °C. Triethylamine (3.15 mL, 22.6 mmol) and trimethylsilyl chloride (1.15 mL, 9.0 mmol) were added dropwise before the cooling bath was removed and the cloudy mixture was then stirred at r.t. for 2.5 h. After full conversion of the starting material the reaction mixture was poured onto a cold saturated aqueous solution of $NaHCO_3$. The mixture was extracted with DCM (3 × 25 mL). The combined organic layer was washed with brine (20 mL), dried over Na_2SO_4 and concentrated. The crude product was then purified via column chromatography on SiO_2 (eluent: DCM/MeOH, 97/3 to 95/5 v/v) to give 2.06 g (76%) of **112** as a white solid; mp 182-185 °C; R_f=0.4 (6% MeOH/DCM); ^{1}H NMR (500 MHz, $CDCl_3$) δ 7.91 (d, J = 7.5 Hz, 1 H, H-6)), 5.67 (d, J = 7.5 Hz, 1 H, H-5), 5.60 (s, 1 H, H-1'), 4.23 (d, J = 13.5 Hz, 1 H, H-4'), 4.14 (dd, J = 11.7, 2.7 Hz, 1 H, H-5'), 4.03 (m, 2 H, H-2', H-3'), 3.95 (dd, J = 13.5, 2.2 Hz, 1 H, H-5'), 0.99 (dd, 28 H, H-^{i}Pr), 0.18 (s, 9 H, TMS); ^{13}C NMR (125 MHz, $CDCl_3$) δ 165.8 (C-2), 155.3 (C-4), 140.1 (C-6), 93.6 (C-5), 91.2 (C-1'), 80.7 (C-4'), 75.8 (C-2'), 67.5 (C-3'), 59.4 (C-5'), 17.2 (CH_3),

17.1 (CH_3), 17.0 (CH_3), 16.9 (CH_3), 16.7 (CH_3), 16.7 (CH_3), 16.6 (CH_3), 16.5 (CH_3), 13.0 (CH), 12.7 (CH), 12.5 (CH), 12.4 (CH), 10.5 (3 C, CH_3,TMS); MS (ESI) *m/z* 580.9 $[M + Na]^+$; HRMS (ESI) calcd for $C_{24}H_{48}N_3O_6Si_3$ (= $[M + H]^+$) *m/z* 558.8184, found 558.8187.

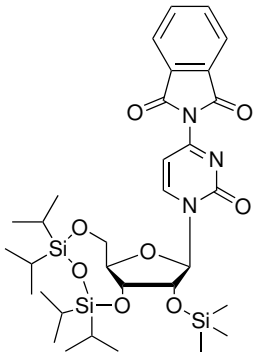

113, $C_{32}H_{49}N_3O_8Si_3$, MW : 688.00

4-(1,2-benzene-dicarboximido)-3',5'-O-(1,1,3,3-Tetraisopropyldisiloxane-1,3-diyl)-2'-O-(trimethylsilyl)-cytidine (113). Compound **112** (400 mg, 0.72 mmol) was coevaporated with dry pyridine (2 × 3 mL) before it was dissolved in dry pyridine (5 mL) at r.t. under nitrogen. DMAP (cat., ≈15 mg) and phthaloyl chloride (0.25 mL, 1.45 mmol), each dissolved in dry DCM (0.5 mL), were added to the stirring solution. The ladder dropwise within 5 min at -5 °C. A white precipitate was formed during the addition and the solution turned slightly yellow. The heterogeneous solution was allowed to warm up to r.t and was stirred for additional 4 h. After complete conversion of the starting material the reaction was quenched by addition of sat. $NaHCO_3$-solution (15 mL). The mixture was extracted with DCM (3 × 20 mL). The combined organic layer was washed with brine (30 mL), dried over Na_2SO_4 and concentrated. The crude product was purified via column chromatography on SiO_2 (eluent: EtOAc/hexane, 55/45 to 75/25 v/v) to give 367 mg (81%) of the title compound **113** as a white solid; mp 187-189 °C; R_f=0.75 (4% MeOH/DCM); ^1H

NMR (500 MHz, $CDCl_3$) δ 8.51 (d, J = 7.2 Hz, 1 H, H-6), 7.94 (td, J = 5.3, 2.1 Hz, 2 H, $H_{arom.}$), 7.82 (td, J = 5.3, 2.1 Hz, 2 H, $H_{arom.}$), 6.66 (d, J = 7.2 Hz, 1 H, H-5), 5.66 (s, 1 H, H-1'), 4.30 - 4.26 (m, 2 H, H-2', H-3'), 4.25 (dd, J = 9.5, 2.1 Hz, 1 H, H-5'), 4.05 (dd, J = 9.5, 3.8 Hz, 1 H, H-4'), 3.99 (dd, J = 13.7, 2.3 Hz, 1 H, H-5'), 1.11 - 0.91 (m, 28 H, H-^{i}Pr), 0.22 (s, 9 H, H-TMS); ^{13}C NMR (125 MHz, $CDCl_3$) δ 164.6 (C-4), 159.2 (C-2), 154.2 (2 C, $C_{arom.}$), 144.6 (2 C, $CH_{arom.}$), 134.8 (C-6), 134.1 (2 C, $C_{carbonyl}$), 131.1 ($CH_{arom.}$), 129.9 ($CH_{arom.}$), 99.7 (C-5), 92.1 (C-1'), 81.5 (C-4'), 75.5 (C-2'), 67.5 (C-3'), 59.26 (C-5'), 17.2 (CH_3), 17.2 (CH_3), 17.0 (CH_3), 16.9 (CH_3), 16.7 (CH_3), 16.7 (CH_3), 16.7 (CH_3), 16.6 (CH_3), 13.1 (CH), 12.8 (CH), 12.6 (CH), 12.5 (CH), 11,1 (3 C, CH_3, TMS); MS (ESI) *m/z* 689.1 $[M + H]^+$; HRMS (ESI) calcd for $C_{32}H_{49}N_3O_8Si_3$ (= $[M + NH_4]^+$) *m/z* 705.3166, found: 705.3165.

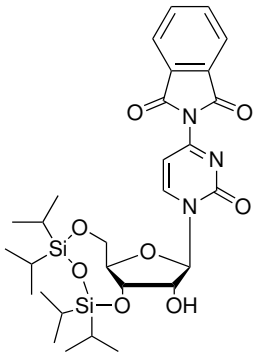

115, $C_{29}H_{41}N_3O_8Si_2$, MW : 615.82

4-(1,2-benzene-dicarboximido)-3',5'-O-(1,1,3,3-Tetraisopropyldisiloxane-1,3-diyl)-cytidine (115). Compound **113** (350 mg, 0.51 mmol) was dissolved in dry DCM (5 mL) before pTsOH (95 mg, 0.5 mmol) was added in portions over 10 min at -5 °C. The mixture was kept at that temperature and stirred for additional 30 min. After full conversion of the starting material the solution was quenched by addition of Et_3N (0.4 mL, 2.5 mmol) at -5 °C. After stirring for another 10 min, the mixture was diluted with sat. $NaHCO_3$-solution

(10 mL). The mixture was extracted with DCM (3 × 10 mL). The combined organic layer was washed with brine (10 mL), dried over Na_2SO_4 and concentrated. The crude product was purified via column chromatography on SiO_2 (eluent: EtOAc/hexane, 70/30 to 80/20 v/v) to give 223 mg (71%) of the title compound **115** as a white foam; R_f=0.55 (4% MeOH/DCM); ^{1}H NMR (500 MHz, $CDCl_3$) δ 8.59 (d, J = 7.2 Hz, 1 H, H-6), 7.98 (dt, J = 7.0, 3.5 Hz, 1 H, $H_{arom.}$), 7.94 - 7.89 (m, 2 H, $H_{arom.}$), 6.90 (d, J = 7.2 Hz, 1 H, H-5), 5.79 (s, 1 H, H-1'), 4.37 - 4.26 (m, 4 H, H-2',3',4',5'), 4.10 (dd, J = 13.5, 1.5 Hz, 1 H, H-5'), 1.33 - 0.77 (m, 28 H, H-^{i}Pr); ^{13}C NMR (125 MHz, $CDCl_3$) δ 171.1 (C-4), 166.4 (C-2), 161.2 (2 C, $C_{arom.}$), 156.8 (2 C, $CH_{arom.}$), 146.3 (C-6), 136.5 ($CH_{arom.}$), 134.1 ($CH_{arom.}$), 132.8 (C-5), 131.9 (2 C, $C_{carbonyl}$), 93.8 (C-1'), 83.4 (C-4'), 75.7 (C-2'), 69.4 (C-3'), 61.1 (C-5'), 18.1 (CH_3), 18.0 (CH_3), 17.9 (CH_3), 17.7 (CH_3), 17.6 (CH_3), 17.5 (CH_3), 17.5 (CH_3), 17.4 (CH_3), 14.7 (CH), 14.4 (CH), 14.2 (CH), 13.8 (CH); MS (ESI) *m/z* 638.9 $[M + Na]^+$; HRMS (ESI) calcd for $C_{29}H_{42}N_3O_8Si_2$ (= $[M + H]^+$) *m/z* 616.4424, found 616.4420.

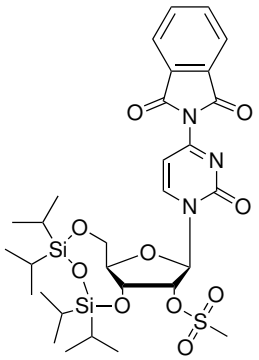

117, $C_{30}H_{43}N_3O_{10}SSi_2$, MW : 693.91

4-(1,2-benzene-dicarboximido)-3'5'-O-(1,1,3,3-Tetraisopropyldisiloxane-1,3-diyl)-2'-O-(methanesulfonyl)cytidine (117). Compound **115** (300 mg, 0.43 mmol) was dissolved in dry DCM (5 mL) under an argon atmosphere before Et_3N (0.3 mL, 2.1 mmol) and mesyl chloride (0.07 mL, 0.84 mmol)

were added to the solution at -5 °C. The resulting solution was stirred for 2 h at r.t. After full conversion of the starting material the mixture was diluted with sat. $NaHCO_3$-solution (10 mL). The mixture was then extracted with DCM (3 × 10 mL) and the combined organic layer was washed with brine (10 mL), dried over Na_2SO_4 and concentrated. The crude product was purified via column chromatography on SiO_2 (eluent: EtOAc/hexane, 20/80 to 30/70 v/v) to give 194 mg (65%) of **117** as a white foam; R_f=0.6 (25% EtOAc/hexane); ^{1}H NMR (500 MHz, $CDCl_3$) δ 8.59 (d, J = 7.2 Hz, 1 H, H-6), 7.98 (dt, J = 7.0, 3.5 Hz, 1 H, $H_{arom.}$), 7.94 - 7.89 (m, 3 H, $H_{arom.}$), 6.90 (d, J = 7.2 Hz, 1 H, H-5), 5.79 (s, 1 H, H-1'), 4.37 - 4.26 (m, 4 H, H-2',3',4',5'), 4.10 (dd, J = 13.5, 1.5 Hz, 1 H, H-5'), 3.38 (s, 3 H, CH_3, mesyl), 1.33 - 0.77 (m, 28 H, H-^{i}Pr); ^{13}C NMR (125 MHz, $CDCl_3$) δ 171.1 (C-4), 166.4 (C-2), 161.2 (2 C, $C_{arom.}$), 156.8 (2 C, $CH_{arom.}$), 146.3 (C-6), 136.5 ($CH_{arom.}$), 134.1 ($CH_{arom.}$), 132.8 (C-5), 131.9 (2 C, $C_{carbonyl}$), 93.8 (C-1'), 83.4 (C-4'), 75.7 (C-2'), 69.4 (C-3'), 61.1 (C-5'), 18.1 (CH_3), 18.0 (CH_3), 17.9 (CH_3), 17.7 (CH_3), 17.6 (CH_3), 17.5 (CH_3), 17.5 (CH_3), 17.4 (CH_3), 14.7 (CH), 14.4 (CH), 14.2 (CH), 13.8 (CH); MS (ESI) *m/z* 716.9 [M + Na]$^+$; HRMS (ESI) calcd for $C_{30}H_{44}N_3O_{10}SSi_2$ (= [M + H]$^+$) *m/z* 694.9133, found 694.9132.

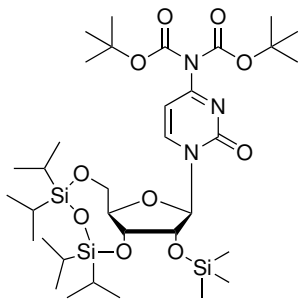

114, $C_{34}H_{63}N_3O_{10}Si_3$, MW : 758.13

N^4-bis-Boc-3',5'-O-(1,1,3,3-Tetraisopropyldisiloxane-1,3-diyl)-2'-O-(trimethylsilyl)-cytidine (114). Compound **112** (3.02 g, 5.4 mmol) was co-

evaporated with dry pyridine (2 × 5 mL) before it was dissolved in dry DCM (35 mL) under an argon atmosphere at r.t. DMAP (650 mg, 5.4 mmol) and di-tert-butyl dicarbonate (4.58 g, 21 mmol) were added to the solution. The reaction mixture was stirred at r.t. for 5 h. After full conversion of the starting material the solution was poured onto cold brine. The resulting mixture was subsequently extracted with DCM (3 × 30 mL). The combined organic layer was washed with brine (30 mL), dried over Na_2SO_4 and concentrated. The crude product was purified via column chromatography on SiO_2 (eluent: EtOAc/hexane, 45/55 to 55/45 v/v) to furnish 3.18 g of the title compound **114** (77%) as a white solid; mp 115-118 °C; R_f=0.7 (5% MeOH/DCM); ^{1}H NMR (500 MHz, $CDCl_3$) δ 8.24 (d, J = 7.6 Hz, 1 H, H-6), 6.95 (d, J = 7.6 Hz, 1 H, H-5), 5.56 (s, 1 H, H-1'), 4.22 (d, J = 13.6 Hz, 1 H, H-4'), 4.18 (d, J = 3.7 Hz, 1 H, H-2'), 4.16 (dd, J = 9.5, 1.8 Hz, 1 H, H-5'), 3.98 (dd, J = 9.5, 3.8 Hz, 1 H, H-3'), 3.93 (dd, J = 13.6, 2.3 Hz, 1 H, H-5'), 1.50 (s, 18 H, Boc), 1.19 - 0.90 (m, 28 H, H-^{i}Pr), 0.16 (s, 9 H, TMS); ^{13}C NMR (125 MHz, $CDCl_3$) δ 162.5 (C-4), 154.2 (C-2), 149.5 (C-6), 143.52 (2 C, $C_{carbonyl}$, Boc) 95.6 (C-5), 92.1 (C-1'), 84.7 (C-5'), 81.5 (C-2'), 75.8 (C-3'), 68.1 (C-5'), 59.6 (2 C, $C_{quat.}$, Boc), 27.9 (6 C, CH_3, Boc), 17.6 (CH_3), 17.5 (CH_3), 17.4 (CH_3), 17.3 (CH_3), 17.0 (CH_3), 16.9 (CH_3), 16.8 (CH_3), 16.8 (CH_3), 13.3 (CH), 13.2 (CH), 12.8 (CH), 12.8 (CH), 12.1 (3 C, (CH_3), TMS); MS (ESI) *m/z* 759.3 $[M + H]^+$; HRMS (ESI) calcd for $C_{34}H_{64}N_3O_{10}Si_3$ (= $[M + H]^+$) *m/z* 759.3894, found 759.3892.

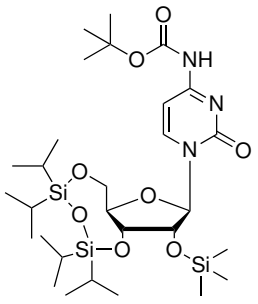

114b, $C_{29}H_{55}N_3O_8Si_3$, MW : 658.02

N^4-Boc-3',5'-O-(1,1,3,3-Tetraisopropyldisiloxane-1,3-diyl)-2'-O-(trimethylsilyl)-cytidine (114b). Compound **112** (2.2 g, 3.9 mmol) was co-evaporated with dry pyridine (2 × 5 mL) before it was dissolved in dry DCM (25 mL) under an argon atmosphere at r.t. DMAP (408 mg, 3.9 mmol) and di-tert-butyl dicarbonate (1.1 g, 5 mmol) were added to the solution. The reaction mixture was stirred at r.t. for 4 h. After full conversion of the starting material the solution was poured onto cold brine. The resulting mixture was subsequently extracted with DCM (3 × 30 mL). The combined organic layer was washed with brine (30 mL), dried over Na_2SO_4 and concentrated. The crude product was purified via column chromatography on SiO_2 (eluent: EtOAC/hexane, 55/55 to 65/45 v/v) to give 2.08 g of the title compound **114b** (81%) as a white foam; mp 127-128 °C; R_f=0.6 (5% MeOH/DCM); ^{1}H NMR (500 MHz, $CDCl_3$) δ 8.32 (d, J = 7.7 Hz, 1 H, H-6), 6.91 (d, J = 7.3 Hz, 1 H, H-5), 5.66 (s, 1 H, H-1'), 4.12 (d, J = 12.9 Hz, 1 H, H-4'), 4.15 (d, J = 3.8 Hz, 1 H, H-2'), 4.11 (dd, J = 9.4, 1.6 Hz, 1 H, H-5'), 3.98 (dd, J = 9.2, 4.8 Hz, 1 H, H-3'), 3.93 (dd, J = 13.2, 3.5 Hz, 1 H, H-5'), 1.56 (s, 9 H, Boc), 1.25 - 0.98 (m, 28 H, H-^{i}Pr), 0.23 (s, 9 H, TMS); ^{13}C NMR (125 MHz, $CDCl_3$) δ 163.1 (C-4), 152.5 (C-2), 147.9 (C-6), 145.5 (1 C, $C_{carbonyl}$, Boc) 96.2 (C-5), 93.5 (C-1'), 85.2 (C-5', 81.5 (C-2'), 77.7 (C-3'), 66.5 (C-5'), 59.2 (1 C, $C_{quart.}$, Boc), 28.1 (3 C, CH_3, Boc), 17.9 (CH_3), 17.1 (CH_3), 16.9 (CH_3), 16.7 (CH_3), 16.6 (CH_3), 16.5 (CH_3), 16.3 (CH_3), 16.2 (CH_3), 13.1 (CH), 13.0 (CH), 12.7 (CH), 12.6 (CH), 12.4 (3 C, (CH_3), TMS); MS (ESI) *m/z* 659.2 $[M + H]^+$.

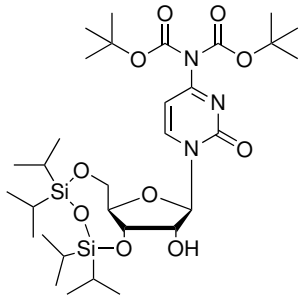

116, $C_{31}H_{55}N_3O_{10}Si_2$, MW : 685.95

N^4-bis-Boc-3',5'-O-(1,1,3,3-Tetraisopropyldisiloxane-1,3-diyl)-cytidine (116). Compound **114** (390 mg, 0.5 mmol) was dissolved in dry DCM (6 mL) before pTsOH (95 mg, 0.5 mmol) was added in portions over 10 min at -5 °C. The mixture was kept at that temperature and stirred for additional 20 min. After full conversion of the starting material the solution was quenched by addition of Et_3N (0.35 mL, 2.5 mmol) at -5 °C. After stirring for another 10 min, the mixture was diluted with sat. $NaHCO_3$-solution (10 mL). The mixture was extracted with DCM (3 × 10 mL). The combined organic layer was washed with brine (10 mL), dried over Na_2SO_4 and concentrated. The crude product was purified via column chromatography on SiO_2 (eluent: EtOAC/hexane, 75/25 to 85/15 v/v) to give 311 mg (90%) of **116** as a white foam; mp 139-143 °C; R_f=0.55 (5% MeOH/DCM); ^{1}H NMR (500 MHz, $CDCl_3$) δ 8.13 (d, J = 7.6 Hz, 1 H, H-6), 7.02 (d, J = 7.6 Hz, 1 H, H-5), 5.75 (s, 1 H, H-1'), 4.28 - 4.15 (m, 4 H; H-2',3',4',5'), 3.98 (dd, J = 13.2, 1.7 Hz, 1 H, H-5'), 3.44 (s, 1 H, OH-2'), 1.53 (s, 18 H, Boc), 1.14 - 0.85 (m, 28 H, H-^{i}Pr); ^{13}C NMR (125 MHz, $CDCl_3$) δ 162.5 (C-2), 154.2 (C-4), 149.4 (2 C, $C_{carbonyl}$, Boc), 143.5 (C-6), 96.0 (C-5), 91.8 (C-1'), 84.8 (C-4'), 81.8 (C-2'), 74.9 (C-3'), 68.4 (C-5'), 59.9 (2 C, $C_{quat.}$, Boc), 27.6 (6 C, CH_3, Boc), 17.4 (CH_3), 17.4 (CH_3), 17.3 (2 C, CH_3), 17.0 (CH_3), 16.9 (CH_3), 16.8 (CH_3), 16.8 (CH_3), 13.3 (CH), 12.9 (CH), 12.8 (CH), 12.4 (CH); MS (ESI) *m/z* 687.0 $[M + H]^+$; HRMS (ESI) calcd for $C_{31}H_{56}N_3O_{10}Si_2$ (= $[M + H]^+$) *m/z* 686.8283, found: 686.8279.

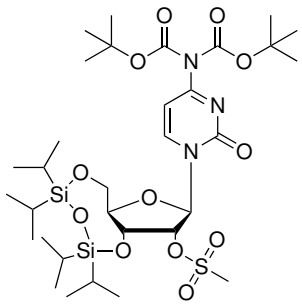

118, $C_{32}H_{57}N_3O_{12}SSi_2$, MW : 764.04

N^4-bis-Boc-3',5'-O-(1,1,3,3-Tetraisopropyldisiloxane-1,3-diyl)-2'-O-(methanesulfonyl)-cytidine (118). Compound **116** (290 mg, 0.42 mmol) was dissolved in dry DCM (4 mL) under an argon atmosphere before Et_3N (0.290 mL, 2.1 mmol) and mesyl chloride (0.065 mL, 0.84 mmol) were added to the solution at -5 °C. The resulting solution was stirred for 1 h at r.t. After full conversion of the starting material the mixture was diluted with sat. $NaHCO_3$-solution (10 mL). The mixture was then extracted with DCM (3 × 10 mL) and the combined organic layer was washed with brine (10 mL), dried over Na_2SO_4 and concentrated. The crude product was purified via column chromatography on SiO_2 (EtOAC/hexane, 45/55 to 55/45 v/v) to give 230 mg (71%) of **118** as a white powder; R_f=0.75 (5% MeOH/DCM); ^{1}H NMR (500 MHz, $CDCl_3$) δ 8.14 (d, J = 7.6 Hz, 1 H, H-6), 7.10 (d, J = 7.6 Hz, 1 H, H-5), 5.81 (s, 1 H, H-1'), 4.96 (d, J = 4.4 Hz, 1 H, H-2'), 4.26 (t, J = 4.7 Hz, 1 H, H-3'), 4.21 (dt, J = 9.6, 4.4 Hz, 1 H, H-4'), 4.12 (dd, J = 9.6, 1.8 Hz, 1 H, H-5'), 3.97 (dd, J = 13.7, 2.4 Hz, 1 H, H-5'), 3.32 (s, 3 H, mesyl), 1.53 (s, 18 H, Boc), 1.17 - 0.81 (m, 28 H, H-^{i}Pr); ^{13}C NMR (125 MHz, $CDCl_3$) δ 162.8 (C-4), 153.9 (C-2), 149.3 (2 C, $C_{carbonyl}$, Boc), 142.6 (C-6), 96.3 (C-5), 89.2 (C-1'), 85.1 (C-2'), 82.5 (C-4'), 81.9 (C-3'), 66.4 (C-5'), 59.0 (2 C,$C_{quart.}$, Boc), 39.2 (CH_3, mesyl), 27.64 (6 C, CH_3, Boc), 17.4 (CH_3), 17.3 (CH_3), 17.2 (CH_3), 17.1 (CH_3), 16.8 (CH_3), 16.7 (CH_3), 16.7 (CH_3), 16.6 (CH_3), 13.3 (CH), 12.9 (CH), 12.7 (CH), 12.5 (CH); MS (ESI) *m/z* 765.1 $[M + H]^+$; HRMS (ESI) calcd for $C_{32}H_{58}N_3O_{12}SSi_2$ (= $[M + H]^+$) *m/z* 765.2043, found: 765.2045.

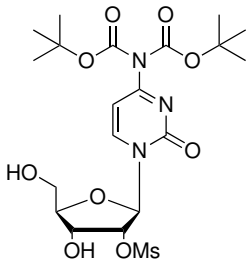

93, $C_{20}H_{31}N_3O_{11}S$, MW : 521.54

N^4-bis-Boc-2'-O-(methanesulfonyl)-cytidine (93). Compound **118** (4.7 g, 6.15 mmol) was dissolved in dry THF (110 mL) before TBAF (3.88g, 12.3 mmol) was added slowly at -10 °C to the stirring solution. The resulting reaction mixture was stirred for additional 20 min at that temperature. After completion of the reaction the solvent was removed under reduced pressure and the resulting crude oil purified via column chromatography on SiO_2 (eluent: EtOAC/hexane, 75/25 to 95/5 v/v) to give 1.44 g the title compound **93** (46%) as a white solid; R_f=0.45 (10% MeOH/DCM); ^{1}H NMR (500 MHz, $CDCl_3$) δ 8.64 (d, J = 7.6 Hz, 1 H, H-6), 7.14 (d, J = 7.6 Hz, 1 H, H-5), 6.06 (d, J = 1.6 Hz, 1 H, H-1'), 5.17 (dd, J = 4.9, 1.6 Hz, 1 H, H-2'), 4.38 (dd, J = 8.1, 4.9 Hz, 1 H, H-3'), 4.10 (dd, J = 5.3, 2.8 Hz, 1 H, H-4'), 4.03 (dd, J = 12.6, 2.2 Hz, 1 H, H-5'), 3.83 (dd, J = 12.6, 2.6 Hz, 1 H, H-5'), 3.34 (s, 3 H, mesyl), 1.58 (s, 18 H, Boc); ^{13}C NMR (125 MHz, $CDCl_3$) δ 164.6 (C-4), 156.6 (C-2), 150.9 (2 C, $C_{carbonyl}$, Boc), 146.3 (C-6), 97.9 (C-5), 90.9 (C-1'), 85.3 (C-2'), 84.1 (C-4'), 68.3 (C-3'), 61.6 (C-5'), 60.4 (2 C,$C_{quart.}$, Boc), 39.02 (CH_3, mesyl), 28.0 (2 C, CH_3), 21.1 (2 C, CH_3), 14.7 (2 C, CH_3); MS (ESI) *m/z* 522.3 $[M + H]^+$.

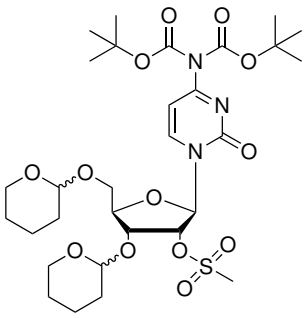

119, $C_{30}H_{47}N_3O_{13}S$, MW : 689.77

N^4-bis-Boc-3',5'-O-bis-tetrahydropyranyl-2'-O-(methanesulfonyl)-cytidine (119). Compound **93** (1.4 g, 2.68 mmol) was dissolved in dry DCM (30 mL) under an argon atmosphere, 3,4-dihydro-puran (2.45 mL, 26.8 mmol) and pTsOH (130 mg, 0.27 mmol) were added to the reaction mixture at 0 °C. The resulting solution was stirred at r.t. for 5 h. After completion of the reaction the mixture was neutralised with Et_3N. Saturated $NaHCO_3$-solution (30 mL) was added and the resulting suspension was then extracted with DCM (3 × 50 mL). The combined organic layer was washed with brine (50 mL), dried over Na_2SO_4 and concentrated. The crude product was purified twice via column chromatography on SiO_2 (eluent: EtOAC/hexane, 40/60 to 65/35 v/v) to furnish 856 mg of precursor **119** (47%) as a white foam (4 diastereomers); HPLC: ≥98% pure (R_t=14.2-15.6 min, 96% MeCN/H_2O); ^{1}H NMR (500 MHz, $CDCl_3$) δ 8.57-8.48 (4 s, 1 H, H-6), 7.14-7.06 (4 s, 1 H, H-5), 5.92-5.87 (4 s, 1 H, H-1'), 5.12-5.07 (m, 1 H), 4.77-4.62 (4 m, 2 H), 4.55-4.45 (m, 1 H), 4.38-4.27 (m, 2 H), 4.02-4.10 (m, 1 H), 3.90-3.75 (m, 3 H), 3.73-3.65 (m, 1 H), 3.63-3.54 (m, 1 H), 3.54-3.41 (m, 3 H), 3.38-3.34 (4 s, 3 H, CH_3, mesyl), 1.82-1.62 (m, 5 H), 1.53-1.52 (m, 18 H, CH_3, Boc), 1.52-1.41 (m, 3 H); MS (ESI) *m/z* 690.7 $[M + H]^+$; HRMS (ESI) calcd for $C_{30}H_{48}N_3O_{13}S$ (= $[M + H]^+$) *m/z* 690.6891, found: 690.6893..

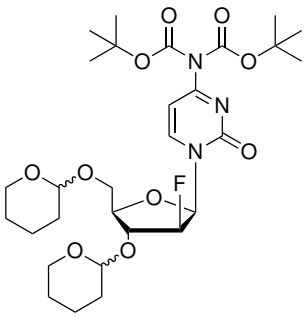

120, $C_{29}H_{44}FN_3O_{13}$, MW : 613.67

N^4-bis-Boc-3',5'-O-bis-tetrahydropyranyl-2'-deoxy-2'-fluoro-arabino-cytidine (120). Fluorination precursor **119** (138 mg, 0.2 mmol) was dissolved in dry DMF (3 mL) in an oven dried Schlenk flask at r.t under an argon atmosphere. Freshly opened 1 M TBAF solution in dry THF (0.6 mL, 0.6 mmol) was added dropwise to the solution. The resulting mixture was stirred at 100 °C for 100 min. After the full conversion of the starting material the solvent was removed under reduced pressure. The crude residue was subsequently purified by column chromatography on SiO_2 (eluent: EtOAc/hexane, 10/90 to 25/80 v/v) to furnish 23 mg (19%) of the fluorinated compound **120** as a colourless oil (four diastereomers); HPLC: ≥95% pure (R_t=17.3 min, 92% MeCN/H_2O); R_f=0.6 (4% MeOH/DCM); ^{1}H NMR (500 MHz, $CDCl_3$) δ 8.44-8.39 (4 s, 1 H, H-6), 7.24-7.17 (4 s, 1 H, H-5), 5.90-5.86 (4 s, 1 H, H-1'), 5.22-5.17 (m, 1 H), 4.82-4.67 (4 m, 2 H), 4.54-4.49 (m, 1 H), 4.36-4.28 (m, 2 H), 4.14-4.10 (m, 1 H), 3.91-3.77 (m, 3 H), 3.70-3.61 (m, 1 H), 3.55-3.48 (m, 1 H), 3.21-3.11 (m, 3 H), 1.88-1.60 (m, 5 H), 1.50-1.46 (m, 18 H, CH_3, Boc), 1.39-1.22 (m, 3 H); ^{19}F NMR (474 MHz, $CDCl_3$) δ -198.6, -198.8, -199.4, -199.2; MS (ESI) *m/z* 636.7 $[M + Na]^+$; HRMS (ESI) calcd for $C_{29}H_{45}FN_3O_{13}$ (= $[M + H]^+$) *m/z* 614.6512, found: 614.6510.

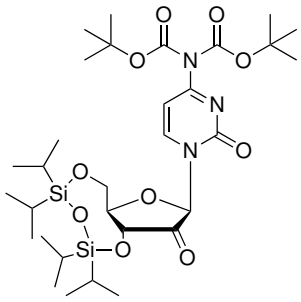

125, $C_{31}H_{53}N_3O_{10}Si_2$, MW : 683.94

N^4-bis-Boc-3',5'O-(1,1,3,3-Tetraisopropyldisiloxane-1,3-diyl)-2'-keto-cytidine (125). A solution of **116** (250 mg, 0.37 mmol) in DCM (5 mL) was cooled to 0 °C before DMP (0.46 g, 1.1 mmol) was added through a funnel to the solution. The resulting cloudy mixture was allowed to warm up to r.t. and was stirred for additional 24 h. After complete conversion of the starting material (monitored by LC-MS) the reaction was quenched with sat. $Na_2S_2O_3/Na_2CO_3$-solution (10 mL). The mixture was then extracted with DCM (2 × 15 mL). The combined organic layer was washed with brine, dried over Na_2SO_4 and concentrated in vacuo. The crude product was subsequently purified by column chromatography on SiO_2 (eluent: EtOAC/hexane, 75/25 to 85/15 v/v) to give 141 mg (57%) of **125** as a white foam; mp 152-154 °C; R_f=0.4 (80% EtOAc/hexane); ^{1}H NMR (500 MHz, $CDCl_3$) δ 8.45 (d, J = 7.5 Hz, 1 H, H-6)), 7.1 (d, J = 7.7 Hz, 1 H, H-5)), 5.75 (s, 1 H, H-1'), 4.26 - 4.2 (m, 4 H; H-2',3',4',5'), 3.92 (dd, J = 13.2, 1.7 Hz, 1 H, H-5'), 1.55 (s, 18 H, Boc), 1.18 - 0.89 (m, 28 H, H-^{i}Pr); ^{13}C NMR (125 MHz, $CDCl_3$) δ 208 (C-2'), 163.5 (C-2), 152.1 (C-4), 149.2 (2 C, $C_{carbonyl}$, Boc), 142.5 (C-6), 96.1 (C-5), 91.5 (C-1'), 84.7 (C-4'), 74.9 (C-3'), 67.2 (C-5'), 57.2 (2 C,$C_{quart.}$, Boc), 26.6 (6 C, CH_3, Boc), 17.2 (CH_3), 17.2 (CH_3), 17.1 (2 C, CH_3), 17.0 (CH_3), 16.9 (CH_3), 16.8 (CH_3), 16.7 (CH_3), 13.3 (CH), 12.8 (CH), 12.8 (CH), 12.4 (CH); MS (ESI) *m/z* 687.0 $[M + H]^+$; HRMS (ESI) calcd for $C_{31}H_{54}N_3O_{10}Si_2$ (= $[M + H]^+$) *m/z* 684.8707, found: 684.8710.

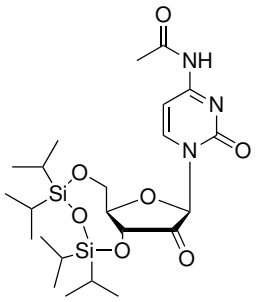

126, $C_{23}H_{39}N_3O_7Si_2$, MW : 525.74

3',5'O-(1,1,3,3-Tetraisopropyldisiloxane-1,3-diyl)-2'keto-N^4-acetylcytidine (126).[233]

DMP oxidation:

A solution of **102** (950 mg, 1.8 mmol) in DCM (15 mL) was cooled to 0 °C before DMP (3.0 g, 7.1 mmol) was added through a funnel to the solution. The resulting cloudy solution was allowed to warm up to r.t. and was stirred for 20 h. After complete conversion of the starting material the reaction was quenched with sat. $Na_2S_2O_3/Na_2CO_3$-solution (20 mL). The mixture was then extracted with DCM (2 × 30 mL). The combined organic layer was washed with brine, dried over Na_2SO_4 and concentrated in vacuo. The crude product was subsequently purified by column chromatography on SiO_2 (DCM/MeOH 98/2 v/v) to furnish 520 mg of the title compound (55%) as a white foam.

Swern oxidation:

Oxalyl chloride (0.2 mL, 1.3 mmol) was dissolved in dry DCM (6 mL) under an argon atmosphere. The solution was cooled to -78 °C before dry DMSO (0.25 mL, 2.8 mmol) was added dropwise to the solution. The mixture was stirred at that temperature for additional 15 min before a solution of compound **102** (300 mg, 0.57 mmol) dissolved in dry DCM (1 mL). Afrer 15 min Et_3N (0.4 mL, 2.8 mmol) was added dropwise and the resulting yellow solution. The mixture was kept additional 15 min at that temperature and was then allowed to warm up r.t. within 30 min. TLC indicated the full conversion of the starting material. The mixture was subsequently poured onto cold brine in a separation funnel followed by an extraction with DCM (2 × 20 mL). The combined organic layer was dried over Na_2SO_4 and concentrated under reduced pressure. The resulting crude mixture was then purified by column chromatography on SiO_2 (DCM/MeOH 97/3 to 95/5 v/v) to furnish 142 mg of the title compound (49%) as a white foam.

mp 145 °C (lit.[233] mp 153 °C); R_f=0.55 (6% MeOH/DCM); ^{1}H NMR (500 MHz, $CDCl_3$) δ 10.51 (s, 1 H, NH), 8.20 (d, J = 7.5 Hz, 1 H, H-6), 7.45 (d, J = 6.3 Hz, 1 H, H-5), 5.81 (s, 1 H, H-1'), 4.28-4.20 (m, 4H), 4.01 (dd, J = 13.3, 2.2 Hz, 1 H, H-5'), 2.30 (s, 3 H, acetyl), 1.13-1.01 (m, 28 H, H-^{i}Pr); ^{13}C NMR (125 MHz, $CDCl_3$) δ ppm 204.1 (C-2'), 170.5 (C-4), 163.1 (C-2), 153.5 (C=O, acetyl), 148.0 (C-6), 96.4 (C-5), 85.4 (C-1'), 80.1 (C-4'), 71.4 (C-3'), 62.6 (C-5'), 23.7 (CH_3), 16.5 (CH_3), 16.4 (CH_3), 16.3 (CH_3), 16.3 (CH_3), 15.9 (CH_3), 15.8 (CH_3), 15.8 (CH_3), 15.6 (CH_3), 12.3 (CH), 12.1 (CH), 11.6 (CH), 11.4 (CH); MS (ESI) *m/z* 548 $[M + Na]^+$.

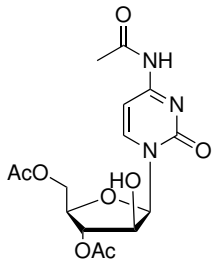

128, $C_{15}H_{19}N_3O_8$, MW : 369.31

3',5'-diacetyl-N^4-acetyl-arabinocytidine (128).[159] N^4-Acetyl cytidine (4.5 g, 15.8 mmol) was azeotropically dried with pyridine (2 × 5 mL). before it was suspended in dry acetonitrile (80 mL) under inert atmosphere. Boron trifluoride etherate (5.45 mL, 45.0 mmol) was added dropwise and the solution was refluxed for 1 h. Acetyl chloride (5.35 mL, 75.0 mmol) was then added via an addition funnel over a period of 15 min. The resulting mixture was refluxed for another 2 h followed by removal of the solvent under reduced pressure. A mixture of diethyl ether/Isopropanol (1.5/1 v/v) was added (3 × 50 mL) to obtain a dark yellow oily residue and a clear filtrate. The crude intermediate was then hydrolised using sat. $NaHCO_3$-solution (70 mL) at r.t for 24 h. The product was filtered and washed with water (3 × 10 mL) before azeotropic drying was performed using pyridine (2 × 5 mL) to give 2.7g of title compound **128** (48%) as a white solid; mp 102-103 °C; R_f=0.45 (10% MeOH/DCM); ^{1}H NMR (500 MHz, $CDCl_3$) δ 10.85 (s, 1 H, NH), 7.97 (d, J = 7.5 Hz, 1 H, H-6), 7.22 (d, J = 7.5 Hz, 1 H, H-5), 6.06 (m, 2 H, H-1', H-2'), 4.96 (s, 1 H, 2'-OH), 4.40 (dd, J = 11.6, 7.5 Hz, 1 H, H-5'), 4.28 (m, 2 H, H-3', H-4'), 4.21 (m, 1 H, H-5'), 2.12 (s, 3 H, CH_3, acetyl), 2.11 (s, 3 H, CH_3, acetyl), 2.06 (s, 3 H, CH_3, acetyl); ^{13}H NMR (125 MHz, $CDCl_3$) δ 172.2 (C-4), 169.3 (C-2), 168.5 (C=O, acetyl), 165.2 (C-6), 157.2 (C=O, acetyl), 143.2 (C=O, acetamide), 101.0 (C-5), 95.3 (C-1'), 81.2 (C-4'), 74.1 (C-2'), 63.3 (C-3'), 58.5 (C-5'), 21.7 (CH_3, acetamide), 21.2 CH_3, acetyl), 21.1 CH_3, acetyl); MS (ESI) *m/z* 370 $[M + H]^+$.

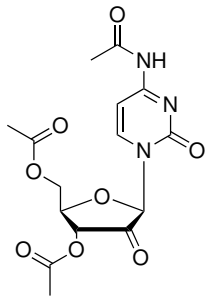

35, $C_{15}H_{17}N_3O_8$, MW : 367.31

3',5'-O-diacetyl-N^4-acetyl-2'-ketocytidine (35).[159]

Starting from Compound 126

Compound **126** (530 mg, 1.0 mmol) was dissolved in dry DCM (8 mL) under nitrogen before a solution of Et_3N (0.8 mL, 5.0 mmol) and $Et_3N \times 3HF$ (0.5 mL, 3.0 mmol) in dry DCM (2 mL) was added dropwise to the reaction mixture at room temperature. The resulting solution was stirred for 1 h. After complete deprotection the mixture was cooled to 0 °C before another aliquot of Et_3N (0.5 mL) and acetyl chloride (0.4 mL, 5.0 mmol) were added dropwise to the reaction mixture. The cloudy solution was allowed to warm up to room temperature and was then stirred over night. The reaction was quenched with sat. $NaHCO_3$-solution and subsequently extracted with DCM (2 × 30 mL). The combined organic layer was dried over Na_2SO_4 and concentrated under reduced pressure. The resulting crude mixture was then purified by column chromatography on SiO_2 (DCM/MeOH 95/5 to 92/8 v/v) to obtain 135 mg of the title compound (32%) as an off-white powder.

Starting from Compound 128

Compound **128** (950 mg, 2.57 mmol) was dissolved in dry MeCN (12 mL) under nitrogen before DMP (3.18 g, 7.5 mmol) to the mixture at 0 °C. The solution was stirred at r.t. for 24 h. After full conversion of the starting material

(monitored LC-MS) the reaction was quenched by adding sat. $Na_2S_2O_3/Na_2CO_3$-solution (10 mL). The mixture was then extracted with DCM (2 × 15 mL). The combined organic layer was washed with brine, dried over Na_2SO_4 and concentrated in vacuo. The crude product was subsequently purified by column chromatography on SiO_2 (DCM/MeOH 95/5 to 92/8 v/v) to obtain 639 mg of the title compound (68%) as an off-white powder.

mp 129-132 °C; R_f=0.6 (8% MeOH/DCM); HPLC: ≥96% pure (R_t=9.6 min, 45% MeCN/H_2O; ^{1}H NMR (500 MHz, $CDCl_3$) δ 10.77 (s, 1 H, NH), 7.81 (d, J = 6.5 Hz, 1 H, H-6), 7.47 (d, J = 6.1 Hz, 1 H, H-5), 6.49 (s, 1 H, H-1'), 4.99-4.85 (m, 1 H, H-4'), 4.43-4.32 (m, 1 H, H-2'), 4.33-4.08 (m, 3 H, H-3', H-5'), 2.28 (s, 3 H, CH_3, acetamide), 2.07 (s, 3 H, CH_3, acetyl), 2.05 (s, 3 H, CH_3, acetyl); ^{13}H NMR (125 MHz, $CDCl_3$) δ 209.4 (C-2'), 171.6 (C-4), 170.3 (C-2), 168.2 (C=O, acetyl), 163.7 (C-6), 154.42 (C=O, acetyl), 145.6 (C=O, acetamide), 103.04 (C-5), 96.4 (C-1'), 80.1 (C-4'), 62.6 (C-3'), 59.51 (C-5'), 24.9 (CH_3, acetamide), 21.3 CH_3, acetyl), 20.5 CH_3, acetyl); MS (ESI) *m/z* 368.1 $[M + H]^+$; HRMS (ESI) calcd for $C_{15}H_{18}N_3O_8$ (= $[M + H]^+$) *m/z* 368.1088, found: 368.1085.

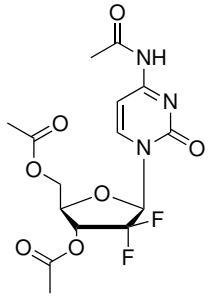

129, $C_{15}H_{17}F_2N_3O_7$, MW : 389.31

3',5'-O-diacetyl-N^4-acetyl-2'-difluoro-deoxycytidine (129).

Acetylation of Gemcitabine:

Gemcitabine (1.0 g, 3.8 mmol) was suspended in dry DCM (15 mL) under nitrogen atmosphere before Et_3N (4.8 mL, 38 mmol) and acetyl chloride (1.36 mL, 19 mmol) were added dropwise to the solution at -10 °C. The mixture was stirred at r.t. for 24 h. After full conversion of the starting material (monitored by LC-MS) the reaction was quenched by pouring the reaction mixture onto ice-cold $NaHCO_3$-solution (50 mL) in a separation funnel. After extraction with DCM (3 × 40 mL) the combined organic layer was washed with brine, dried over Na_2SO_4 and concentrated in vacuo. The crude product was subsequently purified by column chromatography on SiO_2 (DCM/MeOH 98/2 to 96/4 v/v) to obtain 1.37 g of the title compound (93%) as a white powder; mp 129-132 °C; R_f=0.6 (8% MeOH/DCM); HPLC: ≥96% pure (R_t=9.6 min, 45% MeCN/H_2O; ^{1}H NMR (500 MHz, $CDCl_3$) δ 10.59 (s, 1 H, NH), 7.77 (d, J = 7.7 Hz, 1 H, H-6), 7.45 (d, J = 7.7 Hz, 1 H, H-5), 6.36 (t, J = 8.1 Hz, 1 H, H-4'), 5.26 â€“ 5.19 (m, 1 H, H-3'), 4.36 - 4.25 (m, 3 H, H-1',5'), 2.18 (s, 3 H, CH_3), 2.07 (s, 3 H, CH_3), 2.02 (s, 3 H, CH_3); ^{13}H NMR (125 MHz, $CDCl_3$) δ 171.6 (C-4), 170.3 (C-2), 168.2 (C=O, acetyl), 163.7 (C-6), 154.42 (C=O, acetyl), 145.6 (C=O, acetamide), 109.4 (t, ^{1}J(C,F) = 254.7 Hz, C-2'), 103.04 (C-5), 96.4 (t, ^{2}J(C,F) = 27.7 Hz, C-1'), 80.1 (C-4'), 62.6 (t, ^{2}J(C,F) = 22.1 Hz, C-3'), 59.51 (C-5'), 24.9 (CH_3, acetamide), 21.3 CH_3, acetyl), 20.5 CH_3, acetyl); ^{19}F NMR (474 MHz, $CDCl_3$) δ -115.27, -115.76; MS (ESI) *m/z* 390.2 $[M + H]^+$; HRMS (ESI) calcd for $C_{15}H_{18}F_2N_3O_7$ (= $[M + H]^+$) *m/z* 390.1107, found: 390.1108.

Non-radioactive 2'-difluorination of precursor 35 (general procedure):

Precursor **35** (20 mg, 51.4 μmol) was dissolved in the reaction solvent (MeCN, DMF (1.0 mL)) under inert atmosphere. The first fluorination agent (KF/K_{222} or py/HF (1.0 eq.)) was added to the reaction mixture before the organic fluorination agent dissolved in reaction solvent (0.2 mL) (DAST or XtalFluor or Fluolead (10 eq.)) was added dropwise. The resulting mixture was heated to the appropriate reaction temperature and stirred for the appropriate time (2-3 h). The reaction mixture was analysed hourly using LC-MS and TLC. Even though the starting material could not be detected evidence for the formation of the desired 2'-difluorinated compound **129** could not be provided.

5.2.3 Radiochemistry

Production of [^{18}F]fluoride and hot cell equipment

Non-carrier-added [^{18}F]fluoride was produced in an IBA Cyclon 18/9 cyclotron using the ^{18}O(p,n)^{18}F nuclear reaction. ^{18}O-enriched water (enrichment grade 98%, 2.2 mL, Nukem GmbH Germany) was irradiated with 18 MeV protons. Starting activities were between 2.5-55 GBq at the end of bombardment. Radiofluorinations were performed using an Eckert & Ziegler module system and a RNF LAB Laboport vacuum pump N820 (Neuberger, Freiburg, Germany). High-performance liquid chromatography (HPLC) analysis was conducted using an AGILENT Technology 1200 Series System with either an analytical reversed phase column (Phenomenex Synergi 4μ Hydro-RP 80 C-18 4.6 $\cdot$ 250 mm) or a semi-preparative reversed phase column (Phenomenex Synergi 4μ Hydro-RP 80 C-18 10 $\cdot$ 250 mm) coupled with a β-RAM/γ-RAM Model 4 detector (Lablogic Systems, Ltd.) for radioactivity detection. Semi-preparative HPLC was performed with a Smartline pump 100 (Knauer, Germany) and Smartline UV detector 2500 (Knauer, Germany). Radio-TLC was performed using a Canberra

UNISPEC iScan (Meriden, CT, USA) instrument. Radioactivity was determined using a calibrated ion chamber (Capintec CRC-15R). Radioactive material was purified using Sep-Pak Al/C18/QMA cartridges (Waters Corp., Milford, MA, USA). Al cartridges were equilibrated using distilled water (5 mL) and N^2-gas (to dryness). C18 cartridges were equilibrated using distilled water (5 mL) and absolute ethanol (10 mL) followed by N^2-gas (to dryness). QMA cartridges used a Chromafix 30-PS-HCO_3-resin for ion-exchange and were equilibrated using distilled water (5 mL), $NaHCO_3$-solution (0.5 M, 5 mL) and N^2-gas (to dryness). Aqueous tracer solutions were sterilized using Millx-GS 0.22 μm filter units, Millipore, Co. Cork, Ireland.

The automated Eckert & Ziegler synthesis module in the hot cell was configured as shown below (Figure **34**).

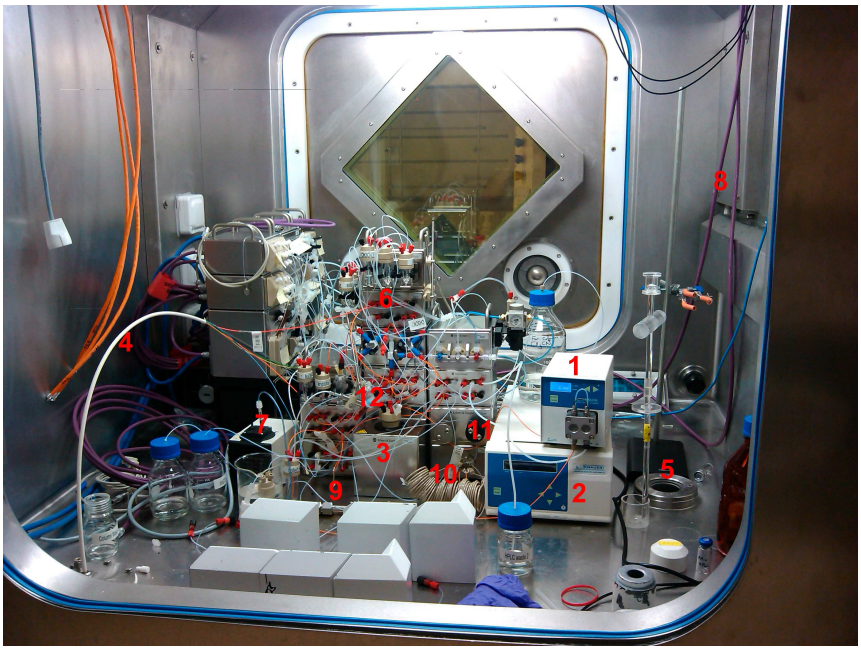

Figure 34: Module system for tracer development at PETIC in the hot cell: (1) prep. HPLC pump; (2) UV detector; (3) reactor; (4) ^{18}F-delivery line; (5) dose calibrator; (6) reagent vials; (7) vacuum pump; (8) argon/nitrogen supply; (9) prep. HPLC column (behind lead brigs); (10) 10 mL HPLC injection loop; (11) HPLC radioactivity detector.

Prior to each experiment all tubing material and vials of the module system were cleaned and dried. All vials were filled with the appropriate reactants/solvents and put in place before radioactivity was delivered. The hot cell remained shut after delivery of radioactivity and thus all reaction parameters such as drying/reaction temperatures, reaction times and reagents were configured using the module system software (Figure **35**).

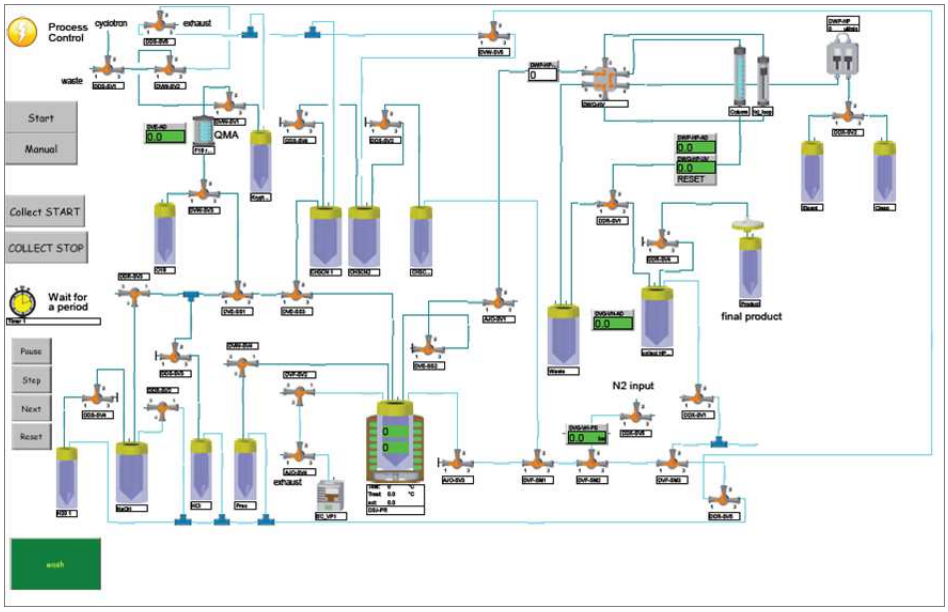

Figure 35: Program configuration of the Eckert & Ziegler module system for general ^{18}F-labelling reactions.

Labelling reactions

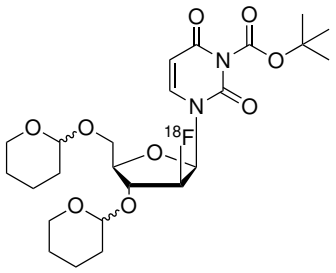

81, $C_{24}H_{35}{}^{18}FN_2O_9$, MW:513.54

N^3-Boc-3',5'-O-bis-tetrahydropyranyl-2'-^{18}F-arabino-uridine (81). Aqueous [^{18}F]fluoride (nca) was trapped on a QMA cartridge and released with an aqueous acetonitrile solution (0.6 mL) containing K_2CO_3 (4.2 mg, 0.03 mmol) and K_{222} (22.6 mg, 0.06 mmol) into a V-vial. The basic [^{18}F]fluoride/K_{222}-mixture was dried by azeotropic evaporation with MeCN (3 × 0.8 mL) at 120 °C. A solution of precursor **79** (10 mg, 0.017 mmol) in dry DMF (0.45 mL) was added to the dried [^{18}F]fluoride/K_{222}-complex. The reaction mixture was heated to 120 °C and stirred for 20 min. The crude reaction mixture was then passed through an Al and a C18 cartridge. The ^{18}F-labelled intermediate was subsequently released using EtOAc (2.0 mL) into a V-vial filled with water (2.0 mL). The heterogeneous mixture was stirred for 5 minutes at r.t. An aliquot of the organic layer was analysed by analytical HPLC and LC-MS. The ^{18}F-labelled intermediate **81** was eluted at R_t=6.3 min (80% MeCN/H_2O (v/v), 1 ml/min flow rate). A spiked sample containing the non-radioactive reference compound confirmed the identity of the intermediate **81** by co-elution. LC-MS gave a strong signal at m/z=512 ($[M-H]^-$) further confirming the identity of **81**. The RCY was calculated to 8.7% (decay-corrected, n = 3) using radio-TLC.

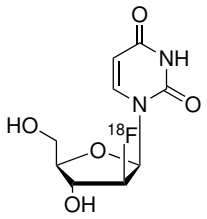

9, $C_9H_{11}{}^{18}FN_2O_5$, MW:245.19

2'-deoxy-2'-^{18}F-arabino-uridine (9). Aqueous [^{18}F]fluoride (nca) was trapped on a QMA cartridge and eluted with an H_2O/acetonitrile solution (0.6 mL, 50/50 v/v) containing K_2CO_3 (4.2 mg, 0.03 mmol) and K_{222} (22.6 mg, 0.06 mmol) into a V-vial. The basic [^{18}F]fluoride/K_{222}-mixture was dried by azeotropic evaporation with MeCN (3 × 0.8 mL) at 120 °C. A solution of precursor **79** (10 mg, 0.017 mmol) in dry DMF (0.45 mL) was added to the dried [^{18}F]fluoride/K_{222}-complex. The reaction mixture was heated up to 120 °C and for 20 min. The solvent was then removed under reduced pressure and a stream of nitrogen at 130 °C. Subsequently, a HCl/MeOH-solution (1 M, 0.3 mL) was added to the crude residue and the mixture was stirred at 70 °C for 10 min. The solvent was evaporated and the residue diluted with a solution of 10% MeCN/H_2O (1 mL). The cooled reaction mixture was then purified using a semi-preparative HPLC column via a 10 mL injection-loop. The product was eluted with 10% MeCN/H_2O (v/v) at a flow of 3mL/min. The appropriate fraction containing ^{18}F-FAU was collected at 15.3 min. An aliquot of the product solution (0.2 mL) was analysed by analytical HPLC (10% MeCN/H_2O, 1mL/min) to verify the purity (≥95%). The specific activity of ≥42 GBq/μmol and RCYs (2.8-3.9%, decay-corrected, n = 3) were calculated with a synthesis time of 178 min.

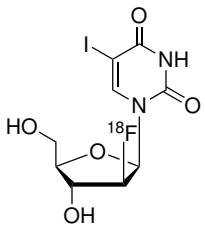

14, $C_9H_{10}{}^{18}FIN_2O_5$, MW:371.09

2'-deoxy-2'-^{18}F-arabino-5-iodouridine (14). Aqueous [^{18}F]fluoride (nca) was trapped on a QMA cartridge and eluted with an aqueous acetonitrile solution (0.6 mL) containing K_2CO_3 (4.2 mg, 0.03 mmol) and K_{222} (22.6 mg, 0.06 mmol) into a V-vial. The basic [^{18}F]fluoride/K_{222}-mixture was dried by azeotropic evaporation with MeCN (3 × 0.8 mL) at 120 °C. A solution of precursor **88** (10 mg, 0.017 mmol) in dry DMF/DMSO (0.3-0.4 mL) was added to the dried [^{18}F]fluoride/K_{222}-complex. The reaction mixture was heated up to 120-140 °C and stirred at that temperature for 20 min. The solvent was then removed under reduced pressure and a stream of nitrogen at 130-140 °C. Subsequently, a HCl/MeOH-solution (1 M, 0.3 mL) was added to the crude residue and the mixture was stirred at 80 °C for 10 min. The cooled crude reaction mixture was analysed using radio-HPLC and radio-TLC by co-elution with the non-radioactive reference standard FIAU. However, the radioactive product **14** could not be detected.

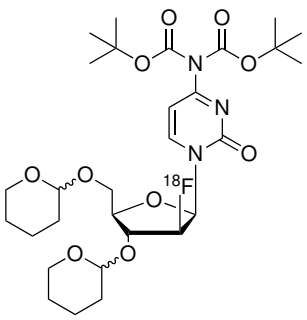

121, $C_{29}H_{44}{}^{18}FN_3O_{10}$, MW : 612.67

^{18}F-FAC-intermediate (121). Aqueous [^{18}F]fluoride (nca) (15 GBq) was trapped on a QMA cartridge before it was eluted with an aqueous solution (0.7 mL) of $KHCO_3$ (22.6 mg/mL) and kryptofix K_{222} (22.6 mg/mL) in acetonitrile (50% H_2O/MeCN v/v). The resulting [^{18}F]fluoride/K_{222}/$KHCO_3$-mixture was dried by co-evaporation under reduced pressure and a stream of nitrogen. The drying process was repeated 3 times (3 × 1 mL MeCN). A solution of precursor **119** (10 mg, 14.5 μmol) in DMF (0.3 mL) was added and the resulting mixture was stirred at 110 °C for 20 min. The crude mixture was passed through an Al and a C18 cartridge. The ^{18}F-labelled intermediate **121** was released using EtOAc (2 mL) and an aliquot (0.2 mL) of the mixture was subsequently analysed by analytical HPLC using co-elution with the non-radioactive reference compound **120**, R_t = 16.7 min (4% H_2O/MeCN (v/v), 1.0 mL/min flow rate). Radio-HPLC confirmed the identity of the ^{18}F-labelled intermediate **121** and the RCY was calculated to 9.4±0.8 (decay-corrected, n = 3).

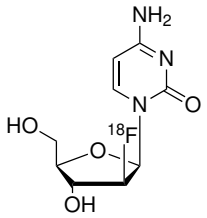

15, $C_9H_{12}{}^{18}FN_3O_4$, MW : 244.21

^{18}F-FAC (15). The procedure for the synthesis of the ^{18}F-labelled intermediate **121** was identical as described above. After the ^{18}F-labelled intermediate was released from the cartridges with EtOAc (2 mL) into a new reaction vial, the solvent was removed under reduced pressure and a stream of nitrogen at 80 °C. Aqueous HCl-solution (2 M, 0.3 mL) was added to the dried residue followed by stirring at 90 °C for 15 min. The solution was then neutralised using a NaOH solution (2 M, 0.3 mL). The resulting mixture was purified by semi-preparative

HPLC. The fraction containing ^{18}F-FAC was collected after 22.5 min with 3% MeCN/H_2O (v/v) and a flow rate of 3.5 mL/min. The collected solution was concentrated and the product taken up in saline before it was flushed through a sterile filter. An aliquot of the final solution was analysed by analytical HPLC to determine identity and purity. ^{18}F-FAC was confirmed and its purity calculated to ≥98% with specific activities ≥1700 mCi/μmol and RCYs between 4.3-5.5% (n = 6, decay-corrected from end of bombardment (EoB)) with a synthesis time of 168 min. Additionally, a carrier-added synthesis was performed according to the above procedure and the product ^{19}F/^{18}F-FAC was saved for decay for 20 half-lives (≈2 days) and subsequently analysed by mass spectrometry; MS (ESI): *m/z* (%): 245.4 (5) $[M + H]^+$, 267.7 (95) $[M + Na]^+$.

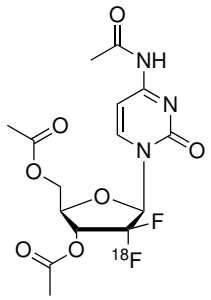

123, $C_{15}H_{17}{}^{18}FFN_3O_7$, MW:388.31

^{18}F-Gemcitabine intermediate (123). Aqueous [^{18}F]fluoride (nca) (8 GBq) was trapped on a QMA cartridge before it was eluted with an aqueous solution (0.7 mL) of $KHCO_3$ (22.6 mg/mL) and kryptofix K_{222} (22.6 mg/mL) in acetonitrile (50% H_2O/MeCN v/v). The resulting ^{18}F/K_{222}/$KHCO_3$-mixture was dried by coevaporation under reduced pressure and a stream of nitrogen. The drying process was repeated 3 times (3 × 1 mL MeCN). A solution of precursor **35** (10 mg, 2.7 μmol) in anhydrous MeCN (0.2 mL) was added followed by the addition of DAST (35 μL, 27 μmol) in anhydrous MeCN (0.2 mL). The resulting mixture was stirred at 60 °C for 30 min and at 90 °C for an additional 60

min. The reaction mixture was cooled to r.t. and the radiolabelled intermediate **123** was then confirmed using radio-HPLC (R_t=7.4 min, 50% MeCN/H_2O (v/v), 1 ml/min flow rate) by co-injection of the non-radioactive reference compound **129**. The crude reaction mixture could be purified using Al and C18 cartridges. The intermediate was released using MeCN (3 mL). The RCY was calculated to 0.3±0.05% (decay-corrected, n = 3) after a synthesis time of 212 min.

5.2.4 Computational procedures

MOE 2010.10 software was used to design each compound and to explore possible conformations. The searching method applied was LowModMD which generates conformations using a short run of Molecular Dynamics (MD) at constant temperature followed by an all-atom energy minimization. Among the conformations, sixteen of them were selected for each compound for quantum mechanics (QM) evaluation. QM calculations were executed for the selected conformations with the GAMESS[214] software. A geometry optimisation was performed in vacuo, using analytical energy gradients with the Restricted Hartree Fock (RHF) wave function.

The 3-21G split valence basis set was used and diffuse sp shell was added to heavy atoms. The initial hessian was guessed and the convergence gradient tolerance was set to 0.0005 Hartree/Bohr. The electrostatic potential was calculated at points determined by Michael Connolly algorithm on the surface of van der Waals fused spheres. Atomic charges were consequently fitted to this potential. The partial net charges of atoms of interest were gathered from each molecule conformation and values were averaged.

6 Appendix

6.1 Selected NMR spectra

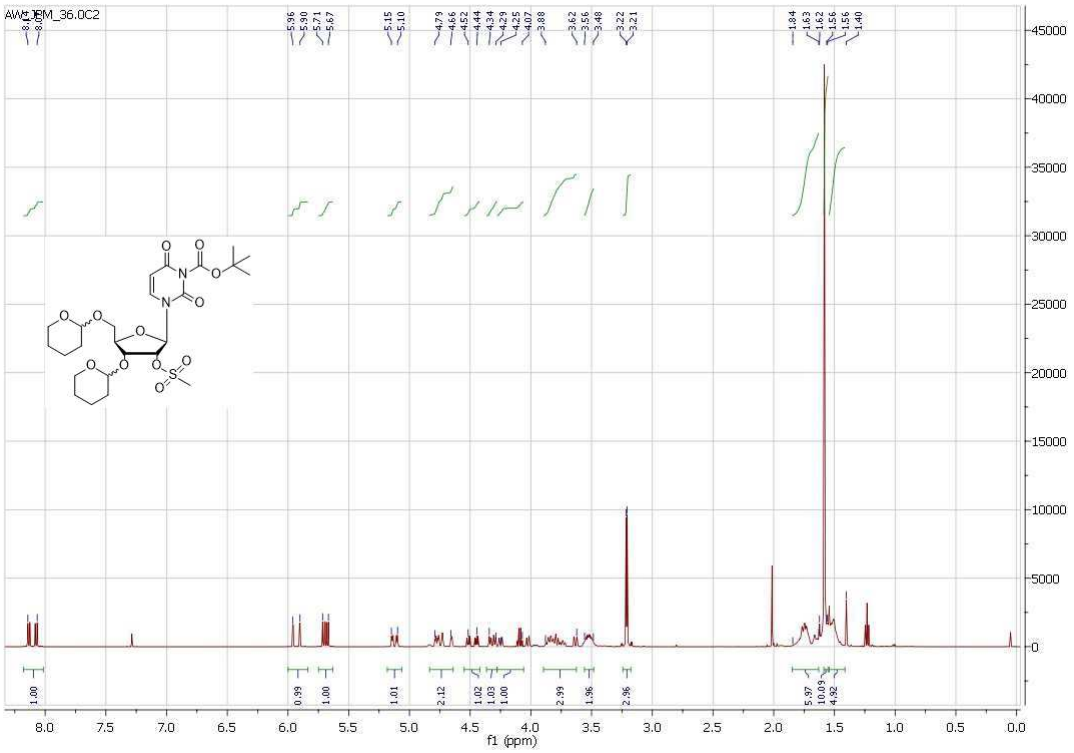

Figure 36: ^{1}H NMR spectrum of mesylate precursor **79** showing the characteristic mesyl-group signals at around 3.2 ppm

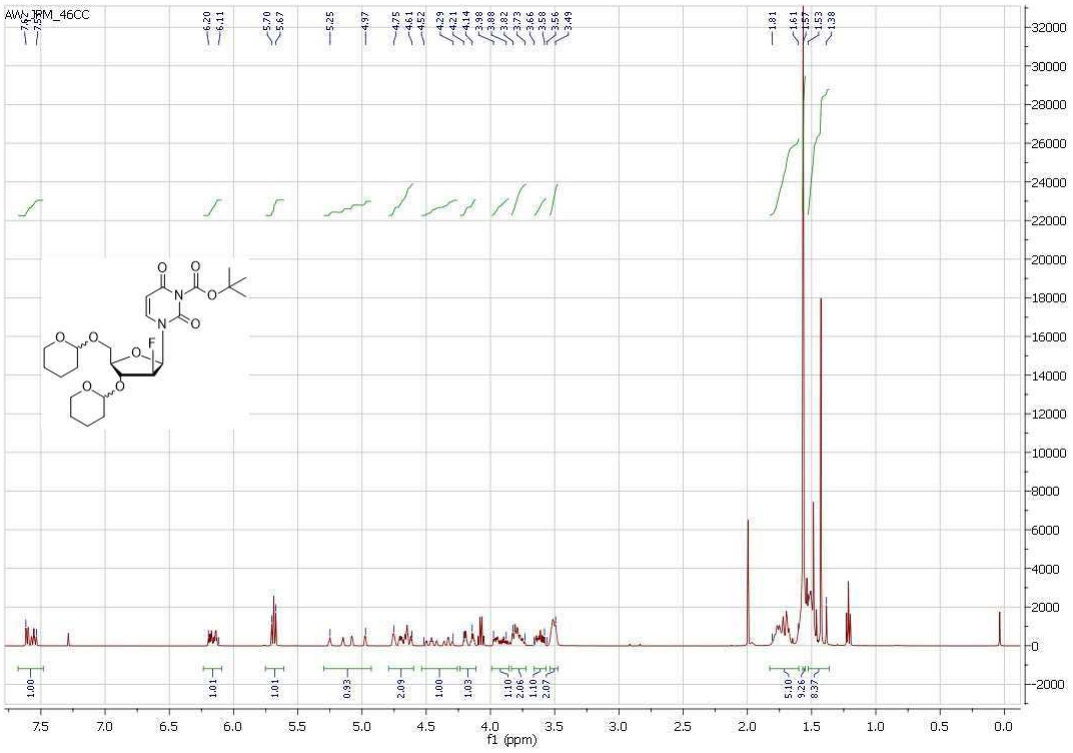

Figure 37: ^{1}H NMR spectrum of the fluorinated FAU intermediate **80**.

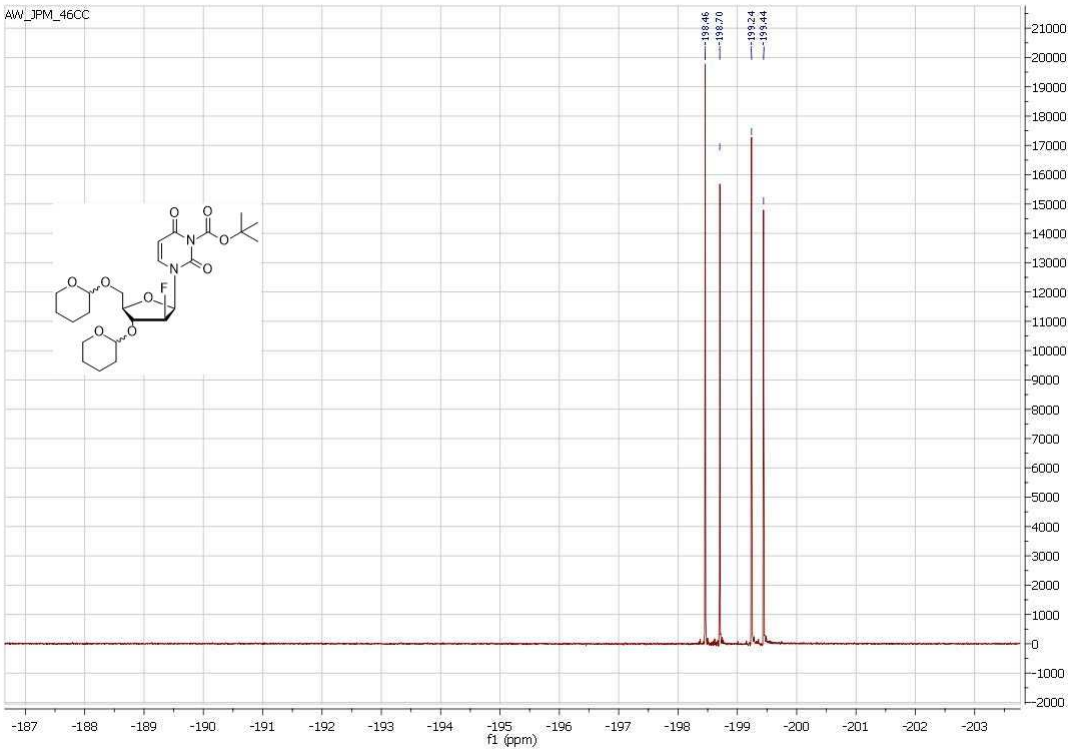

Figure 38: ^{19}F NMR spectrum of the fluorinated FAU intermediate **80**. The four signals correspond to the four diastereomers of the mixture.

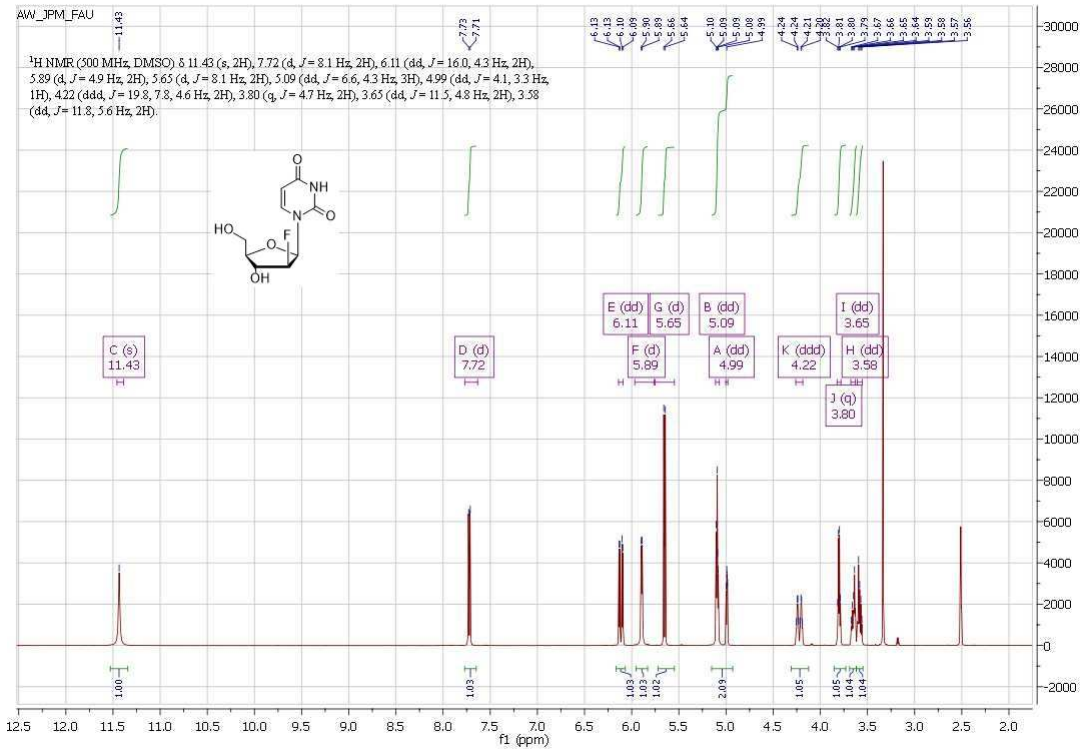

Figure 39: ^{1}H NMR spectrum of FAU (**65**).

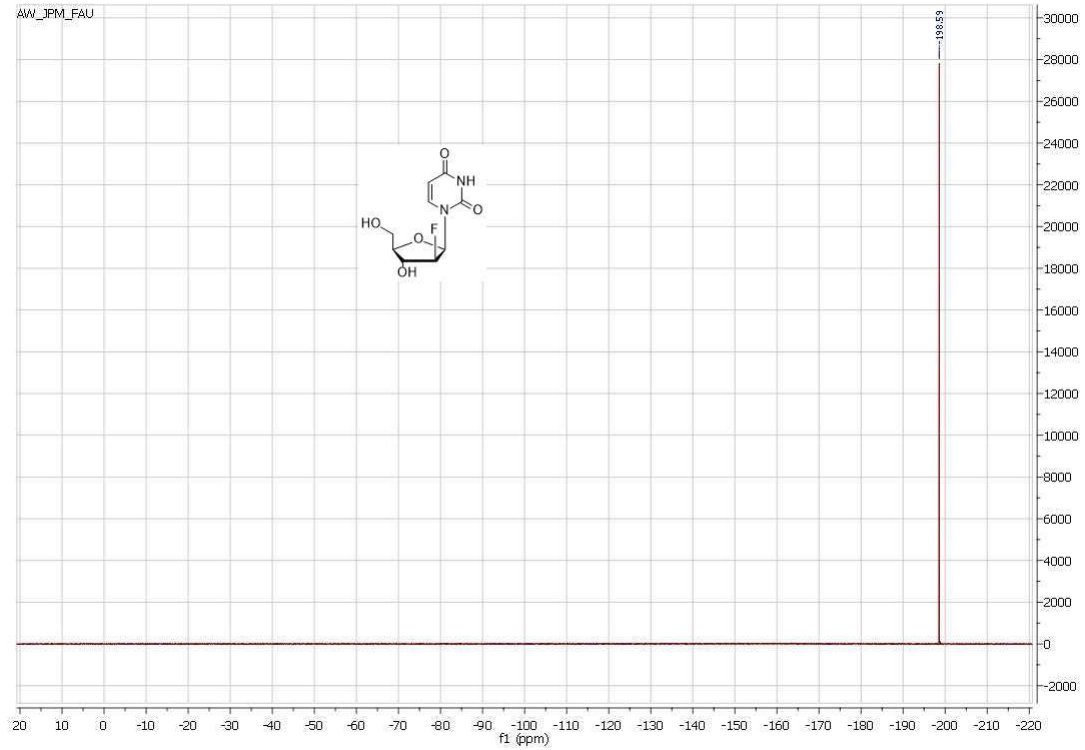

Figure 40: ^{19}F NMR spectrum of FAU (**65**).

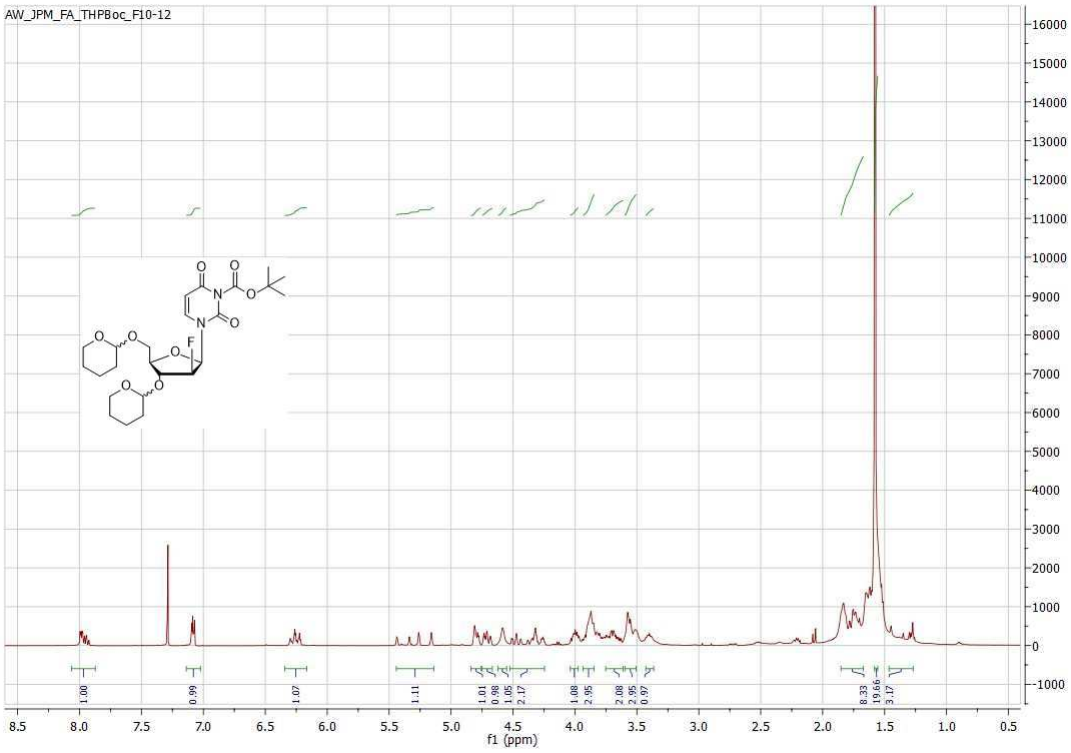

Figure 41: ^{1}H NMR spectrum of FAC-Intermediate **120**.

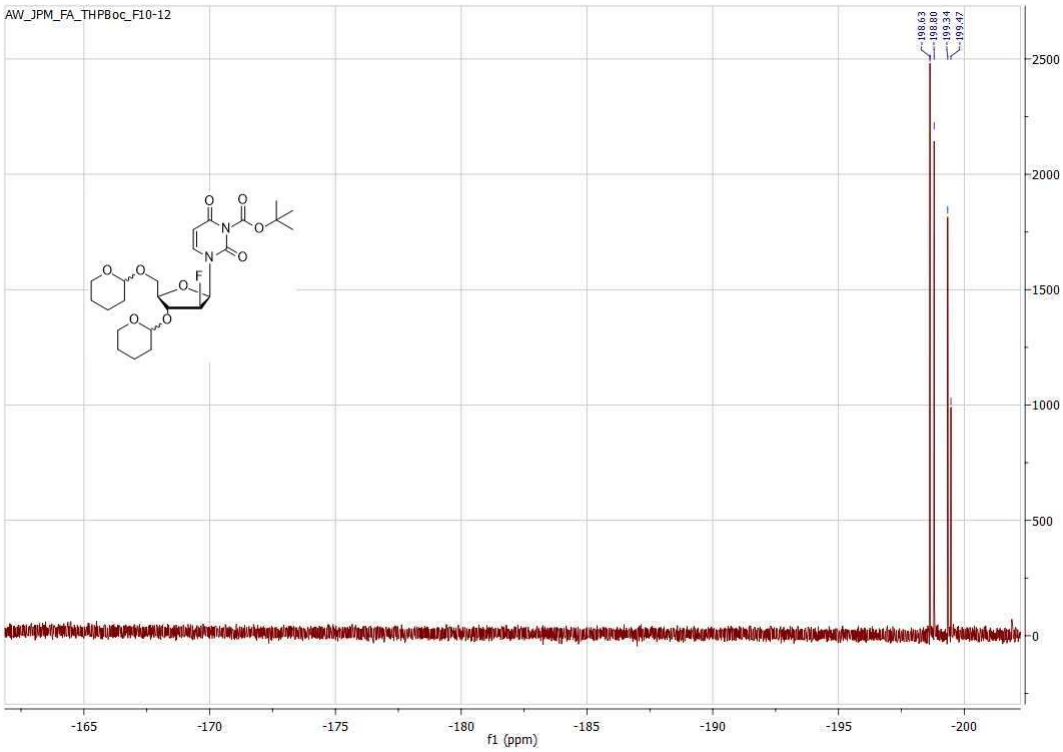

Figure 42: ^{19}F NMR spectrum of FAC-Intermediate **120**.

Bibliography

[1] F. Seela; K. Xua. DNA with stable fluorinated dA and dG substitutes: syntheses, base pairing and 19F NMR spectra of 7-fluoro-7-deaza-2'-deoxyadenosine and 7-fluoro-7-deaza-2'-deoxyguanosine. *Org. Biomol. Chem.*, 6:3552–3560, 2008.

[2] Y. Ma; S. Roy; X. Kong; Y. Chen; D. Liu; R. C. Hider. Design and synthesis of fluorinated iron chelators for metabolic study and brain uptake. *J. Med. Chem.*, 55:2185–2195, 2012.

[3] L. W. L. Woo; D. S. Fischer; C. M. Sharland; M. Trusselle; P. A. Foster; S. K. Chander; A. Di Fiore; C. T. Supuran; G. De Simone; A. Purohit; M. J. Reed; B. V. L. Potter. Anticancer steroid sulfatase inhibitors: Synthesis of a potent fluorinated second-generation agent, in vitro and in vivo activities, molecular modeling, and protein crystallography. *Mol. Cancer Ther.*, 7:2435–2444, 2008.

[4] X. Qiu; X. Xu; F. Qing. Recent advances in the synthesis of fluorinated nucleosides. *Tetrahedron*, 66:789–843, 2010.

[5] S. Daniels; S. F. M. Tohid; W. Velanguparackel; A. D Westwell. The role and future potential of fluorinated biomarkers in positron emission tomography. *Expert Opin. Drug Discov.*, 5:291–301, 2010.

[6] V. Ralevic; G. Burnstock. Receptors for purines and pyrimidines. *Pharmacol. Rev.*, 50:413–492, 1998.

[7] G. Burnstock. Purinergic signaling and vascular cell proliferation and death. *Arterioscler. Thromb. Vasc. Biol.*, 22:364–373, 2002.

[8] G. Burnstock. The past, present and future of purine nucleotides as signalling molecules. *Neuropharmacol.*, 36:1127–1139, 1997.

[9] J. A. Montgomery; J. A. Secrist. Nucleoside analogs as antiviral agents. *Exp. Biol. Med.*, 12:409–416, 1986.

[10] C. M. Galmarini; L. Jordheim; C. Dumontet. Pyrimidine nucleoside analogs in cancer treatment. *Expert Rev. Anticancer Ther.*, 3:717–728, 2003.

[11] P. Liu; A. Sharon; C. K. Chu. Fluorinated nucleosides: Synthesis and biological implication. *J. Fluor Chem.*, 129:743–766, 2008.

[12] H. Lee; Y. Chung; K. Lee; K. S. Byun; S. W. Paik; J. Han; K. Yoo; H. Yoo; J. H. Lee; B. C. Yoo. A 12-week clevudine therapy showed potent and durable antiviral activity in HBeAg-positive chronic hepatitis B. *J. Hepatol.*, 43:982–988, 2006.

[13] A. Pession; R. Masetti; K. Kleinschmidt; A. Martoni. Use of clofarabine for acute childhood leukemia. *Biol. Targets Ther.*, 4:111–118, 2010.

[14] U. Ackermann; G. O'Keefe; S.-T. Lee; A. Rigopoulos; G. Cartwright; J. I. Sachinidis; A. M. Scott; H. J. Tochon-Danguy. Synthesis of a [18F]fluoroethyltriazolylthymidine radiotracer from 2-[18F]-fluoroethyl azide and 5-ethynyl-2'-deoxyuridine. *J. Label Compd. Radiopharm.*, 54:260–266, 2011.

[15] M. C. Koag; H.-K. Kim; A. S. Kim. Fast and efficient microscale radiosynthesis of 3'-deoxy-3'-[18F]fluorothymidine. *J. Fluor Chem.*, 166:104–109, 2014.

[16] C. G. Radu; C. J. Shu; E. Nair-Gill; S. M. Shelly; J. R. Barrio; N. Satyamurthy; M. E. Phelps; O. N. Witte. Molecular imaging of lymphoid organs and immune activation by positron emission tomography with a new [18F]-labeled 2'-deoxycytidine analog. *Nat. Med.*, 14:783–788, 2008.

[17] B. S. Moon; N. H. Jo; K. C. Lee; M. I. El-Gamal; G. I. An; S. H. Hong; T. H. Choi; W. Choi; J. Park; J. Cho; G. J.Cheon; C. Oh. Comparison of D-[18F]-FMAU and L-[18F]-FMAU as PET imaging agents for HSV-TK1 gene expression. *Bull. Korean Chem. Soc.*, 31:3309–3312, 2010.

[18] M. C. Walker; M. C. Y. Chang. Natural and engineered biosynthesis of fluorinated natural products. *Chem. Soc. Rev.*, 43:6527–6536, 2014.

[19] R. Duschinsky; E. Pleven; C. Heidelberger. Synthesis of 5-fluoropyrimidines. *J. Am. Chem. Soc.*, 79:4559–4560, 1957.

[20] T. Furuya; C. A. Kuttruff; T. Ritter. Carbon-fluorine bond formation. *Curr. Opin. Drug Discov. Devel.*, 11:803–819, 2008.

[21] P. L. Bonate; L. Arthaud; W. R. Cantrell; K. Stephenson; J. A. Secrist; S. Weitman. Discovery and development of clofarabine: a nucleoside analogue for treating cancer. *Nat. Rev. Drug Discov.*, 5:855–863, 2006.

[22] M. Che; D.F. Ortiz; I.M. Arias. Primary structure and functional expression of a cDNA encoding the bile canalicular, purine-specific Na(+)-nucleoside cotransporter. *J. Biol. Chem.*, 270:13596–13599, 1995.

[23] S. A. Baldwin; P. R. Beal; S. Y.M. Yao; A. E. King; C. E. Cass; J. D. Young. The equilibrative nucleoside transporter family, SLC29. *Pflugers Arch., EJP*, 447:735–743, 2004.

[24] J. Liou; G. E. Dutschman; W. Lam; Z. Jiang; Y. Cheng. Characterization of human UMP/CMP kinase and its phosphorylation of D- and L-Form deoxycytidine analogue monophosphates. *Cancer Res.*, 62:1624–1631, 2002.

[25] R. E. Lainga; M. A. Walter; D. O. Campbella; H. R. Herschman; N. Satyamurthya; M. E. Phelps; J. Czernina; O. N. Witte; C. G. Radu. Noninvasive prediction of tumor responses to gemcitabine using positron emission tomography. *Proc. Natl. Acad. Sci. USA*, 106:2847–2852, 2009.

[26] L. W. Hertel; G. B. Boder; J. S. Kroin; S. M. Rinzel; G. A. Poore; G. C. Todd; G. B. Grindey. Evaluation of the antitumor activity of gemcitabine (2',2'-difluoro-2'-deoxycytidine). *Cancer Res.*, 50:4417–4422, 1990.

[27] V. Santini; G. D'Ippolito; P.A. Bernabei; A. Zoccolante; A. Ermini; P. Rossi-Ferrini. Effects of fludarabine and gemcitabine on human acute myeloid leukemia cell line HL 60: direct comparison of cytotoxicity and cellular Ara-C uptake enhancement. *Leuk. Res.*, 20:37–45, 1996.

[28] K. Brown; M. Dixey; A. Weymouth-Wilson; B. Linclau. The synthesis of gemcitabine. *Carbohydr. Res.*, 387:59–73, 2014.

[29] J. Pfisterer; M. Plante; I. Vergote; A. du Bois; H. Hirte; A. J. Lacave; U. Wagner; A. Staehle; G. Stuart; R. Kimmig; S. Olbricht; T. Le; J. Emerich; W. Kuhn; J. Bentley; C. Jackisch; H.-J. Lueck; J. Rochon; A. H. Zimmermann; E. Eisenhauer. Gemcitabine plus carboplatin compared with carboplatin in patients with platinum-sensitive recurrent ovarian cancer: An intergroup trial of the AGO-OVAR, the NCIC CTG, and the EORTC GCG. *J. Clin. Oncol.*, 24:4699–4707, 2006.

[30] A. J. Montero; S. Glück. V. Gudena. Gemcitabine and taxanes in metastatic breast cancer: A systematic review. *Ther. Clin. Risk Manag.*, 4:1157–1164, 2008.

[31] S. Réjib; C. Bigand; C. Parmentier; A. Hajri. Gemcitabine-based chemogene therapy for pancreatic cancer using Ad-dCK/UMK GDEPT and TS/RR siRNA strategies. *Neoplasia*, 11:637–650, 2009.

[32] A. Maksimenko; J. Mougin; S. Mura; E. Sliwinski; E. Lepeltier; C. Bourgaux; S. Lepêtre; F. Zouhiri; D. Desmaële; P. Couvreur. Polyisoprenoyl gemcitabine conjugates self assemble as nanoparticles, useful for cancer therapy. *Cancer Lett.*, 334:346–353, 2013.

[33] J. H. Beumer; J. L. Eiseman; R. A. Parise; E. Joseph; J. M. Covey; M. J. Egorin. Modulation of gemcitabine (2',2'-difluoro-2'-deoxycytidine) pharmacokinetics, metabolism, and bioavailability in mice by 3,4,5,6-tetrahydrouridine. *Clin. Cancer Res.*, 14:3529–3535, 2008.

[34] M. Saif; Y. Lee; R. Kim. Harnessing gemcitabine metabolism: a step towards personalized medicine for pancreatic cancer. *Ther. Adv. Med. Oncol.*, 4:341–346., 2012.

[35] E. Mini; S. Nobili; B. Caciagli; I. Landini; T. Mazzei. Cellular pharmacology of gemcitabine. *Ann. Oncol.*, 17:7–12, 2006.

[36] E. Giovannetti; V. Mey; L. Loni; S. Nannizzi; G. Barsanti; G. Savarino; S. Ricciardi; M. Del Tacca; R. Danesi. Cytotoxic activity of gemcitabine and correlation with expression profile of drug-related genes in human lymphoid cells. *Pharmacol. Res.*, 55:343–349, 2007.

[37] X.-M. Tao; J. Wang; J. Wang; Q. Feng; S. Gao; L.-R. Zhang; Q. Zhang. Enhanced anticancer activity of gemcitabine coupling with conjugated linoleic acid against human breast cancer in vitro and in vivo. *Eur. J. Pharm. Biopharm.*, 82:401–409, 2012.

[38] F. H. F. Galvao; J. O. M. Pestana; V. L. Capelozzi. Fatal gemcitabine induced pulmonary toxicity in metastatic gallbladder adenocarcinoma. *Cancer Chemother. Pharmacol.*, 65:607–610, 2010.

[39] M. Slusarczyk; M. Huerta Lopez; J. Balzarini; M. Mason; W. G. Jiang; S. Blagden; E. Thompson; E. Ghazaly; C. McGuigan. Application of ProTide

technology to gemcitabine: A successful approach to overcome the key cancer resistance mechanisms leads to a new agent (NUC-1031) in clinical development. *J. Med. Chem.*, 57:1531–1542, 2014.

[40] M. Vandana; S. K. Sahoo. Long circulation and cytotoxicity of PEGylated gemcitabine and its potential for the treatment of pancreatic cancer. *Biomaterials*, 31:9340–9456, 2010.

[41] Y. Zhang; W. Y. Kim; L. Huang. Systemic delivery of gemcitabine triphosphate via LCP nanoparticles for NSCLC and pancreatic cancer therapy. *Biomaterials*, 34:3447–3458, 2013.

[42] T. E. Bapiro; F. M. Richards; M. A. Goldgraben; K. P. Olive; B. Madhu; K. K. Frese; N. Cook; M. A. Jacobetz; D.-M. Smith; D. A. Tuveson; J. R. Griffiths; D. I. Jodrell. A novel method for quantification of gemcitabine and its metabolites 2,2'-difluorodeoxyuridine and gemcitabine triphosphate in tumour tissue by LC–MS/MS: comparison with [19F] NMR spectroscopy. *Cancer Chemother. Pharmacol.*, 68:1243–1253, 2011.

[43] P. Huang; W. Plunkett. Induction of apoptosis by gemcitabine. *Semin. Oncol.*, 22:19–25, 1995.

[44] R. Bar-Shalom; A.Y. Valdivia; M.D. Blaufox. PET imaging in oncology. *Semin. Nucl. Med.*, 30:150–185, 2000.

[45] M. L. James; S. S. Gambhir. A molecular imaging primer: Modalities, imaging agents, and applications. *Physiol. Rev.*, 92:897–965, 2012.

[46] P. Glover; P. Mansfield. Limits to magnetic resonance microscopy. *Rep. Prog. Phys.*, 65:1489, 2002.

[47] S. G. Nekolla; A. Martinez-Moeller; A. Saraste. PET and MRI in cardiac imaging: from validation studies to integrated applications. *Eur. J. Nucl. Med. Mol. Imaging*, 36(Suppl. 1):S121–S130, 2009.

[48] G. Smith; L. Carroll; E. O. Aboagye. New frontiers in the design and synthesis of imaging probes for PET oncology: Current challenges and future directions. *Mol. Imaging Biol.*, 14:653–666, 2012.

[49] A. Chopra; L. Shan; W. C. Eckelman; K. Leung; M. Latterner; S. H. Bryant; A. Menkens. Molecular imaging and contrast agent database (MICAD): Evolution and progress. *Mol. Imaging Biol.*, 14:4–13, 2012.

[50] C.-M. Lee; L. Farde. Using positron emission tomography to facilitate CNS drug development. *Trends Pharmacol. Sci.*, 27:310–316, 2006.

[51] M. Rudin; R. Weissleder. Molecular imaging in drug discovery and development. *Nat. Rev. Drug Discov.*, 2:123–131, 2003.

[52] M. Piel; I. Vernaleken; F. Roesch. Positron emission tomography in CNS drug discovery and drug monitoring. *J. Med. Chem.*, 57:9232–9258, 2014.

[53] S. M. Ametamey; M. Honer; P. A. Schubiger. Molecular imaging with PET. *Chem. Rev.*, 108:1501–1516, 2008.

[54] M. E. Phelps. Positron emission tomography provides molecular imaging of biological processes. *Proc. Natl. Acad. Sci. USA*, 97:9226–9233, 2000.

[55] T. G. Turkington. Introduction to PET instrumentation. *J. Nucl. Med. Technol.*, 29:1–8, 2001.

[56] M. E. Phelps, editor. *PET: Molecular Imaging and Its Biological Applications.* Springer, 2004.

[57] Magdy Khalil, editor. *Basic Sciences of Nuclear Medicine.* Springer, 2011.

[58] D.W. Townsend. Physical principles and technology of clinical PET imaging. *Ann. Acad. Med. Singapore*, 33:133–145, 2004.

[59] J. S. Karp; S. Surti; M. E. Daube-Witherspoon; G. Muehllehner. Benefit of Time-of-Flight in PET: Experimental and clinical results. *J. Nucl. Med.*, 49:462–470, 2008.

[60] P. C. Ricci; C. M. Carbonaro; D. Chiriu; R. Corpino; N. Faedda; M. Marceddu; A. Anedda. Ce3+-doped lutetium yttrium orthosilicate crystals: Structural characterization. *Mat. Sci. Eng. B*, 146:2–6, 2008.

[61] S. Surti; J. S. Karp; G. Muehllehner; P. S. Raby. Investigation of Lanthanum scintillators for 3-D PET. *IEEE Nucl. Sci. Conf. R.*, 2:1177 – 1181, 2002.

[62] C. L. Melcher. Scintillation crystals for PET. *J. Nucl. Med.*, 41:1051–1055, 2000.

[63] G. Tarantola; F. Zito; P. Gerundini. PET instrumentation and reconstruction algorithms in Whole-Body applications. *J. Nucl. Med.*, 44:756–769, 2003.

[64] B. J. Pichler; M. S. Judenhofer; C. Catana; J. H. Walton; M. Kneilling; R. E. Nutt; S. B. Siegel; C. D. Claussen; S. R. Cherry. Performance test of an LSO-APD detector in a 7-T MRI scanner for simultaneous PET/MRI. *J. Nucl. Med.*, 47:639–647, 2006.

[65] S. Surti; J. S. Karp. Imaging characteristics of a 3-Dimensional GSO Whole-Body PET camera. *J. Nucl. Med.*, 45:1040–1049, 2004.

[66] C. J. Thompson; A. L. Goertzen; J. Thiessen; D. Bishop; G. Stortz; P. Kozlowski; F. Retiere; X. Zhang; V. Sossi. Development of a PET scanner for simultaneously imaging small animals with MRI and PET. *Sensors*, 14:14654–14671, 2014.

[67] G. Arino; M. Chmeissani; G. De Lorenzo; C. Puigdengoles; E. Cabruja; Y. Calderón; M. Kolstein; J. G. Macias-Montero; R. Martinez; E.

Mikhaylova; D. Uzun. Energy and coincidence time resolution measurements of CdTe detectors for PET. *J Instrum.*, 8. pii:C02015, 2013.

[68] M. E. Phelps; E. J. Hoffman; N. A. Mullani; M. M. Ter-Pogossian. Application of annihilation coincidence detection to transaxial reconstruction tomography. *J. Nucl. Med.*, 16:210–226, 1975.

[69] F. H. Fahey. Data acquisition in PET imaging. *J. Nucl. Med. Technol.*, 30:39–49, 2002.

[70] M. A. King; P. H. Pretorius; T. Farncombe; F. J. Beekman. Introduction to the Physics of Molecular Imaging with radioactive tracers in small animals. *J. Cell. Biochem.*, 87(39):221–230, 2002.

[71] M. A. Lodge; R. D. Badawi; R. Gilbert; P. E. Dibos; B. R. Line. Comparison of 2-dimensional and 3-dimensional acquisition for 18F-FDG PET oncology studies performed on an LSO-based scanner. *J. Nucl. Med.*, 47:23–31, 2006.

[72] D. Visvikis; D. Griffiths; D. C. Costa; J. Bomanji; P. J. Ell. Clinical evaluation of 2D versus 3D whole-body PET image quality using a dedicated BGO PET scanner. *Eur. J. Nucl. Med. Mol. Imaging*, 32:1050–1056, 2005.

[73] M. D. Seemann; S. Nekolla; S. Ziegler; F. Bengel; M. Schwaiger. PET/CT: Fundemental Principles. *Eur. J. Med. Res.*, 9:241–246, 2004.

[74] P. E. Kinahan; D. W. Townsend; T. Beyer; D. Sashin. Attenuation correction for a combined 3D PET/CT scanner. *Med. Phys.*, 25:2046, 1998.

[75] N. S. Rehfeld; B. J. Heismann; J. Kupferschläger; P. Aschoff; G. Christ; A. C. Pfannenberg; B. J. Pichler. Single and dual energy attenuation correction in PET/CT in the presence of iodine based contrast agents. *Med. Phys.*, 35:1959–1969, 2008.

[76] M. Defrise; A. Geissbuhler; D. W. Townsend. A performance study of 3D reconstruction algorithms for positron emission tomography. *Phys. Med. Biol.*, 39:305–320, 1994.

[77] H. M. Hudson; R. S. Larkin. Accelerated image reconstruction using ordered subsets of projection data. *IEEE Trans. Med. Imag.*, 13:601–609, 1994.

[78] D. L. Bailey; D. W. Townsend., editor. *Positron Emission Tomography.* Springer, London, 2005.

[79] M. J. Rennie. An introduction to the use of tracers in nutrition and metabolism. *P. Nutr. Soc.*, 58:935–944, 1999.

[80] R. Weissleder; U. Mahmood. Molecular imaging. *Radiology*, 219:316–333, 2001.

[81] F. J. Bonte. The Evolution of Nuclear Medicine. *J. Nucl. Med.*, 36:26N–27N, 1995.

[82] M. Bergstroem; A. Grahnen; B. Langstroem. Positron emission tomography microdosing: A new concept with application in tracer and early clinical drug development. *Eur. J. Clin. Pharmacol.*, 59:357–366, 2003.

[83] G. Hagan; M. Southwood; C. Treacy; R. MacKenzie Ross; E. Soon; J. Coulson; K. Sheares; N. Screaton; J. Pepke-Zaba; N. W. Morrell; J. H. F. Rudd. 18F-FDG PET imaging can quantify increased cellular metabolism in pulmonary arterial hypertension: A proof-of-principle study. *Pulm. Circ.*, 1:448–455, 2011.

[84] S. Vallabhajosula. 18F-labeled positron emission tomographic radiopharmaceuticals in oncology: An overview of radiochemistry and mechanisms of tumor localization. *Semin. Nucl. Med.*, 37:400–419, 2007.

[85] J.-P. Meyer; K. C. Probst; A. D. Westwell. Radiochemical synthesis of 2'-18F-labelled and 3'-18F-labelled nucleosides for positron emission tomography imaging. *J. Label Compd. Radiopharm.*, 57:333–337, 2014.

[86] R. C. Garner; G. Lappin. The phase 0 microdosing concept. *Br. J. Clin. Pharmacol.*, 61:367–370, 2006.

[87] M. Muzia; F. O'Sullivan; D. A. Mankoff; R. K. Doota; L. A. Pierce; B. F. Kurland; H. M. Lindene; P. E. Kinahan. Quantitative assessment of dynamic PET imaging data in cancer imaging. *Magn. Reson. Imaging*, 30:1203–1215, 2012.

[88] O. Jacobson; X. Chen. PET designated fluoride-18 production and chemistry. *Curr. Top. Med. Chem.*, 10:1048–1059, 2010.

[89] L. Koehler; K. Gagnon; S. McQuarrie; F. Wuest. Iodine-124: A promising positron emitter for organic PET chemistry. *Molecules*, 15:2686–2718, 2011.

[90] E. C. Dijkers; T. H. Oude Munnink; J. G. Kosterink; A. H. Brouwers; P. L. Jager; J. R. de Jong; G. A. van Dongen; C. P. Schröder; M. N. Lub-de Hooge; E. G. de Vries. Biodistribution of 89-Zr-trastuzumab and PET imaging of HER2-positive lesions in patients with metastatic breast cancer. *Clin. Pharmacol. Ther.*, 87:586–592, 2010.

[91] Y. Zhang; H. Hong; W. Cai. PET tracers based on Zirconium-89. *Curr. Radiopharm.*, 4:131–139, 2011.

[92] K. K. Wong; M. Piert. Dynamic bone imaging with 99-Tc-labeled diphosphonates and 18F-NaF: Mechanisms and applications. *J. Nucl. Med.*, 54:590–599, 2013.

[93] D. S. Boss; R. V. Olmos; M. Sinaasappel; J. H. Beijnen; J. H. M. Schellens. Application of PET/CT in the development of novel anticancer drugs. *The Oncologist*, 13:25–28, 2008.

[94] M. Schwaiger; H. Wester. How many PET tracers do we need? *J. Nucl. Med.*, 52:36S–41S, 2011.

[95] B. L. Gerber; J. A. Melin; A. Bol; D. Labar; M. Cogneau; C. Michel; J. L Vanoverschelde. Nitrogen-13-ammonia and oxygen-15-water estimates of absolute myocardial perfusion in left ventricular ischemic dysfunction. *J. Nucl. Med.*, 39:1655–1662, 1998.

[96] J. C. Knight; B. Cornelissen. Bioorthogonal chemistry: implications for pretargeted nuclear (PET/SPECT) imaging and therapy. *Am. J. Nucl. Med. Mol. Imaging.*, 4:96–113, 2014.

[97] B. M. Zeglis; K. K. Sevak; T. Reiner; P. Mohindra; S. D. Carlin; P. Zanzonico; R. Weissleder; J. S. Lewis. A pretargeted PET imaging strategy based on bioorthogonal Diels–Alder Click chemistry. *J. Nucl. Med.*, 54:1389–1396, 2013.

[98] A. F. O'Neill; J. L. J. Dearling; Y. Wang; T. Tupper; Y. Sun; J. C. Aster; M. L. Calicchio; A. R. Perez-Atayde; A. B. Packard; A. L. Kung. Targeted imaging of Ewing Sarcoma in preclinical models using a 64Cu-labeled Anti-CD99 Antibody. *Clin. Cancer Res.*, 20:678–687, 2014.

[99] H. Soliman. Immunotherapy strategies in the treatment of breast cancer. *Cancer Control*, 20:17–21, 2013.

[100] R. Tavaréa; M. N. McCracken; K. A. Zettlitza; S. M. Knowlesa; F. B. Salazara; T. Olafsena; O. N. Witte; A. M. Wua. Engineered antibody fragments for immuno-PET imaging of endogenous CD8+ T cells in vivo. *Proc. Natl. Acad. Sci. USA*, 111:1108–1113, 2014.

[101] K. S. Pentlow; M. C. Graham; R. M. Lambrecht; F. Daghighian; S. L. Bacharach; B. Bendriem; R. D. Finn; K. Jordan; H. Kalaigian; J. S. Karp;

W. R. Robeson; S. M. Larson. Quantitative imaging of Iodine-124 with PET. *J. Nucl. Med.*, 37:1557–1562, 1996.

[102] H. T. T. Phan; P. L. Jager; A. M. J. Paans; J. T. M. Plukker; M. G. G. Sturkenboom; W. J. Sluiter; B. H. R. Wolffenbuttel; R. A. J. O. Dierckx; T. P. Links. The diagnostic value of 124-I-PET in patients with differentiated thyroid cancer. *Eur. J. Nucl. Med. Mol. Imaging*, 35:958–965, 2008.

[103] V. V. Belov; A. A. Bonab; A. J. Fischman; Michael Heartlein; P. Calias; M. I. Papisov. Iodine-124 as a label for pharmacological PET imaging. *Mol. Pharmaceutics*, 8:736–746, 2011.

[104] M. K. Robinson; M. Doss; C. Shaller; D. Narayanan; J. D. Marks; L. P. Adler; D. E. Gonzalez Trotter; G. P. Adams. Quantitative immuno-positron emission tomography imaging of HER2-positive tumor Xenografts with an Iodine-124 labeled Anti-HER2 Diabody. *Cancer Res.*, 65:1471–1478, 2005.

[105] W. Jentzen; R. Weise; J. Kupferschläger; L. Freudenberg; W. Brandau; R. Bares; W. Burchert; A. Bockisch. Iodine-124 PET dosimetry in differentiated thyroid cancer: recovery coefficient in 2D and 3D modes for PET/CT systems. *Eur. J. Nucl. Med. Mol. Imaging*, 35:611–623, 2008.

[106] F. Lodi; C. Malizia; P. Castellucci; G. Cicoria; S. Fanti; S. Boschi. Synthesis of oncological [11-C]-radiopharmaceuticals for clinical PET. *Nucl. Med. Biol.*, 39:447–460, 2012.

[107] Z. Tu; R.H. Mach. C-11 radiochemistry in cancer imaging applications. *Curr. Top. Med. Chem.*, 10:1060–1095, 2010.

[108] N. Oyama; H. Akino; H. Kanamaru; Y. Suzuki; S. Muramoto; Y. Yonekura; N. Sadato; K. Yamamoto; K. Okada. 11-C-acetate PET imaging of prostate cancer. *J. Nucl. Med.*, 43:181–186, 2002.

[109] X. Geets; J-F. Daisnea; V. Gregoirea; M. Hamoirb; M. Lonneux. Role of [11-C]-methionine positron emission tomography for the delineation of the tumor volume in pharyngo-laryngeal squamous cell carcinoma: comparison with FDG-PET and CT. *Radiother. Oncol.*, 71:267–273, 2004.

[110] L. K. Shankar; J. M. Hoffman; S. Bacharach; M. M. Graham; J. Karp; A. A. Lammertsma; S. Larson; D. A. Mankoff; B. A. Siegel; A. Van den Abbeele; J. Yap; D. Sullivan. Consensus recommendations for the use of [18F]-FDG PET as an indicator of therapeutic response in patients in National Cancer Institute trials. *J. Nucl. Med.*, 47:1059–1066, 2006.

[111] S. Banister; D. Roeda; F. Dollé; M. Kassiou. Fluorine-18 chemistry for PET: A concise introduction. *Curr. Radiopharm.*, 3:68–80, 2010.

[112] E. L. Cole; M. N. Stewart; R. Littich; R. Hoareau; P. J. H. Scott. Radiosyntheses using Fluorine-18: The art and science of late stage fluorination. *Curr. Top. Med. Chem.*, 14:875–900, 2014.

[113] M. Roteta; E. Garcia-Torano; L. R. Barquero. Standardization of 18F by coincidence and LSC methods. *Appl. Radiat. Isotopes*, 64:10–11, 2006.

[114] R. C. Walker; G. L. Purnell; L. B. Jones-Jackson; K. L. Thomas; J. A. Brito; E. J. Ferris. Introduction to PET imaging with emphasis on biomedical research. *Neurotoxicology*, 25:533–542, 2004.

[115] T. Ido; C-N. Wan; V. Casella; J. S. Fowler; A. P. Wolf. Labeled 2-deoxy-D-glucose analogs: 18F-labeled 2-deoxy-2-fluoro-D-glucose, 2-deoxy- 2-fluoro-D-mannose and 14C-2-deoxy-2-fluoro-D-glucose. *J. Label Compd. Radiopharm.*, 14:175–183, 1978.

[116] M. E. Phelps; S.C. Huang; E.J. Hoffman; C. Selin; L. Sokoloff; D.E. Kuhl. Tomographic measurement of local cerebral glucose metabolic rate in humans with 2'-[18F]fluoro-2-deoxy-D-glucose. *Ann. Neurol.*, 6:371–388, 1979.

[117] R. Weissleder. Molecular imaging in cancer. *Science*, 312:1168–1171, 2006.

[118] A. Almuhaideb; N. Papathanasiou; J. Bomanji. 18F-FDG PET/CT imaging in oncology. *Ann. Saudi Med.*, 31:3–13, 2011.

[119] G. J. Kelloff; J. M. Hoffman; B. Johnson; H. I. Scher; B. A. Siegel; E. Y. Cheng; B. D. Cheson; J. O'Shaughnessy; K. Z. Guyton; D. A. Mankoff; L. Shankar; S. M. Larson; C. C. Sigman; R. L. Schilsky; D. C. Sullivan. Progress and promise of FDG-PET imaging for cancer patient management and oncologic drug development. *Clin. Cancer Res.*, 11:2785–2808, 2005.

[120] J. W. Fletcher; B. Djulbegovic; H. P. Soares; B. A. Siegel; V. J. Lowe; G. H. Lyman; R. E. Coleman; R. Wahl; J. C. Paschold; N. Avril; L. H. Einhorn; W. W. Suh; D. Samson; D. Delbeke; M. Gorman; A. F. Shields. Recommendations on the use of 18F-FDG in oncology. *J. Nucl. Med.*, 49:480–508, 2008.

[121] C. M Galmarini; J. R. Mackey; C. Dumontet. Nucleoside analogues and nucleobases in cancer treatment. *Lancet Oncol.*, 3:415–424, 2002.

[122] J. A. Secrist. Nucleosides as anticancer agents: form concept to the clinic. *Nucleic Acids Symposium Series*, 49:15–16, 2005.

[123] A. Kassis; S. J. Adelstein; G. Mariani. Radiolabeled nucleoside analogs in cancer diagnosis and therapy. *Q. J. Nucl Med.*, 40:301–319, 1996.

[124] J. T. Lee; D. O. Campbell; N. Satyamurthy; J. Czernin; C. G. Radu. Stratification of nucleoside analog chemotherapy using 1-(2'-deoxy-2'-[18F]fluoro-beta-D-arabinofuranosyl)cytosine and 1-(2'-deoxy-2'-[18F]fluoro-beta-L-arabinofuranosyl)-5-methylcytosine PET. *J. Nucl. Med.*, 53:275–280, 2012.

[125] G. R. Morais; R. A. Falconer; I. Santos. Carbohydrate-based molecules for

molecular imaging in nuclear medicine. *Eur. J. Org. Chem.*, 8:1401–1414, 2013.

[126] P. Wells; E. Aboagye; R. N. Gunn; S. Osman; A. V. Boddy; G. A. Taylor; I. Rafi; A. N. Hughes; A. H. Calvert; P. M. Price; D. R. Newell. 2-[11C]thymidine positron emission tomography as an indicator of thymidylate synthase inhibition in patients treated with AG337. *J. Natl. Cancer Inst.*, 95:675–682, 2003.

[127] M. Wagner; U. Seitz; A. Buck; B. Neumaier; S. Schultheiß; M. Bangerter; M. Bommer; F. Leithäuser; E. Wawra; G. Munzert; S. N. Reske. 3'-[18F]fluoro-3'-deoxythymidine ([18F]-FLT) as positron emission tomography tracer for imaging proliferation in a murine B-cell lymphoma model and in the human disease. *Cancer Res.*, 63:2681–2687, 2003.

[128] S. J. Martin; J. A. Eisenbarth; U. Wagner-Utermann; W. Mier; M. Henze; H. Pritzkow; U. Haberkorn; M. Eisenhut. A new precursor for the radiosynthesis of [18F]FLT. *Nucl. Med. Biol.*, 29:263–273, 2002.

[129] S. J. Oh; C. Mosdzianowski; D. Y. Chi; J. Y. Kim; S. H. Kang; J. S. Ryu; J. S. Yeoa; D. H. Moon. Fully automated synthesis system of 3'-deoxy-3'-[18F]fluorothymidine. *Nucl. Med. Biol.*, 31:803–809, 2004.

[130] A.F. Shields. PET imaging with 18F-FLT and thymidine analogs: Promise and pitfalls. *J. Nucl. Med.*, 44:1432–1434, 2003.

[131] N. Graf; K. Herrmann; B. Numberger; D. Zwisler; M. Aichler; A. Feuchtinger; T. Schuster; H. J. Wester; R. Senekowitsch-Schmidtke; C. Peschel; M. Schwaiger; U. Keller; T. Dechow; A. K. Buck. [18F]FLT is superior to [18F]FDG for predicting early response to antiproliferative treatment in high-grade lymphoma in a dose-dependent manner. *Eur. J. Nucl. Med. Mol. Imaging*, 40:34–43, 2013.

[132] C. C. Zhang; Z. Yan; W. Li; K. Kuszpit; C. L. Painter; Q. Zhang; P. B. Lappin; T. Nichols; M. E. Lira; T. Affolter; N. R. Fahey; C. Cullinane; M. Spilker; K. Zasadny; P. O'Brien; D. Buckman; A. Wong; J. G. Christensen. [18F]FLT–PET imaging does not always "Light Up" proliferating tumor cells. *Clin. Cancer Res.*, 18:1303–1312, 2012.

[133] J. F. R. Robertson; K. L. O'Neill; M. W. Thomas; P. G. McKenna; R. W. Blamey. Thymidine kinase in breast cancer. *Br. J. Cancer*, 62:663–667, 1990.

[134] G. Smith; R. Sala; L. Carroll; K. Behan; M. Glaser; E. Robins; Q. Nguyen; E. O. Aboagye. Synthesis and evaluation of nucleoside radiotracers for imaging proliferation. *Nucl. Med. Biol.*, 39:652–665, 2012.

[135] E. T. McKinley; G. D. Ayers; R. A. Smith; S. A. Saleh; P. Zhao; M. K. Washington; R. J. Coffey; H. C. Manning. Limits of [18F]-FLT PET as a biomarker of proliferation in oncology. *PLOS One*, 8:e58938, 2013.

[136] W. Chen; T. Cloughesy; N. Kamdar; N. Satyamurthy; M. Bergsneider; L. Liau; P. Mischel; J. Czernin; M. E. Phelps; D. H.S. Silverman. Imaging proliferation in brain tumors with 18F-FLT PET: Comparison with 18F-FDG. *J. Nucl. Med.*, 46:945–952, 2005.

[137] P. Noordhuis; U. Holwerda; C. L. Van der Wilt; C. J. Van Groeningen; K. Smid; S. Meijer; H. M. Pinedo; G. J. Peters. 5-fluorouracil incorporation into RNA and DNA in relation to thymidylate synthase inhibition of human colorectal cancers. *Ann. Oncol.*, 15:1025–1032, 2004.

[138] J. A. van Laar; C. L. van der Wilt; Y. M. Rustum; P. Noordhuis; K. Smid; H. M. Pinedo; G. J. Peters. Therapeutic efficacy of fluoropyrimidines depends on the duration of thymidylate synthase inhibition in the murine colon 26-B carcinoma tumor model. *Clin. Cancer Res.*, 2:1327–1333, 1996.

[139] Y. Saga; M. Suzuki; H. Mizukami; T. Kohno; Y. Takei; M. Fukushima; K. Ozawa. Overexpression of thymidylate synthase mediates desensitization for 5-fluorouracil of tumor cells. *Int. J. Cancer*, 106:324–326, 2003.

[140] J. L. Eiseman; C. Brown-Proctor; P. E. Kinahan; J. M. Collins; W. Anderson; E. Joseph; D. R. Hamburger; S. Pan; C. A. Mathis; M. J. Egorin and R. W. Klecker. Distribution of 1-(2'-deoxy-2'-fluoro-beta-D-arabinofuranosyl)uracil in mice bearing colorectal cancer Xenografts: Rationale for therapeutic use and as a positron emission tomography probe for thymidylate synthase. *Clin. Cancer Res.*, 10:6669–6676, 2004.

[141] H. Sun; J. M. Collins; T. J. Mangnera; O. Muzika; A. F. Shields. Imaging 18F-FAU [1-(2'-deoxy-2'-fluoro-beta-D-arabinofuranosyl)uracil] in dogs. *Nucl. Med. Biol.*, 30:25–30, 2003.

[142] H. Sun; A. Sloan; T. J. Mangner; U. Vaishampayan; O. Muzik; J. M. Collins; K. Douglas; A. F. Shields. Imaging DNA synthesis with [18F]-FMAU and positron emission tomography in patients with cancer. *Eur. J. Nucl. Med. Mol. Imaging*, 32:15–22, 2005.

[143] H. Sun; J. M. Collins; T. J. Mangner; O. Muzik; A. F. Shields. Imaging the pharmacokinetics of [18F]FAU in patients with tumors: PET studies. *Cancer Chemother. Pharmacol.*, 57:343–348, 2006.

[144] H. Sun; T. J. Mangner; J. M. Collins; O. Muzik; K. Douglas; A. F. Shields. Imaging DNA synthesis in vivo with 18F-FMAU and PET. *J. Nucl. Med.*, 46:292–296., 2005.

[145] O. S. Tehrani; O. Muzik; L. K. Heilbrun; K. A. Douglas; J. M. Lawhorn-Crews; H. Sun; T. J. Mangner; A. F. Shields. Tumor imaging using 1-(2´-deoxy-2´-[18F]fluoro-beta-D-arabinofuranosyl)thymine and PET. *J. Nucl. Med.*, 48:1436–1441, 2007.

[146] D. A. Nathanson; A. L. Armijo; M. Tom; Z. Li; E. Dimitrova; W. R. Austin; J. Nomme; D. O. Campbell; L. Ta; T. M. Le; J. T. Lee; R. Darvish; A. Gordin; L. Wei; H. Liao; M. Wilks; C. Martin; S. Sadeghi; J. M. Murphy; N. Boulos; M. E. Phelps; K. F. Faull; H. R. Herschman; M. E. Jung; J. Czernin; A. Lavie; C. G. Radu. Co-targeting of convergent nucleotide biosynthetic pathways for leukemia eradication. *J. Exp. Med.*, 211:473–486, 2014.

[147] D. Braas; E. Ahler; B. Tam; D. Nathanson; M. Riedinger; M. R. Benz; K. B. Smith; F. C. Eilber; O. N. Witte; W. D. Tap; H. Wu; H. R. Christofk. Metabolomics strategy reveals subpopulation of liposarcomas sensitive to gemcitabine treatment. *Cancer Discov.*, 2:1109–1117, 2012.

[148] Y. Cen; A. A. Sauve. Efficient syntheses of clofarabine and gemcitabine from 2-deoxyribonolactone. *Nucleos. Nucleot. Nucl.*, 29:113–122, 2010.

[149] L. W. Hertel; J. S. Kroin; J. W. Misner; J. M. Tustin. Synthesis of 2-deoxy-2,2-difluoro-D-ribose and 2'-deoxy-2',2'-difluoro-D-ribofuranosyl nucleosides. *J. Org. Chem*, 53:2406–2409, 1988.

[150] W. R. Hasek; W. C. Smith; V. A. Engelhardt. The chemistry of sulfur tetrafluoride. ii. The fluorination of organic carbonyl compounds. *J. Am. Chem. Soc.*, 82:543–551, 1960.

[151] G. S. Lal; G. P. Pez; R. J. Pesaresi; F. M. Prozonic; H. Cheng. Bis(2-methoxyethyl)aminosulfur trifluoride: A new broad-spectrum deoxofluorinating agent with enhanced thermal stability. *J. Org. Chem.*, 64:7048–7054, 1999.

[152] B. J. Paul. K. Dax; M. Albert; J. Oertner. Synthesis of deoxyfluoro sugars from carbohydrate precursors. *Carbohydr. Res.*, 327:47–86, 2000.

[153] A. L'Heureux; F. Beaulieu; C. Bennett; D. R. Bill; S. Clayton; F. LaFlamme; M. Mirmehrabi; S. Tadayon; D. Tovell; M. Couturier. Aminodi-

fluorosulfinium salts: Selective fluorination reagents with enhanced thermal stability and ease of handling. *J. Org. Chem.*, 75:3401–3411, 2010.

[154] J. R. McCarthy; D. P. Matthews; J. P. Paolini. Reactions of sulfoxides with diethylaminosulfur trifluoride: Fluoromethyl phenyl sulfone, a reagent for the synthesis of fluoroalkenes. *Org. Synth.*, 72:209–211, 1995.

[155] M. Lewis; M. E. Meza-Avina; L. Wei; I. E. Crandall; A. M. Bello; E. Poduch; Y. Liu; C. J. Paige; K. C. Kain; E. F. Pai; L. P. Kotra. Novel interactions of fluorinated nucleotide derivatives targeting orotidine 5'-monophosphate decarboxylase. *J. Med. Chem.*, 54:2891–2901, 2011.

[156] R. P. Singh; J. M. Shreeve. Recent advances in nucleophilic fluorination reactions of organic compounds using Deoxofluor and DAST. *Synthesis*, 17:2561, 2002.

[157] T. Umemoto; R. P. Singh; Y. Xu; N. Saito. Discovery of 4-tert-butyl-2,6-dimethylphenylsulfur trifluoride as a deoxofluorinating agent with high thermal stability as well as unusual resistance to aqueous hydrolysis, and its diverse fluorination capabilities including deoxofluoro-arylsulfinylation with high stereoselectivity. *J. Am. Chem. Soc.*, 132:18199–18205, 2010.

[158] D. E. Bergstrom; A. W. Mott; E. De Clercq; J. Balzarini; D. J. Swartling. 3',3'-difluoro-3'-deoxythymidine: comparison of anti-HIV activity to 3'-fluoro-3'-deoxythymidine. *J. Med. Chem.*, 35:3369–3372, 1992.

[159] D. P. Kjell; B. J. Slattery. A convenient synthesis of N4,O3',O2'-triacetyl-2'-ketocytidine. *Nucleos. Nucleot.*, 16:469–474, 1997.

[160] M. G. Straatmann; M. J. Welch. Fluorine-18-labeled diethylaminosulfur trifluoride (DAST): an F-for-OH fluorinating agent. *J. Nucl. Med.*, 18:151–158, 1977.

[161] M. Namavari; Y. Chang; B. Kusler; S. Yaghoubi; B. S. Mitchell; S. S. Gambhir. Synthesis of 2'-deoxy-2'-[18F]fluoro-9-beta-D-arabinofuranosylguanine: a novel agent for imaging T-cell activation with PET. *Mol. Imaging Biol.*, 13:812–818, 2011.

[162] W. Sun; J. Wilson; P. Kumar; E. Knaus; L. Wiebe. Radiosynthesis of 2'-deoxy-2'-[18F]fluorothymidine ([18F)FT), a putative PET agent for imaging HSV1-TK expression. *Curr. Radiopharm.*, 2:75–82, 2009.

[163] V. Gouverneur; K. Mueller., editor. *Molecular Medicine and Medicinal Chemistry: Fluorine is pharmaceutical and medicinal chemistry.*, volume 6. Imperial College Press, 2012.

[164] C. Wodarsky; J. Eisenbarth; K.Weber; M. Henze; U. Haberkorn; M. Eisenhut. Synthesis of 3´-deoxy-3'-[18F]fluoro-thymidine with 2,3'-anhydro-5'-O-(4,4'-dimethoxtrityl)thymidine. *J. Label Compd. Radiopharm.*, 43:1211–1218, 2000.

[165] H.-J. Machulla; A. Blocher; M. Kuntzsch; M. Piert; R. Wei; J.R. Grierson. Simplified labeling approach for synthesizing 3'-deoxy-3'-[18F]fluorothymidine ([18F]FLT). *J. Radioanal. Nucl. Chem.*, 243:843–846, 2000.

[166] M. G. Campbell; T. Ritter. Late-stage fluorination: From fundamentals to application. *Org. Process Res. Dev.*, 18:474–480, 2014.

[167] J. F. Codington; I. L . Doerr; J. J. Fox. Synthesis of 2'- fluorothymidine, 2'-fluorodeoxyuridine, and other 2'-halogeno-2'-deoxynucleosides. *Nucleos. Nucleot.*, 29:558–564, 1963.

[168] R. Mengel; W. Guschlbauer. A simple synthesis of 2-deoxy-2'-fluorocytidine by nucleophilic substitution of, 2,2'-anhydrocytidine with potasium fluoride/crown ether. *Angew. Chem. Int. Ed.*, 17:525, 1978.

[169] K. Hamacher; H. H. Coenen; G. Stoecklin. Efficient stereospecific synthesis of No-Carrier-added 2-[18F]-fluoro-2-deoxy-D-glucose using aminopolyether supported nucleophilic substitution. *J. Nucl. Med.*, 27:235–238, 1986.

[170] M. M. Alauddin; J. Balatoni; J. Gelovani. Synthesis of 3'-deoxy-3'-[18F]fluoro-1-beta-D-xylofuranosyluracil ([18F]-FMXU) for PET. *J. Label Compd. Radiopharm.*, 48:941–950, 2005.

[171] S. Yu. Review of [18F]-FDG synthesis and quality control. *Biomed. Imaging Interv. J.*, 2:e57, 2006.

[172] M. J. Adam. Radiohalogenated carbohydrates for use in PET and SPECT. *J. Label Compd. Radiopharm.*, 45:167–180, 2002.

[173] J. Z. Long; M. S. Jacobson; J. C. Hung. Comparison of FASTlab 18F-FDG production using phosphate and citrate buffer cassettes. *J. Nucl. Med. Technol.*, 41:32–34, 2013.

[174] X. Ma; W.-Y. Tseng; M. Eddings; P. Y. Keng. R. M. van Dam. A microreactor with phase-change microvalves for batch chemical synthesis at high temperatures and pressures. *Lab Chip*, 14:280–285, 2014.

[175] T. J. Mangner; R. W. Klecker; L. Anderson; A. F. Shields. Synthesis of 2'-deoxy-2'-[18F]fluoro-beta-D-arabinofuranosyl nucleosides, [18F]-FAU, [18F]-FMAU, [18F]-FBAU and [18F]-FIAU, as potential PET agents for imaging cellular proliferation. *Nucl. Med. Biol.*, 30:215–224, 2003.

[176] H. G. Howell; P. R. Brodfuehrer; S. P. Brundidge; D. A. Benigni; C. Sapino. Antiviral nucleosides. A stereospecific, total synthesis of 2'-fluoro-2'-deoxy-alpha-D-arabinofuranosyl nucleosides. *J. Org. Chem.*, 53:85–88, 1988.

[177] N. Turkman; V. Paolillo; J. G. Gelovani; M. M. Alauddin. An investigation on stereospecific fluorination at the 2'-arabino-position of a

pyrimidine nucleoside: Radiosynthesis of 2'-deoxy-2'-[18F]fluoro-5-methyl-1-beta-D-arabinofuranosyluracil. *Tetrahedron*, 68:10326–10332, 2012.

[178] H. Cai; Z. Li; P; S. Conti. The improved syntheses of 5-substituted 2'-[18F]fluoro-2'-deoxyarabinofuranosyluracil derivatives ([18F]FAU, [18F]FEAU, [18F]FFAU, [18F]FCAU, [18F]FBAU and [18F]FIAU) using a multistep one-pot strategy. *Nucl. Med. Biol.*, 38:659–666, 2011.

[179] B. Amaraesekera; P. D. Marchis; K. P. Bobinski; C. G. Radu; J. Czernin; J. R. Barrio; R. M. van Dam. High-pressure, compact, modular radiosynthesizer for production of positron emitting biomarkers. *Appl. Radiat. Isotopes*, 78:88–101, 2013.

[180] M. Lazari; K. M. Quinn; S. B. Claggett; J. Collins; G. J. Shah; H. E. Herman; B. Maraglia; M. E Phelps; M. D. Moore; R. M. van Dam. ELIXYS - a fully automated, three-reactor high-pressure radiosynthesizer for development and routine production of diverse PET tracers. *EJNMMI Res.*, 3:52, 2013.

[181] M. Yuna; S. J. Oha; H.-J. Hab; J. S. Ryua; D. H. Moon. High radiochemical yield synthesis of 3'-deoxy-3'-[18F]fluorothymidine using (5'-O-dimethoxytrityl-2'-deoxy-3'-O-nosyl-beta-D-threo pentofuranosyl)thymine and its 3-N-BOC-protected analogue as a labeling precursor. *Nucl. Med. Biol.*, 30:151–157, 2003.

[182] M. R. Javed; S. Chen; H.-K. Kim; L. Wei; J. Czernin; C.-J. Kim; R. M. van Dam; P. Y. Keng. Efficient radiosynthesis of 3'-deoxy-3'-18F-fluorothymidine using Electrowetting-on-Dielectric digital microfluidic chip. *J. Nucl. Med.*, 55:321–328, 2014.

[183] S. Nimmagadda; T. J. Mangner; J. M. Lawhorn-Crews; U. Haberkorn; A. F. Shields. Herpes simplex virus thymidine kinase imaging in mice with (1-(2'-

deoxy-2'-[18F]fluoro-1-beta-D-arabinofuranosyl)-5-iodouracil) and metabolite (1-(2'-deoxy-2'-[18F]fluoro-1-beta-D-arabinofuranosyl)-5-uracil). *Eur. J. Nucl. Med. Mol. Imaging*, 36:1987–1993, 2009.

[184] J. A. Balatoni; M. Doubrovin; L. Ageyeva; N. Pillarsetty; R. D. Finn; J. G. Gelovani; R. G. Blasberg. Imaging herpes viral thymidine kinase-1 reporter gene expression with a new 18F-labeled probe: 2'-fluoro-2'-deoxy-5-[18F]fluoroethyl-1-beta-D-arabinofuranosyl uracil. *Nucl. Med. Biol.*, 32:811–819, 2005.

[185] N. Turkman; J. G. Gelovani; M. M. Alauddin. A novel method for stereospecific fluorination at the 2'-arabino-position of pyrimidine nucleoside: synthesis of [18F]-FMAU. *J. Label Compd. Radiopharm.*, 53:782–786, 2010.

[186] S. H. Kang; S. J. Oh; M. K. Yoon; J. S. Ryu; W. K. Lee; S. J. Choi; K. P. Park; D. H. Moon. Simple and high radiochemical yield synthesis of 2'-deoxy-2'-[18F]fluorouridine via a new nosylate precursor. *J. Label Compd. Radiopharm.*, 49:1237–1246, 2006.

[187] R. Schirrmacher; C. Wängler; E. Schirrmacher. *Fluorine-18 Radiochemistry: Theory and Practice.*, volume 1 of *Munich Radiopharmaceutical Handbook*. Scintomics Print Media and Publishing, 2010.

[188] G. B. Saha., editor. *Basics of PET Imaging: Physics, Chemistry, and Regulations*. Springer, 2nd edition, 2010.

[189] M. S. Berridge; S. M. Apana; J. M. Hersh. Teflon radiolysis as the major source of carrier in fluorine-18. *J. Label Compd. Radiopharm.*, 52:543–548, 2009.

[190] S. Lu; A. M. Giamis; V. W. Pike. Synthesis of [18F]Fallypride in a microreactor: Rapid optimization and multiple-production in small doses for micro-PET studies. *Curr. Radiopharm.*, 2:49–55, 2009.

[191] J. Koziorowski. A simple method for the quality control of [18F]FDG. *Appl. Radiat. Isotopes*, 68:1740–1742, 2010.

[192] R. Nakao; T. Ito; M. Yamaguchi; K. Suzuki. Improved quality control of [18F]FDG by HPLC with UV detection. *Nucl. Med. Biol.*, 32:907–912, 2005.

[193] N. Satyamurthy; M. E. Phelps; J. R. Barrio. Electronic generators for the production of positron-emitter labeled radiopharmaceuticals: Where would PET be without them? *Clin. Posit. Imag.*, 2:233–253, 1999.

[194] A. F. Shields; J. R. Grierson; B. M. Dohmen; H. J. Machulla; J. C. Stayanoff; J. M Lawhorn-Crews. Imaging proliferation in vivo with [18F]FLT and positron emission tomography. *Nat. Med.*, 4:1334–1336, 1998.

[195] J. L. Lim; M. S. Berridge. An efficient radiosynthesis of [18F]fluoromisonidazole. *Appl. Radiat. Isotopes*, 44:1085–1091, 1993.

[196] A. Krasikova. Synthesis modules and automation in F-18 labeling. *Ernst Schering Research Foundation Workshop (PET Chemistry)*, 64:289–316, 2007.

[197] S. Lindegren; H. Jensen; L. Jacobsson. A radio-high-performance liquid chromatography dual-flow cell gamma-detection system for on-line radiochemical purity and labeling efficiency determination. *J. Chromatogr. A*, 1337:128–132, 2014.

[198] Michael F. L'Annunziata, editor. *Handbook of Radioactivity Analysis.* Elsevier, 3rd edition, 2012.

[199] P. J. H. Scott; B. G. Hockley, editor. *Radiochemical Syntheses.*, volume 1. Wiley, 2011.

[200] *Work with ionising radiation: Ionising Radiations Regulations 1999.* HSE, 2000.

[201] A. Bixler; G. Springer; R. Lovas. Practical aspects of radiation safety for using fluorine-18. *J. Nucl. Med. Technol.*, 27:14–16, 1999.

[202] J. Bentley; R. Cosstick. J. W Gaynor. Synthesis of the 3'-thio-nucleosides and subsequent automated synthesis of oligodeoxynucleotides containing a 3'-S-phosphorothiolate linkage. *Nat. Protoc.*, 2:3122–3134, 2007.

[203] H. Moroder; C. Kreutz; K. Lang; A. Serganov; R. Micura. Synthesis, oxidation behavior, crystallization and structure of 2'-methylseleno guanosine containing RNAs. *J. Am. Chem. Soc.*, 128:9909–9918, 2006.

[204] H.G. Howell; P.R. Brodfuehrer; S.P. Brundidge; D.A. Benigni; C. Sapino. Antiviral nucleosides. A stereospecific total synthesis of 2'-fluoro-2'-deoxy-beta-D-arabinofuranosyl nucleosides. *J. Org. Chem.*, 53:85–88, 1988.

[205] S. Han; M. M. Joullie; V. V. Fokin; N. A. Petasis. Spectroscopic, crystallographic and computational studies of the formation and isomerization of cyclic acetals and ketals of pentonolactones. *Tetrahedron: Asymmetry*, 5:2535–2562, 1994.

[206] V. Vanheusden; H. Munier-Lehmann; S. Pochet; P. Herdewijn; S. Van Calenbergh. Synthesis and evaluation of thymidine-5'-O-monophosphate analogues as inhibitors of Mycobacterium tuberculosis thymidylate kinase. *Bioorg. Med. Chem. Lett.*, 12:2695–2698, 2002.

[207] S. G. DiMagno. H. Sun. Anhydrous tetrabutylammonium fluoride. *J. Am. Chem. Soc.*, 127:2050–2051, 2004.

[208] D. P. Cox; J. Terpinski; W. Lawrynowicz. "Anhydrous" tetrabutylammonium fluoride: A mild but highly efficient source of nucleophilic fluoride ion. *J. Org. Chem.*, 49:3216–3219, 1984.

[209] R. K. Sharma; J. L. Fry. Instability of anhydrous tetra-n-alkylammonium fluorides. *J. Org. Chem.*, 48:2112–2114, 1983.

[210] J. G. Tjuvajev; M. Doubrovin; T. Akhurst; S. Cai; J. Balatoni; M. M. Alauddin; R. Finn; W. Bornmann; H. Thaler; P. S. Conti; R. G. Blasberg. Comparison of radiolabeled nucleoside probes (FIAU, FHBG, and FHPG) for PET imaging of HSV-TK1 gene expression. *J. Nucl. Med.*, 43:1072–1083, 2002.

[211] R. Blasberg. PET imaging of gene expression. *Eur. J. Cancer*, 38:2137–2146, 2002.

[212] P. Brader; I. Serganova; R. G. Blasberg. Noninvasive molecular imaging using reporter genes. *J. Nucl. Med.*, 57:167–172, 2013.

[213] A. Matsuda; K. Takenuki; M. Tanaka; T. Sasaki; T. Ueda. Nucleosides and nucleotides. 97. Synthesis of new broad spectrum antineoplastic nucleosides, 2'-deoxy-2'-methylidenecytidine (DMDC) and its derivatives. *J. Med. Chem.*, 34:812–819, 1991.

[214] M. W. Schmidt; K. K. Baldridge; J. A. Boatz; S. T. Elbert; M. S. Gordon; J. H. Jensen; S. Koseki; N. Matsunaga; K. A. Nguyen; S. J. Su; T. L. Windus; M. Dupuis; J. A. Montgomery. General atomic and molecular electronic structure system. *J. Comput. Chem.*, 14:1347–1363, 1993.

[215] C. Serra; C. Aragonbs; J. Bessa; J. Farrhs; J. Vilarrasa. Stabilisation of pyrimidine nucleoside triflates by N-nitro groups. *Tetrahedron Lett.*, 39:7575–7578, 1998.

[216] S. Schiesser; B. Hackner; T. Pfaffeneder; M. Müller; C. Hagemeier; M Truss; T. Carell. Mechanism and stem-cell activity of 5-carboxycytosine decarboxylation determined by isotope tracing. *Angew. Chem. Int. Ed.*, 51:6516–6520, 2012.

[217] H. Tsunoda; A. Ohkubo; H. Taguchi; K. Seio; M. Sekine. Synthesis and

properties of DNA oligomers containing 2'-deoxynucleoside N-Oxide derivatives. *J. Org. Chem.*, 73:1217–1224, 2008.

[218] J. O. Osby; M. G. Martin; B. Ganem. An exceptionally mild deprotection of phthalimides. *Tetrahedron Lett.*, 25:2093–2096, 1984.

[219] S. E. Sen; S. L. Roach. A convenient two-step procedure for the synthesis of substituted allylic amines from allylic alcohols. *Synthesis*, 1:756–758, 1995.

[220] F. Beaulieu; L.-P. Beauregard; G. Courchesne; M. Couturier; F. LaFlamme; A. L'Heureux. Aminodifluorosulfinium tetrafluoroborate salts as stable and crystalline deoxofluorinating reagents. *Org. Lett.*, 11:5050–5053, 2009.

[221] W. J. Middleton. New fluorinating reagents. Dialkylaminosulfur fluorides. *J. Org. Chem.*, 40:574–578, 1975.

[222] J.-P. Meyer; K. C. Probst; I. M. L. Trist; C. McGuigan; A. D. Westwell. A novel radiochemical approach to 1-(2'-deoxy-2'-[18F]fluoro-beta-D-arabinofuranosyl)cytosine (18F-FAC). *J. Label Compd. Radiopharm.*, 57:637–644, 2014.

[223] G. Pascali; L. Matesic; T. L. Collier; N. Wyatt; B. H. Fraser; T. Q. Pham; P. A. Salvadori; I. Greguric. Optimization of nucleophilic 18F radiofluorinations using a microfluidic reaction approach. *Nat. Protoc.*, 9:2017–2029, 2014.

[224] S. H. Liang; D. L. Yokell; R. N. Jackson; P. A. Rice; R. Callahan; K. A. Johnson; D. Alagille; G. Tamagnan; T. L. Collier; N. Vasdev. Microfluidic continuous-flow radiosynthesis of [18F]FPEB suitable for human PET imaging. *Med. Chem. Commun.*, 5:432–435, 2014.

[225] A. Miah; C. B. Reese; Q. Song; Z. Sturdy; S. Neidle; I. J. Simpson; M.

Read; E. Rayner. 2',3'-Anhydrouridine. A useful synthetic intermediate. *J. Chem. Soc., Perkin Trans. 1*, 19:3277–3283, 1998.

[226] J. Shi; J. Du; T.i Ma; K. W. Pankiewicz; S. E. Patterson; P. M. Tharnish; T. R. McBrayer; L. J. Stuyver; M. J. Otto; C. K. Chu; R. F. Schinazic; K. A. Watanabe. Synthesis and anti-viral activity of a series of D- and L-2'-deoxy-2'-fluororibonucleosides in the subgenomic HCV replicon system. *Bioorg. Med. Chem.*, 13:1641–1652, 2005.

[227] S. Manfredini; P. G. Baraldi; E. Durini; L. Porcu; A. Angusti; S. Vertuani; N. Solaroli; E. De Clercq; A. Karlsson; J. Balzarini. Design, synthesis and enzymatic activity of highly selective human mitochondrial thymidine kinase inhibitors. *Bioorg. Med. Chem. Lett.*, 11:1329–1332, 2001.

[228] Y. Aoyama; T. Sekine; Y. Iwamoto; E. Kawashima; Y. Ishido. Efficient synthesis of 2'-bromo-2'-deoxy-3',5'-O-TPDS-pyrimidine nucleosides by boron trifluoride catalized reaction of 2,2'-anhydro-(1-beta-D-arabinofuranosyl)pyrimidine nucleosides with lithium bromide. *Nucleos. Nucleot.*, 15:733–738, 1996.

[229] N. Ciliberti; S. Manfredini; A. Angusti; E. Durini; N. Solaroli; S. Vertuani; L. Buzzoni; M. C. Bonache; E. Ben-Shalom; A. Karlsson; A. Saada; J. Balzarini. Novel selective human mitochondrial kinase inhibitors: Design, synthesis and enzymatic activity. *Bioorg. Med. Chem.*, 15:3065–3081, 2007.

[230] H. M.-P. Chuia; M. Meroueha; S. A. Scaringeb; C. S. Chow. Synthesis of a 3-methyluridine phosphoramidite to investigate the role of methylation in a ribosomal RNA hairpin. *Bioorg. Med. Chem.*, 10:325–332, 2002.

[231] R. Z. Sterzycki; I. Ghazzouli; V. Brankovan; J. C. Martin; M. M. Mansuri. Synthesis and Anti-HIV activity of several 2'-fluoro-containing pyrimidine nucleosides. *J. Med. Chem.*, 33:2150–2157, 1990.

[232] F. Wohlrab; T. Haertlé; T. Trichtinger; W. Guschlbauer. 2'-deoxy-2'-fluorouridine-5'-phosphate: an alternative substrate for thymidylate synthetase from Escherichia coli K12. *Nucleic Acids Res.*, 12:4753–4759, 1978.

[233] K. Okuda; A. C. Seila; S. A. Strobel. Synthesis of isotopically labeled puromycin derivatives for kinetic isotope effect analysis of ribosome catalyzed peptide bond formation. *Tetrahedron*, 60:12101–12112, 2004.

[234] M. Sekine. General method for the preparation of N3- and O4-substituted uridine derivatives by phase-transfer reactions. *J. Org. Chem*, 54:2321–2326, 1989.